WOODHEAD PUBLISHING IN MATERIALS

Hybrid laser–arc welding

Edited by Flemming Ove Olsen

CRC

WP

Hybrid laser–arc welding

Related titles:

MIG welding guide
(ISBN 978-1-85573-947 5)
Gas metal arc welding (GMAW) also referred to as MIG (metal inert gas) is one of the key processes in industrial manufacturing. *MIG welding guide* provides comprehensive, easy-to-understand coverage of this widely used process. The reader is presented with a variety of topics from the choice of shielding gases, filler materials, welding equipment and lots of practical advice. The book provides an overview of new developments in various processes such as: flux cored arc welding; new high productive methods; pulsed MIG welding; MIG-brazing; robotic welding applications and occupational health and safety. This is essential reading for welding engineers, production engineers, designers and all those involved in industrial manufacturing.

Advanced welding processes
(ISBN 978-1-84569-130-1)
This book introduces the range of advanced welding techniques currently in use. It covers gas tungsten arc welding (GTAW), gas metal arc welding (GMAW), high energy density processes such as laser welding, and narrow gap welding methods. The book reviews general issues such as power sources, filler materials and shielding gases. Particular attention is given to monitoring and process control as well as to automation and robotics.

Computational welding mechanics
(ISBN 978-1-84569-221-6)
This book begins by discussing the physics of welding before going on to review modelling methods and options as well as validation techniques. It also reviews applications in areas such as fatigue, buckling and deformation, improved service life of components and process optimisation. Some of the numerical methods described in the book are illustrated using software available from the author which allows readers to explore CWM in more depth.

Details of these and other Woodhead Publishing materials books can be obtained by:

- visiting our web site at www.woodheadpublishing.com
- contacting Customer Services (e-mail: sales@woodheadpublishing.com; fax: +44 (0) 1223 893694; tel.: +44 (0) 1223 891358 ext. 130; address: Woodhead Publishing Limited, Abington Hall, Granta Park, Great Abington, Cambridge CB21 6AH, UK)

If you would like to receive information on forthcoming titles, please send your address details to: Francis Dodds (address, tel. and fax as above; e-mail: francis.dodds@woodheadpublishing.com). Please confirm which subject areas you are interested in.

Hybrid laser–arc welding

Edited by
Flemming Ove Olsen

CRC Press
Boca Raton Boston New York Washington, DC

WOODHEAD PUBLISHING LIMITED
Oxford Cambridge New Delhi

Published by Woodhead Publishing Limited, Abington Hall, Granta Park, Great Abington, Cambridge CB21 6AH, UK
www.woodheadpublishing.com

Woodhead Publishing India Private Limited, G-2, Vardaan House, 7/28 Ansari Road, Daryaganj, New Delhi – 110002, India

Published in North America by CRC Press LLC, 6000 Broken Sound Parkway, NW, Suite 300, Boca Raton, FL 33487, USA

First published 2009, Woodhead Publishing Limited and CRC Press LLC
© 2009, Woodhead Publishing Limited
The authors have asserted their moral rights.

This book contains information obtained from authentic and highly regarded sources. Reprinted material is quoted with permission, and sources are indicated. Reasonable efforts have been made to publish reliable data and information, but the authors and the publishers cannot assume responsibility for the validity of all materials. Neither the authors nor the publishers, nor anyone else associated with this publication, shall be liable for any loss, damage or liability directly or indirectly caused or alleged to be caused by this book.

Neither this book nor any part may be reproduced or transmitted in any form or by any means, electronic or mechanical, including photocopying, microfilming and recording, or by any information storage or retrieval system, without permission in writing from Woodhead Publishing Limited.

The consent of Woodhead Publishing Limited does not extend to copying for general distribution, for promotion, for creating new works, or for resale. Specific permission must be obtained in writing from Woodhead Publishing Limited for such copying.

Trademark notice: Product or corporate names may be trademarks or registered trademarks, and are used only for identification and explanation, without intent to infringe.

British Library Cataloguing in Publication Data
A catalogue record for this book is available from the British Library.

Library of Congress Cataloging in Publication Data
A catalog record for this book is available from the Library of Congress.

Woodhead Publishing ISBN 978-1-84569-370-1 (book)
Woodhead Publishing ISBN 978-1-84569-652-8 (e-book)
CRC Press ISBN 978-1-4398-0214-4
CRC Press order number: N10051

The publishers' policy is to use permanent paper from mills that operate a sustainable forestry policy, and which has been manufactured from pulp which is processed using acid-free and elemental chlorine-free practices. Furthermore, the publishers ensure that the text paper and cover board used have met acceptable environmental accreditation standards.

Typeset by SNP Best-set Typesetter Limited, Hong Kong
Printed by TJ International Limited, Padstow, Cornwall, UK

Contents

Contributor contact details *ix*
Preface *xi*

Part I Characteristics of hybrid laser–arc welding 1

1 Advantages and disadvantages of arc and laser welding 3
E. W. Reutzel, Pennsylvania State University, USA
1.1 Introduction 3
1.2 Arc welding 3
1.3 Laser welding 15
1.4 Acknowledgments 25
1.5 References 25

2 Fundamentals of hybrid laser–arc welding 28
S. Katayama, Osaka University, Japan
2.1 Introduction 28
2.2 Plasma characteristics including interaction between laser beam and arc 29
2.3 Dynamic behavior 34
2.4 Melt dynamics and melt pool stability 37
2.5 Formation and prevention mechanism of porosity 41
2.6 References 44

3 Heat sources of hybrid laser–arc welding processes 47
A. Mahrle and E. Beyer, Dresden University of Technology, Germany
3.1 Introduction 47

3.2	Laser beam heat sources	48
3.3	Arc heat sources	59
3.4	Combinations of laser beams and arcs	68
3.5	Future trends	77
3.6	References	78
4	Effect of shielding gas on hybrid laser–arc welding M. Gao and X. Y. Zeng, Huazhong University of Science and Technology, China	85
4.1	Introduction	85
4.2	Common types and physical properties of shielding gases	86
4.3	Effects of shielding gas in hybrid welding	92
4.4	Effects of shielding gas on mechanical properties of the hybrid weld	100
4.5	Conclusions and sources of further information and advice	103
4.6	References	103
5	Properties of joints produced by hybrid laser–arc welding V. Kujanpää, Lappeenranta University of Technology, Finland	106
5.1	Introduction	106
5.2	Microstructure of hybrid laser–arc welds	106
5.3	Hardness	112
5.4	Strength	116
5.5	Toughness	118
5.6	Fatigue properties	120
5.7	Corrosion properties	123
5.8	References	124
6	Quality control and assessing weld quality in hybrid laser–arc welding J. K. Kristensen, FORCE Technology, Denmark	127
6.1	Introduction	127
6.2	Weldability of typical structural materials	127
6.3	Weld quality	134
6.4	Assessment of weld properties	136
6.5	Conclusions	138
6.6	Acknowledgements	139
6.7	References	139

Part II Applications of hybrid laser–arc welding 141

7 Hybrid welding of magnesium alloys 143
L. Liu, Dalian University of Technology, China
7.1 Introduction 143
7.2 Weldability of magnesium alloys 144
7.3 Low-power laser–arc hybrid welding process 145
7.4 Numerical simulation 162
7.5 Infrared temperature measurement 167
7.6 Spectral diagnosis 168
7.7 Interaction between laser beam and arc plasma 172
7.8 Practical application 173
7.9 Conclusions and future trends 175
7.10 References 175

8 Shipbuilding applications of hybrid laser–arc welding 178
J. K. Kristensen, FORCE Technology, Denmark
8.1 Introduction 178
8.2 The approval of laser-based welding in shipbuilding 179
8.3 Industrial examples 184
8.4 Conclusions 190
8.5 References 191

9 Industrial robotic application of laser-hybrid and laser-hybrid-tandem welding 192
H. Staufer, Fronius International GmbH, Austria
9.1 Introduction 192
9.2 Laser-hybrid process for industrial applications 193
9.3 Applications and case studies in the automotive industry 195
9.4 Applications in shipbuilding 199
9.5 Synergies by LaserHybrid 204
9.6 The laser-hybrid-tandem welding process in the automotive industry 205
9.7 Application of LaserTandem welding in the pipeline industry 207
9.8 LaserTandem welding system 209
9.9 Laser-hybrid welding with three arcs: principles of laser-hybrid and laser-hybrid-tandem welding 211
9.10 Conclusions 214
9.11 References 215

10 Hybrid laser–arc welding of aluminium 216
C. Thomy, BIAS – Bremer Institut für angewandte Strahltechnik GmbH, Germany
10.1 Introduction 216
10.2 Aluminium and its alloys 217
10.3 Fusion welding of aluminium alloys 219
10.4 Hybrid laser–arc welding processes for aluminium alloys 228
10.5 Properties of hybrid laser–arc welds 245
10.6 Applications 258
10.7 Future trends 261
10.8 References 262

11 Hybrid laser–arc welding of dissimilar metals 270
C. Thomy, BIAS – Bremer Institut für angewandte Strahltechnik GmbH, Germany
11.1 Introduction 270
11.2 Specific aspects of and state-of-the-art in joining of dissimilar metals 271
11.3 Basic features of laser MIG hybrid welding for dissimilar metals 277
11.4 Process and joint properties 278
11.5 Application potentials 288
11.6 Future trends 291
11.7 References 291

Part III Hybrid laser–arc welding of steel 297

12 Hybrid laser–arc welding of steel 299
S. Katayama, Osaka University, Japan
12.1 Introduction 299
12.2 Hybrid laser–arc welding of steel and high tensile strength steel 300
12.3 Hybrid laser–arc welding of Zn-coated steel 307
12.4 Hybrid laser–arc welding of stainless steel 309
12.5 References 309

Index *312*

Contributor contact details

(* = main contact)

Editor

Professor Flemming Ove Olsen
IPU
Produktionstorvet
Bygning 425
DK-2800 Kgs. Lyngby
Denmark
Email: foo@ipu.dk

Chapter 1

Dr E. W. Reutzel
The Applied Research Laboratory
The Pennsylvania State University
P.O. Box 30
State College
PA 16804-0030
USA
Email: ewr101@psu.edu

Chapters 2 and 12

Professor S. Katayama
Joining and Welding Research Institute (JWRI)
Osaka University
11-1 Mihogaoka
Ibaraki
Osaka 567-0047
Japan
E-mail: katayama@jwri.osaka-u.ac.jp

Chapter 3

Dr Achim Mahrle*
Dresden University of Technology,
Institute of Surface and Manufacturing Technology,
Postbox, 01062 Dresden
Germany
Email: achim.mahrle@iws.fraunhofer.de

Professor Eckhard Beyer
Dresden University of Technology,
Institute of Surface and Manufacturing Technology,
Postbox, 01062 Dresden, and
Fraunhofer IWS,
Winterbergstraße 28, 01277 Dresden
Germany

Chapter 4

Dr Ming Gao* and Professor Xiaoyan Zeng
Wuhan National Laboratory for Optoelectronics
Huazhong University of Science and Technology
H107 room, H zone,
1037# Luoyu Road
Wuhan
Hubei 430074
China
Email: mgao@mail.hust.edu.cn; hust_gm@163.com

Chapter 5

Professor V. Kujanpää
Lappeenranta University of Technology and VTT
Box 20, FI-53851
Lappeenranta
Finland
E-mail: Veli.kujanpaa@lut.fi

Chapters 6 and 8

Professor J. K. Kristensen
Technical Vice President
Welding and Production Innovation
FORCE Technology
Park Allé 345
2605 Brøndby
Denmark
E-mail: jek@force.dk

Chapter 7

Professor L. Liu
School of Material Science and Engineering
Dalian University of Technology
2 Linggong Road
Dalian City 116024
Liaoning Province
China
E-mail: liulm@dlut.edu.cn

Chapter 9

H. Staufer
Fronius International GmbH
Wels
Austria
E-mail: staufer.herbert@fronius.com

Chapters 10 and 11

Claus Thomy
BIAS – Bremer Institut für angewandte Strahltechnik GmbH
Klagenfurter Strasse 2
D-28359 Bremen
Germany
Email: thomy@bias.de

Preface

Since the beginning of the 1980s, the industrial applications of high power lasers have been increasing and today lasers are a well established high technology industrial tool. Welding is one of the main applications of high power lasers. The potential of high brightness energy sources such as lasers and electron beams to perform high-quality narrow welds at high production rates is outstanding and many welding applications of these two processes have been developed through the years. Starting from spot welding and fine pulsed welding, which mainly use Nd–YAG lasers, seam welding using continuous-wave CO_2 lasers also became an industrial process in the 1980s.

The major problem in using laser (and electron beam) welding was often the stringent joint tolerances these two processes demanded. Laser beams heat only the seam and a small area around it, creating a narrow weld. If a wide gap is used, a weld with an underfill or an undercut results or, in some cases, part of the beam is transmitted through the gap rather than welding the metal.

For many years it was considered impossible to use these techniques in heavy industry with its use of relatively coarse components. However, as the output of high-power lasers increased to a level high enough to produce welds 5 mm wide, the process became viable for heavy industrial applications.

It was at this point that a research paper from the late 1970s came into the mind of some scientists and engineers involved in laser welding. The paper was one of two dealing with combining an arc process with a laser beam: one paper on arc-augmented laser cutting and one on arc-augmented laser welding. Both papers were part of the steady stream of innovative papers from the team around Professor William M. Steen, at that time working at Imperial College in London. He applied his 2-kW British Oxygen

Company (BOC) lasers in many different experiments, including those reviewed in these two studies. At that time, others in the laser welding community were busy concentrating on making narrow cut and keyhole welds, and the idea of combining this fine and precise heat source with an old fashioned arc source was not considered mainstream research at that time.

However, when bridging the gap in heavy section welding or when reducing the hardness in steel by reducing the cooling rate became topical in laser welding, this old research paper came into our minds, and a number of my colleagues started to study this process more carefully. By this time we had larger and more reliable laser sources than the two 2-kW laboratory lasers at Imperial College. As a result, promising results came out of the first research into laser hybrid welding. Large heavy-industry projects with potential laser welding applications, such as the shipbuilding projects in Europe and Japan, stimulated this development, and soon many research groups around the world took up the challenge of bringing the two heat sources together. The laser hybrid process that emerged from this research is not a simple process and the equipment is not cheap. However, laser hybrid welding has now found its way into a range of industrial applications.

In this book, a summary is presented of recent research on the hybrid laser–arc welding process and its applications. This provides a snapshot of this advanced technology at a particular point in time but developments will continue. New types of laser, the disc laser and the high-power fibre laser, will certainly improve this technology in the future. The results of research using these new laser sources are included in this book, but much more will certainly follow in the near future as a result of the many research teams throughout the world that are active in developing this important process. It has been a pleasure to have had the opportunity to be editor of this book on laser hybrid welding, and to bring together a team of highly competent authors to write it. My thanks to them for sharing their research in furthering our understanding and use of this process.

1

Advantages and disadvantages of arc and laser welding

E. W. REUTZEL, Pennsylvania State University, USA

Abstract: This chapter provides historical background for gas metal arc (GMAW), gas tungsten arc (GTAW), and laser welding technologies, and a summary of practical considerations when employing each technique, and seeks to elucidate the advantages and disadvantages of each.

Key words: arc welding, gas metal arc welding (GMAW), gas tungsten arc welding (GTAW), laser welding.

1.1 Introduction

Ever since the bronze age, mankind has had a desire to metallurgically join separate components in order to build ever more complex tools and structures. For centuries, blacksmithing techniques and forge welding were the only known methods of joining such materials. Charcoal furnaces were used to heat iron parts to a temperature at which permanent metallurgical bonds could be created by hammering or rolling. Late in the 19th century, dramatic developments in the ability to harness and utilize electricity resulted in the development of practical arc welding techniques. Then, in the 1960s, the birth of lasers enabled focused light energy to be used to melt and fuse metal components. Through decades of development, these welding techniques have been advanced and refined, and now many of their relative benefits and drawbacks are well defined. In this chapter, a historical and technical background is provided for arc and laser welding technologies, and the advantages and disadvantages of each are elucidated.

1.2 Arc welding

1.2.1 Brief history of arc welding

Most people credit the birth of the electric arc to Sir Humphrey Davy, who, in 1801, demonstrated that an arc could be created, maintained, and manipulated with a battery-powered high-voltage electric circuit. Through careful manipulation of the carbon leads, the arc could be maintained and was

found to cast off substantial light and heat. It was not until much later, when suitable electric generators became available, that the arc began to be employed for more practical uses, such as the development of the carbon arc street lamp in the 1870s, that the electric arc technology became more widespread.

In 1881, Auguste De Meritens was perhaps the first to use an electric arc to melt and join metal when he patented a method to utilize the heat from a carbon arc to weld lead plates for storage batteries. Shortly thereafter, from 1885 to 1887, Nikolai Bernados and Stanislav Olszewaski were issued patents that described a manually manipulated carbon arc welding process. This technique was employed commercially soon after in the production of tanks and garden furniture, and, by 1892, for the maintenance of locomotives. The technique had limited application because, by its very nature, it introduces carbon into the weld metal resulting in a brittle end product.

In 1889, N. G. Slavianoff and Charles Coffin independently developed techniques in which the carbon rod was replaced with a metal electrode. This development signified a major improvement because the rod not only provided heat, but also because as the electrode was consumed it directly introduced supplemental metal to fill the joint. The technological advance was slow to gain widespread acceptance owing to the poor supply of satisfactory electrodes. The bare metal electrodes produced brittle and weak welds.

In the first decades of the 1900s, covered electrodes were introduced that served to both stabilize the arc (carbonates and silicates patented by Oscar Kjellberg in 1907) and eventually to purify the weld metal (blue asbestos and sodium silicate patented by A. P. Strohmenger in 1912). Despite these advances, the high cost of producing the electrodes limited its widespread use until World War I, when arc welding was found to offer faster production for bombs, torpedoes, ships, and even aircraft fuselages compared with conventional techniques such as riveting and gas welding, use of which was constrained owing to gas shortages.

After the war, use of arc welding was still limited owing to the high production cost of quality electrodes. In 1927, an extrusion process was developed whereby a coating could be inexpensively applied to a metal core. The availability of low-cost electrodes with tailored coatings enabled the shielded-arc electrode welding process to grow significantly. In the 1930s, international treaties that limited the gross tonnage of national navies encouraged the expansion of arc welding for shipbuilding applications by reducing weight compared with conventional joining methods.

In 1935, the submerged arc process was developed, in which granular flux is deposited immediately ahead of the bare steel filler wire electrode in order to provide adequate shielding for the arc, as well as flux to prevent oxidation of the molten weld puddle. By 1946, the process was refined for

use in a hand-held, semi-automatic gun with controlled voltage and current to decrease the dependence of bead quality on operator skill. Owing to the granular nature of the flux, the process was, and remains, only suitable for downhand welding.

In the late 1920s and early 1930s, arc welding processes were developed that utilized inert gases as a process shielding agent. These gas-based arc processes were often employed with a high melting point tungsten electrode and helium (He) or argon (Ar) shielding to produce the arc. The process became known as Tungsten Inert Gas (TIG) welding, and later changed to the more generic Gas Tungsten Arc Welding (GTAW), as it was recognized that certain applications may benefit from utilization of non-inert process gases. This process enabled welding of reactive metals such as aluminium and magnesium for which suitable fluxes could not be developed. An additional benefit is that the absence of flux significantly reduced potential for slag inclusions. Owing to the relatively low heat input, the process was not suitable for joining of thick sections of conductive materials. The process was modified in 1953 to direct the arc through a nozzle, resulting in a weld process eventually known as plasma-arc welding.

Though process concepts in which an inert gas is used to shield a weld process that utilizes a consumable weld electrode were first introduced in the 1920s, it was not until 1948 that the Metal Inert Gas (MIG) welding process was commercialized. In the 1950s the process became quite widespread and a desire to reduce gas costs led to the use of less expensive reactive gases such as carbon dioxide (CO_2), and so the process is now commonly referred to as the Gas Metal Arc Welding (GMAW) process.

Additional arc welding and manufacturing developments in the 1950s and 1960s led to the commercial use of consumable, tubular electrodes that encased fluxing and shielding agents. The process eventually became known as Flux Cored Arc Welding (FCAW), and is employed both with and without gas shielding. This self-shielded electrode enabled quite high deposition rates for automated and semi-automated equipment.

In the ensuing years, tremendous advances in manufacturing technology, metallurgy, robotics, power electronics and power source technology (including most recently computer technology), and in the scientific understanding of the arc welding process, have resulted in arc welding becoming a critical enabler for modern society. Scarcely a modern building or manufactured article exists that does not rely upon arc welding for some portion of its fabrication. Today, arc welding is extensively used in such indisposable and ubiquitous industries such as buildings and construction, bridges, heavy machinery, automobiles, trains, ships, mining equipment, oil and gas, and windpower.

According to the US Census Bureau, 1995 *Annual Survey of Manufactures*, more than $2b US of arc welding machines and electrodes were shipped

from the USA (or 66% of $3.3 billion shipped from all welding-related industries). According to the 1996 *Occupational Outlook Handbook* published by the US Department of Labor and Statistics, welders and those who use welding as an integral part of the occupation comprise more than two million workers, or more than 1% of the US workforce. According to the American Welding Society report, welding-related expenditures in US industry exceeded $34 billion in 2000, equivalent to $325 for every household in the USA. These figures serve to reinforce the substantial impact that welding has on the US and world economy.

The history and data provided in Section 1.2.1 were compiled from a variety of sources, including JFLAW 2000, Anon 1961, Miller and Crawford 2002, Dodds, Hanson and Zampogna 1997.

1.2.2 Gas metal arc welding (GMAW)

The gas metal arc welding (GMAW) process is a broad category of methods that join metals by use of an arc that heats the metals to their melting point. A welding arc is a high-temperature, ionized column of gas (or plasma) that spans between the continuously fed consumable electrode (typically 0.035–0.063 in., 0.89–1.60 mm in diameter) and the workpiece. The arc temperature is typically of the order of 6600 °C (for comparison, the melting point of iron is 1539 °C, and that of aluminum is 660 °C), and is sustained by high current (typically 100 to 450 A) provided by a welding power supply offering relatively low potential (typically 15 to 35 V). Upon solidification, the parts are permanently metallurgically fused. There is a variety of metal transfer modes that can be employed by changing the operating parameters to balance between a desire to increase welding rate and simultaneously limit heat input to decrease distortion and metallurgical degradation.

Equipment

Welding equipment comprises a variety of components necessary to generate the arc. The power supply provides the electrical voltage and current necessary to sustain the arc. The current is fed through cables to the contact tip, located in the welding torch, which provides a low resistance electrical connection to the consumable electrode filler wire. The other lead from the power supply connects to the workpiece to complete the electrical circuit. The filler wire is fed to the welding torch, which may be water cooled, from a wire spool by means of a wire feeder. The wire feeder can strictly push the wire, or a push–pull type configuration may be employed for soft metals, such as aluminium alloys. The shielding gas is fed coaxially through the torch around the contact tip to ensure adequate coverage for arc stabilization and process shielding. The torch can be manipulated manually, or can be attached

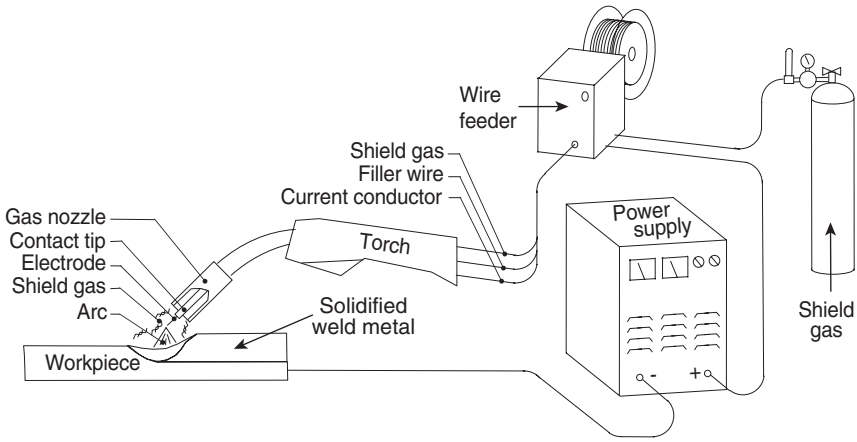

1.1 Schematic of a typical gas metal arc weld (GMAW) set up (not to scale).

to mechanized equipment or robotics. A schematic of a typical GMAW setup is shown in Fig. 1.1.

Shield gas

The arc forms in a shield gas between the consumable electrode and the metal component being welded. The shield gas can be any of a variety of gas mixtures that are used to form and stabilize the arc, as well as to shield the molten weld pool from oxidation with the atmosphere and from other atmospheric contaminants. The selection of shield gas is heavily dependent on the alloys that are being joined, the desired weld transfer mode and quality requirements, and the economics of the manufacturing process. Argon (Ar) is a commonly used component of shield gas mixtures for joining a variety of metals, in part because it offers an inert environment to prevent oxidation of the hot metal as it solidifies and cools. Its low ionization potential helps to ensure an easily formed path for electron flow and so it provides a constricted, stable arc and relatively deep penetration profile. Varying amounts of other reactive gases, such as CO_2 and oxygen (O_2), are often introduced when joining ferrous alloys. Carbon dioxide is relatively inexpensive and its reactivity produces a broader and hotter arc that results in a more fluid weld puddle, a broad, deep penetration profile, and often increased spatter. The presence of oxygen leads to oxidation of alloy contaminants, which can aid in scavenging undesirable contaminants from the weld zone and lead to improved properties. However, it also contributes to the formation of slag on the weld surface, which can be detrimental in some

manufacturing operations, e.g. it must be removed to ensure adhesion of paints and coatings. A variety of other gases are also used to produce other effects. The selection of an appropriate shield gas for a given weld application involves a delicate balance between conflicting requirements, and welding equipment, material, and gas suppliers provide information that can aid the selection process.

Filler wire

The consumable electrode is selected to balance cost of the process with throughput and quality requirements. Electrode alloys and configurations are formulated to provide a variety of beneficial functions, such as improving feedability and process stability, deoxidation and scavenging of weld puddle contaminants (especially with flux cored wires), increased conductivity for higher heat and puddle fluidity, and replacing key substrate alloying elements that are volatilized and lost during the weld process.

Weld modes

Historically, constant voltage power supplies have been employed in the majority of GMAW applications. With this type of power supply, there are three primary modes of transferring filler material from the consumable electrode to the weldment.

Short circuit metal transfer

At relatively low current and voltage, short circuit transfer mode (or 'short arc') occurs. In this case, when the trigger of the welding torch is pressed, the consumable electrode is continuously fed toward the workpiece. After it contacts the workpiece, electrical resistance of the electrode causes it to heat up and melt and the arc is formed. As the electrode continues to feed, the tip of the electrode wire begins to melt and a droplet forms on the end of the wire. The transfer of the molten electrode droplet to the workpiece occurs when the drop actually touches the workpiece and is drawn into the molten puddle through surface tension forces. When the contact occurs, it creates a short circuit that momentarily extinguishes the arc. For standard carbon steel with the power supply operating in constant voltage mode, this mode will typically occur at 180 A and 20 V, corresponding to roughly 210 in. min^{-1} wire feed speed with 0.045 in. (1.14 mm) wire. Owing to the necessity of using thin wires and low wire feed speeds, this process is limited in deposition rate. However, it generates relatively little heat, and therefore creates minimal distortion and offers additional advantages in certain applications. The low heat results in a small

and relatively non-fluid melt pool, so this mode is effective in joining of thin materials and for welding out-of-position. A side effect is that the low heat process can sometimes result in incomplete fusion of the weld bead, and the short circuit event and corresponding sharp increase in current can result in excessive spatter. Changing the inductance of the power supply or circuit can be used to adjust the rate of current rise in order to minimize spatter generation.

Globular metal transfer

At slightly higher current and voltage, the arc is sustained as the electrode is fed, and the molten droplet that forms on the end of the wire grows large enough (typically larger than the wire diameter) to allow gravity to pull it off the wire and into the molten puddle before a short circuit occurs. The dominating effect of gravity on droplet transfer makes out-of-position welding nearly impossible, and in practice, short circuiting is never completely avoided. As the large drops are formed and suspended above the workpiece, they are subject to violent turbulence found within the arc, and therefore are rarely of regular shape and are often subject to irregular trajectories that result in excessive spatter. This weld mode offers higher welding speeds and greater metal deposition rates relative to the short circuit metal transfer mode, but the excessive spatter associated with the process limits its widespread use.

Spray metal transfer

At still higher current and voltage, electromagnetic forces acting on the tip of the electrode will tend to 'pinch off' the molten droplet and forcefully direct it to the workpiece, resulting in axial spray transfer. The droplets tend to be smaller than the wire diameter, and will come off at much higher velocity than exhibited in globular mode transfer. Short circuiting rarely occurs, if at all, and the arc is continuously sustained leading to a very stable process with minimal spatter. For standard carbon steel with the power supply operating in constant voltage mode, this mode will typically occur at up to 350 A and 29 V, corresponding to roughly 380 in. min^{-1} (965 cm) wire feed speed with 0.045 in. (1.14 mm) wire. The higher energy used in the process results in a hotter and more fluid weld bead yielding high weld speeds and deposition rates with excellent weld fusion, but resulting in greater distortion and limiting minimum workpiece thickness and out-of-position welding relative to the short circuit metal transfer mode. Additionally, gas mixtures required to produce ensure stability with this weld mode are typically more costly than gases that can be utilized in the short circuit metal transfer mode.

Recent power source advances

Recent advances in power supply technology have introduced new metal transfer modes that do not fit neatly into the conventional categories of metal transfer.

Power source technology has undergone great advances since the 1950s, leading to the development of various modes of metal transfer for the GMAW process. In the late 1950s, power supplies were developed that enabled small diameter electrodes, down to 0.035 inch (0.89 mm), to employ short-circuiting mode transfer for lower heat input to decrease distortion. In the 1960s, in an attempt to decrease spatter and heat input while eliminating incomplete fusion defects, pulsed power supplies were introduced that enabled the pulsed spray transfer mode, with high peak current and low background current. In the 1970s, power source technology was rapidly advanced, and improvements in high-speed, transistor-controlled thyristor power sources, and in the welding engineer's understanding of the relationship between pulse frequency and wire feed speed, enabled the introduction of so called synergic power supplies. Whereas previous power supplies required the welder to set both wire feed speed and voltage or pulse parameters based on experience and intuition, this technology allows the operator to select wire feed speed alone, with the power supply providing optimal voltage or pulse parameters, i.e. single knob control. In the 1980s, power supply manufacturers began to introduce inverter-based transformers that enabled high-speed control of the waveform of individual pulses. The computer technology and digital control that exploded in the 1990s enabled real-time, reactive control of the waveform of each individual pulse to produce stable and smooth droplet transfer while ensuring minimal heat input and complete fusion for welding of various substrate thicknesses. Several key aspects of these advances are described below.

Pulsed spray transfer

As power supplies advanced, it became possible to modify the voltage waveform to effectively overcome some of the drawbacks of purely constant voltage welding systems. Based on knowledge of the specific welding process (desired wire feed speed, metal alloy, shield gas composition, etc.) welding current can be cycled at a specified rate from a high peak current to a low background current. In this manner, the metal droplets can be expelled in a stable and spatter-free manner during the high current portion of the pulse, thus approaching the stability found with a standard spray transfer mode. Complete weld fusion is also ensured through the high current pulse, but the drop to a lower background current level serves to limit overall heat input, thus limiting distortion and enabling out-of-position

welding. The pulse parameters are typically mapped out for individual alloy/shield gas combinations by the power supply manufacturer to enable single knob control for the operator, thus greatly simplifying parameter selection. This is often referred to as synergic control.

Real time adaptive control

As computer technology advanced and became less expensive throughout the 1990s, it became possible to monitor the arc electrical characteristics, such as voltage and current, in real time, and to actively control or adapt the waveform to achieve optimal and repeatable results. For example, to achieve the most robust pulsed spray mode weld process with the least amount of spatter, it may be desirable to force expulsion of only a single drop per pulse. However, changing process conditions, such as varying contact tip to workpiece distance or slight variations in wire feed speed, may lead to instability in conventional feed-forward pulsing systems. By monitoring the circuit characteristics and developing high-speed computer control algorithms, it is possible to vary the voltage or current based on feedback in real time to prevent multiple or no drops per pulse. Another example of real-time power supply control targets reduction of spatter in the low heat input processing realm. In this case, it is possible to carefully monitor the process to determine when the wire has contacted the workpiece and produces a short circuit. In an uncontrolled, constant voltage power supply, the sharp increase in current during the short circuit often results in a violent expulsion of molten metal or spatter. Adaptive computer algorithms can utilize sensor feedback to force the power supply to change voltage, current, or wire feed characteristics in real time to achieve a more gentle and spatter free droplet transfer. As computer technology and the understanding of arc dynamics and metal transfer continue to advance, it is likely that further advances in real time GMAW process control will be developed and commercialized in the future.

Advantages

The GMAW process offers several advantages relative to many other welding processes. First, the welding equipment can be relatively inexpensive relative to other high-cost processes like laser welding. The ability to feed filler wire directly into the weld pool with integral gas shielding results in a relatively simple process that, at its most basic level, is relatively easy to learn and use, and yet also lends itself to mechanization or automation. The wire is fed from a roll, and therefore can produce longer length welds without error-prone starts and stops, enabling faster deposition rates than when using the limited electrode length from shielded metal arc welding.

The filler metal can aid in accommodating gaps and can be tailored to achieve desired metallurgical properties by adding alloying elements that may be lost through volatilization. The relatively high heat input of certain welding modes can also benefit metallurgical properties by slowing the cooling rate down to prevent formation of undesirable metallurgical phases and to limit cracking. Conversely, in other modes the relatively low heat input enables out-of-position welding, e.g. vertical-up or even overhead welding. When properly tuned, the process can achieve relatively high welding rates with little or no spatter. With appropriate changes in parameters and process conditions, the process is amenable to the joining of a wide variety of metals.

Disadvantages

The GMAW process does suffer several disadvantages relative to some other welding processes. Owing to the fact that proper parameter selection is sometimes difficult to achieve, there is a likelihood of production of weld spatter. In using low heat input welding modes, improper technique can result in a lack of fusion. The fact that heat is provided over the relatively broad area of the arc means that deep penetration is not possible. High deposition rate welding modes require high heat input which can result in undesirable distortion. Additionally, since the heat is transferred through the surface of the workpiece and conducts into the interior, the heating pattern and fusion zone are often asymmetric, leading to a tendency to distortion. In certain welding modes, arc blow can result in process instability and spatter. More equipment is involved compared with shielded metal arc welding, and so it tends to be a bit less portable. GMAW is not suitable for single-pass joining of thick materials, and so multi-pass welds are often required resulting in high heat input and significant consumption of filler material. The transfer of filler material occurs over space and the loss of a droplet of material from the electrode dramatically changes arc characteristics, thus resulting in undesirable spatter formation. The gas requirement makes welding in windy environments difficult, unlike shielded metal arc welding, though welding in such conditions is feasible using the related FCAW process.

The information and data provided in Section 1.2.2 were compiled from a variety of sources, including O'Brien 1991, Nadzam 2006, and JFLAWF 2000.

1.2.3 Gas tungsten arc welding (GTAW)

The gas tungsten arc welding (GTAW) process is a method that joins metals by use of an arc that heats the metals to their melting point to create a melt

puddle or weld pool. The welding arc is a high-temperature, ionized column of gas (or plasma), producing temperatures normally ranging from 5000 to 30 000 K, that spans between a non-consumable tungsten electrode and the workpiece. The welder can add filler material to the molten weld puddle if required, manually or through a wire feeding system, or operate without added filler in the so-called autogenous mode. Gas, fed through the welding torch, serves as a medium for the formation of the arc and also shields the molten metal from atmospheric contamination. The arc is normally initiated with a brief high frequency alternating current to breakdown the shield gas, and is sustained by current (typically 50 to 400 A, though can be much higher or lower) provided by a welding power supply offering relatively low potential (typically 8 to 12 V). Direct current with electrode negative and workpiece positive is typically used, though use of electric positive or high-frequency alternating current, up to 50 000 cycles per second (typically less than 500 Hz), is common in aluminum welding to aid in breaking down the thermally stable aluminum oxide layer. Upon solidification of the melt puddle, the parts are permanently, metallurgically fused.

Equipment

Welding equipment comprises a variety of components necessary to generate the arc. The power supply provides the voltage and current (direct or alternating) necessary to sustain the arc. The current is fed through cables to the tungsten electrode, located in the welding torch. The other lead from the power supply must connect to the workpiece to complete the electrical circuit once the arc is established. Most metals are welded with the circuit connected as direct current electrode negative, sometimes referred to as direct polarity, in which electrons flow from the tungsten to strike the workpiece, and metal and gas ions travel from the workpiece to the electrode. In this case, approximately 70% of the generated heat is concentrated on the workpiece, leading to a more concentrated arc with deeper penetration enabling faster travel speeds than can be achieved with an electrode-positive configuration. Certain materials, like aluminum and magnesium, readily form an insulative, high melting point oxide layer in air that must be removed before welding. Alternating current circuits, typically square wave with varying percentage of time at the negative versus the positive portion of the cycle, are normally used with these materials because, during the electrode-positive portion of the cycle, the gas ions flowing to the workpiece serve to break up and chip away the oxide layer.

The welding torch, which may be water cooled, not only holds the tungsten electrode, but also feeds the shielding gas to provide adequate coverage for arc stabilization and process shielding. Various shield gases are used, though typically inert Argon or Helium are used, with the higher ionization energy

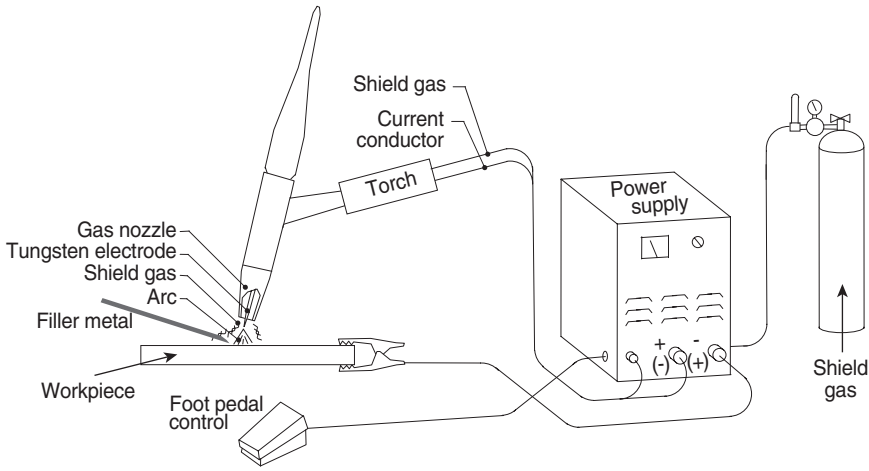

1.2 Schematic of a typical gas tungsten arc weld (GTAW) set up (not to scale).

of He leading to a more constricted and deeper penetrating arc. A schematic of a typical GTAW setup is shown in Fig. 1.2.

Advantages

With the GTAW process, it is possible to join more kinds of metals than GMAW and many other arc welding processes because the arc does not require use of a consumable electrode. Additionally, since wire feeders are not required, the process tends to be a bit more portable. In GTAW, the heat source and filler metal are controlled independently, thus simplifying the development of process parameters and enabling use of a broader range of filler materials. Pinpoint control of heat input enables the potential to produce narrow heat-affected zones, which can result in improved mechanical properties of the joint. Additional benefits of the high degree of heat source control include excellent control of penetration and low distortion, which makes the process good for joining of thin materials. With the GTAW process, it is possible to produce welds with no slag because no flux is required. The process produces an arc that is very stable relative to GMAW, with arc fluctuations resulting from expulsion of metal from the tip of the consumable electrode, and consequently there is significantly reduced potential for sparks or spatter. The GTAW process produces little smoke or fumes, unless caused by the materials or contamination, since no flux is employed. The GTAW process is generally considered quite clean, and a skilled welder can produce very high quality weld deposits.

Disadvantages

The GTAW process tends to offer relatively low filler metal deposition and low speeds compared with GMAW because the filler material is fed in cold and not automatically fed into the puddle. Unlike shielded metal arc or gas metal arc welding, the GTAW process required the welder to use both hands, and thus superior hand-eye coordination and operator skill is a necessity. The arc tends to be hotter than other arc welding processes, and so arc rays tend to be brighter and potentially more hazardous, and the ultraviolet emissions from the arc generate undesirable ozone and nitrous oxides. When GTAW is employed in an alternating current mode, such as typically used for aluminum welding, the process is quite noisy and distracting. Additionally, tungsten inclusions in the joint are possible. The GTAW process is generally not suitable for thick materials like GMAW because molten droplets from a consumable electrode are not forcefully ejected deep into the melt puddle. If high frequency arc starts are utilized, it is possible that the resultant high energy electromagnetic noise may be deleterious to electronic equipment nearby.

The information and data provided in Section 1.2.3 were compiled from a variety of sources, including O'Brien 1991, Nadzam 2006, and JFLAWF 2000.

1.3 Laser welding

1.3.1 Brief history of lasers and laser welding

Development of lasers

In the early 20th century, Albert Einstein changed the world as he strove to understand and develop theories to explain the nature of physical phenomena. In 1917, he introduced the concept of stimulated emission, which refers to the fact that a photon of light may produce another photon of light with the same phase, frequency, polarization, and direction of travel by perturbing an electron that is already in an excited energy state. The perturbing photon is not destroyed and, thus, the process can serve as a kind of optical amplification. This concept serves as the foundation for the subsequent development of the laser, an acronym for Light Amplification by Stimulated Emission of Radiation.

In 1958, a paper published by Arthur Schawlow and Charles Townes describes the potential to build devices to produce monochromatic and coherent light through stimulated emission in the ultraviolet, visible, and infrared wavelengths. This publication, and a subsequent patent filed in 1960, have cemented their status as the inventors of the laser. It was not until 1960, though, that Theodore Maiman built and demonstrated the first

working laser system based on a ruby crystal. Several other lasing media were investigated shortly thereafter, with the first fiber laser demonstrated by Elias Snitzer in 1961, and the first direct diode laser demonstrated by Robert Hall, Gunther Fenner, and co-workers in 1962. It was not until 1964 that the workhorse cutting and welding laser technologies prevalent today were invented: (i) the Nd:YAG laser, with emission of light energy at a wavelength of 1064 nm, was described by J. E. Geusic, H. M. Marcos, and L. G. Van Uitert, and (ii) the CO_2 laser, with emission at a wavelength of 10.6 μm, was described by C. K. N. Patel. The first available commercial Nd:YAG lasers were low power pulsed systems, and the first CO_2 lasers offered powers limited to 100 W. Today, Nd:YAG lasers are commercially available with continuous wave operation offering output power up to 8 kW, and CO_2 lasers are available off-the-shelf offering output power up to 20 kW, with research facilities hosting systems up to 150 kW.

Newer technology is raising the bar on capability across a variety of laser technologies. Direct diode lasers with fiber delivery are now commercially available at powers up to 10 kW, with wall-plug efficiencies reaching nearly 50%. The relatively poor beam quality generated with this technology yields a large spot and low irradiance (power per unit area, and sometimes mistakenly referred to as energy density), though this is usually sufficient and sometimes preferred for welding processes, particularly in cladding operations. Single-mode fiber lasers are now available that offer output power greater than 3 kW at 25% wall plug, and deliver high beam quality that can produce a very small spot with extremely high irradiance. The unique characteristics offered by the low cost and extreme energy density of these single-mode laser systems promise development of new welding techniques and applications in the coming years. Multi-mode fiber laser technology, which produce larger spot size and lower irradiance, can now achieve output powers to 50 kW at 25% wall plug efficiency in commercially available systems, again promising new applications for high speed and thick section welding.

Development of laser welding

Quite early during the development of laser technology, it was recognized that lasers could offer advantages in processing and joining of metals. The fact that the laser light energy is coherent enables it to be delivered to and focused onto a substrate using relatively inexpensive reflective or refractive optics. Depending on wavelength and focusing optic material, the light energy will be focused to a small spot on the substrate, resulting in high irradiance whose energy is readily absorbed by the substrate and converted to heat. If enough energy is provided to a particular spot, the metal substrate will heat up and melt, thus enabling fusion welding.

Throughout the 1960s, several studies of the applicability and use of lasers for welding were published (Dunlap and Williams 1962, MacNielle 1963, Bahun and Engquist 1964, Fairbanks and Adams 1964, Pfluger and Maas 1965, Miller and Ninnikhoven 1965, Anderson and Jackson 1965, Adams 1965, Smith and Thompson 1967, Epperson and Cohen 1968, Gagliano *et al*. 1969, Rykalin and Oglov 1969, to name a few). Owing to the relatively low laser power available at the time, much of the early work focused on joining of small components for the electronics industry. By the early 1970s, the advent of multi-kilowatt CO_2 lasers sparked interest from other industries, and several papers discussed deep-penetration and high-speed welding with CO_2 lasers offering output power to 20 kW (Locke *et al.* 1972, Baardsen *et al.* 1973, Locke and Hella 1974).

Since the CO_2 laser beam is of wavelength in the far infrared (10.6 μm), the laser beam energy must be transmitted to the workpiece with so called hard optics, i.e. mirrors and lenses. As a result, systems are complex and require high levels of maintenance to maintain proper cleanliness and alignment along the beam path. The shorter wavelength of the Nd:YAG laser, at 1064 nm and in the near-infrared regime, allow it to be transmitted by fiber optics, thus greatly simplifying the beam delivery aspects and easing integration into mechanized, semi-automated, or automated systems. Initially, Nd:YAG lasers were greatly limited in maximum available power, but, by the late 1980s, the availability of high power (>1 kW) continuous-wave Nd:YAG lasers spurred several welding studies (Yamada *et al.* 1987, Cieslak and Fuerschbach 1988, Hoult 1990a, Hoult 1990b). The promise of high-power laser welding through a fiber has encouraged continual efforts to produce systems capable of ever higher output powers, and recent publications discuss the characteristics of 8 and 10 kW Nd:YAG laser beam welding (Russell and Hilton 2001, Ishide *et al.* 2003, Nakabayashi *et al.* 2003, Greses *et al.* 2004).

Whereas multi-kilowatt CO_2 and Nd:YAG lasers have been commercially available for two decades or more, direct diode lasers suitable for welding processes have become available only more recently, and many researchers were involved in early welding studies (Sepold *et al.* 1997, McEuen 1998, Kugler *et al.* 1998, Marince *et al.* 1999). More recently, work has focused on the joining of thermoplastics and polymers, joining of thin materials, of laser cladding and deposition activities.

The first reference to fiber laser welding that could be located discusses the potential for early fiber lasers to aid in microwelding applications (Toenshoff *et al.* 1998, Hecht 1998), and follow up work beginning in 2002 continued to explore potential applications (Miyamoto *et al.* 2002, Park *et al.* 2003). Only as commercially available systems have become widely available has interest in single-mode fiber laser welding expanded. The first 1 kW single-mode fiber laser was introduced in 2004 and it was not until

late 2007 that a 3 kW single-mode system was released as a commercial product. As available power increases for these high brightness laser systems, new applications are being explored (Beyer *et al.* 2007). Additionally, fiber lasers have only recently been combined into multi-kilowatt, multimode systems. The first 1 kW multimode fiber laser was introduced in May 2002, a 10 kW was released in March 2003, and now up to 50 kW are available (Shiner 2004). Recently published welding results show great promise for joining of thick sections and high-speed welding of thin section (Vollertsen and Thomy 2005, Shiner 2005).

The history and data provided in Section 1.3.1 were compiled from a variety of sources, including Steen 2003, Duley 1999, Migliore 1996, and other publications referenced throughout.

1.3.2 Lasers and laser welding

Laser light is actually a coherent form of electromagnetic radiation propagating through space with a discrete wavelength. As is well known, light exhibits properties of both discrete particles and of waves. For the purpose of describing the interaction of a laser beam with materials, it can be thought of as an oscillating electric field vector and its associated magnetic field vector. When the oscillating electric field interacts with the elastically bound electrons in a substrate material, the electrons are set in motion in the form of an induced vibration. For opaque materials, some of the incident energy is reflected and some is absorbed into the material, the proportion of which depends on material, wavelength, substrate temperature, surface films, angle of incidence, and surface roughness. Electrons that are free to oscillate and re-radiate without disturbing the atomic structure, such as those contained in the free electron gas present in metals, result in reflection of the incident radiation. As other electrons try to vibrate, especially those bound to specific atoms, however, they are constrained by the material lattice structure, and the vibrational energy is transmitted through the substrate. This induced vibration is observed as heat.

If enough energy is supplied to the substrate through this mechanism to effectively eliminate mechanical strength in the material bonds, the result is melting of the substrate. While metals are typically quite reflective to infrared laser beam energy when in their solid state (>90% reflectivity is typical), the additional atomic disorder when the material melts decreases reflectivity significantly (~50% reflectivity is typical). If the molten zone is used to melt a common region between two components, and the heat source is subsequently removed so that the molten zone can cool, solidify, and fuse the components together, then the process can be referred to as welding. If the heat provided by the laser beam is controlled to only allow melting while limiting evaporation, then the process is often referred to as

conduction mode welding. This can be achieved by balancing the heat provided to the substrate by the laser with heat conducted away from the region through the substrate, or by moving the laser beam spot relative to the substrate so as to limit the total amount of energy deposited by the incident beam in a single spot. Typically, this is achieved by operating the beam out of focus, so the irradiance is relatively low.

When the laser beam interaction with the substrate is of sufficiently high irradiance, the bonds between the atoms themselves can be broken, thus resulting in vaporization. If intensity is higher still, then electrons from the vaporized metal atoms and from gases in the interaction zone can be removed from the atoms, resulting in ionized gas and plasma. This high-temperature vapour and plasma will tend to expand, resulting in a recoil force that pushes on the surrounding molten material, thus balancing the forces on the molten material and leading to formation of a cavity or keyhole. Welding in this mode is often referred to as the keyhole welding, and it typically occurs when laser irradiance is in the order of 10^6 W cm^{-2}. When irradiance is even higher, say at $>10^7$ W cm^{-2}, the process often results in excessive spatter: at such irradiance, melting occurs within a microsecond. The keyhole typically will contain both evaporated substrate and ionized gas or plasma. It is maintained through a balance of the recoil force with vapor pressure, surface tension, and hydrostatic forces caused by friction effects from the moving vapor acting on the surface of the molten liquid. Once a keyhole is formed, penetration will increase dramatically compared with conduction mode welding, as the beam energy has additional opportunities for absorption to the substrate material through multiple reflections in the keyhole and through Fresnel absorption. The vapor and plasma in the keyhole is at extremely high temperatures, ~2000 K for Nd:YAG and ~6000–10 000 K for CO_2 welding (Greses 2001), and gains additional energy through absorption through the inverse bremsstrahlung effect and reradiation to the substrate through blackbody effects. This plasma can serve to absorb, scatter, and defocus the laser beam, especially in the case of long wavelength CO_2 welding, and can thus limit penetration. Consequently, shield gases with high ionization potential, such as He, can be selected to limit this absorption. Additionally, high velocity gas jets are often used to redirect the escaping plasma out of the path of the laser beam. The superheated plasma is also known to reradiate heat back to the surface of the substrate enough to effect the fusion zone profile to contribute to the so called nail head effect.

Historically, the literature has drawn a sharp distinction between these two modes, though in reality there exists a continuum between conduction and keyhole mode welding (Martukanitz 2005). Owing to the varying physical processes occurring at the two ends of this continuum, it is a convenient distinction, as illustrated in Fig. 1.3, and it is often observed that conduction

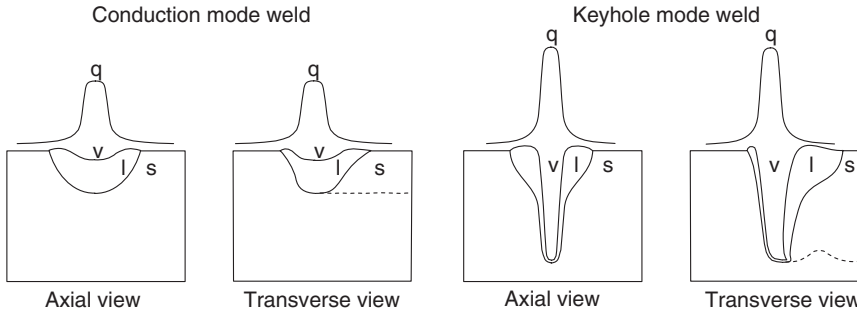

1.3 Illustration of conduction mode and keyhole mode weld definitions.

mode welding tends to be a more stable process, as without a keyhole the weld is less susceptible to gas entrapment and formation of porosity. With the keyhole mode process, instabilities in the flow of molten metal within the keyhole can result in creation of vapor bubbles at the root of the keyhole through keyhole collapse, which can be trapped during solidification resulting in fusion zone porosity. In some cases, higher heat processes will maintain a molten puddle long enough for bubbles formed through keyhole stability, or through volatilization of alloy elements or surface contaminants, to migrate to the surface of the molten puddle and escape to the atmosphere.

As the energy used for welding is contained in such a limited area during laser keyhole welding, the surrounding material is not appreciably heated and cooling rates are much higher than with conventional arc welding processes owing to higher travel speeds. A benefit of this efficient energy use is a limiting of the size of the heat-affected zone and a sharp decrease in the generation of residual plastic strains. Consequently, laser welds tend to result in significantly less distortion than found when employing conventional welding processes. However, this fast cooling rate can be accompanied by formation of cracks along the weld centerline, as contamination and alloying additions are pushed along the solidification front to the center of the weld puddle. Additionally, undesirable microstructures that are brittle and exhibit limited ductility are often formed as a result of the rapid cooling rates.

Equipment

Laser beam welding comprises a variety of components and considerations necessary to consistently perform high-quality lasers welds. These can be

broadly broken into two categories: (i) laser, beam, and optics, and (ii) process gases and ancillary process equipment/considerations.

Laser, beam, and optics

There are several types of lasers utilized for laser beam welding. As previously mentioned, historically CO_2 lasers operating at a far-infrared 10.6 μm wavelength and Nd:YAG lasers operating at a near-infrared 1064 nm wavelength have been the workhorses for laser welding. More recently, fiber lasers and direct diode lasers have entered the arena, both operating at near-infrared wavelengths. Laser beams at far-infrared wavelengths tend to be less well absorbed in metals than near-infrared laser beams, though, once the keyhole is formed, absorption increases dramatically in both cases. Owing to the longer wavelength, CO_2 laser beams cannot be delivered through fiber optics and must therefore be delivered by reflective mirrors which are often water cooled. All the other lasers mentioned above can be delivered by a fiber. The ability to deliver laser beam energy through a fiber simplifies the integration of lasers into mechanized and automated welding systems. Additionally, the longer wavelength of the CO_2 laser beam is absorbed more readily in the welding plasma and, thus, use of gases and nozzles for plasma suppression is a necessity for deep penetration. All lasers mentioned above can be operated in a continuous wave (CW) mode or in a pulsed mode. Pulsed welding is sometimes utilized to reduce capital costs, since the pulsed lasers have been shown capable of welding deeper and faster than CW lasers operating at the same average power. Additionally, various researchers have shown that clever manipulation of the pulse parameters can help reduce formation of porosity owing to increasing the stability of the keyhole, through techniques such as tying the pulse rate of the laser beam power to the oscillation frequency of the melt puddle.

The optics required to deliver the beam to the focusing optics, including the fiber, all affect the ability to produce a sufficiently small spot to reach the required irradiance of ~10^6 W cm^{-2}. With CO_2 lasers, larger reflective optics are sometimes used to help with heat management and to compensate for beam divergence that occurs as the beam is reflected from mirror to mirror through space to the focusing optics. With fiber delivered beams, the fiber diameter has a direct correspondence to the minimum possible spot size such that the spot diameter can never be less than the fiber diameter. Until recently, 600 μm diameter fibers were typical for delivery of high power Nd:YAG laser beams, though recent developments in technology now permit delivery of high-power fiber and Nd:YAG lasers being delivered through fibers with diameter as small as 100 μm. Single mode fiber lasers of up to 3 kW power now exist that can transmit the laser

through a fiber with a much smaller diameter, and are capable of producing spot size with ~10 μm diameter. When a larger spot size is acceptable, then the focal length can be increased to provide additional separation of the optics from the processing zone, thus limiting potential damage to optics from spatter and other process emissions. Fibers can be step index or gradient index, impacting the outgoing beam quality and the ability to focus the beam.

Once the beam is delivered to the desired weld location, focusing optics must be used to collimate and focus the beam to the desired shape and size. Transmissive optics are typically used for near-infrared laser beams and far-infrared laser beams up to about 5 kW, and water-cooled reflective optics are used for higher power far-infrared laser beams. In both cases, it is customary to apply anti-reflective (AR) coatings to increase the transmission efficiency of the optic. Simple spherical lenses based on purely geometrical optic laws can be utilized for focusing the laser beam, though more complex lens combinations are normally utilized to compensate for spherical aberrations. At high power levels, water cooling is employed to limit any thermally induced distortion that could impact the characteristics of the focused beam. The complexity of these focusing lens assemblies can lead to high cost, so, in most cases, to prevent damage, a relatively inexpensive and disposable cover lens is placed between the welding area and the focus optics, typically in an easily removable lens cartridge. Damage can be caused by spatter or fumes from the welding process that coat the optic, thus creating a hot spot as the laser is absorbed that will eventually lead to fracture of the lens. Several companies now offer cover lens monitoring systems that observe any scattered light from spatter or other deposits on the cover lens, and notify the operator when the cover lens should be changed. Damage can also occur owing to so-called back reflection of the laser off the substrate back into the focusing optics, which can result in thermal excursion that can damage the fiber or even the laser. As such, the head is often positioned 5 degrees off of normal, so that the bulk of reflected energy does not proceed directly back into the focusing head.

Several variations on the standard focusing optics can be integrated for different applications. Sensors and imaging equipment can be incorporate into the optics train through use of selectively reflecting mirrors. These can be used for scientific exploration as well as process monitoring and control, thermal sensing, and even for seam tracking. High-speed scanning optics can manipulate the beam over a large area very rapidly, without the need to move high-inertia robotic or positioners. Typical uses include spot welding in the automotive industry. Other optics can be used to create twin spots, either longitudinal or transverse to the welding direction, in an attempt to help stabilize the weld keyhole. The beam can also be rotated or oscillated rapidly to help stabilize the welding process (Martukanitz 2005).

Process gases and ancillary process equipment/considerations

Various process gases are utilized during laser welding to mitigate several potential problems in the process. As mentioned previously, with CO_2 laser beam welding the beam is strongly absorbed in the plasma emitted from the keyhole. As such, gases with high ionization potential, such as He, are often used for plasma suppression. The gas can be fed coaxially, though it is often fed from the side of the interaction zone at high velocity so that the emitted plasma is actually blown out of the way of the beam path. This also serves to help deflect process emissions and spatter that could result in lens damage. However, especially when welding with high brightness lasers that are prone to generation of spatter, additional gas may be required for lens protection, and sometimes high flow rate air knives are used for the purpose. Finally, depending on the material, additional process shielding gas can be used to help prevent oxidation of the substrate at high temperatures. A sketch of a laser welding head with multiple gas assist is shown in Fig. 1.4.

The focal spot is typically located on the top surface of the substrate, though sometimes it is positioned a few millimeters below the surface leading to deeper penetration when welding of thick sections. The beam waist, which describes the length at which the beam is nominally in focus and irradiance is relatively constant, will increase when focal length is increased, and will also affect the welding process.

The travel speed and power are selected to achieve the desired penetration while maintaining a robust keyhole and sufficient weld quality. These

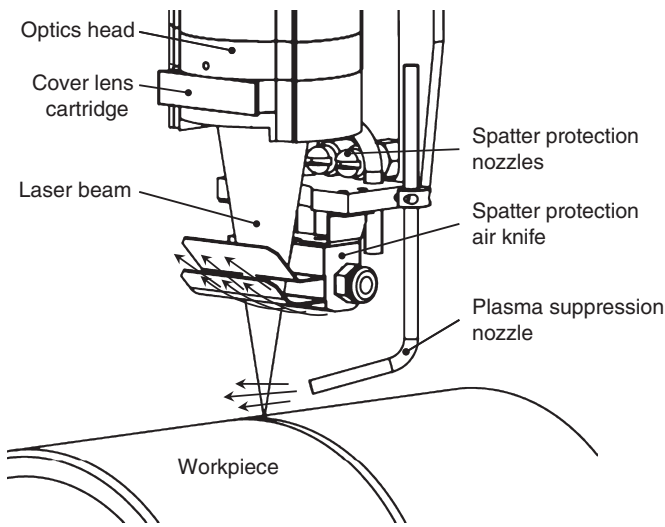

1.4 Sketch of a laser welding head with multiple gas assist.

are affected by all the aforementioned process variables, and are also strongly affected by material properties, especially thermal diffusivity. The material also affects the mechanical properties of the fusion zone, and sometimes filler material can be added to the melt puddle to compensate for any volatilized alloying elements. In butt joints, gaps in the joint can permit the laser beam to traverse through without being absorbed and converted to heat, so filler material is often used to compensate for gaps. Filler material is also used to compensate for gaps in lap joints, in which case the gap can lead to undercut.

In addition to safety considerations typical of conventional arc welding techniques, laser welding presents additional hazards. When feasible, the weld process is entirely enclosed within an interlocked, light-tight enclosure. This is especially true with near-infrared laser beams, which are focused by the human eye and are thus especially hazardous.

Only the most basic aspects of laser light and its interaction with materials that are deemed particularly germane to the overall topic of the book have been discussed herein. Many of the referenced texts serve as excellent sources of additional detail.

Advantages

The laser welding process offers many potential advantages over conventional arc welding technologies. The ability to perform deep penetration welds with keyhole mode makes it possible to weld extremely thick substrates with a single weld pass, thus presenting fewer opportunities for defects. The ability to weld thick sections in a single pass can also have a substantial impact on the amount of required consumables and subsequent reduction in hazardous emissions. The precisely controlled beam energy enables low heat input that can result in significantly reduced distortion. Low heat can also lead to improved metallurgical microstructures in the heat-affected zone and sometimes in the fusion zone, which can result in improvement to mechanical properties of direct interest to designers, such as fatigue and formability. The precisely controlled heat and keyhole weld mode can also lead to welding at speeds which are impossible with arc processes (up to 10 m min^{-1}). The non-contact nature of the laser energy as a heat source has led to the use of scanning systems that can move the welding heat source through space much more rapidly than would be possible with physical manipulation of welding torches.

Disadvantages

Lasers of high power, and their associated optics, currently require a significantly higher capital investment than conventional arc welding equip-

ment. Until recently, the low energy efficiency (1–2% in the case of lamp-pumped Nd:YAG lasers) could be considered a disadvantage of the technology, though now fiber lasers and direct diode lasers offer up to 30% wall plug efficiency, or higher, and eliminate this as a significant disadvantage of the technology. Joint fit up, and therefore fixturing, is critical and gap must be limited or filler material must be added to ensure adequate fusion. Fast cooling rates associated with high-speed laser welding can lead to centreline cracking, hot cracking, liquation cracking, or formation of brittle and non-ductile solidification microstructures. Increased safety concerns, especially with eye safety of Nd:YAG, fiber lasers, and direct diode lasers, leads to added implementation complexity and cost. The safety issues also make it difficult to utilize laser welding technology in portable or manual operations. Spatter can occur at high irradiance levels, and can damage costly optics.

The information and data provided in Section 1.3.1 were compiled from a variety of sources, including Steen 2003, Duley 1999, Migliore 1996, Ready and Farson 2001, and other publications referenced throughout.

1.4 Acknowledgments

The author would like to thank Dr Richard P. Martukanitz and Stephen W. Brown for their contributions and helpful advice.

1.5 References

ADAMS JR C M (1965), 'Laser welding', *American Society of Tool and Manufacturing Engineers – Technical Papers*, SP65-99, 14 pp.

ANDERSON J E, JACKSON J E (1965), 'Theory and application of pulsed laser welding', *Welding Journal*, **44**(12), 1018–1026.

ANON (1961), *Welding and the World of Metals*, Memco News, MILLER Electric Manufacturing Co., June 1961, 31 pp.

BAARDSEN E L, SCHMATZ D J, BISARO R E (1973), 'High speed welding of sheet steel with a CO_2 laser', *Welding Journal*, **52**(4), 227–229.

BAHUN C J, ENGQUIST R D (1964), 'Metallurgical applications of lasers', *Metals Engineering Quarterly*, **4**(1), 27–35.

BEYER E, PFOHL P, HERWIG P, IMHOFF R (2007), 'Welding and cutting of copper with high brightness lasers', *Proceedings of the International Congress on Lasers and Electro-Optics (ICALEO 2007)*, 98–101.

CIESLAK M J, FUERSCHBACH P W (1988), 'On the weldability, composition, and hardness of pulsed and continuous Nd:YAG laser welds in aluminum alloys 6061, 5456, and 5086', *Metallurgical Transactions B*, 19B, 319–329.

COHEN M I, EPPERSON J P (1968), 'Application of lasers to microelectronic fabrication', *Advances in Electronics and Electron Physics*, SUPPL 4, 139–186.

DODDS J, HANSON K I, ZAMPOGNA M J (1997), *1995 Annual Survey of Manufactures*, US Department of Commerce, Bureau of the Census, M95(AS)–1, 71 pp.

DULEY W W (1999), *Laser Welding*, USA, Published by John Wiley & Sons, Inc., A Wiley – Interscience Publication.

DUNLAP G W, WILLIAMS D L (1964), 'High-power laser for welding applications', *Proceedings of the National Electronics Conference*, **18**(1551), 601–606.

FAIRBANKS SR, R H, ADAMS JR C M (1964), 'Laser beam fusion welding', *Welding Journal*, **43**(3), 97s–102s.

GAGLIANO F P, LUMLEY R M, WATKINS L S (1969), 'Lasers in Industry', *Proceedings of the IEEE*, **57**(2), 114–147.

GEUSIC J E, MARCOS H M, VAN UITERT L G (1964), 'Laser oscillations in Nd-doped yttrium aluminum, yttrium gallium and gadolinium garnets', *Physical Review Letters*, **4**(10), 182–184.

GRESES J, HILTON P A, BARLOW C Y, STEEN W M (2001), 'Spectroscopic studies of plume/plasma in different gas environments', *Proceedings of the International Congress on Lasers and Electro-Optics (ICALEO 2001)*, 10 pp.

GRESES J, HILTON P A, BARLOW C Y, STEEN W M (2004), 'Plume attenuation under high power Nd:yttrium-aluminium-garnet laser welding', *Journal of Laser Applications*, **16**(1), 9–15.

HALL R N, FENNER G E, KINGSLEY J D, SOLTYS T J, CARLSON R O (1962), 'Coherent light emission from GaAs junctions', *Physical Review Letters*, **9**(9), 366–368.

HECHT J (1998), 'Fiber lasers prove versatile', *Laser Focus World*, **34**(7), 4 pp.

HOULT A P (1990), 'Welding with supra kilowatt solid state lasers', *Proceedings of the SPIE High-Power Solid State Laser and Applications Conference*, **1277**, 209–216.

ISHIDE T, TSUBOTA S, NAYAMA M, SHIMOKUSU Y, NAGASHIMA T, OKIMURA K (2000), '10 kW class YAG laser application for heavy components', *Proceedings of IEEE – High Power Lasers in Manufacturing*, **3888**, 543–550.

JFLAWF (2000), *The Procedure Handbook of Arc Welding – 14th ed.*, Cleveland, OH, Published by The James F. Lincoln Arc Welding Foundation.

LOCKE E V, HELLA R A, 'Metal processing with a high-power CO_2 laser', *IEEE Journal of Quantum Electronics*, **QE-10**(2), 179–185.

LOCKE E, HOAG E, HELLA R (1972), 'Deep penetration welding with high power CO_2 lasers', *IEEE Journal of Quantum Electronics*, **QE-8**(2 pt 2), 132–135.

MACNEILLE S M (1963), 'Laser beam welding – how good is it', *Tool and Manufacturing* Engineer, **50**(6), 59–63.

MAIMAN T H (1960), 'Stimulated Optical Radiation in Ruby', *Nature*, **187**(4736), 493–494.

MARINCE M E, MARTUKANITZ R P, HAAKE J M, COOK C M (1999), 'Investigation of a direct diode laser for manufacturing applications (welding, hardening, surfacing, etc.)', *Proceedings of the International Congress on Lasers and Electro-Optics (ICALEO 1999),* A207–A216.

MARTUKANITZ, R P, 'A critical review of laser beam welding', *Proceedings of SPIE – The International Society for Optical Engineering*, **5706**, Critical Review: Industrial Lasers and Applications, 2005, p. 11–24.

MCEUEN K (1998), 'Direct use of diode lasers: an overview', *Proceedings of the SPIE Laser Diodes and Applications III*, **3415**, 72–78.

MIGLIORE L, ed. (1996), *Laser Materials Processing*, New York, Marcel Dekker, Inc.

MILLER C, CRAWFORD M H (2002), *Welding Related Expenditures, Investments, and Productivity Measurement in U.S. Manufacturing, Construction, and Mining Operations*, May 200, 90 pp.

MILLER K J, NINNIKHOVEN J D (1965), 'Laser welding', *Machine Design*, **37**(18), 120–125.

MIYAMOTO I, PARK S J, OOIE T (2003), 'Precision microwelding of thin metal foil with single-mode fibre laser', *Proceedings of the SPIE 4th Intenational Symposium on Laser Precision Microfabrication*, **5063**, 297–302.

NADZAM J, ed. (2006), *GMAW Welding Guide: Gas Metal Arc Welding, Carbon, Low Alloy, and Stainless Steel and Aluminum, Gas Metal Arc Welding Guidelines*, Cleveland, OH, Published by Lincoln Electric, 96 pp.

NAKABAYASHI T, WANI F, HAYAKAWA A, SUZUKI S, YASUDA K (2003), 'Thick plate welding with Nd:YAG laser and COIL', *Proceedings of the SPIE 1st International Symposium on High-Power Laser Macroprocessing*, **4831**, 416–421.

O'BRIEN R L, ed. (1991), *Welding Handbook, Volume 2. Welding Processes – 8th ed.*, Miami, FL, Published by the American Welding Society, pp. 74–109, pp. 110–155.

PARK S J, OHMURA E, MIYAMOTO I (2002), 'Micro welding of ultra thin metal foil using Yb-fiber laser', *Proceedings of the SPIE 3rd International Symposium on Laser Precision Microfabrication*, **4830**, 52–56.

PATEL C K N (1964), 'Continuous-wave laser action on vibrational–rotational transitions of CO_2', *Physical Review*, **136**(5A), A1187–A1193.

PFLUGER A R, MAAS P M (1965), 'Laser beam welding electronic-components leads', *Welding Journal*, **44**(6), 264s–269s.

READY J F, FARSON D F, eds. (2001), *LIA Handbook of Laser Materials Processing*, USA, Published by the Laser Institute of America.

RUSSELL J D, HILTON P A (2001), 'The development of a 10 kW Nd:YAG laser facility', *Proceedings of the 7th International Aachen Welding Conference*, (1), 299–310.

SCHAWLOW A L, TOWNES C H (1958), 'Infrared and optical masers', *Physical Review*, **112**, 1940–1949.

SCHAWLOW A L, TOWNES C H (1960), 'Masers and maser communication system', US Patent No. 2,929,922.

SHINER B (2004), 'Fiber Frenzy', *Industrial Laser Solutions*, **19**(6), 4 pp.

SHINER, B (2005), 'Materials progress: fiber laser enables 50% faster pipeline welding', *Advanced Materials and Processes*, **163**(6), 28.

SMITH J F, THOMPSON A (1967), 'Metalworking lasers in engineering service applications', *Proceedings of the IEEE 9th Annual Symposium on Electron, Ion, and Laser Beam Technology*, Berkeley, CA, 268–277.

SNITZER E (1961), 'Optical maser action of Nd^{+3} in a barium crown glass', *Physical Review Letters*, **7**(12), 444–446.

STEEN W M (2003), *Laser Material Processing – 3rd ed.*, London, Published by Springer-Verlag London Limited.

VOLLERTSEN F, THOMY C (2005), 'Welding with fiber lasers from 200 to 17000 W', *Proceedings of the International Congress on Lasers and Electro-Optics (ICALEO 2005)*, 254–263.

YAMADA T, YOSHIDA S, ISHIDA S, FUJIMORI Y, ISHIKAWA K (1987), 'Continuously pumped 1-kW Nd:YAG laser and applications', *Proceedings of the Conference on Lasers and Electro-Optics*, 190–191.

2

Fundamentals of hybrid laser–arc welding

S. KATAYAMA, Osaka University, Japan

Abstract: The fundamental behavior of hybrid laser–arc welding, including arc plasma characteristics, laser-induced plume behavior, and the interaction of a laser beam with its induced plume, arc plasma and droplet transfer is discussed. Melt flows, keyhole behavior, and bubbles generation in the molten pool leading to the porosity formation in the weld fusion zones are then described.

Key words: induced plasma, hybrid welding, droplet transfer, laser–arc welding, keyhole behavior, porosity.

2.1 Introduction

Hybrid laser–arc welding is noted as a promising joining process since it can compensate for the drawbacks or weaknesses in laser welding and arc welding by utilizing both features. Laser welding has gained great popularity as promising joining technology with high quality, high precision, high performance, high speed, good flexibility and low deformation or distortion, in addition to the recognition of easy and wide applications owing to congeniality with a robot, reduced man-power, full automation, systematization, production lines, etc.[1] Applications of laser welding are increasing. The defects or drawbacks of lasers and their welding are high costs of laser apparatuses, difficult melting of highly reflective or highly thermal-conductive metals, small gap tolerance, and easy formation of welding defects such as porosity in deeply penetrated weld fusion zones. Arc welding is most widely used in joining applications because the machines are cheap and easy in operation, and the welding processes are highly stable and effective. The drawbacks are shallow penetration of weld beads in most cases, slower welding speeds, easier formation of humping weld beads at high speed welding, etc. On the other hand, hybrid welding with CO_2, YAG, diode, disk, or fiber laser and TIG, MIG, MAG, plasma or another arc heat source has been receiving considerable attention because it can achieve many advantages such as deeper penetration, higher welding speeds, wider gap tolerance, better weld bead surface appearance and reduced welding defects leading to a smaller amount of porosity in addition to complements of the drawbacks of both individual processes.[1–15]

In this chapter, therefore, to understand the fundamentals of hybrid laser–arc welding and to properly utilize the hybrid welding process on the basis of better understanding of its phenomena, arc plasma characteristics, laser-induced plume behaviour, the interaction between a laser beam or its induced plume and arc plasma, droplet transfer, melt flows, keyhole behaviour, and bubbles generation in the molten pool leading to the porosity formation in the weld fusion zones will be described and discussed in detail.

2.2 Plasma characteristics including interaction between laser beam and arc

In hybrid laser–arc welding, understanding of physical phenomena is important since all states of solid, liquid, vapor and plasma exist in a small space. Hybrid laser-TIG arc and laser-MIG arc welding situations are schematically shown in Fig. 2.1 (a) and (b).[14,15] (In this chapter, for example, when a YAG laser optics head or TIG torch is a leading heat source, hybrid YAG laser–TIG or TIG–YAG laser welding is used depending upon the heat source arrangement.) A keyhole is generally formed in the molten pool with the laser beam of high power density, and simultaneously a plume (light emission), vapors, ultrafine particles or fume and spatters are formed in the space. TIG arc plasma, and MIG arc plasma and droplets from a MIG wire also exist above the molten pool in respective welding processes.

Spectroscopic measurement was performed as indicated in Fig. 2.2 (a) and (b), and the analysis results of light-emitted parts at a height of about 1 mm above the surface of the pool during TIG, YAG laser and hybrid welding are shown in Fig. 2.2 (c), (d) and (e),[16] respectively. Emissions from neutral argon (Ar) atoms and Ar plasma and from neutral metallic atoms are chiefly observed during TIG and YAG laser welding, respectively. In

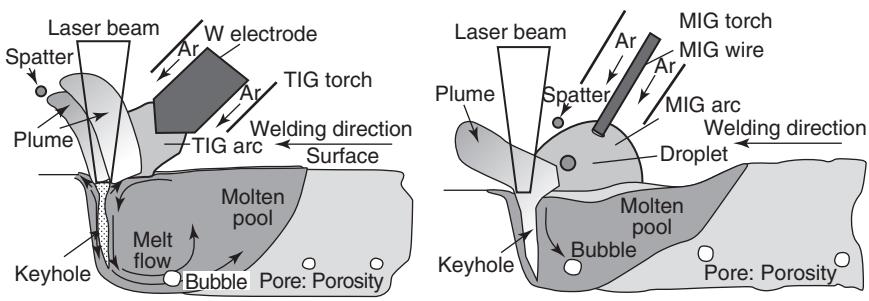

2.1 Schematic representation of hybrid laser–TIG (a) and laser–MIG welding.

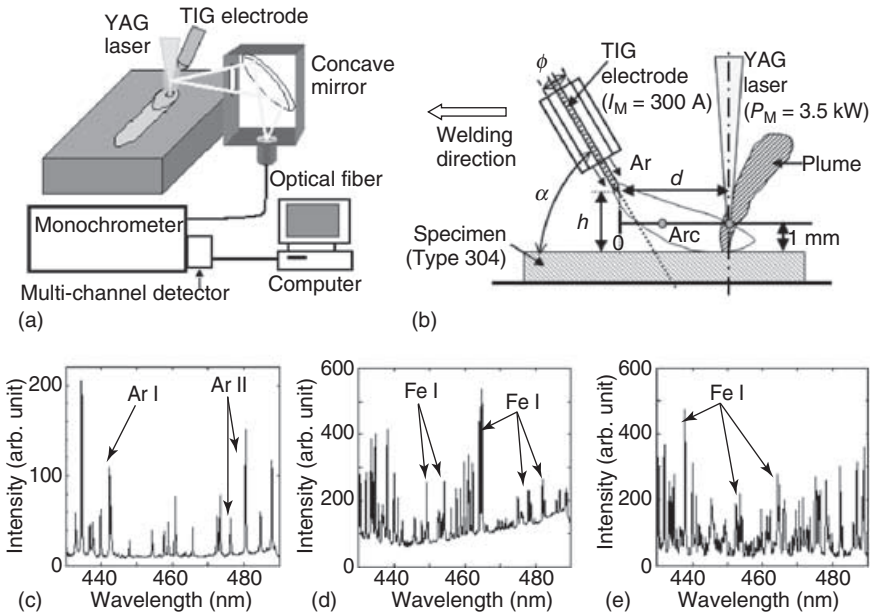

2.2 Schematic arrangement for spectroscopic analyses of plume and/or plasma formed during welding, measurement locations and results during TIG, YAG laser and hybrid TIG–YAG laser welding.

hybrid welding, the emission of neutral metallic atoms, which is dominant above the keyhole inlet, is brighter than in laser welding. The emission of plume light with shorter wavelengths increases in hybrid welding. It means that the plume temperature is higher in hybrid welding than in laser welding. The plasma emission intensity increases with an increase in arc current.

High-speed video observation and arc current or voltage measurement are performed to determine the behavior of arc plasma and a laser-induced plume and their interaction with a laser beam. Figure 2.3 (a) and (b) show arc plasmas during TIG welding and hybrid TIG-YAG laser welding (when the TIG torch is leading) with the inclined laser beam, and the measurement results of arc voltages during both processes are indicated in Fig. 2.4.[16,17] An increase in arc voltage is noted during hybrid welding, and the amount of this increase is in direct proportion to the YAG laser power. The plume, which evolves toward the incident laser beam, affects the phenomenon that the arc column becomes brighter and longer, leading to an increase in the arc voltage in this hybrid welding.[16,17] In the case of a hybrid CO_2 laser and pulsed MAG welding, the arc approaches a laser-induced plume at low voltages but covers the molten pool just below the wire at high voltages,[18,19] as shown in Fig. 2.5.[19] It is often seen that a laser-induced plume acts as an

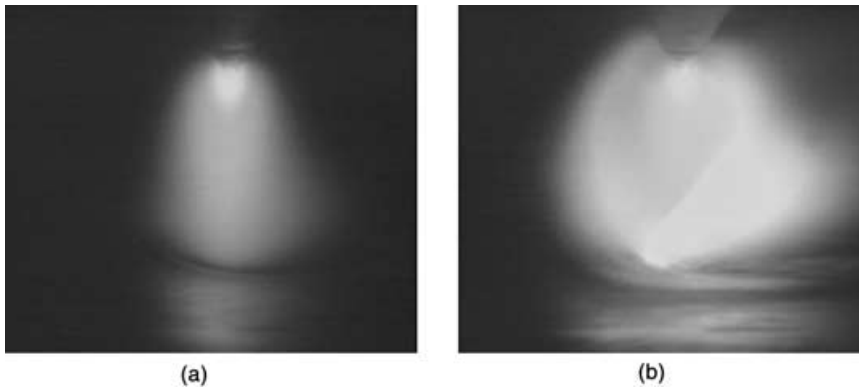

2.3 Observation results of arc behaviour of Type 304 steel during (a) TIG and (b) hybrid TIG–YAG laser welding.

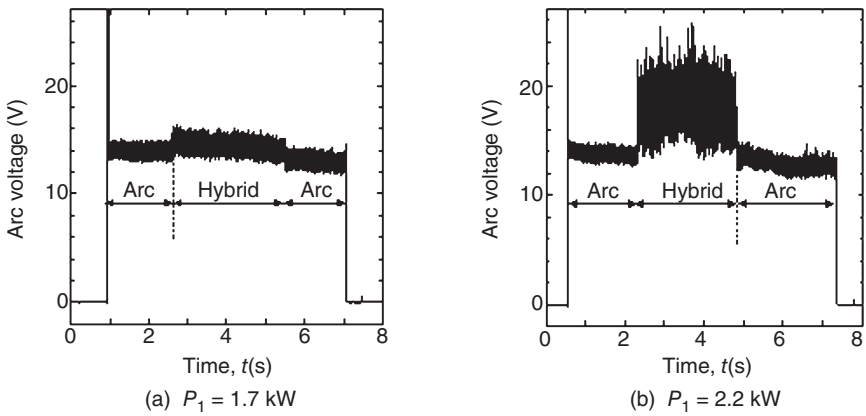

2.4 Voltage variation during TIG welding and hybrid welding.

arc current path between the electrode or wire and the plate when the laser beam and the heat source are close together. The interaction between the arc and the laser-induced plume generally depends upon the type of laser and a shielding gas, the arc current, the distance between an electrode and a plate, the distance between a laser-irradiation spot and an electrode target on the plate, and the inclination of the electrode.

Vapors and a plume (light emission) of evaporated metallic elements are formed during laser welding and, in CO_2 laser welding with Ar shielding gas, the gas plasma is also formed. The situations and phenomena of laser welding mainly depend upon the type or wavelength of lasers, shielding gas and welding conditions, as schematically shown in Fig. 2.6.[1] In particular, in

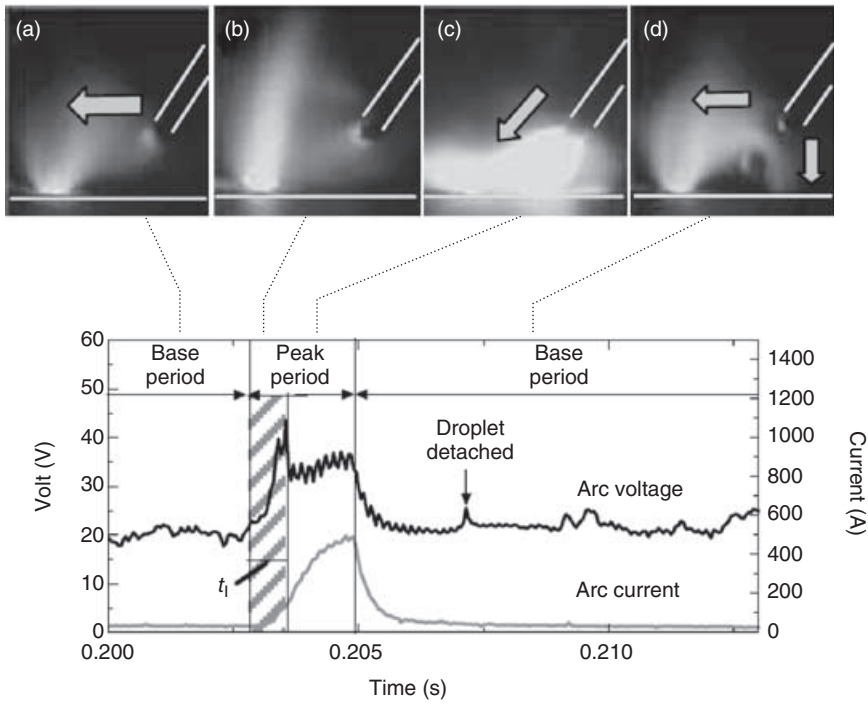

2.5 Variation in arc voltage and current and high speed images during transition of base to peak periods in hybrid welding. Pulse frequency: 50 Hz, leading arc, DLA: 3 mm, $v = 2$m min^{-1}.

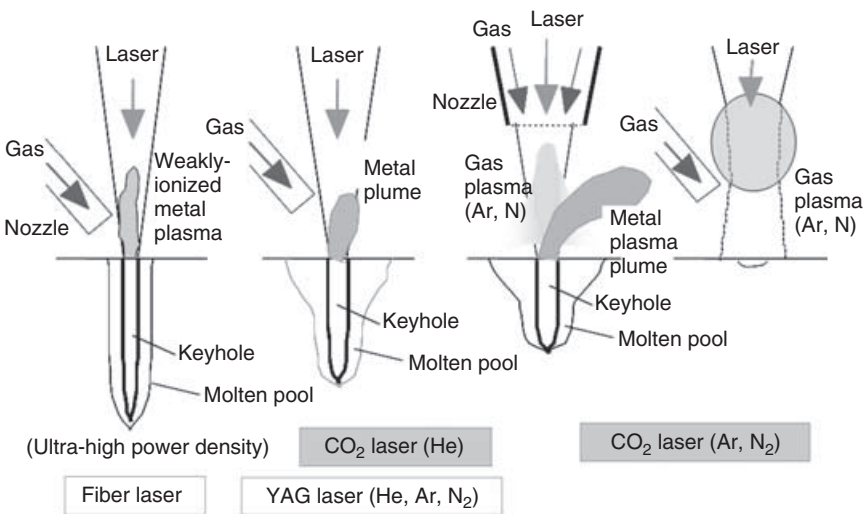

2.6 Schematic representation of plume, plasma and keyhole behavior during fiber, YAG and CO_2 laser welding, showing effect of plasma on energy transfer and consequent weld penetration.

the case of laser and hybrid welding with high power CO_2 lasers, a helium (He) shielding gas or a mixed gas with a high He content is recommended instead of the use of Ar shielding gas because Ar plasma absorbs incident laser energy and/or acts to defocus the laser beam.[7,18–22] The interaction of a laser beam to a laser-induced plume was visually investigated using a probe fiber, argon ion or diode laser.[23,24] The results suggest that the absorption (or attenuation) of laser energy at the wavelengths of less than 1.1 μm is caused by Rayleigh scattering.[23,24] Moreover, the refraction or deflection angles of the probe fiber laser are approximately 0.6 and 2.5 mrad on average and at the maximum, respectively.[23–25] It is concluded that the attenuation of laser energy and the refraction or deflection of a laser beam only to a laser-induced plume or ultrafine particles are small if the plume is normally depressed to a small size for cases using YAG, disk, or fiber lasers of about 1 μm wavelength.[23–25]

The reflected laser beams during YAG laser welding and hybrid TIG–YAG laser welding were observed together with the behavior of the laser-induced plume. Examples of the results, shown in Fig. 2.7,[16,26] indicate that the brightness and shape of the reflected beams are almost the same during laser welding and during hybrid welding. It is therefore concluded that the effects of the plume and arc plasma on the shielding of incident laser beams are small in hybrid welding with lasers of about 1 μm wavelength. The interaction between a laser beam and an Ar plasma or a

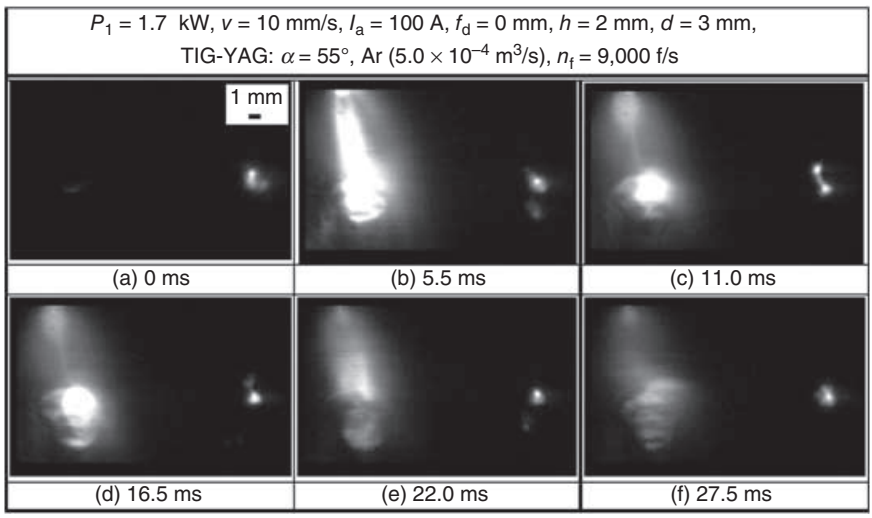
P_1 = 1.7 kW, v = 10 mm/s, I_a = 100 A, f_d = 0 mm, h = 2 mm, d = 3 mm,
TIG-YAG: α = 55°, Ar (5.0×10^{-4} m^3/s), n_f = 9,000 f/s
1 mm
(a) 0 ms
(b) 5.5 ms
(c) 11.0 ms
(d) 16.5 ms
(e) 22.0 ms
(f) 27.5 ms

2.7 Simultaneous observation results of TIG arc and reflected laser beam during hybrid TIG–YAG laser welding of Type 304 steel.

laser-induced plume exists,[23–25] but the small effect may be attributed to the short distance between the interaction area and the plate surface. In other words, the effect of the refraction or deflection can be minimized by such a localized high-temperature field.

2.3 Dynamic behavior

The behavior of an arc and laser-induced plume has been observed by high-speed video cameras without or through filters of given wavelengths during hybrid welding. Photographs taken from the upper side location or from the upper back location during hybrid TIG–YAG laser welding (TIG torch: leading) are shown in Fig. 2.8.[16] The arc is sometimes concentrated around the keyhole inlet near the TIG electrode,[16,26–28] from which a bright

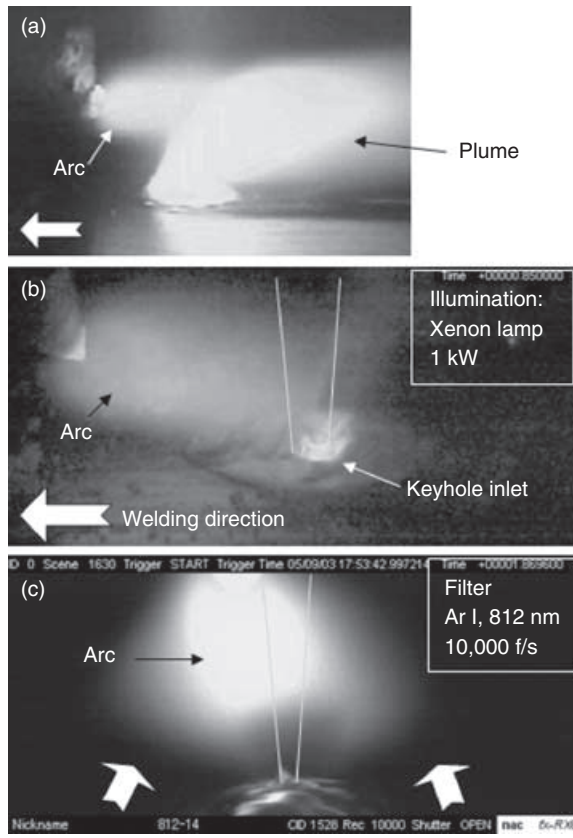

2.8 CCD and high-speed video observation results of arc and plume behavior during hybrid TIG–YAG laser welding.

evaporation occurs in addition to the laser-induced plume (as shown in Fig. 2.19b). In general, the arc barely enters the keyhole to reach the bottom, although there is a proposal in the mechanism[3] that the arc enters the inside of the keyhole and thus acts effectively on melting efficiency.

Figure 2.9 shows the cross-sections of A5052 alloy welds obtained by hybrid YAG laser-pulsed MIG welding with an inclined A5356 alloy wire at the different target distances (d) between the wire and the laser beam, and examples of the video pictures observed during hybrid welding.[15] Droplets transfer slightly ahead away from the wire target (see Fig. 2.10). Consequently, at $d = 0$ mm, the laser beam hits or irradiates a flying droplet. In other words, the droplets block or prevent the laser beam irradiation, thus generally resulting in shallower weld penetration at $d = 0$ mm than at $d = 2$ mm.

Figure 2.10 demonstrates the examples of video pictures observed during hybrid YAG laser–MAG or MAG–YAG laser welding of steel at low and high voltages. At low voltages, short-circuit transfer easily occurs, causing severe spattering in hybrid laser–MAG welding. On the other hand, in hybrid MAG–YAG laser welding at a high voltage, the wire melts above the surface, and smooth droplet transfer from the wire to the molten pool is observed, resulting in the formation of sound deep welds.

In general, MIG welding of steels and stainless steels in pure Ar or He gas is unstable, and thus the welding is performed in the shielding gas with a small amount of oxygen such as Ar–2 to 5% O_2 or Ar–20% CO_2 mixed gas,[21] and therefore this process is named MAG welding. As shown in Fig. 2.11, MIG welds are not good; on the other hand better hybrid welds are produced. It is thus confirmed in hybrid pulsed MIG–YAG laser or YAG

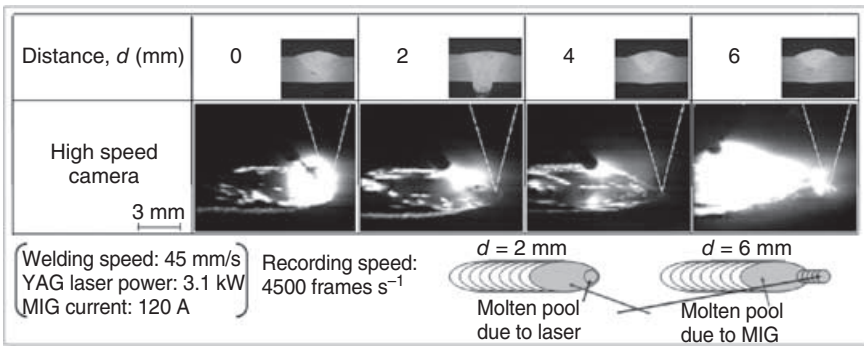

2.9 Cross sections of A5052 welds obtained by hybrid YAG laser-pulsed MIH welding with A5356 wire and welding phenomena, showing effect of target distance between wire and laser beam (d) on penetration.

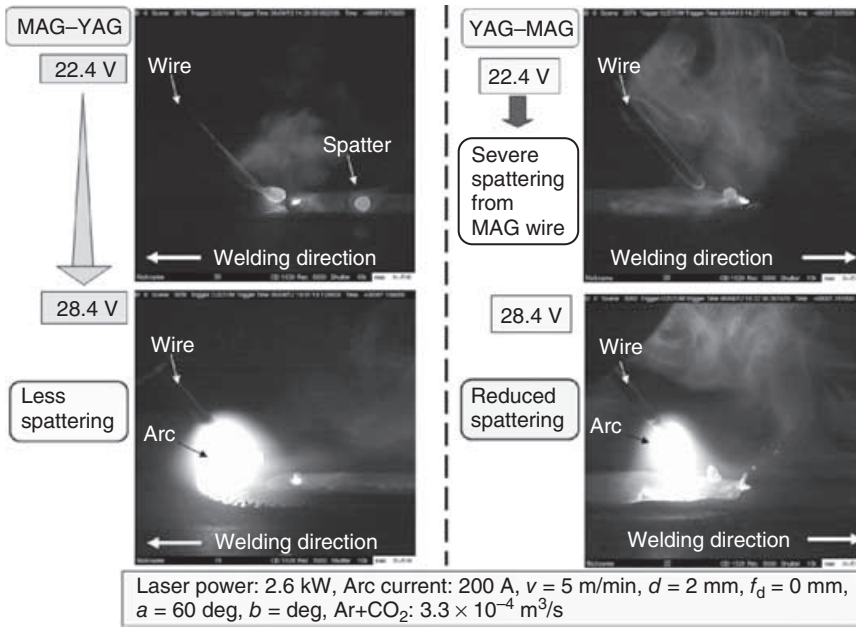

2.10 Arc and droplet behavior during hybrid YAG laser–MAG or MAG–YAG laser welding of steel at low and high voltages.

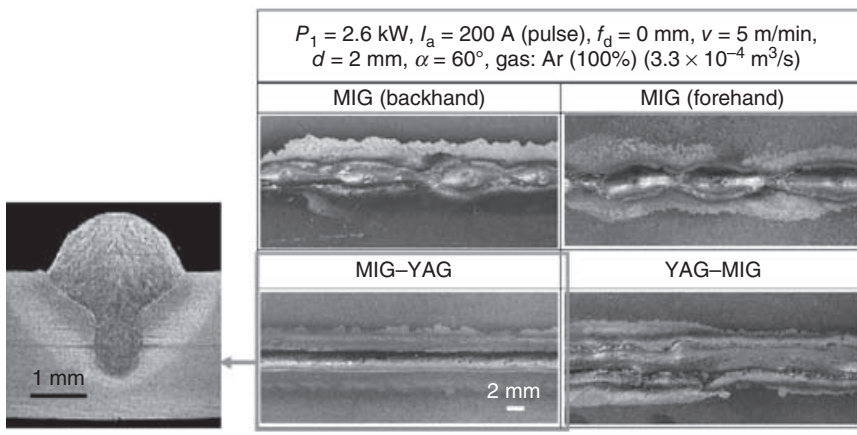

2.11 Comparison of MIG welds and hybrid YAG laser–MIG or MIG–YAG laser welds in steel with Ar gas, and cross section of good weld made by hybrid MIG–YAG laser welding.

laser-pulsed MIG welding of steels or stainless steels that stable welds can be produced even in pure Ar shielding gas.

In hybrid laser–TIG welding, the generation of spatters (splashing the melt around the keyhole inlet) accompanied by a laser-induced plume is suppressed owing to the formation of a wider molten pool enough to accommodate keyhole expansion, while, in hybrid laser-MIG, MAG or CO_2 arc welding, spatters are easily generated under the normal conditions of short-circuit transfer of droplets from the wire. Moreover, in the case of hybrid laser–MAG welding with the forward inclination of the wire, droplets are apt to fly on the solid part in front of the molten puddle, resulting in the formation of spatters. Therefore, to suppress spattering in the hybrid laser–MIG, MAG or CO_2 arc welding process, the utilization of pulsed arc is recommended,[15,27] and droplets from a wire should be transferred onto the molten pool or just in front of the molten pool.

2.4 Melt dynamics and melt pool stability

High-speed video and x-ray transmission in-situ observation have been carried out during laser and hybrid welding to determine keyhole stability and melt flows in the molten pool. To understand melt flows near the molten pool surface during hybrid TIG–YAG laser welding, the movement of ZrO_2 particles was observed with a high-speed video camera. Examples of Type 304 surfaces observed during hybrid welding at the TIG arc currents of 100 and 200 A are shown in Figs. 2.12 and 2.13, respectively.[16,28] The schematic

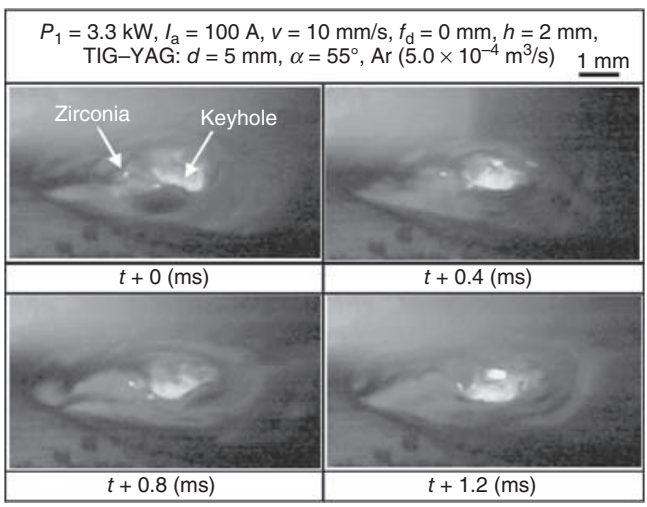

2.12 Observation results of molten pool surface and ZrO_2 particle tracer during hybrid TIG–YAG laser welding at 100 A in Ar gas.

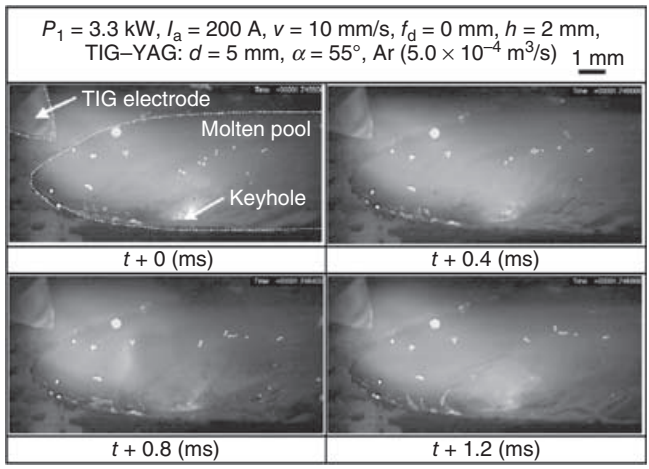
P_1 = 3.3 kW, I_a = 200 A, v = 10 mm/s, f_d = 0 mm, h = 2 mm,
TIG–YAG: d = 5 mm, α = 55°, Ar (5.0×10^{-4} m^3/s)
1 mm
TIG electrode
Molten pool
Keyhole
t + 0 (ms)
t + 0.4 (ms)
t + 0.8 (ms)
t + 1.2 (ms)

2.13 Observation results of molten pool surface and ZrO_2 particle tracer during hybrid TIG–YAG laser welding at 200 A in Ar gas.

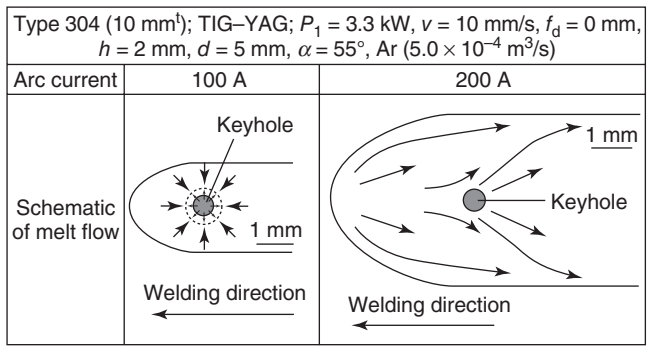
Type 304 (10 mm^t); TIG–YAG; P_1 = 3.3 kW, v = 10 mm/s, f_d = 0 mm,
h = 2 mm, d = 5 mm, α = 55°, Ar (5.0×10^{-4} m^3/s)
Arc current
100 A
200 A
Schematic of melt flow
Keyhole
1 mm
Welding direction
1 mm
Keyhole
Welding direction

2.14 Schematic melt flow patterns on molten pool surface during hybrid TIG–YAG laser welding at 100 A and 200 A.

summary of melt flows on the surface is represented in Fig. 2.14.[16,28] At 100 A, ZrO_2 particles first approach the keyhole inlet but soon flow away from the keyhole inlet owing to stream shear stress caused by laser-induced plume ejected from the inlet. Nevertheless, the particles approach the inlet again probably owing to the surface tension-driven flows and the electromagnetic convection. At 200 A, the surface of the molten pool becomes concave owing to the high arc pressure, and ZrO_2 particles approach a keyhole inlet but soon flow away to the rear molten pool owing to a strong arc plasma stream in addition to the plume ejection. Such melt flows are

also observed during hybrid MAG–CO_2 laser welding of HT (high tensile strength) steel.

The melting of Pt wire and the movement of W particles inside the molten pool are also observed by an x-ray real-time transmission system. An observation example of Type 304 subjected to hybrid welding at 100 A is shown in Fig. 2.15.[16,28] It is observed that the Pt wire melts and flows down towards the keyhole and then backwards to the bottom of the molten pool. The W particle is heavy, but moves widely. The measured examples of W movement at 100 and 200 A are compared in Figs. 2.16 and 2.17.[16,28] These suggest that a molten pool in hybrid welding is longer and wider than that in laser welding. The melt flows are different between 100 and 200 A resulting in a different hybrid weld bead geometry. It is generally understood that the weld bead geometry is chiefly determined by the melt flows in the molten pool.

The melt flows in the molten pools during hybrid welding with YAG laser or fiber laser and MIG, and with CO_2 laser and MAG arc were observed. The melt flows are strongly induced with higher arc currents, resulting in a

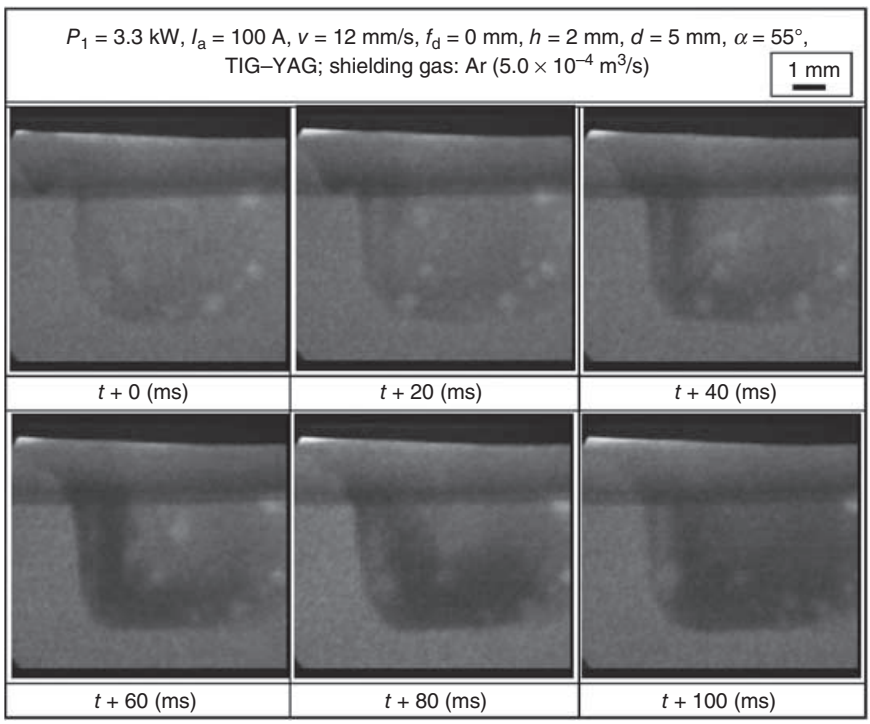

2.15 X-ray transmission observation results during hybrid welding with Ar gas at 100 A in air, showing diffusion of Pt inside molten pool.

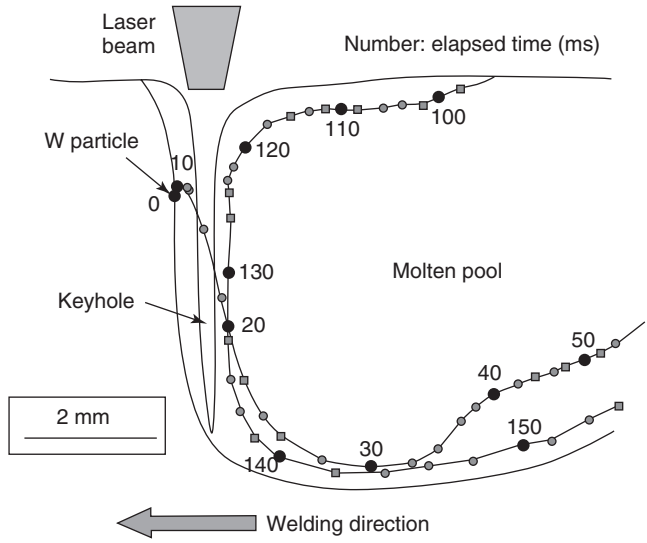

2.16 Motion of W particle observed during hybrid welding with Ar gas at 100 A in air, showing melt flows inside molten pool.

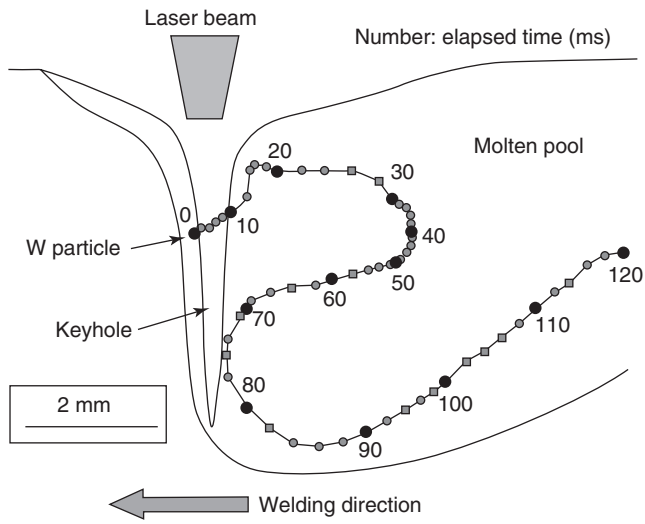

2.17 Motion of W particle observed during hybrid welding with Ar gas at 200 A in air, showing melt flows inside molten pool.

wider molten pool. The mixing of filler wire components takes place more completely in hybrid welding than in laser welding owing to the effect of arc electromagnetic convection.

The melt flows during hybrid CO_2 laser–MAG and MAG–CO_2 laser welding of thick HT steel plate have been investigated.[29] The different melt flows are observed between these. For example, in hybrid CO_2 laser–MAG welding the flows down the keyhole wall are dominant, but in hybrid MAG–CO_2 laser welding the backward flows on the surface of the molten pool are strong. These are understood by considering the melt flows induced by the arc plasma stream and surface tension,[29] and it is consequently confirmed that the distribution of alloying elements is different by the heat source arrangement.

YAG–MIG and MIG–YAG hybrid welding were carried out on A5052 aluminum alloy. Slightly easier melting or higher speed for full penetration welding is achieved in MIG–YAG welding. Better surface appearances of weld beads are observed in YAG–MIG hybrid welding. Therefore, hybrid YAG–MIG and MIG–YAG welding are recommended for the production of aluminum alloy weld joints from the viewpoints of better surface appearances and deeper penetrations, respectively.[14,30]

2.5 Formation and prevention mechanism of porosity

The cross-sections and x-ray inspection results of weld beads, and transmission observation results of molten pools of hybrid TIG–YAG laser welding are shown in Fig. 2.18.[16,28] The effect of the arc current on weld penetration,

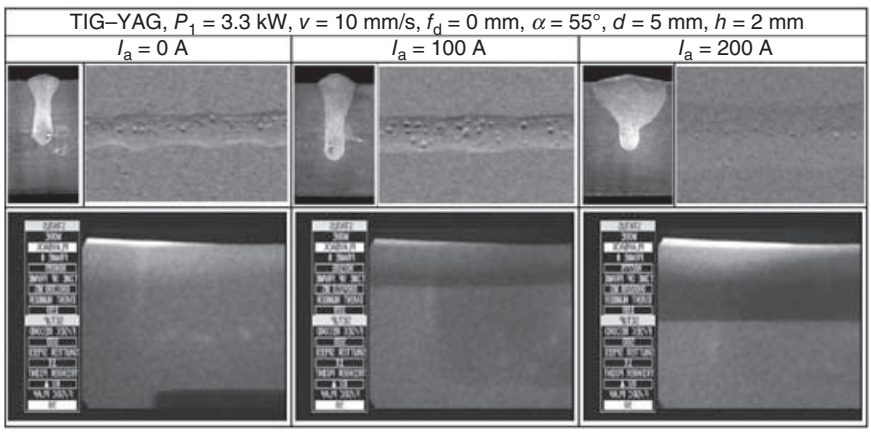

2.18 Cross-sections and x-ray inspection results of weld beads, and transmission real-time observation results of molten pools of hybrid TIG–YAG laser welding.

porosity formation tendency, keyhole behavior, and bubble generation in Type 304 steel with low S content can be compared. The phenomena of hybrid welding at 100 and 200 A in the air are schematically summarized in Fig. 2.19.[16,28] The diameter of the keyhole inlet becomes slightly larger with an increase in the arc current. In the YAG laser welding, bubbles are generated from the bottom part of the keyhole probably because of intense evaporation from the front wall and/or collapse of a deep keyhole. The bubbles are trapped by the solidifying front, resulting in the formation of pores and porosity. At 100 A, a keyhole is slightly larger and deeper, since the surface tension driven flows and electromagnetic flows are superimposed on the downward flows of the melt near the keyhole wall and thereafter the melt flow from the keyhole tip to the rear part along the bottom of the molten pool. These melt flows deepen the bottom of the molten pool, leading to a deeper weld. Big bubbles are often generated from a larger keyhole to form larger-sized pores. At 200 A, the surface of the molten pool is concavely depressed owing to the higher arc pressure, the keyhole inlet diameter is much larger, and other fast melt flows owing to the arc plasma stream cause the molten pool to widen, resulting in a wide bead. In addition, the generation of bubbles is reduced, resulting in the decreased porosity. Porosity reduction at 200 A is attributed to the reduction in bubble generation, but not to the disappearance of bubbles from the molten pool surface in TIG (leading)-YAG laser hybrid welding of Type 304 steel. Bubble formation tendency depends upon the arc current. High arc current can render a keyhole shallower and more stable under the current conditions.

Hybrid laser–MIG welding of aluminum alloys is applied in car production lines.[8] The weld beads become larger and deeper with an increase in the MIG current.[30] Figure 2.20 gives a comparison of cross-section, surface

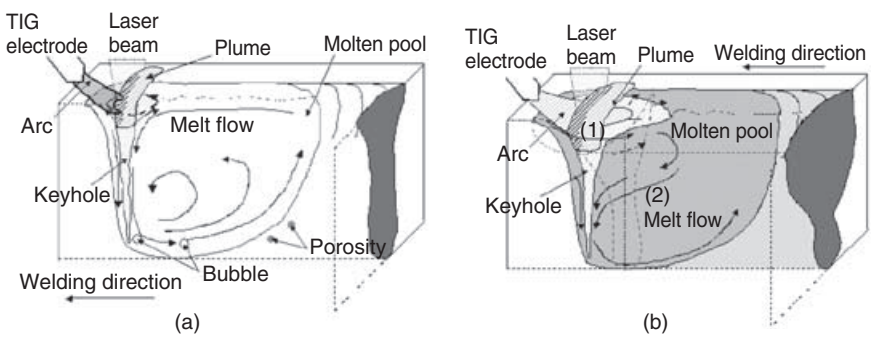

2.19 Schematic welding phenomena during hybrid TIG–YAG laser welding at (a) 100 and (b) 200 A, showing melt flows, bubble and porosity formation or no porosity.

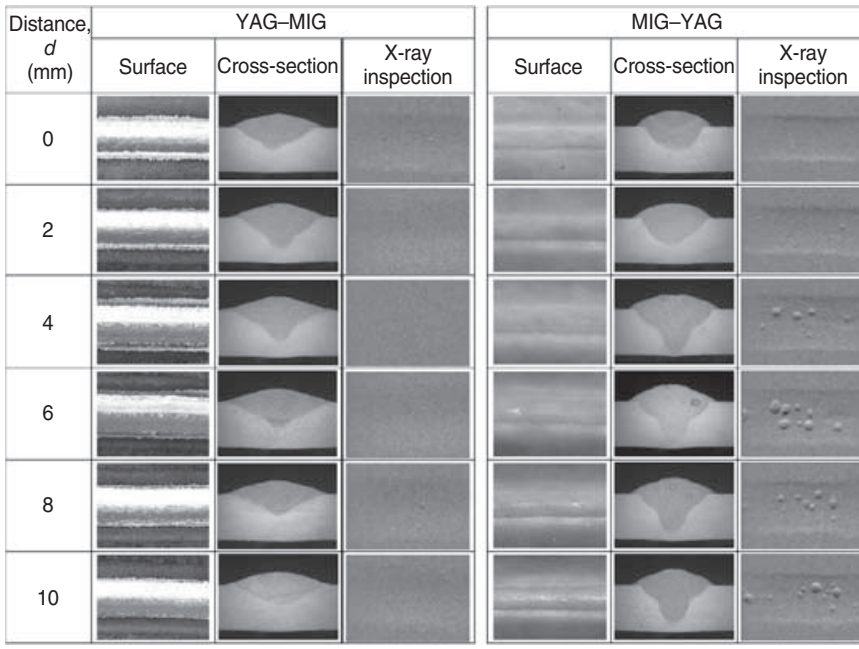

2.20 Comparison of surface, cross section and x-ray inspection results between (a) YAG laser–MIG or (b) MIG–YAG laser showing effect of distance (*d*) on weldability.

and x-ray inspection results of hybrid YAG laser–MIG and MIG–YAG laser weld beads in A5052 aluminum alloy in Ar shielding gas at the laser power of 3 kW, the focal point and the different distances between the laser beam and the wire target.[30] MIG–YAG laser welds generally appear to be slightly deeper and larger than YAG laser–MIG ones. The surface appearances of YAG laser–MIG welds are always better than those of MIG–YAG ones.[15,30] Porosity is reduced in A5052 hybrid weld beads at the laser power of 3 kW and at the high MIG current of 240 A.[15,30] Welding phenomena, molten pool geometry, melt flows inside the pool, bubble and porosity formation are schematically indicated in Fig. 2.21.[15,30] At 120 A, a lot of bubbles are generated and trapped by the solidifying front, resulting in porosity formation. On the other hand, at 240 A, some bubbles may be generated. However, all bubbles disappear from the concave surface of the molten pool, resulting in no porosity. Therefore, the mechanism of bubble disappearance is effective in shallow welds. In deeply penetrated MIG-YAG laser welds, it is confirmed that an inclined laser beam is beneficial to reduce porosity.[30]

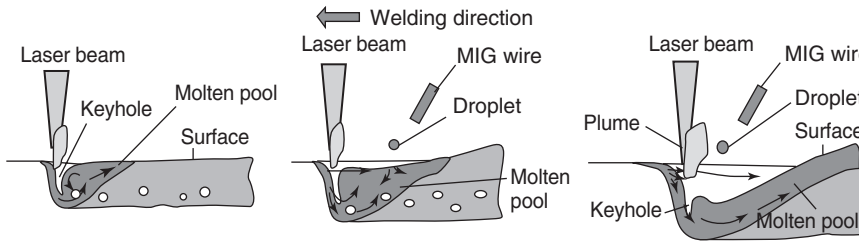

2.21 Schematic welding phenomena during laser welding and during hybrid YAG laser–MIG welding at 120 and 240 A, showing melt flows, bubble and porosity formation or no porosity.

It is interesting to know that the concave molten pool surfaces induced at high TIG and MIG currents suppress the bubble formation in stainless steels and act as a disappearance site in aluminum alloys, respectively.[27]

2.6 References

1 KATAYAMA S, '*New development in laser welding*', in *New developments in advanced welding*, ed. by Ahmed N, 2005, Cambridge, England, Woodhead Publishing Limited, 158–197.
2 STEEN V M and EBOO M, 'Arc augmented laser beam welding', *Metal Construction*, 1979 **7**(7) 332–335.
3 BEYER E, DILTHEY U, IMHOFF R, MAJER C, NEUENHAHN J and BEHLER K, 'New aspects in laser welding with an increased efficiency', *Proc. of Int. Congress on Applications of Lasers & Electro-Optics (ICALEO) '94*, Orlando, LIA, 1994, 183–192.
4 ISHIDE T, TSUBOTA S, WATANABE M and UESHIRO K, 'Latest MIG, TIG arc–YAG laser hybrid welding system', *Journal of the Japan Welding Society*, 2003 **72**(1) 22–26.
5 ISHIDE T, TSUBOTA S, and WATANABE M, 'Latest MIG, TIG arc-YAG laser hybrid welding systems for various welding products', *Proc. of SPIE (First Int. Sym. on High Power Laser Macroprocessing)*, Osaka, JLPS, 2002 **4831** 347–352.
6 PETRING D, FUHRMANN C, WOLF N and POPRAWE R, 'Investigation and applications of laser–arc hybrid welding from thin sheets up to heavy section components', *Proc. of the 22nd ICALEO '03*, Jacksonville, LIA, 2003 Section A, 1–10 (CD:301).
7 ABE N, KUNUGITA Y and MIYAKE S, 'The mechanism of high speed leading path laser–arc combination welding, *Proc. of ICALEO '98*, Orlando, LIA, 1998 **85** Section F, 37–45.
8 STAUFER H, 'Laser hybrid welding and laser brazing: State of the art in technology and practice by the examples of the Audi A8 and VW-Phaeton', *Proc. of 3rd Int. WLT-Conf. on Lasers in Manufacturing 2005*, Munchen, 2005 203–208.
9 TSUEK J and SUBAN M, 'Hybrid welding with arc and laser beam', *Science and Technology of Welding and Joining*, 1999 **4**(5) 308–311.
10 BEYER E, 'Laser technology for new markets – application highlights', *6th International Laser Market place 2003*, Anwendung im Dialog, 2003 5–15.

11 KUTSUNA M and CHEN L, 'Interaction of both plasma in CO_2 laser–MAG hybrid laser–hybrid welding of carbon steel, *IIW*, 2002, Doc.XII-1708–02.
12 SCHUBERT E, WEDEL B and KOHLER G, 'Influence of the process parameters on the welding results of laser–GMA welding, *Proc. of ICALEO '02*, *(Laser Materials Processing Conference)* Scottsdale, LIA, 2002 Session A – Welding (CD).
13 NAITO Y, MIZUTANI M and KATAYAMA S, 'Observation of keyhole behavior and melt flows during laser–arc hybrid welding', *Proc. of the 22nd ICALEO '03*, Jacksonville, LIA, 2003, (CD: 1005).
14 NAITO Y, MIZUTANI M, KATAYAMA S and BANG H-S, '*Proc. of the 23rd ICALEO '04*, San Francisco, LIA, 2004 Hybrid laser welding (CD: 207).
15 UCHIUMI S, WANG J B, KATAYAMA S, MIZUTANI M, HONGU T and FUJII K, 'Penetration and welding phenomena in YAG laser–MIG hybrid welding of aluminum alloy', *Proc. of the 23rd ICALEO '04*, San Francisco, LIA, 2004, Hybrid laser welding (CD: P530).
16 NAITO Y, 'Fundamental study of hybrid welding phenomena with YAG laser and TIG arc', Doctor Thesis, Osaka University, Japan, 2005 (in Japanese).
17 NAITO Y, MIZUTANI M and KATAYAMA S, 'Electrical measurement of arc during hybrid welding – welding phenomena in hybrid welding using YAG laser and TIG arc (Third report)', *Quarterly Journal of the Japan Welding Society (JWS)*, 2006 **24**(1) 45–51 (in Japanese).
18 SUGINO T, TSUKAMOTO S, NAKAMURA T and ARAKANE G, 'Fundamental study on welding phenomena in pulsed laser-GMA hybrid welding', *Proc. of the 24th ICALEO '05 (Laser Materials Processing Conference)*, LIA, Miami, 2005 **98** Paper #302 108–116 (CD).
19 SUGINO T, TSUKAMOTO S, ARAKANE G and NAKAMURA T, 'Effect of interaction between the arc and laser plume on metal transfer in pulsed GMA/CO_2 laser hybrid welding', *On-line Proc. the 4th Int. Congress on Laser Advanced Materials Processing (LAMP '06)*, JLPS, Kyoto, 2006, #198, 1–6.
20 TSUKAMOTO S, HIRAOKA K, ARAI Y and IRIE H, 'Characterization of laser induced plasma in CO_2 laser welding', *Proc. 5th Int. Conf. 'Trends in Welding Research'*, ASM & AWS, 1998 431–436.
21 CHAE H, KIM C, KIM J and RHEE S, 'Development of hybrid laser-rotating arc process', *On-line Proc. the 4th Int. Congress on Laser Advanced Materials Processing (LAMP '06)*, JLPS, Kyoto, 2006, #237, 1–4.
22 SCHITTENHELM H, MULLER J, BERGER P and HUGEL H, 'Investigation on cw CO_2-laser induced welding plasmas using differential interferometry', *Proc. of the 19th ICALEO '99 (Laser Materials Processing Conference)*, LIA, San Diego, 1999 **87**(2) Section E 195–204.
23 KAWAHITO Y, KINOSHITA K, KATAYAMA S, TSUBOTA S and ISHIDE T, 'Visualization of interaction between laser beam and YAG-laser induced plume', *Proc. of the 24th ICALEO '05 (Laser Materials Processing Conference)*, LIA, Miami, 2005 **98** Paper #P530 920–928 (CD).
24 KAWAHITO Y, KINOSHITA K, MATSUMOTO N, MIZUTANI M and KATAYAMA S, 'Interaction between laser beam and plasma/plume induced in welding of stainless steel with ultra-high power density fiber laser', *Quarterly Journal of the Japan Welding Society*, 2007 **25**(3) 461–467 (in Japanese).
25 KAWAHITO Y, KINOSHITA K, MATSUMOTO N, MIZUTANI M and KATAYAMA S, 'High-speed observation and spectroscopic analysis of laser-induced plume in

high-power fiber laser welding of stainless steel', *Quarterly Journal of the Japan Welding Society*, 2007 **25**(3) 455–460 (in Japanese).

26 NAITO Y, MIZUTANI M and KATAYAMA S, 'Penetration characteristics in YAG laser and TIG arc hybrid welding, and arc and plasma/plume behavior during welding – welding phenomena in hybrid welding using YAG laser and TIG arc (First report)', *Quarterly Journal of the Japan Welding Society*, 2006 **24**(1) 32–38 (in Japanese).

27 KATAYAMA S, KAWAHITO Y and MIZUTANI M, 'Plume behaviour and melt flows during laser and hybrid welding', *Proc. of 4th Int. WLT-Conf. on Lasers in Manufacturing 2007*, Munchen, 2007 265–271.

28 NAITO Y, MIZUTANI M and KATAYAMA S, 'Elucidation of penetration characteristics, porosity prevention mechanisms and flows in molten pool during laser–arc hybrid welding – welding phenomena in hybrid welding using YAG laser and TIG arc (Fourth report)', *Quarterly Journal of the Japan Welding Society*, 2006 **24**(2) 149–161 (in Japanese).

29 TSUKAMOTO S, Private communication (2008).

30 KATAYAMA S, UCHIUMI S and BRIAND F, 'Production of sound deep-penetration hybrid weld in aluminum alloy with YAG laser and MIG arc', *Proc. of the 25th ICALEO '06*, LIA, Scottsdale, 2006 Paper 1903 953–959 (CD).

3

Heat sources of hybrid laser–arc welding processes

A. MAHRLE and E. BEYER, Dresden University of Technology, Germany

Abstract: In this chapter, the different types of heat sources commonly used in hybrid laser–arc welding are discussed. First, the most important characteristics of laser beams and the available high-power laser types for welding purposes are presented. Then, several methods of welding with electric arcs are described in detail. Finally, various ways of combining electric arcs with laser beams to hybrid laser–arc processes are shown.

Key words: welding heat source, laser beam, electric arc, laser beam welding, arc welding, laser–arc welding, hybrid welding.

3.1 Introduction

In welding engineering, the term heat source generally refers to type of thermal tool, which is used in the fusion welding process. As the heat source progresses along the weld path, its energy is transformed into internal energy at the weld zone between the parts to be joined. Provided there is a sufficiently high amount of deposited energy, the base material and sometimes some additional material (filler) are locally melted, thus forming the weld bead and, after resolidification, the weld seam. There are many different types of welding heat sources and, in such a way, numerous possibilities are available to join separate workpieces together (e.g. Lesnewich 1976, Weman 2003, Messler 2004). Figure 3.1 shows a schematic presentation of the most common fusion welding methods. The applied heat sources for fusion welding comprise electric arcs, laser and electron beams. Each of these welding tools has its own characteristics and the choice of one specific heat source for any particular welding assignment depends on a multitude of factors. A distinctive feature that can be used to categorise welding heat sources is the achievable intensity. Laser and electron beams are referred to as high-energy density heat sources since their intensities are commonly much higher than the intensity of electric arcs.

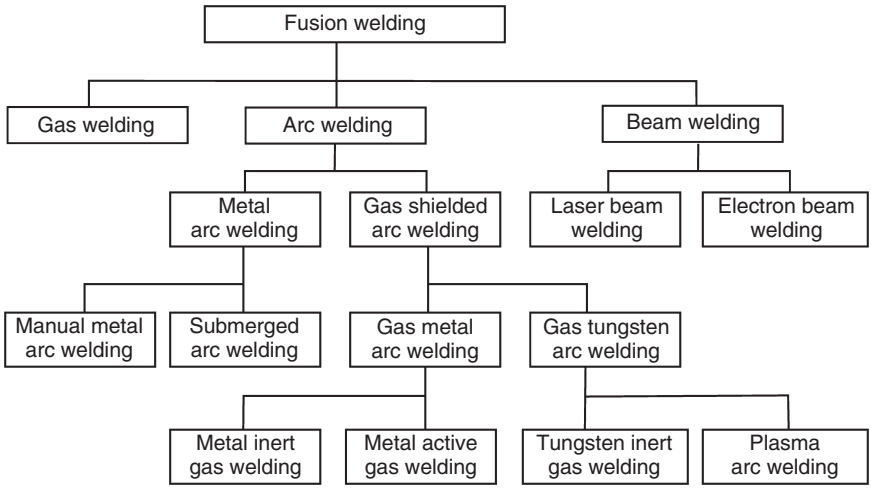

3.1 Schematic presentation of the most common fusion welding methods.

In recent years, combinations of high energy density and low energy density heat sources further increased the variety of welding tools. The most proven technique consists of a combination of an electric gas-shielded arc and a laser beam. Such combinations are referred to as hybrid laser–arc processes. In principle, laser–arc combinations are relatively simple to realise since both heat sources usually work under atmospheric pressure conditions and require similar gas shielding of the weld zone. However, the knowledge of the relevant properties of each individual heat source is an essential precondition in searching for useful process combinations and optimal parameter constellations.

3.2 Laser beam heat sources

Focused laser beams belong to the highest power density welding heat sources available to welding engineering today. The emitted electromagnetic radiation of coherent and nearly monochromatic laser light is usually concentrated to very small spot sizes with diameters in the sub-millimetre range. For welding purposes, intensities up to several 10^{12} W m^{-2} are commonly realised. The incident laser radiation is either absorbed or reflected since weldable metals such as steel and aluminium are opaque, i.e. non-transparent, at wavelengths of typical materials processing lasers. The absorbed laser energy is transferred into internal energy of the material being welded within a very thin surface layer causing heating, melting and even evaporation and plasma formation. Conventionally, laser beam welding

is carried out without additional filler metal. The weld and the heat-affected zone are usually shielded from the atmosphere by a blanket of inert gas, typically argon (Ar), helium (He) or mixtures of the two gases.

3.2.1 Beam characteristics

The most important characteristics of laser beam sources are the available optical output power P_L, the wavelength λ of the emitted radiation and the beam parameter product (BPP) as a measure of the beam focusability or quality, respectively. These quantities that depend on a specific laser system, see section 3.2.3, determine the achievable intensity or irradiance of the laser beam at the surface of the material being welded. The averaged value $I_{L,0}$ of the intensity is defined as ratio of laser power P_L to the cross-sectional area $A_{L,0}$ of the beam. For the common case of circular beams with the radius w_0, it is

$$I_{L,0} = \frac{P_L}{A_{L,0}} = \frac{P_L}{\pi w_0^2} \tag{3.1}$$

The smallest value of w_0 that can be achieved by focusing the beam (e.g. through a lens) can be estimated under usual focusing conditions according to the relation

$$w_0 = \frac{2f}{D}\mathrm{BPP} \tag{3.2}$$

as a function of the focal length f of the lens and the initial beam diameter D before focusing, see Fig. 3.2 (Hügel 1992). The BPP corresponds to the

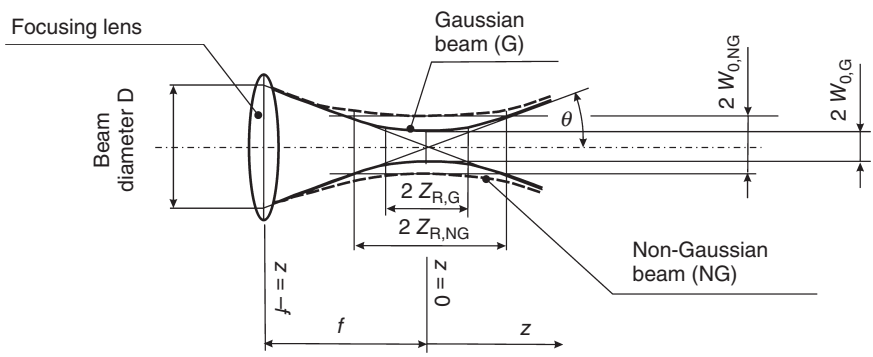

3.2 Beam propagation of a Gaussian and a non-Gaussian beam after focusing through a lens.

product of the beam waist radius w_0 and the half-angle θ of the so-called far-field divergence as a measure for how fast the beam expands from the beam waist at $z = 0$. The BPP is constant for laser systems with ideal beam delivery optics. For a Gaussian beam (index G), also referred to as an ideal or diffraction-limited beam with the best beam quality physically possible, the BPP is proportional to the emitted laser wavelength according to the relation

$$\mathrm{BPP_G} = w_{0,\mathrm{G}}\theta_\mathrm{G}\frac{\lambda}{\pi} = \mathrm{const} \tag{3.3}$$

Actual or non-Gaussian beams (index NG) possess a $\mathrm{BPP_{NG}}$ that is always greater than $\mathrm{BPP_G}$. Introducing the so-called beam propagation ratio M^2 as a dimensionless ratio of both BPPs (DIN EN ISO 11145, 2002) it is

$$\mathrm{BPP_{NG}} = w_{0,\mathrm{NG}}\theta_\mathrm{NG} = \mathrm{M^2BPP_G} = \mathrm{M^2}\frac{\lambda}{\pi} \tag{3.4}$$

The beam propagation ratio M^2 is an often used quantity as a relative measure of laser beam quality. For Gaussian beams, it is $M^2 = 1$ whereas real beams are characterised by $M^2 > 1$. The actual value of M^2 strongly depends on the laser type. Other factors having an impact on M^2 are spherical aberrations and thermal lensing effects during beam delivery. Consequently, M^2 also depends on the optics used (lenses, protection glasses, beam splitters) and the laser power as well. This fact becomes especially important for laser beams with an initial high quality (Abt *et al.* 2007).

Further characteristic details of the beam propagation during focusing are shown in Fig. 3.2. For a given focal length f of a lens, the focus radius $w_{0,\mathrm{NG}}$ of an actual beam is M^2 times greater than the radius $w_{0,\mathrm{G}}$ of a diffraction-limited laser beam. With respect to the definitions (3.3) and (3.4) of the BPP for ideal and real beams, the angle θ follows under the considered conditions to

$$\theta = \theta_\mathrm{NG} = \frac{M^2}{w_{0,\mathrm{NG}}}\frac{\lambda}{\pi} = \frac{M^2}{M^2 w_{0,\mathrm{G}}}\cdot\frac{\lambda}{\pi} = \frac{\lambda}{w_{0,\mathrm{G}}\pi} = \theta_\mathrm{G} \tag{3.5}$$

The beam radius $w_{\mathrm{z,NG}}$ of an actual laser beam at any distance z from the beam waist can be calculated with the beam propagation equation

$$\frac{w_{\mathrm{Z,NG}}(z)}{w_{0,\mathrm{NG}}} = \sqrt{1+\left(\frac{M^2\lambda z}{\pi w_{0,\mathrm{NG}}^2}\right)^2} = \sqrt{1+\left(\frac{\theta_\mathrm{NG} z}{w_{0,\mathrm{NG}}}\right)^2} = \sqrt{1+\left(\frac{z}{z_{\mathrm{R,NG}}}\right)^2} \tag{3.6}$$

where z_R is the corresponding Rayleigh length that denotes the distance between the origin of the beam waist at $z = 0$ and the point along the propagation line where the beam waist radius $w_{0,NG}$ is increased by 41.4% (or by the factor that corresponds to the square root of 2). In the case of a circular beam, the cross-sectional area is doubled at this point. According to equation (3.6), the Rayleigh length of a laser beam is defined to be

$$z_{R,NG} = \frac{w_{0,NG}}{\theta_{NG}} = \frac{w_{0,NG}^2}{BPP_{NG}} = \frac{\pi w_{0,NG}^2}{M^2 \lambda} \tag{3.7}$$

The Rayleigh length is one possible definition of the depth of focus DOF as a measure of the length of the beam waist region over which the spot size does not change significantly and the laser intensity remains approximately constant (Latham and Kar 2001). In this way, depth of focus can have an important impact on the geometry of the weld seam and the achievable weld penetration depth in addition to the effects of the focal intensity $I_{L,0}$ of the applied laser beam. This fact becomes especially important in the case of strongly focused laser beams with small focus radii w_0, which, in turn, give rise to short Rayleigh lengths or increased divergence angles, respectively (Weberpals *et al.* 2005, 2006).

3.2.2 Welding modes

When a laser beam with the intensity $I_{L,0}$ according to equation (3.1) impinges on the surface of a metallic workpiece, only the part

$$P_{L,A} = \pi w_0^2 A I_{L,0} = \pi w_0^2 I_{L,A} \tag{3.8}$$

penetrates into a substrate with the absorptivity A. The absorbed laser power $P_{L,A}$ is mainly dissipated, i.e. transferred into internal energy of the material, in a thin layer with the thickness

$$l_A = \frac{\lambda}{4\pi k} \tag{3.9}$$

This quantity is commonly referred to as the absorption depth l_A as a function of the wavelength λ of the laser radiation and the damping constant or extinction coefficient k. Typical values of the absorption depth in metals lies in the order of some hundredth of the laser wavelength (Pedrotti 1996). Thus, metals can be considered to be opaque and the part

$$P_{L,0} - P_{L,A} = (1 - A) P_{L,0} = R P_{L,0} = P_{L,R} \tag{3.10}$$

where $R = 1 - A$, is the reflected portion of the incident laser power that is lost and does not contribute to the heating of the material being welded. It becomes obvious that the optical properties of absorptivity and reflectivity have an important impact on the energy transfer efficiency of laser beams as welding heat source.

In general, the absorptivity A and reflectivity R are complicated functions of the polarisation state of the laser radiation, the angle of incidence between laser beam and irradiated surface, as well as the fundamental optical properties index of refraction n and extinction coefficient k, which in turn depend on the wavelength λ of the laser light and several properties of the material such as the free electron density n_e and the temperature T (Modest 2001). Characteristic reflectivity values at typical wavelengths of materials processing lasers are listed in Table 3.1 for different metals at room temperature (Kreutz 1991). However, it must be considered that the given values are valid for smooth surfaces only. For technical surfaces, the absorptivity is additionally affected by the surface conditions of the irradiated sample including surface roughness, surface layers and oxide films (Steen 1998, Modest 2001).

Finally, the overall dissipated laser power and, thus, the heat input or energy transfer efficiency of laser beams as a ratio of delivered (incident) laser power to dissipated (absorbed) laser power depends to a high degree on the realised welding mode. In laser beam welding, three different laser welding modes can be distinguished based on the chosen welding parameters (primarily on the energy density per unit length) and the properties of the material being welded. These welding modes involve the heat conduction mode, the penetration mode and the keyhole or deep-penetration mode. Figure 3.3 shows schematic diagrams of the conduction and keyhole welding process as the most often used laser welding modes.

Table 3.1 Reflectivity values of selected metals at room temperature for typical wavelengths of materials processing laser systems

Material	Reflectivity at 10.6 μm wavelength	Reflectivity at 1.06 μm wavelength
Aluminium	0.98	0.96
Iron	0.96	0.70
Gold	0.99	0.97
Copper	0.99	0.95
Nickel	0.97	0.74
Silver	0.99	0.96
Tantalum	0.95	0.85
Titanium	0.92	0.58
Zinc	0.97	0.84

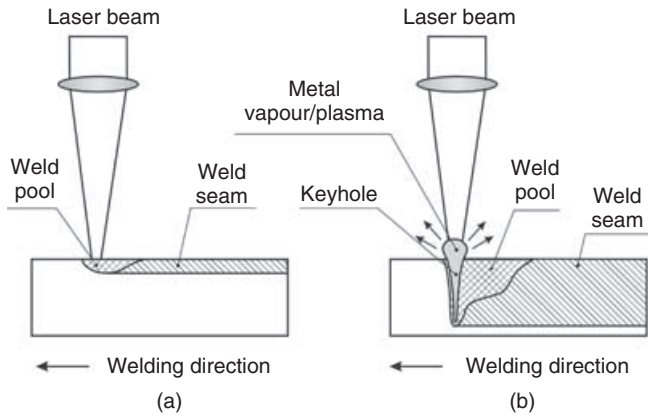

3.3 Schematic diagrams of (a) conduction mode laser beam welding and (b) keyhole mode laser beam welding.

The heat conduction mode is a laser welding variant, in which the absorbed laser energy only induces a melting of the samples to be welded, i.e. the conduction mode is a type of pure fusion welding process and the maximum value of the temperature at the weld pool surface lies between the melting and the boiling point of the material (Ready *et al.* 2001). In this case, the laser acts as a surface heat source and the energy transfer efficiency is mainly determined by the absorptivity of the surface. The dissipated energy is transferred into the bulk material by heat conduction and, within the melt pool, by the convective heat transfer as result of the melt pool fluid flow that is in turn induced by (I) the buoyancy effect as a result of the temperature-dependent density and (II) the Marangoni effect in consequence of surface tension gradients at the free weld pool surface. The latter is able to significantly determine the weld pool shape and size and, thus, the geometry of the resultant weld seam (e.g. Pitscheneder *et al.* 1996, 1998). In order to achieve acceptable penetration depths, the conduction mode laser welding process must be carried out at relatively slow welding speeds. Typical aspect ratios of penetration depth to weld seam width lie in the range 0.2 to 1. Thus, the conduction-limited laser welding process is preferably applied for welding of thin metal sheets and micro-joining purposes.

At increased values of laser intensity, the material being welded is heated up to its boiling point. In addition, some of the material will evaporate and the resultant recoil pressure squeezes the liquid melt to the side. The subsequent depression of the weld pool surface, allowing the laser radiation to penetrate deeper into the material, gives rise to the formation of a drill hole within the weld pool which is called the 'keyhole'. The corresponding laser welding process termed to be deep penetration or keyhole mode welding

is the most preferred laser welding mode (e.g. Dawes 1992, Beyer 1995, Duley 1999). A fully developed and stable vapour channel acts like a black body that absorbs the greatest amount of the incident laser radiation (Steen 1998). In this case, the laser beam can be considered as an effective and highly concentrated volumetric welding heat source. As a result of the fact that the keyhole formation depends mainly on the focal laser beam intensity, the penetration depth which is achievable by use of laser beam welding heat sources shows a distinctive threshold behaviour, see Figure 3.4, whereby the defined threshold intensity is generally a function of the thermal properties of the material to be welded and, the welding feed rate as well as the laser wavelength and power (e.g. Beyer 1985).

The efficiency of keyhole laser welding processes is furthermore affected by plasma effects that occur at high laser intensities where the evaporated metal becomes ionised and forms a plasma with free electrons that are capable of interacting with the incident laser radiation preferably by the process of inverse bremsstrahlung (Matsunawa 1991). That the type and strength of the interaction strongly depend on the laser wavelength was primarily observed in welding processes with CO_2 lasers, see section 3.2.3. As a result, the beam propagation characteristics can be significantly deteriorated during passing a plasma plume owing to absorption and refraction effects. However, those negative effects can be diminished or even suppressed by use of appropriate shielding gases with a high ionisation potential, such as He or He-Ar mixtures with high He content (e.g. Beck *et al.* 1995).

The keyhole mode is the preferred mode for welding of thicker materials at high welding speeds. Aspect ratios lie typically between three and ten but sometimes even higher if highly focused laser beams with high beam

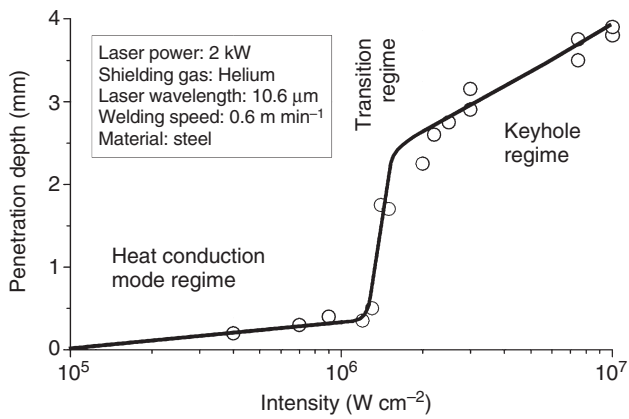

3.4 Penetration depth versus intensity for laser beam welding processes.

quality such as fibre lasers, see section 3.2.3, are applied. The required energy input per unit length is relatively small, thus often distortion-free joining of the parts to be welded is feasible with minimized residual welding stresses. Process inherent disadvantages of the keyhole mode includes (I) the often high requirements for seam preparation and clamping, (II) eventual instabilities of the keyhole leading to spattering, spiking and/or porosity, (III) high thermal gradients within the weld and the heat-affected zone sometimes inducing weld defects such as cracks in crack-susceptible materials, and (IV) undesired interactions between the laser radiation and the metallic vapour forming a plasma as described above.

The third laser welding mode called penetration mode induces a welding regime somewhere between conduction mode welding and keyhole welding. In this mode, the laser intensity at focus is too low to produce a small and stable keyhole as in deep penetration welding. However, a relatively large melt pool surface depression is created being able to trap the incident laser power at the central weld pool indentation by multiple reflections. As a result, the laser energy is more efficiently absorbed than in the conduction mode and aspect ratios up to 3:1 can be achieved (Kugler 2001a).

In addition to the various welding modes, laser welding processes can be further classified in terms of their dependence on the temporal control of the energy deposition, i.e. to distinguish between continuous-wave (CW) and pulsed-wave (PW) processes. In CW processes as the most used process regime for welding purposes, the realised energy density per unit length, i.e. the ratio of laser intensity to welding speed, determines the welding mode whereas in PW applications, the welding mode primarily depends on the pulse energy and the pulse repetition rate (Tzeng, 2000).

3.2.3 Laser types

There are many different types of lasers but only a few of them possess the required high output power necessary for welding purposes. Currently, the most commonly used high-power laser types are still the carbon dioxide (CO_2) and the Nd:YAG (neodymium: yttrium–aluminium–garnet) laser. However, recently Yb:YAG (ytterbium: yttrium–aluminium–garnet) disc and Yb fibre lasers with high output powers and high beam quality have become available and are being increasingly used for welding applications. A fifth laser type that was in the past preferred for conduction mode welding processes is the high-power diode laser. The most important characteristics of these laser sources such as the emitted wavelength of the used lasing medium, the power conversion efficiency, i.e. the ratio of optical output to electrical input power, the maximum output power available, the theoretical beam quality as well as the mobility of the laser system and the characteristic maintenance interval are listed in Table 3.2. Additionally,

Table 3.2 Feature comparison for typical materials processing laser sources

	CO_2 laser	Nd:YAG laser (lamp-pumped)	Nd:YAG laser (diode-pumped)	Disc laser	Fibre laser	Diode laser (fibre-coupled)
Lasing medium	Gas mixture	Crystalline rod	Crystalline rod	Crystalline disc	Doped fibre	Semiconductor
Emitted wavelength (μm)	10.6	1.06	1.06	1.03	1.07	0.808–0.98
Power efficiency (%)	10–15	1–3	10–30	10–20	20–30	35–55
Maximum output power (kW)	20	6	6	8	50	8
BPP at 4 kW (mm mrad)	4	25	12	2	0.35	44
M^2 at 4 kW	1.2	75	35	6	1.1	150
Fibre beam delivery	No	Yes	Yes	Yes	Yes	Yes
Typical fibre diameter at 4 kW (mm)	–	0.6	0.4	0.1–0.2	0.03–0.1	0.4
Mobility	low	low	low	low	high	high
Maintenance interval (h)	1000	500	10000	>25000	>30000	>25000

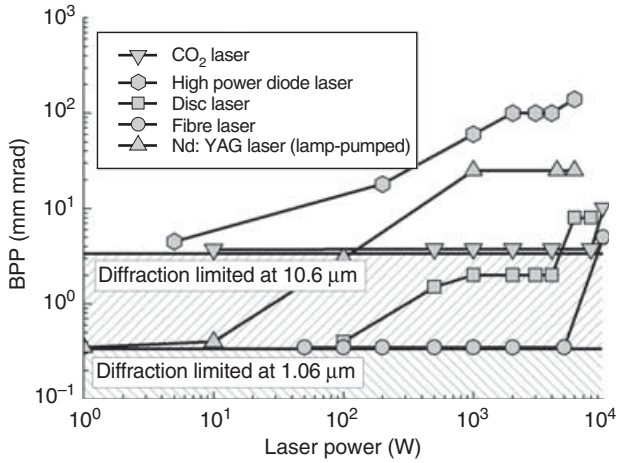

3.5 Characteristic beam parameter products (BPP) vs. laser power for different laser types.

typical values of BPP as a characteristic measure of the beam quality are shown in Fig. 3.5 as a function of the laser power in the range up to 10 kW.

Carbon dioxide laser

The CO_2 laser is, in general, the most popular gas laser for materials processing purposes today. The lasing medium is CO_2 mixed with N_2 and He in different amounts, depending on the laser resonator design, the operating pressure and the operating mode, i.e. continuous or pulsed. The excitation of the CO_2 molecules is realised by means of an electric discharge through the gas mixture. Laser radiation is primarily emitted at a wavelength of 10.6 μm. Typically, conversion efficiencies lie in the range 12 to 14%. For a long time, CO_2 lasers have been the highest CW power sources available for laser materials processing. The maximum power output of current commercial systems amounts 20 kW.

The most frequently mentioned disadvantages of CO_2 lasers are associated with the long wavelength of the emitted radiation. One consequence is that most materials that are transparent within the visible range of the electromagnetic spectrum, e.g. glass, are opaque for CO_2 laser radiation. Consequently, required transmission elements of the laser resonator and the beam guidance must be manufactured from special and more expensive materials such as zinc selenide and beam deflection and focusing must be realised by means of reflective optics such as gold-coated or multilayer-coated copper substrates (e.g. Davis and Berkmanns 2001).

Another consequence of the long wavelength is the high reflectivity of metals commonly used in materials processing, see Table 3.1, and the increased interaction of the radiation with laser-induced plasmas, see section 3.2.2. Thus, effective plasma suppression in CO_2 laser welding usually requires gas shielding with He that exhibits a high ionisation potential.

Nd:YAG laser

The Nd:YAG laser is still the most prevalent solid-state laser in use. A Nd-doped YAG crystal serves as lasing medium with an emitted wavelength of 1.06 μm. The excitation energy is optically provided either by high-intensity electric-discharge lamps (lamp-pumped) or laser diodes (diode-pumped). In contrast to gas lasers, the rod-shaped Nd:YAG laser crystal is optically active and the output beam quality decreases with increased output power (e.g. Kugler 2001b). Consequently, the beam quality is considerably lower than the beam quality of CO_2 lasers but owing to the shorter wavelength, Nd:YAG lasers can achieve similar focus spot sizes to a CO_2 laser of 10 times better (smaller) M^2 value. The maximum commercially available CW output power of Nd:YAG lasers is currently limited to 6 kW.

The shorter output wavelength of Nd:YAG lasers offers some important advantages. First, the beam can be carried through optical fibres and focused with ordinary lenses giving important benefits for use in robot welding and welding of complex three-dimensional structures. Secondly, the absorptivity of most metals is significantly improved. This fact is especially important for conduction-mode welding processes as well as for the value of the threshold intensity for keyhole mode welding. Finally, there is no significant interaction between the incident laser radiation and the generated metal vapour and, therefore, the problem of a perturbing plasma as present in deep penetration laser welding with CO_2 lasers does not occur at the power intensities typically used. As a consequence, Ar or Ar gas mixtures can be used as shielding gas instead of the more expensive He.

Disc and fibre laser

In recent years, promising disc and fibre laser systems as special types of diode-pumped solid state lasers with characteristic geometries of the laser-active medium (disc and fibre, respectively) have been developed that simultaneously offer high optical output powers, high conversion efficiencies, high beam qualities and a short emission wavelength around 1 μm, see Table 3.2. Besides the already mentioned advantage of the possible beam delivery through optical fibres, disc and fibre lasers allow a strong focusing of the laser radiation to remarkably smaller focus radii if compared with

typical focus dimensions reached with the established CO_2 laser (due to the longer wavelength of 10.6 μm) and the Nd:YAG laser (owing to thermal effects in the rod-shaped laser-active crystal). In addition, the characteristics of the new laser sources are continuously improved (e.g. Gapontsev *et al.* 2007). Consequently, disc and fibre lasers are increasingly applied for several welding purposes (e.g. Thomy *et al.* 2005, Verhaeghe and Hilton 2005, Kinoshita *et al.* 2006, Liu *et al.* 2006a, Ream 2006, Seefeld and O'Neill 2007, Göbel *et al.* 2007, Beyer *et al.* 2007, Zhang *et al.* 2007, Brockmann *et al.* 2007, Katayama *et al.* 2007, Beyer 2008, Iammi 2008).

To date, continuous-wave disc lasers are commercially available with output powers up to 8 kW (Trumpf 2008). At this power, the BPP amounts to 8 mm mrad. The preferably used diode-pumped laser-active medium is Yb:YAG with a laser wavelength of 1.03 μm. Fibre laser systems deliver even higher powers up to 50 kW (multimode). Single-mode fibre lasers with nearly diffraction-limited (Gaussian) beams ($M^2 < 1.1$) are currently available up to 5 kW. The active gain medium of fibre lasers is commonly an optical fibre doped with Yb leading to laser wavelengths in the range 1.06 to 1.07 μm.

Diode laser

For a long time, high-power diode laser (HPDL) systems were limited to low output powers and low beam qualities which lead to rectangular spot sizes with typical lengths of several millimetres. The resultant focal intensities only permitted welding applications in the heat conduction mode. However, the continuous improvement in the laser beam power and beam quality which can be achieved has led to the possibility for deep penetration welding processes as well (e.g. Li 2000, Walsh *et al.* 2003). Currently, direct HPDLs with output powers up to 10 kW and fibre-optic-coupled HPDLs with output powers up to 8 kW are available. With the latter systems the beam quality is similar to the beam quality of Nd:YAG lasers, and actual HPDLs are capable of directly competing with this more common laser type. The emitted wavelength of HPDLs depends on the material properties of the semiconductor, the temperature and the driving current (Li 2000). Typical values lie between 0.8 and 1 μm. One important advantage of HPDL systems is their compact size and low weight making them particularly suitable for use in conjunction with robotic control.

3.3 Arc heat sources

Nowadays, the welding arc is still the most applied welding heat source. It is based on an electrical gas discharge under atmospheric pressure conditions between the two open terminals, i.e. the welding electrode

and the workpiece to be welded, of the usually high-amperage and low-voltage welding current circuit. The gaseous zone between the welding electrode and the workpiece is partially ionised with typical ionisation degrees in the order of few percent. The resultant visible plasma arc closes the welding current circuit and ensures the continuous transfer of electrical energy between the electrode and the workpiece to be welded. The current transfer is primarily realised by the flow of electrons from the negatively charged cathode to the positively charged anode. Both electrode positive (EP) and electrode negative (EN) polarity can be applied depending on the materials to be welded and the required heat input. The choice of the polarity type does significantly influence the welding result because of the different amounts of energy that are dissipated within the cathodic and anodic spot. As a rule of thumb, approximately 70% of the total amount of heat is generated at the anode and 30% at the cathode (Kou 1987).

It is obvious that the presence of the plasma within the weld zone is a necessary precondition of the arc welding technique. Furthermore, the plasma properties have an essential influence on the efficiency of the welding arc. Compared with the gaseous state of matter, a plasma is characterised by the presence of free electrons and ionised atoms (ions). The relative number of such free charge carriers can be expressed by the ionisation grade. For single ionisation, the number of ions n_i is approximately equal to the number of electrons, i.e. $n_i = n_e$. The ionisation grade χ is then defined as the ratio of free electrons n_e to the total number n of elementary particles, i.e. the sum of electrons n_e and neutral atoms n_n per volume. Using such a definition, the electron density is given by the equation

$$n_e = \chi(n_e + n_n) = \chi n = \frac{\chi p}{k_B T_{Pl}} \tag{3.11}$$

where p is the ambient pressure, k_B the Boltzmann constant, and T_{Pl} the temperature of the plasma. The ionisation degree χ and the plasma temperature T_{Pl} are not independent from each other. The relationship between these quantities is described by the Eggert–Saha equation

$$\frac{\chi^2}{1-\chi} = \left(\frac{2\pi m_e}{h^2}\right)^{3/2} \frac{(k_B T_{Pl})^{5/2}}{p} \exp\left(-\frac{E_i}{k_B T_{Pl}}\right) = f(E_i, T_{Pl}) \tag{3.12}$$

where h is the Planck constant, E_i the ionisation energy and m_e the electron mass (e.g. Hippler *et al.* 2001). Consequently, the ionisation grade is a function of the ionisation energy E_i that, in turn, depends on the type of the atoms to be ionised. Calculated values of the ionisation grade of different elements vs. temperature at atmospheric pressure are shown in Fig. 3.6. It

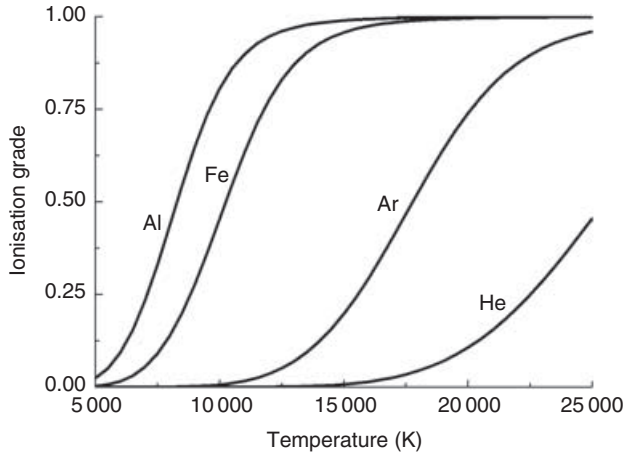

3.6 Ionisation grade vs. temperature of typical elements present in the welding zone.

can be concluded that the properties of the arc plasma strongly depends on the gas composition. As a result, the plasma temperature of arcs containing metal vapour components lies typically around 5000 K whereas arcs containing only inert gas components such as Ar or He reach temperature values up to 20 000 K and more (Schellhase 1985).

However, most of the delivered electrical power is not dissipated within the arc column but at the tip of the electrode and the surface of the workpiece where the arc root enters the weld zone. Achievable power intensities of welding arc sources range from 10^4 to 10^8 W m^{-2} (e.g. Radaj 1999). For a given material, the actual value depends on a multitude of controllable welding parameters including the welding amperage, the current mode (direct constant, direct pulsed or alternating), the shape, size, polarity and composition of the welding electrode, and the shielding gas type. Welding arcs burn not necessarily in a steady-state manner but can be intermittent, subject to interruptions by electrical short circuiting or continuously non-steady, e.g. being influenced by an alternating directional or pulsed flow of current or by turbulent flow of the plasma medium (Manz *et al.* 1976).

A special feature of arc welding heat sources is their inherent ability to add filler metal with consumable electrodes that melt during the welding procedure, see section 3.3.1. In this case, energy and mass transfer from the arc source to the weld zone must be considered as strongly coupled. Alternatively, arc welding processes with non-consumable electrodes also exist, see section 3.3.2.

3.3.1 Arc sources with consumable electrodes

There are variants of arc welding with consumable electrodes including (I) the shielded metal arc welding (SMAW) process using electrodes with an external flux coating, (II) the submerged arc welding (SAW) process using a layer of flux that covers the weld zone and protects the molten material from reaction with oxygen and nitrogen in the air, and (III) the gas metal arc welding (GMAW) process, in which the weld zone is protected by a shielding gas (e.g. Lesnewich *et al.* 1976). With respect to hybrid laser–arc processes, the last variant, i.e. the GMAW process, is of primary interest.

The GMAW technique uses a bare and continuously fed electrode wire with a composition that is equal or similar to the base metal composition. Characteristically, only one current mode with direct current and electrode positive (DCEP) polarity is used. With this current type the majority of the heat is generated at the electrode ensuring high filler metal deposition rates. The continuously fed electrode melts and forms together with the molten material after cooling and resolidification the weld seam. Both electrode and base material are shielded from the atmosphere by use of a shielding gas. The welding procedure is schematically shown in Fig. 3.7.

Depending on the used shielding gas type, two variants are to be distinguished; these are metal inert gas (MIG) welding preferably applied for joining of aluminium, copper and stainless steel and metal active gas (MAG) welding for joining of mild steels, low-alloyed steels and nickel alloys. Active gases used in MAG welding comprise CO_2 and diverse gas mixtures, which are based on Ar and contain additions of O_2, CO_2 and He.

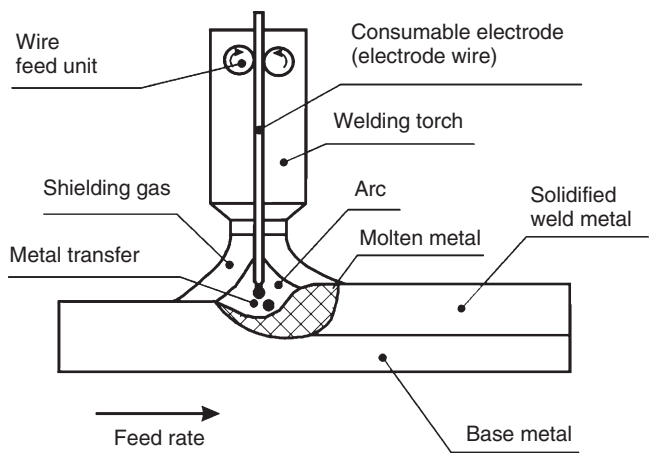

3.7 Schematic diagram of gas–metal arc welding with consumable electrode.

In GMAW processes, the geometry, metallurgy and resultant weld quality is determined by the type of metal transfer between electrode and weld pool. Depending on the current density, the arc power and the shielding gas type, different methods of metal transfer must be distinguished. These are called short-circuiting or short-arc, globular, spray and rotating metal transfer (Schellhase 1985). These basic metal transfer modes are schematically sketched in Fig. 3.8.

Short-circuiting or dip transfer occurs for low values of welding current and arc voltage. In this regime, the arc periodically extinguishes while a short-circuiting bridge of molten metal is formed between electrode and weld pool. Just as the metal transfer into the molten base metal is completed, the arc is reignited again. The frequency of the short-circuiting regime lies in the range 20 to 200 Hz (Manoharan 2006). Since the heat input and the metal deposition rate are low, the short-circuiting mode allows welding of thin materials without large amounts of distortion or residual stress in the weld area.

The globular transfer occuring during GMAW with higher welding amperage and CO_2 or CO_2-rich gas mixtures is characterised by a longer arc length and a metal transfer in the form of large droplets with a diameter typically greater than the diameter of the electrode wire. The droplets detach either by gravity or by short-circuiting, often leaving an uneven weld seam surface or causing spatter. The globular mode is limited to welding ferrous materials with a thickness of 3 mm or more.

At sufficiently high welding amperages, the use of Ar or Ar-rich gas mixtures gives rise to the formation of the spray transfer mode. The current value at which the metal transfer mode changes to the spray mode is sometimes called transition current (Manoharan 2006). In the spray transfer mode, the filler metal from the electrode is transferred in the form of many fine droplets at increased rate of droplet detachment. The last can be

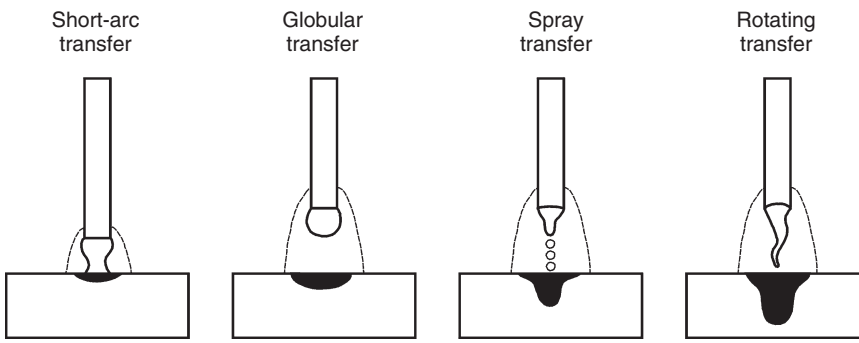

3.8 Basic metal transfer modes in gas–metal arc welding.

controlled by a modified process variant that uses pulsed current in a frequency range between 50 and 300 Hz. For each current pulse, one molten droplet detaches from the electrode. The spray and the pulsed spray transfer mode are mainly applied for welding of non-ferrous metals such as aluminium. Advantages involve the possible high-deposition rates, the good fusion and penetration characteristics, the good weld appearance as well as the absence of spatter during the welding process. However, as the globular transfer mode, the spray transfer mode can be only used for welding of thicker metal sheets with a thickness greater than or equal to approximately 3 mm.

The rotating metal transfer mode sets in at further increased values of the welding current. In this regime, the filler wire electrode begins to rotate under the influence of the surrounding magnetic field. The rotating metal transfer mode allows high deposition rates but the rotating arc is difficult to control, and, consequently, this variant is rarely realised.

Besides the different metal transfer modes of conventional GMAW processes, there are several advancements with specific shielding gas mixtures, which appear under various trade names and provide an increased productivity based on high wire feed speeds and melting rates, respectively. One example is the transferred ionised molten energy (TIME) process that involves a four-component gas mixture consisting of 65% Ar, 26.5% He, 8% CO_2 and 0.5% O_2 (Church and Imaizumi 1990). However, the theory that the type of shielding gas is capable of increasing the achievable melting rates is still controversially discussed (Suban and Tuŝek 2001).

Another development concerns the reduction of the thermal input during GMAW as well as the improved control of material transfer as recently realised in the cold metal transfer (CMT) process developed by Fronius International. The CMT process is based on a dip-transfer arc. However, in contrast to the conventional procedure, an oscillating wire feeding is applied including an interruption of the power supply during the short-circuit period. As the cycle begins, the wire is initially moved towards the work piece. At the moment the short-circuit is detected, the feed direction of the wire is reversed until the short circuit is reopened. After that, the process starts again whereby one droplet detaches from the electrode during each cycle. The CMT process allows spatter-free metal transfer at reduced thermal input (Fronius 2004). These benefits have led to its use for different welding applications. Among others, the CMT process was applied for light-gauge welding (in the range 0.3 and 0.8 mm thickness), for joining of hot galvanized and electrolytically galvanised sheets as well as for brazing of aluminium to steel sheets (Potesser *et al.* 2006, Agudo *et al.* 2007).

3.3.2 Arc sources with non-consumable electrodes

Arc sources with non-consumable electrodes exclusively use tungsten (W) as electrode material. Associate welding processes are then referred to as

gas tungsten arc welding (GTAW). The melting point $\vartheta_{m.p.}(W) = 3350\,°C$ of W is very high compared with the melting points of base materials usually welded and, consequently, high amperages can be realised without melting of the electrodes. Figure 3.9 shows a schematic diagram of the GTAW process, in which the tungsten electrode, the molten metal area and the heat-affected zone are all shielded from the surrounding atmosphere by inert gases such as Ar, He or Ar–He mixtures. An advantage of the GTAW process is that the addition of filler material is separated from the electric circuit. This separation enables an independent determination of amperage and filler metal deposition rate when trying to establish optimal parameters for a given welding problem. In cases where an externally fed filler wire is used, the type of filler metal is usually equal or similar to the chemical composition of the base material. However, in many instances, an addition of filler material is not necessary at all, e.g. when welding thinner materials, edge joints, and flanges. In theses cases, there is no transfer of metal across the arc, and, consequently, there are no molten droplets of spatter to contend with. As a result, often high-quality welds are achievable using the GTAW process. Known variants of GTAW are the tungsten inert gas (TIG) welding process, and the plasma arc welding (PAW) process.

The heat input of a TIG arc into the workpiece depends on the current type and polarity, the amperage, the arc length, the shielding gas composition, the shape and size of the electrode as well as on the chemical composition of the material to be welded. Several choices of polarity and welding current type are feasible, including direct current electrode negative (DCEN), direct current electrode positive (DCEP), alternating current (AC), and pulsed direct current (PDC), see Fig. 3.10.

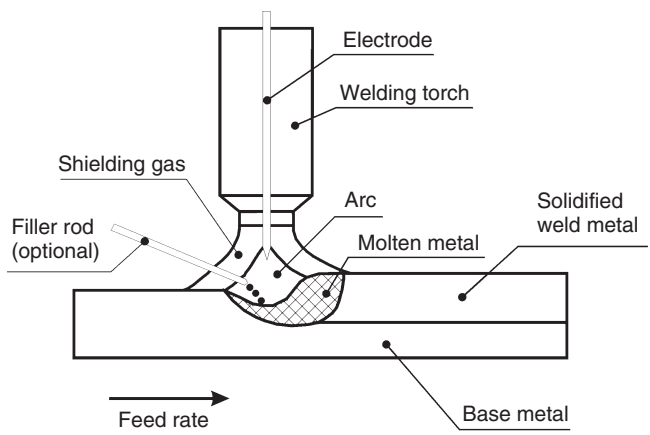

3.9 Schematic diagram of tungsten inert gas welding with non-consumable electrode.

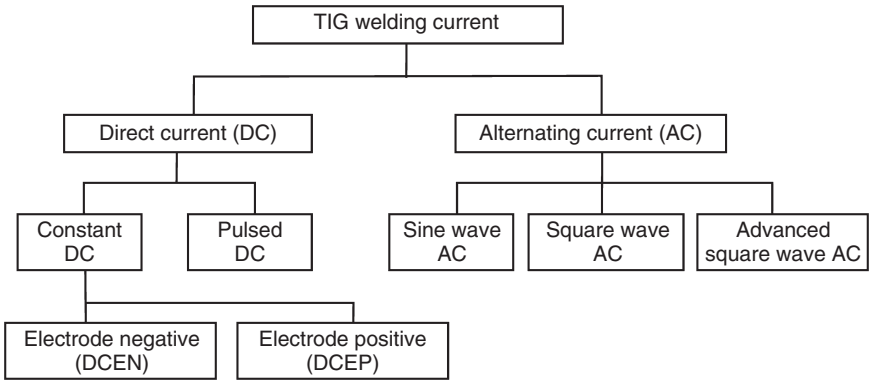

3.10 Schematic presentation of the common TIG welding process variants.

DCEN polarity, sometimes also referred to as straight polarity, is the most commonly used polarity type for TIG welding. The greatest amount of heat is generated in the space of the anodic arc root at the surface of the material to be welded. Consequently, the tungsten electrode dissipates only a relatively small portion of the total heat energy ensuring the highest current carrying capacity of a given electrode size. In addition, the electrode tip is usually sharpened to a conical shape which leads to a more concentrated arc shape. As a consequence, narrow heat-affected zones and deep penetration can be achieved.

The DCEN mode is not applicable for welding of all types of metal. Aluminium for example forms a tenacious oxide layer with a high melting point temperature at its surface and cannot be welded with DCEN polarity. A remedy is the use of DCEP polarity, also termed reverse polarity, leading to a destruction of the oxide layer within the weld zone by evaporation, thermal decomposition and demolition. This phenomenon is called the cleaning effect of the cathodic spot (Schellhase 1985). However, the great disadvantage of the DCEP polarity type is the small current carrying capacity of the welding electrode even with large electrode diameters. To obtain the advantages of both polarities in welding of aluminium commonly alternating current is used. AC–TIG welding combines the good cleaning action of the positive polarity with moderate penetration of the negative polarity current type. The best results are not achieved with conventional sine wave AC but with square wave AC power sources. Modern power supplies with advanced or variable square wave current output have a balance control in order to vary the length of time of the electrode negative and electrode positive cycles. Furthermore, an independent determination of current frequency, electrode negative current level and electrode positive current level

is possible. The ability to separately control these parameters provides an efficient balancing of heat input and cleaning action.

A special direct current type also applied in TIG welding is a pulsed current regime that periodically changes the output current level in a square waveform, i.e. the current level jumps between a maximum and a minimum value without change of the current polarity. The majority of pulsed TIG welding is done in a frequency range of 0.5 to 20 pulses per second with intent to reduce the heat input. In contrast, high frequency pulsing with 200 to 500 pulses per second is used to increase the stiffness of the arc leading to a stabilisation of the arc root and a suppression of arc wandering.

Advancement of the conventional TIG welding process has led to the plasma arc welding process. This variant is based upon a specific torch design, where the tungsten electrode is located within a water-cooled copper nozzle. Two separate gas flows are used, namely the plasma gas and the shielding gas. The inner plasma gas, usually Ar, flows through the copper nozzle, becomes ionised and exits through the constricted orifice of the nozzle at high velocities and with high temperature. The resulting plasma jet is additionally squeezed by the cold shielding gas that is delivered through the outer nozzle. The constriction of the plasma gas flow provides a more concentrated arc that has a significantly higher intensity than a TIG arc at the same amperage, see Fig. 3.11. The plasma arc is stable even at low welding current, less sensitive to arc length variations, and the high arc root intensity allows deep and narrow penetration at increased welding speeds.

In addition to the conventional working regime with the arc between the electrode and the workpiece (transferred arc), there is an alternative mode of operation, in which the plasma arc is burning between the electrode and the constricting nozzle (non-transferred arc). These non-transferred arcs

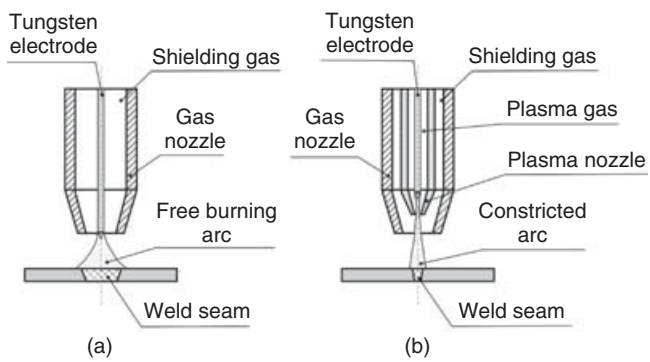

3.11 Schematic diagram of a plasma torch used for (a) tungsten inert gas welding compared with (b) a torch used for plasma arc welding.

are typically applied for plasma spraying processes whereas the transferred arc is the common mode of operation for welding purposes.

The different variants of PAW are distinguished by their dependence on the current range including (I) micro plasma welding, (II) medium or melt-in mode plasma welding and (III) keyhole plasma welding (Weman 2003). Plasma welding with amperages between 0.1 and 15 A is termed micro plasma welding. The resultant stable arc can be applied for welding of sheet thicknesses from 1 mm down to 0.1 mm. The micro plasma welding process provides an advanced level of accuracy for high quality welds in miniature or precision applications. Metal thicknesses in the range between 1 and 3 mm are weldable with the medium or melt-in plasma welding mode. The higher penetration depths are not only a result of the increased current level up to 100 A but also of the surface depression of the liquid weld metal under the influence of the plasma stream pressure. Finally, in the third variant being keyhole plasma welding, the plasma stream pressure is strong enough to drill through the liquid weld bead and to form a keyhole. The molten metal is pressed sidewards, flows around the keyhole and fills the joint behind the jet in a similar way as in deep penetration laser beam welding, see section 3.2.2, where the keyhole is formed by the ablation pressure of the evaporated base material. Plasma welding in the keyhole mode with current levels greater than 100 A allows full penetration welds up to approximately 10 mm thickness.

3.4 Combinations of laser beams and arcs

Laser beams and electric arcs are quite different welding heat sources but both work under a gaseous shielding atmosphere at ambient pressure that makes it possible to combine these heat sources to a unique welding technique referred to as laser–arc hybrid welding (from Latin *hybrida*, a thing made by combining two different elements). In laser–arc welding processes the laser beam as a high-energy density heat source commonly serves as the primary heat source enabling deep penetration mode welding while the arc as secondary heat source undertakes additional functions in order to improve the process stability, reliability and efficiency as well as the quality of the resultant weld seam. In contrast to this definition, heat source combinations where the arc acts as primary heat source are called laser-augmented or laser-supported arc welding processes.

The concept of hybrid laser–arc welding was introduced in the 1970s by Steen and Eboo (Steen and Eboo 1979, Steen 1980) who combined a 2-kW CO_2 laser and a TIG arc for welding and cutting applications. These early investigations already showed that the combination of laser beams and arcs within a common process zone is more than a simple combination of two heat sources. As a result of their initial experiments, it could be

demonstrated that the laser radiation had an essential impact on the arc behaviour leading to a stabilised arc column and a contraction of the arc spot.

Since then, Steen's idea has been developed by many researchers and welding engineers and various laser–arc combinations were examined and developed (e.g. Beyer *et al.* 1994, Seyffahrt *et al.* 1994, Behler *et al.* 1997, Maier 1999, Shibata *et al.* 2001, Ono *et al.* 2002, Behler 2003, Keller 2003, Staufer and Graf 2004, Shi *et al.* 2005, Dilthey *et al.* 2005, Song *et al.* 2006, Reutzel *et al.* 2006, Liu *et al.* 2006b, Staufer 2007). Combinations have involved setups with a common process zone, arrangements where the laser and the arc act separately, as well as setups with more than two sources (e.g. Seyffarth and Krivtsun 2002, Ishide *et al.* 2003, Bagger and Olsen 2005, Mahrle and Beyer 2006). The corresponding technological developments are motivated, on the one hand, by the enhanced capability of the combined process, and, on the other hand, by the fact that deficiencies of the individual processes can be compensated for by the other one. For example, probably the most important feature of laser beam heat sources is their precise control of the spot intensity by the independent determination of laser power and focus diameter, see section 3.2.1. Usually small focus diameters in the sub-millimetre range are realised in order to achieve high intensities enabling deep penetration at high welding speeds. As a result, the welding energy per unit length is comparatively small making the generation of distortion-free welds feasible. However, the extreme focusability of laser beams has also disadvantageous consequences including the high demands to joint fit-up tolerances and accurate seam tracking. These disadvantages can be overcome by the use of an additional arc heat source that widens the weld bead and thus increases the gap bridging ability. Other reported improvements of laser–arc processes involve increases in (I) the welding speed and/or the weldable material thickness, (II) the weld quality with reduced susceptibility to pores and cracks, and (III) the process stability and efficiency (e.g. Beyer *et al.* 1996, Dilthey *et al.* 1999, Hackius *et al.* 2000, Walz *et al.* 2001, Dilthey and Keller 2001, Jokinen *et al.* 2003, Fujinagi *et al.* 2003, Liming *et al.* 2004, Hu and den Ouden 2005, Choi 2006).

3.4.1 Basic setups

Hybrid laser–arc heat sources can be classified by the type of the heat sources to be combined as well as by the arrangement of the selected heat sources relative to each other (Mahrle and Beyer 2006). Principal variation possibilities can be derived from the Fig. 3.12 and 3.13. The specification of setups for hybrid laser–arc processes consequently involves the choice of at least one primary and one secondary heat source as well as the determination of the geometrical relations in the arrangement of these heat sources.

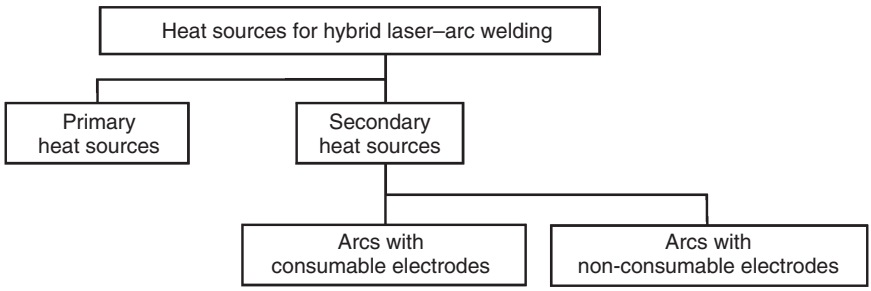
Heat sources for hybrid laser–arc welding
Primary heat sources
Secondary heat sources
Arcs with consumable electrodes
Arcs with non-consumable electrodes

3.12 Schematic presentation of heat sources available for hybrid laser–arc combinations.

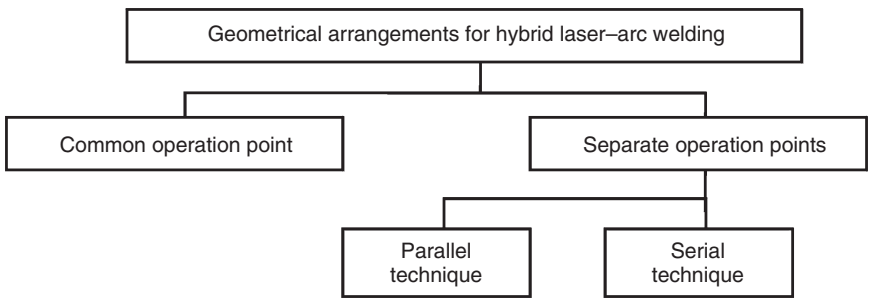

3.13 Geometrical arrangements for hybrid laser–arc welding.

The various high-power laser types commonly used for welding purposes, including the CO_2 laser, the Nd:YAG laser, the disc and fibre laser as well as the fibre-coupled high-power diode laser, are capable of serving as primary heat sources. In recent years, the most proven laser systems for hybrid technology developments were CW CO_2 and Nd:YAG lasers mainly because of their prevalence in laboratory and industrial environments. However, disc, fibre and fibre-delivered high-power diode lasers also meet all requirements to act as primary heat sources, and it is expected that these laser types will be increasingly applied for future hybrid technology developments.

Besides the required laser power and beam quality that both determine the achievable penetration depth, one main criterion for the selection of the primary laser beam heat source is the wavelength of the emitted radiation, which can restrict the choice of the usable shielding gas type. For example, welding with a CO_2 laser commonly needs gas mixtures with a

high He content or pure He in order to suppress plasma shielding effects whereas for the other high-power laser types Ar and Ar-based gas mixtures with additions of active gas components such as CO_2 or O_2 can be used. Consequently, hybrid combinations with Nd:YAG, disc, fibre or high-power diode lasers offer more flexibility in influencing the metallurgy of the weld pool and the metal transfer of the arc welding process (when using consumable electrodes) by allowing greater choice of suitable shielding gases.

As secondary heat sources, either arcs with consumable electrodes, i.e. gas metal arcs, or arcs with non-consumable electrodes, i.e. gas tungsten or plasma tungsten arcs can be chosen. The essential criterion for the choice of the electrode type is usually the necessity of filler metal for solving a specific welding problem. If any addition of filler metal is required then procedures with consumable electrodes should be applied, otherwise arcs with non-consumable electrodes are preferred. The specification of each particular process combination usually depends on the specific demands of the welding problem to be solved. Considering the various possible process regimes of each individual heat source as described in the previous sections 3.2 and 3.3, the specification of appropriate processing parameters for hybrid laser–arc techniques must be regarded as a challenging task.

In addition to a specified heat source combination, the geometrical arrangement of the chosen heat sources plays the most important role for the capability and efficiency of the hybrid process as well as for the properties of the generated joints. It is important to distinguish between techniques with common and separated operation points. Realising a common operation point means that the arc root and the laser beam spot centre are directed into the same surface location on the material being welded. This is exactly accomplished by a coaxial configuration of the laser beam and the electric arc. Technical realisations of such an arrangement comprise for example (I) the use of a special mirror system that turns the laser radiation around a coaxially placed electrode (Steen 1979), (II) the use of a set of several rod electrodes on a cylindrical insulator that allows the beam to be focused throughout (Hashiura *et al.* 1985), and (III) the direct use of ring-shaped or hollow electrodes. Although those coaxial solutions are still technically interesting, the majority of practically realised hybrid laser–arc combinations have used arrangements where a conventional welding torch and electrode are inclined in relation to the incident laser beam. Figure 3.14 shows possible arrangements with inclined welding torches in the plane along (left hand side) and across (right hand side) the welding direction.

The first variant is the preferred arrangement for conventional hybrid laser–arc seam welding. The arc roots into the laser-generated keyhole where the vaporised metal offers an easy to ionise conductive medium

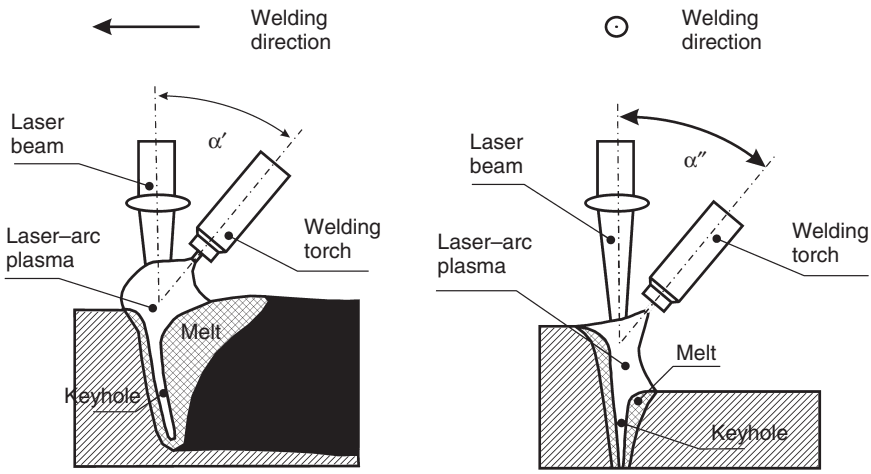

3.14 Schematic diagrams of hybrid laser–arc welding with a common operation point.

because of its low ionisation potential. Beyer *et al.* (1994) used such an arrangement with a Nd:YAG laser as primary and a TIG arc as secondary heat source and found that the available laser power mainly determines the achievable penetration depth, whereas the control of the arc parameters allows for adjustment of the weld seam width. As a result, the requirements for edge preparation could be reduced. Furthermore, by combining the arc and the laser beam in an optimal way, the same welding depth was achieved with reduced laser power or, alternatively, an increase of the welding speed was possible. The second variant with a transversely inclined welding torch was applied by the same research group for welding of tailored blanks, i.e. plates with different thicknesses as shown in Fig. 3.14, on the right hand side, where the combined impact of both heat sources (I) reduced the edge preparation requirements, (II) increased the volume of the molten material, (III) improved the weld appearance with a smooth transition zone between the sheets because the arc was burning preferably to the edge of the thicker plate, and (IV) increased the process efficiency resulting in significantly higher welding speeds compared with the laser welding process alone.

One important advantage of the individual and independent arrangement of the selected heat sources is the fact that both operation points can be easy separated by changing the inclination angles or leaving a certain distance between the laser beam axis and the welding torch. This allows the user to adapt the characteristics of the resultant hybrid heat source, for example the effective intensity distribution, to special requirements and/or specific boundary conditions of a particular welding problem. In addition,

possible undesired interactions between the laser radiation and the electric arc, e.g. an attenuation of the laser beam intensity by scattering or reflection and absorption effects within the arc column, can be minimised or avoided. Furthermore, the many possibilities to arrange both heat sources relative to each other offers a great potential for process optimisation.

Various operation points imply a temporal and/or local separation of the selected heat sources. Several configurations can be realised as already schematically represented in Fig. 3.13. A parallel arrangement is characterised by a distance in the vertical or horizontal direction along the path between both heat sources. In contrast, the primary and the secondary heat source are moved along the same weld path in serial arrangements but with a certain working distance, realising either a pre-running (leading arc) or post-running (trailing arc) of the secondary heat source. The pre-running variant enables an effective preheating of the region to be welded. This can increase (I) the efficiency of the primary laser beam heat source because energy losses by heat conduction are reduced and (II) the quality of the resultant weld seam owing to stabilised keyhole behaviour. In comparison, the post-running arrangement with small distances to the leading beam is also capable of increasing the efficiency and stability of the laser beam welding process owing to interactions between laser and arc within a common process plasma and a modified thermal impact on the material being welded. In addition, applying greater distances to the leading laser beam, the post-running variant can be applied to act as a short-time post-heat treatment of the laser weld seam that can favourably change the microstructure and improve the properties of the weld. Regarding the thermal load of the material to be welded it must be considered that there is an essential difference between parallel and serial process arrangements. Using a serial order, the additional energy is dissipated within the same weld seam region, whereas in parallel arrangements the energy is distributed to different areas.

In practice, however, it is not always possible to strictly distinguish between parallel and serial arrangements because both types of displacement are often applied simultaneously. Figure 3.15 schematically shows a hybrid laser arc welding process with strictly separated operation points in parallel (vertical) and serial order (trailing arc). The specific Y-groove seam preparation enables welding of the root, i.e. the bottom part of the joint, with the laser beam and the final top layer by a successive arc welding process with consumable electrodes. Seyffahrt *et al.* (1994) used such an arrangement with the aim of increasing the weldable plate thickness according to the specific requirements of the shipbuilding industry. The process can be carried out as a two-step variant (multi-pass) with different welding speeds of both heat sources and as a one-step variant (single-pass) with an aligned feed rate of both heat sources. Even though the laser beam and the

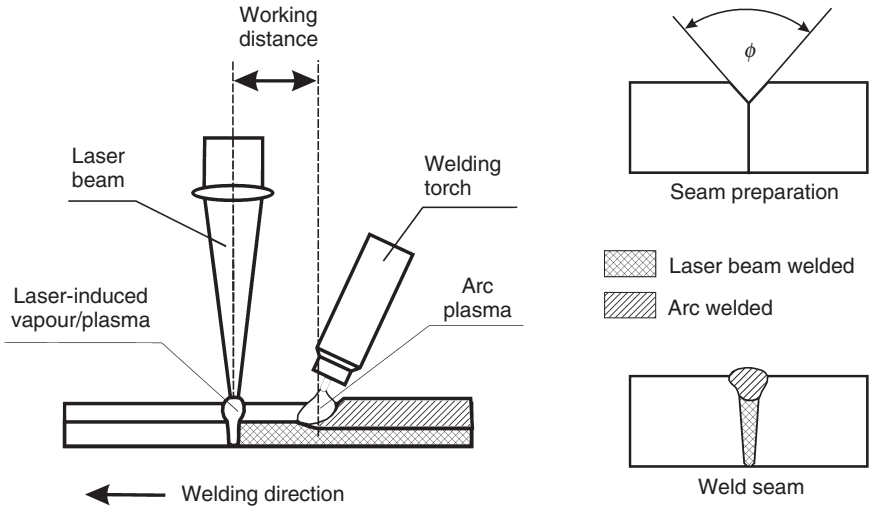

3.15 Schematic diagram of hybrid laser–arc welding with separate operation points.

arc do not cooperate directly, some synergistic effects result. First, the fixation of the workpieces by the laser-welded joint diminished welding distortions after the arc welding (MAG) process. Secondly, the additional energy of the arc led to an annealing of the laser-welded joint with the effect that the hardness of the seam was favourably reduced.

In addition to the previously discussed variants with either a common operation point or strictly separated operation points there is a transition regime, in which both heat sources are capable of directly interacting despite a certain working distance between them. Investigations by Matsuda *et al.* (1988) showed that the welding results, in addition to the principal parameters such as laser power, arc amperage and feed rate, strongly depend on the distance between laser beam and electrode (serial displacement) as well as on the focal position of the laser beam (parallel displacement). In the case of the CO_2 laser combinations with TIG and MIG having up to 5 kW laser power, arc currents in the range 100 to 400 A, an inclined welding torch (45 °) with respect to the incident laser beam, and an effective suppression of plasma formation by means of He gas shielding, it was found that the maximum value of penetration is achieved at the smallest possible distance between laser beam axis and electrode tip. This phenomenon is mainly caused by the fact that the laser beam at small distances to the tip of the welding electrode strikes the deepest part of the melt pool surface, which is commonly depressed by the arc forces present. In addition,

the focal position must be set to coincide with the surface depression in order to reach the maximum penetration depth possible, i.e. the optimal focus position depends on parameters such as arc current and welding speed.

Subsequent investigations with a similar experimental setup combining a CO_2 laser with 7 kW output power and a MIG arc with 9.75 kW power were carried out by Abe *et al.* (1997) who additionally analysed the behaviour of the laser and arc plasma by means of high-speed photographs. Using He as assist gas, the welding speed, the assist gas flow rate and the distance between laser and arc were varied for welding experiments on mild steel plates. It was found that the laser-induced plasma is capable of stabilising the arc column. Initially, at a distance of 3 mm between the laser beam axis and the electrode tip, one single plasma was observed for a feed rate of 2 m min^{-1}. Increasing the welding speed led to the appearance of two separate plasmas, i.e. the laser-generated and the arc plasma, but the arc plasma remained under the arc torch whereas it was shifted increasingly backwards when arc welding alone was performed. The strength of the stabilising effect depends on the distance between laser beam and arc and disappears for greater displacements.

Research results by Beyer *et al.* (1996) showed that the type of interaction in hybrid setups with separated operation points strongly depends on the type of the selected laser beam source as well as on the properties of the material being welded. Combining a Nd:YAG laser beam and a TIG arc with a working distance of some millimetres, it has been found that the arc column is pushed away from the laser-generated keyhole and the escaping metal vapour stream, respectively. However, this behaviour was only observed when welding steel with a comparatively good conduction surface. In contrast, when welding aluminium, which normally has a poorly conducting oxide layer at the surface, the arc was deflected towards the keyhole. Realising the same experimental set-up with a CO_2 laser, the guiding of the arc was detected for both materials.

In summary, it is not possible to give general recommendations for optimal basic setups in hybrid laser–arc welding because there are many specific factors of influence that must be taken into account. The most proven arrangements combine the laser beam and the electric arc within a common process zone leading to a single process plasma and a common weld pool. CO_2 lasers seem to be capable of stabilising and guiding the electric arc even at certain distances between the laser beam axis and electrode tip. However, the usable shielding gas type is restricted to He or gas mixtures with a high He content in order to suppress plasma shielding effects. The other available high-power laser types offer the advantage of a shorter wavelength giving more flexibility with respect to the usable shielding gas type.

3.4.2 Setups with more than two sources

Besides the conventional hybrid laser–arc processes with one laser beam as primary and one electric arc as secondary heat source, there have also been some technological developments that make use of two or even more electric arcs. Possible basic configurations already applied for different reasons are schematically presented in Fig. 3.16. The first arrangement (a) was realised by Winderlich (2003) using a CO_2 laser as primary heat source and two trailing TIG torches as secondary heat sources. During the process, the first TIG arc (torch 1) was operating at the same side as the laser beam, and the second (torch 2) at the opposite side with the purpose to generate an optimal notch-free weld seam geometry appropriate for dynamic loading. Compared with the pure laser beam welding process, the fatigue resistance could be increased by approximately 50%.

The second set-up (b) is characterised by two separate arc welding torches acting at the same side as the laser beam. The laser beam and the welding arcs are all aligned along the weld line with the leading arc (torch 1) in a backhand configuration and the trailing arc (torch 2) in a forehand configuration. Such an arrangement, also referred to as Hydra (hybrid welding with double rapid arc) process, was originally applied by Dilthey and Keller (2001) who combined a CO_2 laser welding process with two GMAW processes. In comparison with the conventional hybrid laser–arc process with only one arc as secondary heat source the deposition rate of the filler material could be further increased leading to higher welding speeds and a reduced thermal load. Alternative configurations of the Hydra process also comprise variants where the arcs are arranged parallel to the weld line either in a leading or trailing position relative to the laser beam axis. The inclination angles can be varied so that both

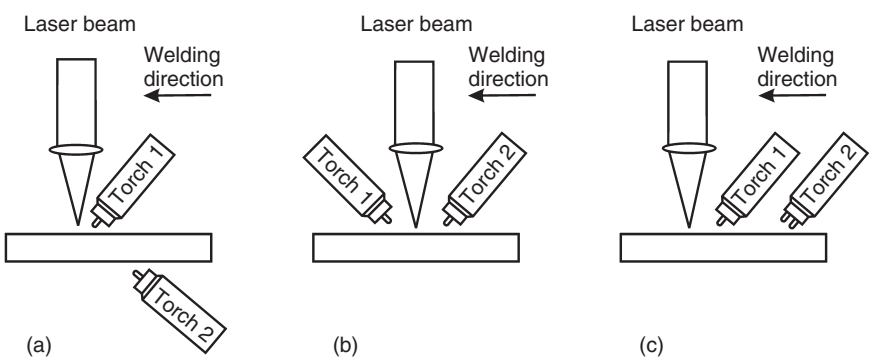

3.16 Schematic diagrams of hybrid laser–arc processes with two secondary heat sources.

backhand and forehand configurations can be realised. Concerning the gap bridging ability, the best results were achieved with two leading arcs (Wieschemann 2001).

The special feature of the third variant (c), recently realised by Staufer (2007) is the application of a tandem welding process (torch 2) as additional heat source. Tandem wire welding methods which make use of two consumable electrodes (each with its own power source) are commonly used for increasing the welding productivity by increasing the deposition rate of the filler material. In combination with the conventional hybrid laser–arc process (laser beam and torch 1) the cooling rates of the weld can be systematically controlled by varying the distance between the hybrid and the tandem-arc process.

3.5 Future trends

In recent years, many variants of the laser–arc processes have been developed and fundamentally investigated demonstrating good potential for robust and efficient solutions for practical welding problems. Industrial applications of the hybrid welding technique have been realised in the automotive (e.g. Graf and Staufer 1999, Ono *et al.* 2002, Staufer *et al.* 2003) and the shipbuilding sector (e.g. Jokinen *et al.* 2000, Jasnau *et al.* 2002, McPherson *et al.* 2005). Other industrial branches that already make use of hybrid laser–arc heat sources involve pipe-line and offshore installations, the aerospace and aviation industry, the power-generation industry and the off-road and heavy vehicles sector (Wouters 2005). Owing to the reported improvements in productivity, efficiency and quality, it can be expected that hybrid welding methods will be increasingly adopted for future industrial welding applications as a promising alternative to conventional welding methods.

So far, probably the most important feature of hybrid laser–arc heat sources was the capability of offering an increased gap bridging ability at simultaneously low energy inputs per unit length owing to the high welding speeds which were achievable. However, the high flexibility of the process also allows for an efficient control of the weld seam properties, including the weld seam shape (e.g. El Rayes *et al.* 2004, Kaplan *et al.* 2007), porosity (e.g. Naito *et al.* 2003) and microstructure (e.g. Moore *et al.* 2004, Liu *et al.* 2006c). Whilst most of the reported work was carried out on steels and aluminium alloys it has also been proven that the hybrid technique is capable of improving the weld and process characteristics for welding of other materials such as magnesium (e.g. Liu *et al.* 2005, Song *et al.* 2006).

The high flexibility of the hybrid laser–arc process is associated with a high number of additional parameters, which must be adapted for optimal welding results. This process complexity issue could still be a restricting

factor with regard to widespread adoption of hybrid laser–arc sources in industry. However, commercial welding heads that integrate a laser beam with a conventional arc source are already available (e.g. Graf and Staufer 1999, Ishide *et al.* 2003) which can provide efficient control of all of the relevant parameters of the hybrid welding process for different applications.

To date, the most proven laser systems for hybrid laser–arc processing were CO_2 and Nd:YAG lasers. However, the recently developed and now commercially available disc and fibre laser systems should also be considered as an attractive alternative to the conventional laser beam sources because of their unique properties combining high output power and excellent beam quality with the advantages of a short wavelength, see section 3.2.3. It is consequently expected that, by use of these new laser sources, the further development of innovative hybrid laser–arc variants can be supported. Initial investigations that made use of the fibre laser as the primary heat source in hybrid laser–arc welding confirmed this assumption (Liu *et al.* 2007, Thomy *et al.* 2007).

Another interesting trend is the rediscovered use of low-power laser beams for guidance and stabilisation of electric arc welding processes, referred to as laser-assisted or laser-enhanced arc welding methods. A characteristic feature of these processes is the fact that only low intensities of laser radiation are applied, i.e. the required laser power is small compared with the total arc power, and the laser acts as a secondary heat source only. Early in the 1990s, it was already demonstrated that a low-energy CO_2 laser beam with an output power of merely 100 W is capable of (I) supporting the arc ignition, (II) increasing the stability of the arc, (III) improving the weld quality, and (IV) allowing higher welding speeds owing to a reduced arc size and higher arc amperages, respectively (Cui 1991, Finke *et al.* 1991, Cui *et al.* 1992, Decker *et al.* 1995). Recent investigations have been demonstrated also stabilizing effects of Nd:YAG radiation on a tungsten inert gas welding (TIGW) process, as well as of diode laser radiation (wavelength $\lambda = 0.808\ \mu m$) on a gas metal arc welding (GMAW) process (Kling *et al.* 2007, Hermsdorf *et al.* 2008).

3.6 References

ABE, N *et al.* (1997), 'Dynamic observation of high-speed laser–arc combination welding of thick steel plates', in Fabbro *et al.*, *Proc. of the Laser Materials Processing Conference ICALEO'97*, Orlando, Laser Institute of America, 155–163.

BAGGER, C and OLSEN F O (2005), 'Review of laser hybrid welding', *Journal of Laser Applications*, **17**(1), 2–14.

BECK, M *et al.* (1995), 'The effect of plasma formation on beam focusing in deep penetration welding with CO_2 lasers', *Journal of Physics D: Applied Physics*, **28**, 2430–2442.

BEHLER, K *et al.* (1997), 'Kombination von Laserstrahl- und Metallschutzgasschweißen zum Fügen unlegierter Stähle', *Schweißen und Schneiden'97*, DVS-Berichte, Band 186, DVS-Verlag Düsseldorf, 182–186.

BEHLER, K (2003), 'Hybrid welding technology – a flexible method for industrial applications', *Proc. of the LASERAP'05*, Les Hauts de Marquay (France), 56–72.

BEYER, E (1985), *Einfluss des laserinduzierten Plasmas beim Schweißen mit CO_2 Lasern*, Dissertation, Technische Hochschule Darmstadt.

BEYER, E (1995), *Schweißen mit Laser*, Berlin – Heidelberg, Springer.

BEYER, E *et al.* (1994), 'New aspects in laser welding with an increased efficiency', in Dwayne *et al.*, *Proc. of the Laser Materials Processing Conference ICALEO'96*, Orlando, Laser Institute of America, 183–192.

BEYER, E *et al.* (1996), 'Hybrid laser welding technique for enhanced welding efficiency', in Duley, W *et al.*, Proc. of the *Laser Materials Processing Conference ICALEO'96*, Orlando, Laser Institute of America, 157–166.

BEYER, E *et al.* (2007), 'Welding and cutting of copper with high brightness lasers', *Proc. of the 26th Int. Congress on Applications of Lasers and Electro Optics*, Orlando (USA), paper 208, 98–101.

BEYER, E (2008), 'High power laser materials processing – new developments and trends', *Proc. of the 3rd Pacific Int. Conf. on Applications of Lasers and Optics*, Bejing (China), 5–9.

BROCKMANN, R *et al.* (2007), 'High performance industrial disc lasers for a broad range of applications', *Proc. of the 26th Int. Congress on Applications of Laser and Electro-Optics ICALEO 2007*, Orlando (USA), paper 1603, 866–870.

CHOI, H W *et al.* (2006), 'Using a hybrid laser plus GMAW process for controlling the bead humping defect', *Welding Journal*, **85**(8), Welding Research Supplement, 174s–179s.

CHURCH, J and IMAIZUMI, H (1990), 'T.I.M.E. process', *IIW/IIS* Doc. XII-1999-90.

CUI, H (1991), *Untersuchung der Wechselwirkungen zwischen Schweißlichtbogen und fokussiertem Laserstrahl und der Anwendungsmöglichkeiten kombinierter Laser-Lichtbogentechnik*, Dissertation, TU Braunschweig (Germany).

CUI, H *et al.* (1992), 'Laserinduziertes Fokussieren des WIG-Lichtbogens', *Schweißen und Schneiden'92*, DVS-Verlag Düsseldorf (Germany), DVS-Berichte, Band **146**, 139–143.

DAVIS, J and BERKMANNS J (2001), 'Carbon dioxide lasers', in Ready, J F and Farson D F, *LIA Handbook of Laser Materials Processing*, Orlando, Laser Institute of America, Magnolia Publishing, Inc., 27–35.

DAWES, C (1992), *Laser Welding – A Practical Guide*, Cambridge, Abington Publishing.

DECKER, I *et al.* (1995), 'Laserstrahl-WIG-Schweißen von Aluminiumlegierungen', *Schweißen und Schneiden'95*, DVS-Verlag Düsseldorf (Germany), DVS-Berichte, Band **170**, 96–99.

DILTHEY, U *et al.* (1999), 'Erweiterte Möglichkeiten beim Schweißen von Aluminiumlegierungen durch den Laser-MIG-Hybridprozess', *Aluminium*, **75**. Jahrgang, 64–75.

DILTHEY, U and KELLER, H (2001), 'Prospects in laser GMA hybrid welding of steel', *Proc. of the First Int. WLT-Conf. on Lasers in Manufacturing*, AT Fachverlag, 453–465.

DILTHEY, U *et al.* (2005), 'Laserstrahl-MSG-Hybridschweißen – Neue Fertigungsmöglichkeiten für den Rohrbau', *Schweißen und Schneiden*, **57**(7), 323–329.

DILTHEY, U and KELLER, H (2001), 'Einsatz der Hybrid- und Hydra-Schweißverfahren zur Wirtschaftlichkeitssteigerung im Schiffbau', *Proc. Schweißen und Schneiden 2001*, Düsseldorf, DVS-Verlag, 56–62.

DIN EN ISO 11145 (2002), *Laser und Laseranlagen*, Normenausschuss Feinmechanik und Optik im DIN Deutsches Institut für Normung e.V.

DULEY, W W (1999), *Laser Welding*, New York, John Wiley & Sons.

EL RAYES, M *et al.* (2004), 'The influence of various hybrid welding parameters on bead geometry', *Welding Journal*, **83**(5), Welding Research Supplement, 147s–153s.

FINKE, B R *et al.* (1991), 'Auswirkungen eines unterstützenden Laserstrahls auf den WIG-Schweißprozess', *Lectures and Posters of the 3rd Int. Beam Technology Conf., DVS-Verlag Düsseldorf (Germany)*, DVS-Berichte, Band **135**, 149–151.

FRONIUS (2004), 'CMT: Cold Metal Transfer', Brochure, Fronius International GmbH.

FUJINAGI, S *et al.* (2003), 'Improvements of welding characteristics of aluminium alloys with YAG laser and TIG arc hybrid system', *Proc. of the First Int. Symposium on High-Power Laser Macroprocessing, 2002, Proc. of SPIE*, **5831**, 301–306.

GAPONTSEV, V *et al.* (2007), 'Der Faserlaser – Schweißen und Schneiden von 100 W bis 20 kW', *Große Schweißtechnische Tagung 2007*, DVS-Verlag Düsseldorf (Germany), DVS-Berichte, Band **244**, 3–7.

GRAF, T and STAUFER H (1999), 'Laser hybrid process at Volkswagen', *IIW*-Doc. XII-1730–02.

GÖBEL, G *et al.* (2007), 'New application possibilities for fibre laser welding', *Proc. of the 26th Int. Congress on Applications of Laser and Electro-Optics ICALEO 2007*, Orlando (USA), paper 209, 102–108.

HACKIUS, J *et al.* (2000), 'Innovation in laser hybrid technology for aluminium welding', *Proc. of the Laser Materials Processing Conference ICALEO 2000*, Orlando (USA), B8–B19.

HASHIURA, M *et al.* (1985), *Laser working device*, Claim 60–106688, Japan.

HERMSDORF, J *et al.* (2008), 'Guidance and stabilisation of electric arc welding using Nd:YAG laser radiation', *Proc. of the 3rd Pacific Int. Conf. on Application of Lasers and Optics*, paper 707, 335–340.

HIPPLER, R *et al.*, (2001), *Low Temperature Plasma Physics*, Berlin, Wiley-VCH.

HU, B and DEN OUDEN, G (2005), 'Synergetic effects of hybrid laser/arc welding', *Science and Technology of Welding and Joining*, **10**(4), 427–431.

HÜGEL, H (1992), *Strahlwerkzeug Laser*, Stuttgart, Teubner.

IAMMI, J *et al.* (2008), 'Fibre laser welding of Ti6Al4V', *Proc. of the 3rd Pacific Int. Conf. on Applications of Lasers and Optics, Bejing (China)*, paper 601, 152–157.

ISHIDE, T *et al.* (2003), 'Latest MIG, TIG arc–YAG laser hybrid welding systems for various welding products', in Miyamoto, L. *et al.*, *First Int. Symposium on High-Power Laser Macroprocessing, Proc. of SPIE*, **4831**, 347–352.

JASNAU, U *et al.* (2002), 'Nd:YAG laser–gas metal arc hybrid welding: a change for the use of the advantages of laser technology and flexible automation in shipbuilding and steel construction', *Proc. of the Int. Conf. on Robotic Welding, Intelligence and Automation RWIA'2002*, Shanghai, December 9–12.

JOKINEN, T *et al.* (2000), 'Welding of ship structural steel A36 using a Nd: YAG laser and gas–metal arc welding', *Journal of Laser Applications*, **12**(5), 185–188.

JOKINEN, T *et al.* (2003), 'Optimisation of parameters in hybrid welding of aluminium alloy', *Proc. of the First Int. Symposium on High-Power Laser Macroprocessing, 2002, Proc. of SPIE*, **5831**, 307–312.

KAPLAN, A F H *et al.* (2007), 'Shaping and optimising hybrid weld seam geometries', in Vollertsen *et al.*, *Proc. of the 4th Int. WLT-Conf. on Lasers in Manufacturing LIM 2007*, Munich, AT-Fachverlag GmbH, 73–77.

KATAYAMA, S *et al.* (2007), 'Weld penetration and phenomena in 10 kW fibre laser welding', *Proc. of the 26th Int. Congress on Applications of Lasers and Electro-Optics ICALEO 2007*, Orlando (USA), paper P540, 353–359.

KELLER, H (2003), 'CO_2-Laserstrahl-MSG-Hybridschweißen von Baustählen im Blechdickenbereich von 12 bis 25 mm', Dissertation, RWTH Aachen (Germany), Shaker Verlag.

KINOSHITA, K *et al.* (2006), 'Phenomena of welding with high power fibre laser', *Proc. of the 25th Int. Congress on Applications of Lasers and Electro-Optics ICALEO 2006*, Scottsdale (USA), paper 902, 535–542.

KLING, R *et al.* (2007), 'Minimale Laserleistung mit Lasern angepasster Strahleigenschaften für das Laser/MSG-Hybrid-Schweißen in Fertigungssystemen für die Fahrzeugfertigung', in *Die Verbindungsspezialisten*, DVS-Verlag Düsseldorf, DVS-Berichte, Band **244**, 409–418.

KOU, S (1987), *Welding Metallurgy*, New York, John Wiley & Sons.

KREUTZ, E W (1991), 'Bearbeitbarkeit von Werkstoffen mit Laserstrahlung', in Bimberg D, *Materialbearbeitung mit Lasern*, Ehningen bei Böblingen, expert-Verlag, 94–99.

KUGLER, T R (2001a), 'Fusion front penetration', in Ready, J F and Farson D F, *LIA Handbook of Laser Materials Processing*, Orlando, Laser Institute of America, Magnolia Publishing, Inc., 310–313.

KUGLER, T R (2001b), 'Nd:YAG lasers', in Ready, J F and Farson D F, *LIA Handbook of Laser Materials Processing*, Orlando, Laser Institute of America, Magnolia Publishing, Inc., 37–44.

LESNEWICH, A *et al.* (1976), 'Survey of processes for joining and cutting materials', in Weisman, C (ed.), *Welding Handbook*, 7th edition, vol. 1: Fundamentals of Welding, American Welding Society, Miami (USA), 1–32.

LI, L (2000), 'The advances and characteristics of high-power diode laser materials processing', *Optics and Lasers in Engineering*, **34**, 231–253.

LIMING, L *et al.* (2004), 'Hybrid laser–TIG welding, laser beam welding and gas tungsten arc welding of AZ31B magnesium alloy', *Materials Science and Engineering A*, **381**, 129–133.

LIU, L *et al.* (2005), 'Pore formation during hybrid laser-tungsten inert gas arc welding of magnesium alloy AZ31B – mechanism and remedy', *Materials Science and Engineering A*, **390**, 76–80.

LIU, Z *et al.* (2006a), 'Fibre laser welding of 780 MPa high strength steel', *Proc. of the 25th Int. Congress on Applications of Lasers and Electro-Optics ICALEO 2006*, Scottsdale (USA), paper 1101, 562–568.

LIU, Z *et al.* (2006b), 'CO_2 laser – MAG hybrid welding of 590 MPa high-strength steel', *Quarterly Journal of the Japan Welding Society*, **24**(1), 17–25.

LIU, Z *et al.* (2006c), 'Microstructure and mechanical properties of CO_2 laser-MAG hybrid welding of high-strength steel', *Quarterly Journal of the Japan Welding Society*, **24**(4), 334–349.

LIU, Z *et al.* (2007), 'Laser and Laser–MAG hybrid welding of high-strength steel using fiber laser and CO_2 laser', *Quarterly Journal of the Japan Welding Society*, **25**(2), 254–260.

MAHRLE, A and BEYER, E (2006), 'Hybrid laser beam welding – classification, characteristics and applications', *Journal of Laser Applications*, **18**(3), 169–180.

MAIER, C (1999), *Laserstrahl-Lichtbogen-Hybridschweißen von Aluminiumwerkstoffen*, Dissertation, RWTH Aachen (Germany), Shaker Verlag.

MANOHARAN, S (2006), 'Arc Welding Processes', in Raj, B, Shankar, V and Bhaduri, A K, *Welding Technology for Engineers*, Oxford, Alpha Science International Ltd., 116–156.

MANZ, A F *et al.* (1976), 'Physics of welding', in Weisman, C (ed.), *Welding Handbook*, 7th edition, vol. 1: *Fundamentals of Welding*, American Welding Society, Miami (USA), 1–32.

MATSUDA, J *et al.* (1988), 'TIG or MIG arc augmented laser welding of thick mild steel plate', *Joining and Materials*, July 1988, 31–34.

MATSUNAWA, A (1991), 'Beam – plasma interaction in laser materials processing by different wavelength', in Waidelich, W, *Laser in der Technik*, Proc. of the 10. Int. Congr. Laser '91, Berlin, Springer, 263–271.

MCPHERSON, N A *et al.* (2005), 'Laser and laser-assisted arc welding processes for DH 36 microalloyed steel ship plate', *Science and Technology of Welding and Joining*, **10**(4), 460–467.

MESSLER, R W (2004), *Principles of Welding*, Weinheim, WILEY-VCH Verlag GmbH.

MODEST, M F (2001), 'Reflectivity and absorptivity of opaque surfaces', in Ready, J F and Farson D F, *LIA Handbook of Laser Materials Processing*, Orlando, Laser Institute of America, Magnolia Publishing, Inc., 175–182.

MOORE, P L *et al.* (2004), 'Microstructure and properties of laser/arc hybrid welds and autogenous laser welds in pipeline steels', *Science and Technology of Welding and Joining*, **9**(4), 314–322.

NAGAYAMA, H *et al.* (2007), 'Weld penetration and welding phenomena of aluminium alloy with high power fiber laser', *Proc. of the 26th Int. Congress on Applications of Laser and Electro-Optics ICALEO 2007*, Orlando (USA), paper P513, 916–924.

NAITO, Y *et al.* (2003), 'Observation of keyhole behaviour and melt pool flow during laser–arc hybrid welding', *Proc. of the Laser Materials Processing Conference ICALEO 2003*, Paper 1005.

ONO, M *et al.* (2002), 'Development of laser–arc hybrid welding', *NKK Technical Review*, **86**, 8–12.

PEDROTTI, F *et al.* (2002), *Optik für Ingenieure*, 2nd edition, Springer, 602.

PITSCHENEDER, W *et al.* (1996), 'Role of sulphur and processing variables on the temporal evolution of weld pool geometry during multi-kilowatt laser beam welding of steel', *Welding Journal*, **75**(3), Welding Research Supplement, 71s–80s.

PITSCHENEDER, W *et al.* (1998), 'Experimental and numerical investigation of transport phenomena in conduction mode weld pools' in: Cerjak, H (ed.), *Mathematical Modelling of Weld Phenomena 4*, London, IOM Communications, 2–25.

RADAJ, D (1999), *Schweißprozesssimulation – Grundlagen und Anwendungen*, DVS-Verlag Düsseldorf.

READY, J F *et al.* (2001), 'Conduction welding', in Ready, J F and Farson D F (eds.), *LIA Handbook of Laser Materials Processing*, Orlando, Laser Institute of America, Magnolia Publishing, Inc., 307–359.

REAM, S (2006), 'High-speed fiber laser welding for fuel cell components', *Proc. of the 25th Int. Congress on Applications of Lasers and Electro-Optics ICALEO 2006*, Scottsdale (USA), paper 1302, 586–594.

REUTZEL, E W *et al.* (2006), 'Joining pipe with the hybrid laser-GMAW process: weld test results and cost analysis', *Welding Journal*, **85**(6), 66–71.

SCHELLHASE, M (1985), *Der Schweißlichtbogen – ein technologisches Werkzeug*, Berlin, Verlag Technik.

SEEFELD, T and O'NEILL, W (2007), 'High brightness laser cutting and welding', *Proc. of the Fourth Int. WLT-Conference on Lasers in Manufacturing*, Munich (Germany), 311–320.

SEYFFARTH, P and KRIVTSUN I V (2002), *Laser–Arc Processes and their Applications in Welding and Material Treatment*, London, Taylor & Francis.

SEYFFAHRT *et al.* (1994), 'Combination of laser beam arc welding', *Proc. of the 5th European Conference on Laser Treatments of Materials ECLAT'94*, Düsseldorf, DVS-Verlag, 377–395.

SHI, S *et al.* (2005), 'Hybrid Nd:YAG laser – MAG welding of thick section steel with adaptive control', *The Industrial Laser User*, **38**, 34–37.

SHIBATA, K *et al.* (2001), 'Laser-MIG hybrid welding of aluminium alloys', Proc. of the First Int. WLT-Conf. on Lasers in Manufacturing, AT Fachverlag Stuttgart, 436–443.

SONG, G *et al.* (2006), 'Overlap welding of magnesium AZ31B sheets using laser–arc hybrid process', *Materials Science and Engineering A*, **429**, 312–319.

STAUFER, H and GRAF, T (2004), 'Laser-Hybridschweißen und Laserlöten anhand von Praxisbeispielen aus dem Automobilbau', Tagungsband zum Aachener Kolloquium für Lasertechnik'04, 107–120.

STAUFER, H *et al.* (2003), 'Hybrid welding for the automotive industry', *Industrial Laser Solutions*, February 2003.

STAUFER, H (2007), 'Laser-tandem hybrid welding on mild and high-strength steels', *Proc. of the 4th Int. WLT-Conf. on Lasers in Manufacturing*, Munich, 67–72.

STEEN, W M (1979), 'Methods and apparatus for cutting and welding', United States Patent 4,167,662.

STEEN, W M and EBOO, M (1979), 'Arc-augmented laser welding', *Metal Construction*, **11**(7), 332–335.

STEEN, W M (1980), 'Arc-augmented laser processing of materials', *J. Appl. Phys.*, **51**(11), 5636–5641.

STEEN, W M (1998), *Laser Material Processing*, 2nd edition, London, Springer.

SUBAN, M and TUŠEK, J (2001), 'Dependence of melting rate in MIG/MAG welding on the type of shielding gas used', *Journal of Materials Processing Technology*, **119**, 185–192.

THOMY, C *et al.* (2005), 'Application of high power fibre lasers for joining of steel and aluminium alloys', *Proc. of the Third Int. WLT-Conference on Lasers in Manufacturing*, Munich (Germany), 27–32.

THOMY, C *et al.* (2007), 'Fibre laser GMA hybrid welding of thin sheet material', in Vollertsen, F *et al.*, *Lasers in Manufacturing, Proc. of the 4th Int. WLT-Conf. on Lasers in Manufacturing*, Munich, 85–90.

TRUMPF (2008), *Lasers: solve every task perfectly*, Trumpf Laser GmbH + Co, Schramberg (Germany).

TZENG, Y F (2000), 'Process characterisation of pulsed Nd:YAG laser seam welding', *International Journal of Advanced Manufacturing Technology*, **16**, 10–18.

VERHAEGHE, G and HILTON, P (2005), 'Battles of the sources – using a high-power Yb fibre laser for welding steel and aluminium', *Proc. of the Third International WLT-Conference in Manufacturing*, Munich (Germany), 33–38.

WALSH, C *et al.* (2003), 'Characteristics of high-power diode-laser welds for industrial assembly', *Journal of Laser Applications*, **15**(2), 68–76.

WALZ, C *et al.* (2001), 'Laser-GMA welding and its influence on bead geometry and process stability', *Proc. of the First Int. WLT-Conf. on Lasers in Manufacturing,* AT Fachverlag, 444–452.

WEMAN, K (2003), *Welding processes handbook*, Cambridge, Woodhead.

WIESCHEMANN, A (2001), *Entwicklung des Hybrid- und Hydraschweißverfahrens am Beispiel des Schiffbaus*, Aachen, Shaker.

WINDERLICH, B (2003), Erhöhte Dauerschwingfestigkeit von Schweißverbindungen durch Laserstrahl-Hybridschweißen mit integrierter Wurzellagenschweißung, *IWS Jahresbericht 2003*, Dresden, Fraunhofer Institut für Werkstoff- und Strahltechnik IWS.

WOUTERS, M (2005), *Hybrid Laser-MIG Welding: An Investigation of Geometrical Considerations*, Licentiate Thesis, Luleå University of Technolgy.

ZHANG, X *et al.* (2007), 'High-power fiber laser welding of thick steel at low welding speed', *Proc. of the 26th Int. Congress on Applications of Laser and Electro-Optics, Orlando (USA)*, paper 1601, 850–857.

4

Effect of shielding gas on hybrid laser–arc welding

M. GAO and X. Y. ZENG, Huazhong University of Science and Technology, China

Abstract: The effects of shielding gas, including gas composition and nozzle arrangements, on the welding properties of hybrid laser–arc welding are examined. The types of gas and their effects on single laser and arc welding are reviewed, in order to clarify the significance of shielding gas in hybrid laser–arc welding. The effects of shielding gas parameters on the plasma-suppressing effect, laser–arc synergy effects and bead shape in hybrid laser–arc welding are described and the selection and optimization range of shielding gas composition, gas flow and nozzle arrangements are summarized.

Key words: shielding gas, laser-induced plasma, bead shape, laser–arc welding.

4.1 Introduction

Shielding gas is the crucial welding parameter that must be considered in single laser and arc welding. It has an important effect on process stability and the quality of welded joints. In laser welding, the main purpose of shielding gas is to reduce the amount of laser-induced plasma and achieve stable deep penetration welding, while in arc welding, it is used to obtain a stable arc, desirable arc characteristics and the droplet transfer mode (in metal inert gas, MIG welding). In addition to these effects, the shielding gas must be used to isolate the molten pool and the solidifying high-temperature metal from the environmental atmosphere.

It is, therefore, clear that shielding gas must also play an important role in hybrid laser–arc welding, in which a laser beam is coupled with the arc. The main shielding gas parameters are the gas components, flow rate and arrangement of the gas nozzles. Because of the different, and sometimes opposite, physical qualities of the laser-induced plasma and arc column, shielding gases need to balance the different requirements of the two plasmas (Bagger 2005, Campana 2008, Fellman 2003, Tani 2007). In general, the different requirements of shielding gases during hybrid laser–arc

welding are as follows: (a) composition: the gases have to be inert with respect to the working materials, and also at high temperatures, but some active (oxidative or reductive) gases can prove useful for improving arc stability and bead shape; (b) flow: the kinetic energy of the gas flux must change the laser-induced plasma plume in order to achieve a high coupling coefficient between laser and material, but it must be low enough not to blow the liquid phase away from the bead; (c) ionization potential: high ionization potentials help to reduce the amount of plasma during welding and thus lead to deep penetration, although they often lead to arc instability. For these reasons, mixed gases are predominantly used in the study and industrial applications of hybrid welding, especially for hybrid CO_2 laser–arc welding, owing to the strong laser-induced plasma.

In this chapter, the common types of shielding gases used in hybrid welding are examined and their effects on welding characteristics, bead shape and the mechanical properties of the joint are discussed.

4.2 Common types and physical properties of shielding gases

The gases commonly used in laser and arc welding are helium (He), argon (Ar), carbon dioxide (CO_2), oxygen (O_2), nitrogen (N_2) and hydrogen (H_2). Table 4.1 presents the basic chemical and physical properties of these gases. The ionization energy of gases, a very important parameter for both laser and arc welding, can influence the formation and ionization of the arc column, arc shape and energy distribution in the arc, while also affecting the shape and amount of laser-induced plasma, as well as the process stability of laser welding. Figure 4.1 shows the thermal conductivity of gases as a function of temperature, which affects the arc shape of arc welding and the plasma shape of laser welding. Figures 4.2 and 4.3 show gas enthalpy and electrical conductivity as a function of temperature, which mainly affect arc formation, arc shape and temperature conductivity in the arc.

4.2.1 Inert gases

Helium and argon are the two gases usually used in laser and arc welding. As shown in Table 4.1 and Fig. 4.1, helium has higher ionization energy and thermal conductivity. In laser welding, helium is the preferred shielding gas owing to its good plasma-suppressing effect for the laser beam. Argon is also generally used in laser welding, especially for solid lasers, such as Nd:YAG, fiber and diode lasers. In these lasers, the plasma-shielding effect for the laser beam is not significant because the absorption of laser-induced plasma is small for the relatively short wave of the laser beam. Therefore, laser welding with solid lasers also provides the desired results using argon

Table 4.1 Basic chemical and physical properties of the gases commonly used in laser and arc welding (Tusek, 2000)

Type of gas	Content in the air (vol.%)	Boiling point at 1.013 bar (°C)	Atomic weight and mean molecular weight reps	Density at 15°C, 1 bar (kg m^{-3})	Relative density with regard to the air (=1) at 15°C, 1 bar	Dissociation and ionization energies (eV)[c]	Chemical activity
Hydrogen (H_2)	0.5×10^{-6}[a]	−252.9	2.016	0.085	0.06	4.48 13.59 –	Reducing
Argon (Ar)	0.934	−185.9	39.948	1.669	1.38	– 15.76 27.50	Inert
Helium (He)	5.2×10^{-6}[a]	−268.9	4.002	0.167	0.14	– 24.56 54.10	Inert
Nitrogen (N_2)	78.084	−195.8	28.013	1.170	0.91	9.76 14.55 29.60	Reactive
Carbon dioxide (CO_2)	0.033[a]	−78.5[b]	44.011	1.849	1.44	5.80	Oxidizing
Oxygen (O_2)	20.946	−183.0	31.998	1.337	1.04	13.62 35.20	Oxidizing

[a] It is not obtained from the atmosphere.
[b] Sublimation temperature.
[c] 1 eV = 1.6×10^{-6} J; ionization energy of the majority of metals ranges between 6 and 9 eV.

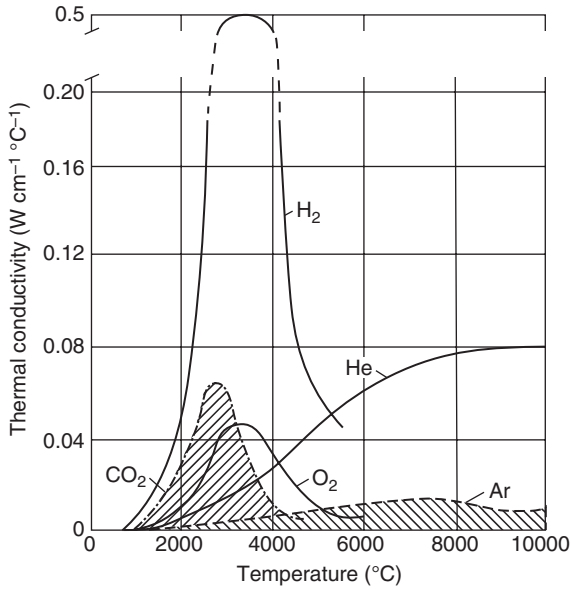

4.1 Thermal conductivity of gases as a function of temperature (Tusek, 2000).

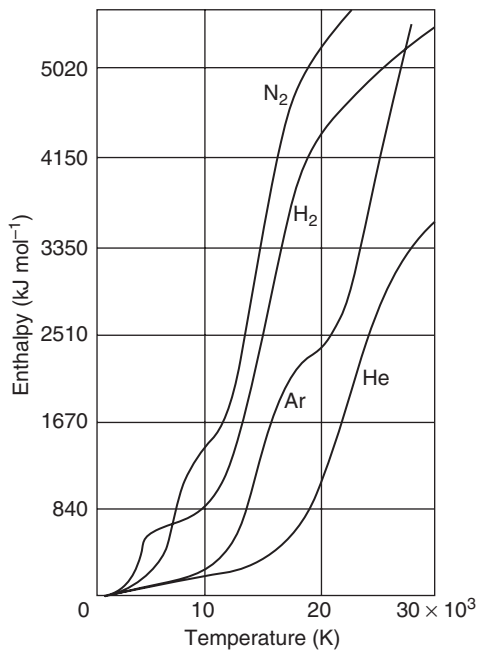

4.2 Gas enthalpy as a function of temperature (Tusek, 2000).

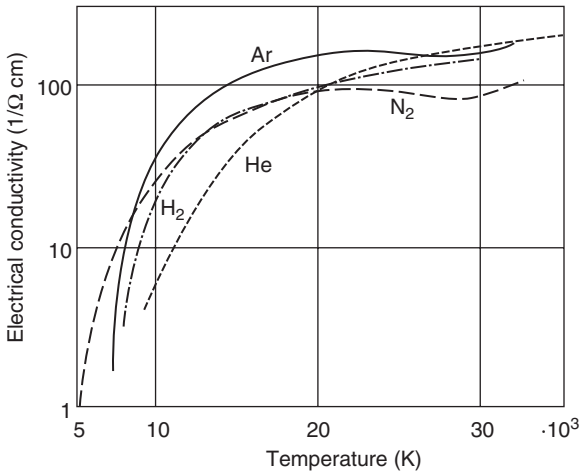

4.3 Electrical conductivity of gases as a function of temperature (Tusek, 2000).

as the shielding gas. However, for laser welding of thick plates, especially using CO_2 lasers, the increasing laser power forms strong laser-induced plasma which cannot be suppressed by argon alone. The laser beam will be defocused and process stability decreased. Occasionally, the welding properties are even changed from deep penetration welding to heat conduction welding, making a partially penetrated weld.

In many conditions, helium must be used for laser welding. However, helium is very expensive outside the United States, at a cost of over 10–20 times that of argon. For this reason, there has been a trend to reduce its use in shielding gases, and mixed helium–argon gases have been considered for laser welding and hybrid welding. Studies have shown (Kern 1997, Tang 1997) that in CO_2 laser welding, when helium and argon are mixed at a ratio of 3:1, the shielding gas can produce good results. However, in general, for a stable process and reliable weld penetration, helium is the only usable shielding gas in CO_2 laser welding of thick plates (Jokinen 2003, Ono 2002, Tsukamoto 2001).

In arc welding including tungsten inert gas (TIG) and metal inert/active gas (MIG/MAG) welding, argon is the most commonly used inert gas, owing to the stable ignition of the arc in the argon environment. In MIG/MAG welding with argon shielding gas, the spray transfer mode can be obtained easily with very few spatters owing to the decrease of the threshold current. Moreover, the high density of argon relative to air gives good protection for the weld pool. Compared with argon, helium arc has higher arc voltage with the same arc length, higher arc temperature and greater heat input

because of greater thermal conductivity. These advantages facilitate the welding of thick parts and enhance the welding speed. However, because of helium's high ionization energy during the MIG arc welding process, there is high spot pressure on the droplets, which makes the transfer of droplets difficult and increases the threshold current of spray transfer. Process stability is also reduced for this reason. Nowadays, therefore, argon–helium mixed shielding gas is usually considered when arc welding thick non-ferrous metals, such as aluminum alloys, copper alloys and titanium alloys.

4.2.2 Active gases

CO_2 and O_2 are the usual active gases used in arc welding, but they are seldom used in laser welding. In addition to CO_2 arc welding, they are usually used as assistant gases mixed with argon in TIG and MAG welding. The main purpose of the two gases is to improve welding properties and suppress some problems, such as cathode drift and weld morphology defects. Lu has studied the effects of oxygen content on He–O_2 and Ar–O_2 shielded TIG welding of low carbon 304 stainless steel (Lu 2004 a&b, 2007). This study demonstrated that when the oxygen disassociates from O_2 at high temperature and enters into the weld pool, subsequently reaching a critical content, the surface tension can be changed, thus influencing the flow of melted metal and consequently the weld shape. As shown in Fig. 4.4, under the same welding parameters, when the O_2 content in Ar–O_2 shielding gas is 0.1 and 0.3%, respectively, the weld shapes are obviously different. When the oxygen content is high in the shielding gas, the liquid metal flow driven by the surface tension is transferred from the pool edges to the center and lower parts, making a narrow, deep weld. When the oxygen content is lower, the melted metal flow is transferred from the pool center to the edges, making a wide and shallow weld. In MAG welding, moreover, the two active gases promote the refining of the metal droplets and subsequently decrease the threshold current of spray transfer.

Because of the oxidation characteristics, the addition of these two gases must be limited; otherwise the mechanical properties of the joints will be decreased. In general, for the welding of stainless steel and high-alloy steel, the oxygen content is in the range of 1–5%, while for the welding of common low carbon and low alloy steel without high demand, the highest content of oxygen can reach 20% (Jiang 1980).

4.2.3 Other gases

Nitrogen and hydrogen are other gases that are used infrequently in laser welding and arc welding. Hydrogen is a colorless, odorless and tasteless gas.

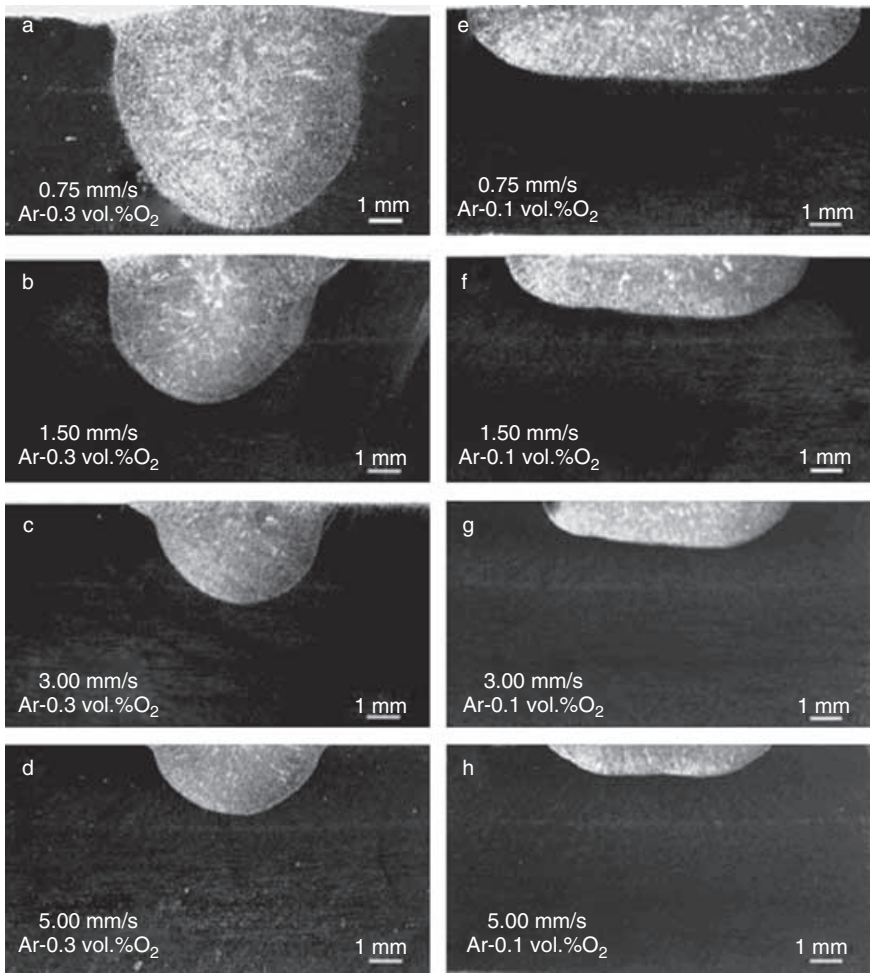

4.4 The effects of oxygen content in Ar–O_2 mixture on weld shape of TIG welds.

It is non-toxic and flammable (ignition point at 560 °C). It is much lighter than air (see Table 4.1) and explosive in a mixture with air and oxygen over a very wide range. Of all the gases, it has the highest thermal conductivity, high enthalpy and is a reducing gas, which means that it combines with oxygen and hinders oxide formation. As a shielding gas, hydrogen is used in addition to other gases, mainly argon, but also helium in smaller quantities. Hydrogen is used to a greater extent as a plasma gas with argon, or as a component in the argon–hydrogen mixture when arc welding high-alloy stainless steels. In general, the addition of hydrogen is in the range of 4–8%.

The main purpose of including hydrogen is the increase of arc temperature and heat input for the substrate and, consequently, an increase in welding speed or efficiency. Moreover, owing to hydrogen's deoxidizing effect, it can be used in the welding of nickel alloy to eliminate CO pores. However, its content must be lower than 6% to suppress hydrogen pores.

Nitrogen is also a colorless, odorless and tasteless gas and is non-toxic. It is the main component of air. As shown in Table 4.1, the ionization of nitrogen requires relatively high energy because it consumes some energy when it disassociates from N_2 to the N atom. This phenomenon facilitates plasma-suppression for laser welding. Compared with argon, the advantages of nitrogen are its lower cost and better plasma-suppressing effect in laser welding, while its disadvantages are the nitrogen pores and decrease of weld strength resulting from the nitrogen compound. Nitrogen is, therefore, seldom used in laser welding requiring demand for high quality joints. Nitrogen is usually employed as an addition to argon in the arc welding of copper and copper alloys and the ratio of Ar–N_2 is 4:1. When welding austenitic stainless steel, some nitrogen added to the argon shielding gas can improve arc stiffness and weld shape.

To date, only Bagger has used pure nitrogen in the hybrid CO_2 laser–TIG welding of 4 mm X6Cr17 steel to 2 mm 316L austenitic stainless steel, obtaining good results and fulfilling product demands (Bagger 2004). Apart from this, nitrogen and hydrogen are seldom used in hybrid laser–arc welding. However, given their applications in single laser and arc welding, they should play an important role in the hybrid welding of some special materials, such as copper alloys, nickel alloys and stainless steels.

4.3 Effects of shielding gas in hybrid welding

4.3.1 Selection and effects of gas compositions

In hybrid welding using solid lasers, because the laser beam is not sensitive to the laser-induced plasma, pure argon produces a stable synergistic effect between the laser and the arc. In the hybrid YAG laser–TIG welding of aluminum carried out by Fujinaga (2003), using pure argon shielding gas, the penetration depth of the hybrid weld (10 mm) was nearly twice that of the single laser weld, indicating the obvious enhanced laser–arc synergy effect. However, in the pure argon shielded hybrid YAG laser–TIG welding of 304 stainless steel carried out by Natio (2006), the penetration depth of the hybrid weld was only 0.5 mm deeper than that of the single laser weld (5 mm). Natio's study also demonstrates that the increase in the gas ratio of O_2 to argon shielding gas influences the shape of the weld beads, especially at an arc current of 100 A, in YAG laser and hybrid welding: the surface widths decrease and the penetration becomes deep with the increase

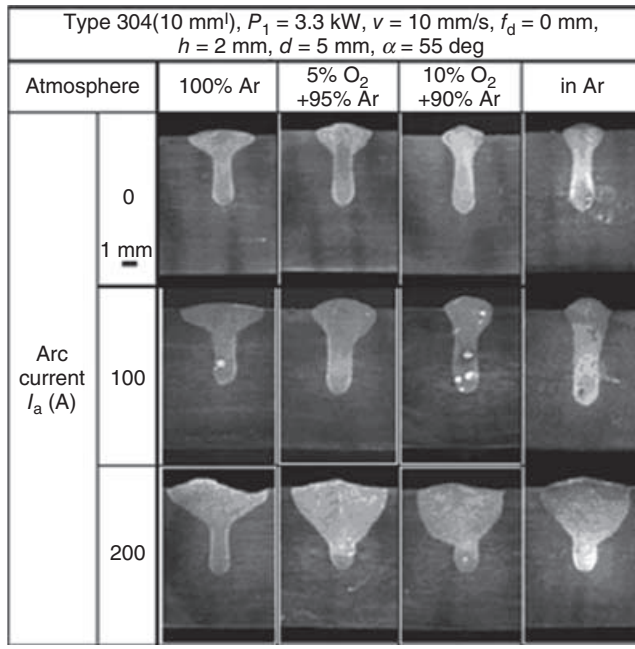
Type 304(10 mm^{l}), P_1 = 3.3 kW, v = 10 mm/s, f_d = 0 mm,
h = 2 mm, d = 5 mm, α = 55 deg
Atmosphere
100% Ar
5% O_2 +95% Ar
10% O_2 +90% Ar
in Ar
Arc current I_a (A)
0
100
200
1 mm

4.5 Effects of oxygen content on the hybrid YAG laser–TIG weld shape of 304 stainless steel.

in oxygen ratio, Fig. 4.5. Moreover, under these conditions the 'nail head' disappears in the atmosphere of the higher ratio. In addition, at any arc current, the welds in the air are similar to those in the atmosphere of the higher oxygen ratio, signifying that the oxygen in the atmosphere affects the geometries of the hybrid weld beads.

In hybrid CO_2 laser–arc welding, the composition of the shielding gas should be considered because of the strong plasma-defocusing effect. In general, helium must be used in hybrid CO_2 laser–arc welding in order to obtain the deep penetration weld mode as a result of the high ionization energy of helium. As shown in Fig. 4.6, under the same conditions, the penetration depth of the hybrid CO_2 laser–TIG weld with low helium content in the shielding gas is shallow, owing to heat conduction welding. However, the weld penetration depths increase with the increasing helium content in the He–Ar mixed shielding gas. When the helium content is greater than 50%, the 3 mm stainless steel plate is fully penetrated and the hybrid welding mode clearly presents deep penetration welding.

However, helium is expensive. The helium arc has high voltage and high spot pressure on the electrode, which does not promote arc stability,

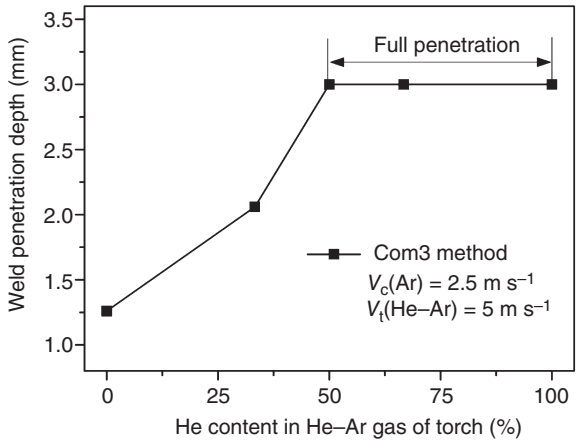

4.6 Effects of helium content in He–Ar shielding gas on penetration depth of CO_2 laser–TIG hybrid weld, the substrate is 316L stainless steel plate with 3 mm thickness.

especially for the stability of droplet transfer in the MIG/MAG arc. Pure helium, therefore, is not the most desirable shielding gas for hybrid CO_2 laser–arc welding. Apart from some hybrid CO_2 laser–TIG welding studies using pure helium shielding gas, hybrid CO_2 laser–arc welding usually employs He–Ar binary mixed shielding gas (Bagger 2003, Chen 2003, Xiao 2001). For low carbon or stainless steels, He–Ar–O_2 or He–Ar–CO_2 triple mixed shielding gases are used by adding a small quantity of CO_2 or O_2 to the He–Ar mixed shielding gas (Fellman 2006, Jasnau 2004, Nilsson 2003). According to the studies of Fellman and Tani, the helium content of the He–Ar–CO_2/O_2 mixed shielding gas for hybrid CO_2 laser–MAG welding should be greater than 30% in order to obtain effective plasma-suppression and the synergy effect between the laser and arc. However, when the helium content is too high, as shown in Fig. 4.7a–c, many spatters disappear, indicating an unstable welding process (Gao 2007a). Moreover, the helium content has obvious effects on the hybrid weld shape. As shown in Fig. 4.8, increased helium content can reduce the weld crown width, increase the root width and make the face of the weld cross-section smoother. The greater the helium content of the shielding gas, the more energy can be contained in the energy source, with more penetrating ability. The plasma-suppressing effect of the helium also reduces the effective size of the energy source, thus reducing the tendency for a 'nail-head' weld bead profile. The smoother weld cross-section is the result of the higher energy and higher arc pressure. It should be pointed out that the effects of the helium content on the width of the weld cross-section are smaller when the joints have a groove gap,

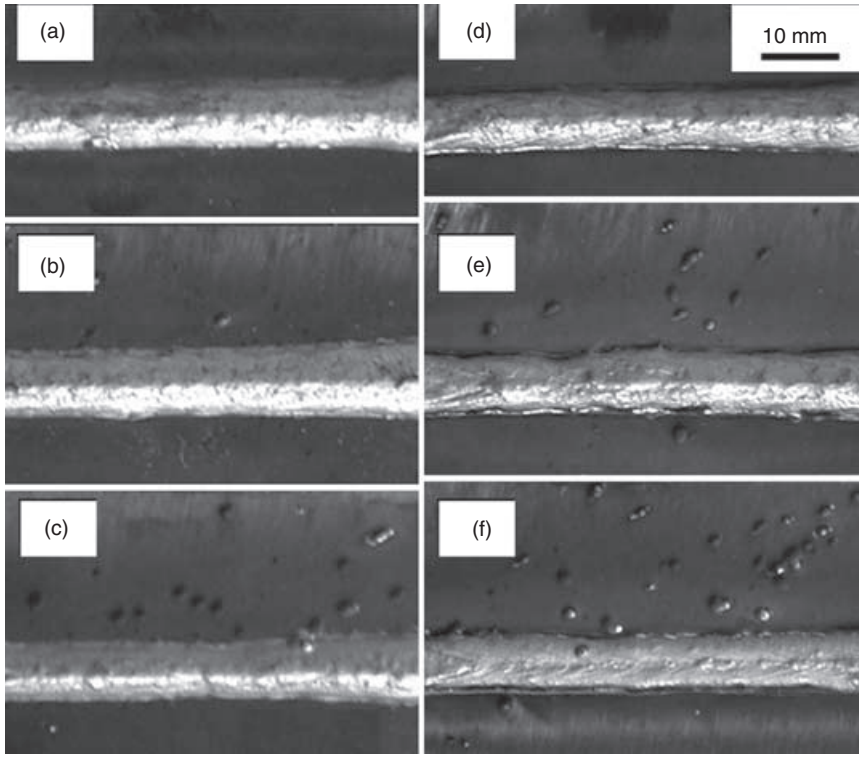

4.7 Effect of CO_2 and He content in shielding gas on spatter of hybrid laser-MAG welding for mild steel, He–Ar mixed gas: (a) He 20%, (b) He 60%, (c) He 100%, Ar balance; CO_2–Ar mixed gas: (d) CO_2 10%, (e) CO_2 30%, (f) CO_2 50%.

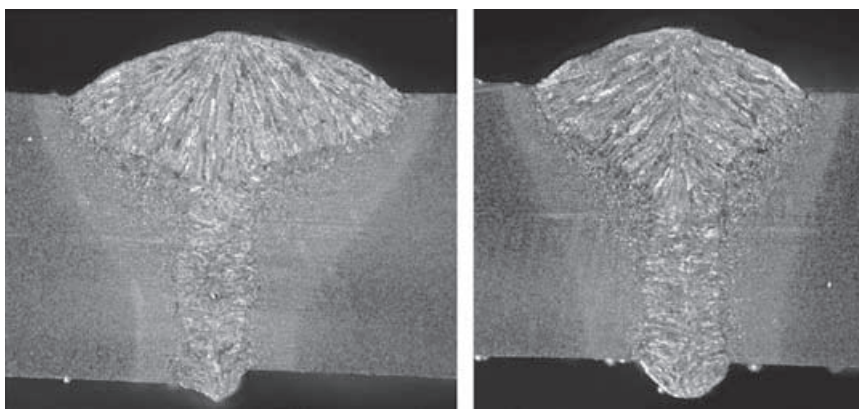

(a) (b)

4.8 Effect of He on hybrid weld bead cross section width in close-fitting I-butt joints: (a) 30% He, (b) 80% He; 2% CO_2, balance argon. Plate thickness is 6 mm.

because the filler wire feed rate is small in relation to the groove volume and so there is a smaller amount of weld metal in the weld pool.

The study of Fellman and his co-authors (Fellman 2006) on the hybrid CO_2 laser–MAG welding of carbon steel also demonstrated that a small addition of CO_2 and O_2 to He–Ar shielding gas can improve the bead shape of hybrid welding. When the CO_2 content is in the range of 0–2%, the undercut and root cavity are easily formed in the hybrid weld, especially at the end of the weld; when the CO_2 content is in the range of 5–10%, these weld defects disappear and a smooth weld bead transition can be produced with the base materials. As shown in Fig. 4.9, CO_2 content also has an obvious effect on hybrid weld shape. The change of bead shape resulting from the CO_2 is similar to that of helium. This is because CO_2 may disassociate in the high temperature environment of arc welding, resulting in an increase in arc pressure. When the CO_2 content is higher, the large arc pressure will throw metal droplets away from the weld and make spatters. As shown in Fig. 4.7d–f, the spatters increase significantly with the increasing CO_2 content in the CO_2–Ar mixture. With the addition of O from CO_2 disassociation, the surface tension may cause the melted metal to flow from the surround to the center and lower part as discussed above, and consequently make a smoother weld face. Moreover, the CO_2 disassociation absorbs the energy from its surroundings, indicating that CO_2 also has a good plasma-suppressing effect for the laser beam. In fact, Gao demonstrated in his study (Gao 2007a), that the CO_2–Ar mixture can also produce good laser–arc synergistic interaction and the weld penetration obtained is only a little lower than in the case of He–Ar shielding gas.

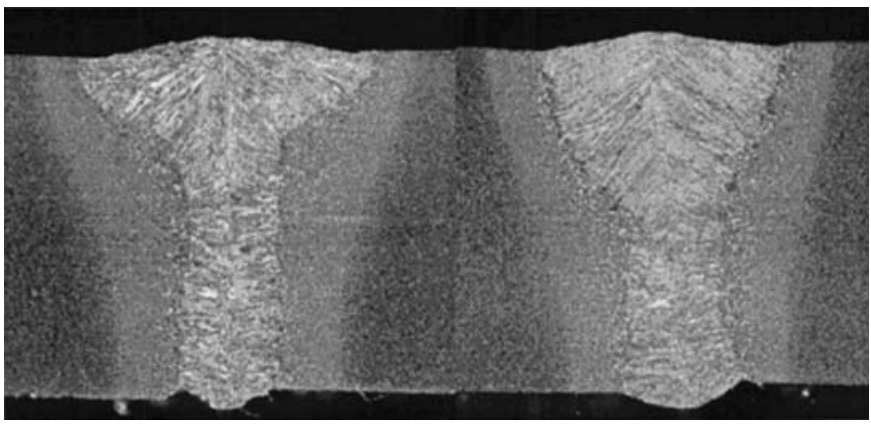

4.9 Effect of carbon dioxide on hybrid weld bead cross section width: 0% CO_2 (left), 10% CO_2 (right); 40% He, balance argon. A gap of 0.8 mm was present in the joint. Plate thickness 6 mm.

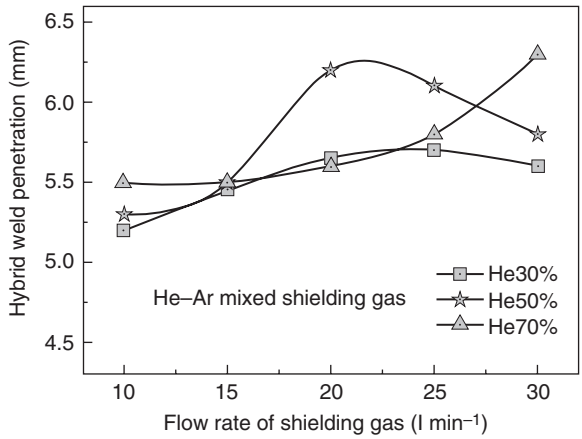

4.10 Effects of shielding gas flow on the weld penetration of hybrid laser–MAG welding for mild steel, He–Ar mixed shielding gas, plate thickness 7 mm.

In addition to shielding gas composition, gas flow is the other important consideration for hybrid welding. Gao (2007c) showed that corresponding to a constant gas composition, as shown in Fig. 4.10, there is an optimal gas flow to obtain the deepest weld penetration depth and, therefore, the greatest welding efficiency. Gas flow that is too small cannot produce good plasma-suppressing for the laser beam, while gas flow that is too great may produce turbulence on the pool surface, reducing the shielding results of the weld pool. In general, when the helium content in the shielding gas is low, the gas flow should be greater in order to produce good plasma-suppressing and a full penetrated weld. When the helium content in the shielding gas is high, the gas flow can be reduced to save costs. However, due to the low density of helium, the gas flow can be too small to guarantee good shielding results of the weld pool. According to research results (Fellman 2006, Gao 2007a, Tani 2007), the appropriate gas flow for hybrid laser–arc welding should be in the range of 15–30 l min^{-1}.

4.3.2 Optimization and effects of gas nozzle arrangement

The arrangement of the gas nozzles is a significant factor for the stability and efficiency of hybrid welding, and it is also an important consideration in the design of the hybrid welding head. Though many hybrid welding studies have achieved a good laser–arc synergy effect by using only the single arc weld torch, some studies have shown that multiple gas nozzles can produce an improved laser–arc synergy effect and a more stable process

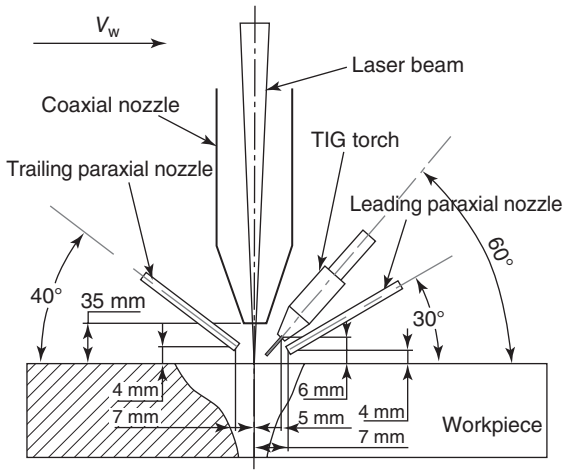

4.11 Schematic diagram of gas nozzle arrangement of hybrid CO_2 laser–TIG welding.

Table 4.2 Combinations of shielding gas

Methods	Combination of nozzles
Com1	TIG torch only
Com2-trailing	TIG torch + trailing paraxial nozzle
Com2-leading	TIG torch + leading paraxial nozzle
Com3	TIG torch + coaxial nozzle

(Gao 2007b). As shown in Fig. 4.11 and Table 4.2, in the study of hybrid CO_2 laser–TIG welding for 316L stainless steel, three shielding gas arrangements were considered based on three gas nozzles (weld torch, coaxial nozzle and paraxial nozzle). The results showed that with a similar ratio of He–Ar mixed shielding gas, the gas arrangement method has an important effect on the process stability and weld penetration depth. As shown in Fig. 4.12a, the weld produced by the Com1 method has a discontinuous and scraggy surface morphology with an obvious crook at the beginning of the weld and a shallow penetration (0.78 mm), which is far lower than that of laser-only welding (2.1 mm), and even lower than that of pure TIG welding (1.0 mm). As shown in Fig. 4.12b in the Com2 method, the weld surface and cross-section indicate that the laser and arc do not act linearly, which also results in shallow weld penetration. However, the weld obtained by the Com3 method, as shown in Fig. 4.12c, has a continuous and uniform surface morphology, showing a stable welding process and full weld penetration.

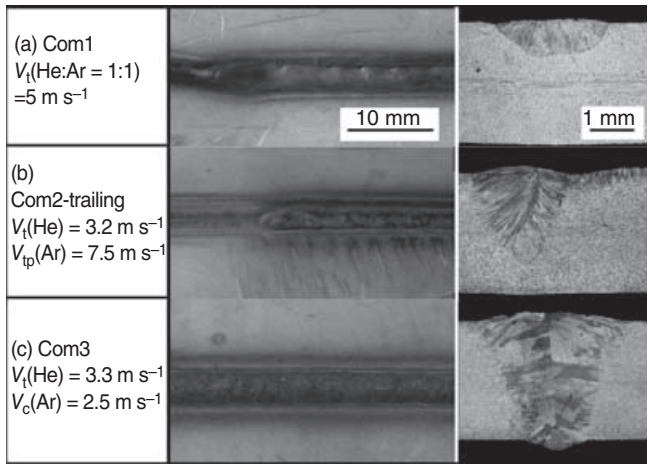

4.12 Effects of gas nozzle arrangement on weld surface and cross-section shape in hybrid CO_2 laser–TIG welding, 316L stainless steel with 3 mm thickness.

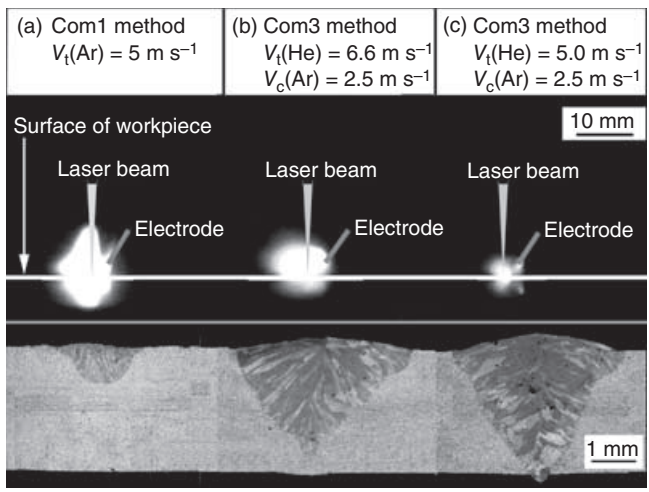

4.13 Effects of gas nozzle arrangement on plasma shape and weld penetration depth in hybrid CO_2 laser-TIG welding, 316L stainless steel with 3 mm thickness.

The arrangement of the gas nozzles also has a major influence on the plasma-suppressing effect of hybrid welding. As shown in Fig. 4.13a&b, when the arrangement method and gas composition is inappropriate, the plasma swells and climbs to a great height aligned with the laser beam axis (far higher than the height of the electrode tip), and this is accompanied

with shallow weld penetration. However, when the shielding gas parameters are appropriate, as shown in Fig. 4.13c, the plasma is controlled and of very small height aligned with the laser beam axis (slightly higher than the height of the electrode tip), and this is accompanied with full penetration. The results and discussion of this study demonstrated that the full penetrated weld cannot be generated by the pure TIG torch method, but it can be reached by the hybrid protecting method. With the full penetration weld of the hybrid protecting method, combining the torch and paraxial nozzle, the shielding gas parameter range is very narrow, but the range of the hybrid protecting method coupling the torch and coaxial nozzle is quite wide. Moreover, the effect of shielding gas arrangements on the plasma shape is achieved in two ways: laser–arc plasma interaction and gas flow direction and velocity.

For the hybrid welding head, multiple gas nozzles complicate the design and increase its volume, which does not facilitate the welding of 3D structures. Study of the gas nozzle arrangement and its practical effects is, therefore, significant for the design of the hybrid welding head – the key hybrid welding technology for industrial applications. Nowadays, Fraunhofer ILT has designed a hybrid welding head in which the laser beam and arc are surrounded by a common water-cooled nozzle device with an integrated contact tube (see Fig. 4.14a&b) (Kaierle 2000, Petring 2003). This arrangement provides the closest laser and arc proximity. The process gas flows out of an annular channel nearly coaxial to the laser beam. A diffusing aperture within the channel enables a homogeneously distributed stream of the assist gas onto the welding zone. Thus, a transverse suction of air is avoided and effective protection of the weld bead is ensured (Fig. 4.14a). Moreover, a minimal but sufficient leak gas flow in the upward direction avoids process gas contamination by air via the laser beam entrance. This hybrid welding head can provide a good synergy laser–arc effect and has been used in production.

4.4 Effects of shielding gas on mechanical properties of the hybrid weld

Because the shielding gas has some effects on weld shape, morphology defects and alloy compositions of the hybrid weld, it also has an influence on the mechanical properties of the hybrid weld. In the study carried out by Fellman, the best impact strength was achieved in welds made using the shielding gases 60%Ar+40%He and 50%Ar–40%He–10%CO_2. Hardness testing revealed that the values were well below the accepted limit of 350 HV in all sections of the weldment. The lowest average hardnesses around the weld area were achieved by using 50%Ar–40%He–10%CO_2 as shielding gas. The test pieces for transverse tensile strength tests all failed

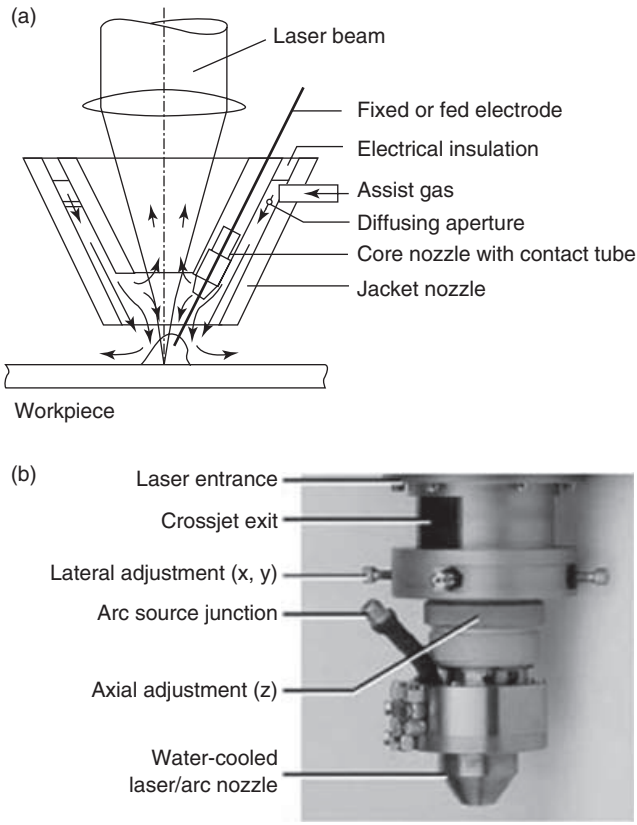

4.14 Schematic diagram (a) and entity (b) of Fraunhofer ILT hybrid welding head.

in the base metal. Welding procedure testing indicated that the changes in shielding gas composition did not have a significant effect on the properties of a hybrid CO_2 laser–GMA weld.

Gao (2007c) confirms the above results. As shown in Fig. 4.15, with the changing helium content (except for the helium content of 20% with a weld not fully penetrated), the impact toughness and tensile strength are nearly constant, tested using notched specimens. Figure 4.16 presents the effects of O_2–Ar and He–Ar mixed shielding gas on the microhardness of hybrid CO_2 laser–MAG welded mild steel (Gao 2007a). The microhardness of the He–Ar hybrid weld is higher that that of the CO_2–Ar hybrid weld. Using He–Ar shielding gas, the increasing helium content increases microhardness slowly. With CO_2–Ar shielding gas, when the CO_2 content is greater than 30%, weld microhardness decreases dramatically. This is because the

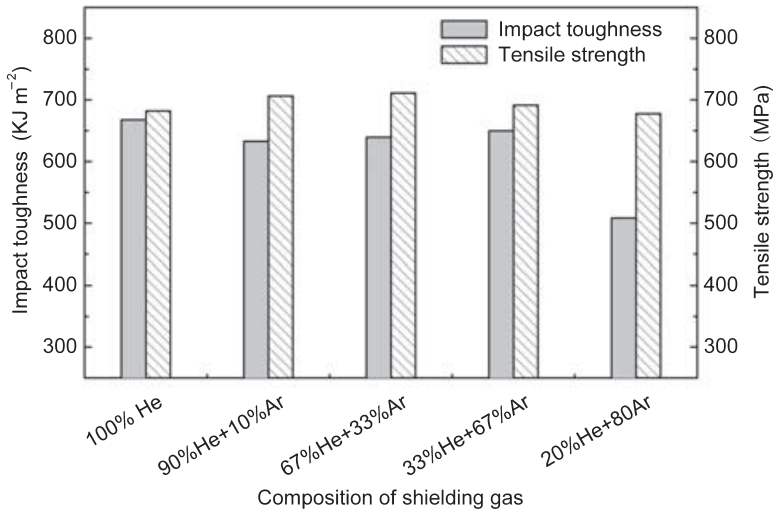

4.15 Effects of shielding gas on mechanical properties of hybrid CO_2 laser–MIG welded mild steel with 6 mm thickness.

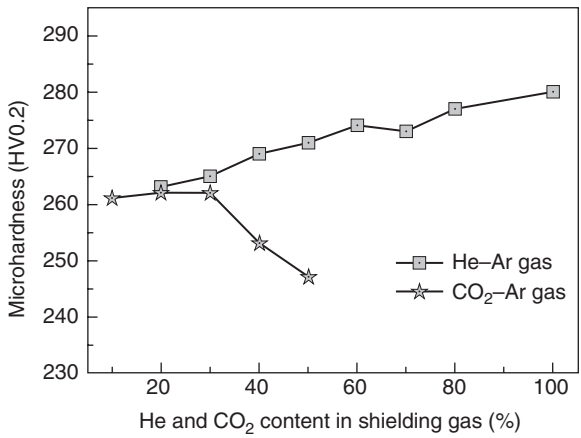

4.16 Effects of shielding gas on microhardness of hybrid CO_2 laser–MAG welded mild steel with 7 mm thickness.

oxygen atoms can be disassociated from CO_2 at high temperature and recombine with the carbon atoms in the weld pool to form CO gas escaping from the pool. This then reduces the carbon content of the weld and decrease weld microhardness.

All the above studies showed that inert gases in the shielding gas do not have a significant effect on the mechanical properties of the hybrid weld,

while CO_2 has a relatively great effect on it, especially high CO_2 content in shielding gas. However, because very few studies exist on this subject, and only on the carbon steel, the effects of shielding gas on the mechanical properties of the hybrid weld are not sufficiently clear.

4.5 Conclusions and sources of further information and advice

Research into shielding gas indicates its important effect on the welding properties of hybrid laser–arc welding, including process stability, laser–arc synergy effects, bead shape and joint mechanical properties. In hybrid CO_2 laser–arc welding, shielding gas has a more important role because of its strong plasma-defocusing effect. For a constant combination of laser beam and arc heat sources, there should be an optimal combination and composition of types of shielding gas, which also vary according to the types of welded materials.

However, studies examining shielding gas effects in the field of hybrid laser–arc welding have only been carried out to a limited extent. Outstanding issues concern the practical plasma-suppressing effects to achieve the greatest laser–arc synergy effect or deepest weld penetration. Theoretical understanding is greatly lacking, and only a few studies include mathematical modeling to discuss the effect mechanism of shielding gas in hybrid welding. Moreover, except for some studies of carbon steel, few investigations have addressed the effects of the hybrid laser–arc weld on the mechanical properties of the joint and the weld microstructure. Apart from steels, the effect on other materials has been little considered. Studies of gas nozzle arrangements, which are important for the design of the hybrid welding head, are also scarce.

As a result, many advances have been derived from experimentation in the field of shielding gas research in hybrid laser–arc welding. These results are useful for the selection of shielding gas parameters and the understanding of hybrid welding. However, more modeling should be carried out to clarify the mechanism of their effect and further related experiments should focus on materials with bad weldability, such as high-strength steel, magnesium alloys and copper alloys, in order to improve the understanding of shielding gas in hybrid laser–arc welding.

4.6 References

BAGGER C, OLSEN F O (2003), Comparison of plasma, metal inactive gas (MIG) and tungsten inactive gas (TIG) processes for laser hybrid welding', *Proceedings of ICALEO 2003*, LMP, paper 302.

BAGGER C, SONDRU L DE C, OLSEN F O (2004), 'Laser/TIG hybrid welding of pot for induction heater', *Proceeding of ICALEO 2004*, LMP, Hybrid laser welding, 60–69.

BAGGER C, OLSEN F O (2005), 'Review of laser hybrid welding', *J Laser Appl*, **17**, 2–14.

CAMPANA G, ASCARI A, FORTUNATO A, TANI G (2008), 'Hybrid laser–MIG welding of aluminum alloys: the influence of shielding gas', *Appl Surf Sci*, in press. doi:10.1016/j.apsusc.2008.07.169

CHEN Y B, LEI Z L, LI L Q (2003), 'Study of welding characteristics in CO_2 laser–TIG hybrid welding process', *Proceeding of ICALEO 2003*, LMP, paper 306.

FELLMAN A, JERNSTROM P, KUJANPAA V (2003), 'CO_2–GMA hybrid welding of carbon steel – the effect of shielding gas composition', *Proceeding of ICALEO 2003*, LMP, paper 308.

FELLMAN A, KUJANPAA (2006), 'The effect of shielding gas composition on welding performance and weld properties in hybrid CO_2 laser–gas metal arc welding of carbon manganese steel', *J Laser Appl*, **18**, 12–20.

FUJINAGA S, OHASHI R, KATAYAM S, MATSUNAWA A (2003), 'Improvements of welding characteristics of aluminum alloys with YAG laser and TIG arc hybrid system', *Proceedings of SPIE*, **4831**, 301–306.

GAO M, ZENG X Y, HU Q W, YAN J (2007), 'Effects of shielding gas in CO_2 laser–MAG hybrid welding', *Transactions of the China Welding Institution*, **28**(2), 85–88.

GAO M, ZENG X Y, HU Q W (2007), 'Effects of gas shielding parameters on weld penetration of CO_2 laser–TIG hybrid welding', *J Mater Process Technol*, **184**,177–183.

GAO M (2007), 'Study on technology, mechanism and quality controlling of CO_2 laser–arc hybrid welding', PhD dissertation, *Huazhong University of Science and Technology*, Wuhan, PR China.

JASNAU U, HOFFMANN J, SEYFFARTH P (2004), 'Nd:YAG laser–GMA hybrid welding in shipbuilding and steel construction', *in Tan T J et al.*: *Robotic welding, intelligence and automation, LNCIS 299*, 14–24, Berlin, Springer.

Jiang H Z (1980), 'Arc welding and electro-slag welding', *China Machine Press*, Beijing.

JOKINEN T, KARHU M, KUJANPAA V (2003), 'Welding of thick austenitic stainless steel using Nd:yttrium–aluminum–garnet laser with filler wire and hybrid process', *J Laser Appl*, **15**, 220–224.

KAIERLE S, BONGARD K, DAHMEN M (2000), 'Innovative hybrid welding process in an industrial application', *Proceeding of ICALEO 2000*, LMP section C, 1–10.

KERN M, BECK M, BERGER P, HUGEL H (1997), 'Process stabilizing potential of shielding gas mixtures in laser welding with CO_2 lasers', *Proceeding of SPIE 1997*, **3092**, 526–529.

LU S P, FUJII H, NOGI K (2004), 'Sensitivity of marangoni convection and weld shape variations to welding parameters in O_2-Ar shielded GTA welding', *Script Mater*, 51, 271–277, doi:10.1016/j.scriptamat.2004.03.004.

LU S P, FUJII H, NOGI K (2004), 'Marangoni convection and weld shape variations in Ar–O_2 and Ar–CO_2 shielded GTA welding', *Mater Sci Eng A*, **380**, 290–297, doi:10.1016/j.msea.2004.05.057.

LU S P, FUJII H, NOGI K, SATO T (2007), 'Effect of oxygen content in He–O_2 shielding gas on weld shape in ultra deep penetration TIG', *Sci Technol Weld Join*, **12**, 659–665. doi: 10.1179/174329307X238425.

NATIO Y, MIZUTANI M, KATAYAMA S (2006), 'Effect of oxygen in ambient atmosphere on penetration characteristics in single yttrium–aluminum–garnet laser and hybrid welding', *J Laser Appl*, **18**, 21–27.

NILSSON K, HEIMBS S, ENGSTROM H, KAPLAN F H (2003), 'Parameter influence in CO_2-laser/MIG hybrid welding', *IIW Doc*, IV-843–03.

ONO K, ADACHI K, MIYAMOT I, INOUE T (2002), Influence of oxide film on weld characteristics of mild steel in CO_2 laser welding', *J Laser Appl*, **14**, 73–77.

PETRING D, FUHRMANN C, WOLF N, POPRAWE R (2003), 'Investigations and applications of laser–arc hybrid welding from thin sheets up to heavy section components', *Proceedings of ICALEO 2003*, LMP section A, 1–10.

TANG X H, ZHU H H, ZHU G F (1997), 'Study of plasma control in high-power CO_2 laser welding', *Chin J Lasers*, **24**, 174–178 (in Chinese).

TANI G, CAMPANA G, FORTUNATO A, ASCARI A (2007), 'The influence of shielding gas in hybrid laser–MIG welding', *Appl Surf Sci*, **253**, 8050–8053, doi:10.1016/j.apsusc.2007.02.144.

TUSEK J, SUBAN M (2000), 'Experimental research of the effect of hydrogen in argon as a shielding gas in arc welding of high alloy stainless steel', *Int J Hydrogen Energy*, **25**, 369–376.

TSUKAMOTO S, KAWAGUCHI I, ARAKANE G, HONDA H (2001), 'Suppression of porosity using pulse modulation of laser power in 20 kW CO_2 laser welding', *Proceedings of ICALEO 2001*, LMP, paper 1702.

XIAO R S, AMBROSY C, ZUO T C, HUGEL H (2001), 'New approach to improve the laser welding process of aluminum by using an external electrical current', *J Mater Sci Lett*, **20**, 2163–2165.

5

Properties of joints produced by hybrid laser–arc welding

V. KUJANPÄÄ, Lappeenranta University of Technology, Finland

Abstract: Hybrid laser welding is quite a tolerant process, as far as welding parameters and their selection are concerned. In ordinary steels, which are easy to weld with conventional or laser welding methods, hybrid laser welding has no major problems, either. Mechanical properties can be maintained in the acceptable range in most of the cases. The most challenging materials are high or ultra-high strength steels, where attention is to be paid on welding conditions and welding parameters to guarantee acceptable properties. Hybrid laser welding gives a potential process for carbon steels, stainless steels and aluminium alloys for most applications.

Key words: hybrid laser welding, mechanical properties, hardness, microstructure, fatigue, steel joints.

5.1 Introduction

Hybrid laser welding is quite a tolerant process, if welding parameters and their selection are concerned. In ordinary steels, which are easy to weld with conventional or laser welding methods, hybrid laser welding has no major problems, either. As seen in previous chapters, the major advantages are the higher production speed and higher tolerances compared with ordinary laser welding, and higher production speed, higher penetration and lower distortions compared with arc welding processes. On the other hand, the heat-affected zone as well as the weld zone tend to be wider than in the laser process and narrower than in arc processes. This causes differences in the mechanical and corrosion properties of the weld.

5.2 Microstructure of hybrid laser–arc welds

The microstructure of the melted zone of hybrid laser–arc welds is governed by cooling rate and composition. The heat-affected zone is additionally affected by the original microstructure, i.e. the base metal microstructure.

5.2.1 Carbon steel hybrid welds

As seen earlier, hybrid laser welding allows much higher welding speeds to be used compared with laser welding and the same penetration. In heavy section laser–arc hybrid welding the penetration is mainly determined by the laser power alone, but by increasing the arc power the welding speed may be increased to a high level even for a relatively large gap. Thus, an increased ability to bridge a gap as well as a significant increase in speed may be taken advantage of by using the hybrid process as compared with the traditional high power laser welding process, and the heat input per unit length is typically not increased significantly (Kristensen 2007). A cross-section of an arc–laser hybrid weld in 12 mm structural steel is shown in Fig. 5.1 together with a pure laser weld. For the given gap, the welding speed is roughly doubled for the hybrid weld compared with the one obtained by the laser process alone.

Many factors affect cross-section. In Fig. 5.2 the effect of shielding gas is described. The addition of CO_2 in the shielding gas increases remarkably the cross-section area (Fellman *et al.* 2003).

The laser–GMA hybrid welds have the same microstructures as the ordinary welds that are base metal, granular pearlite zone, fine grain zone,

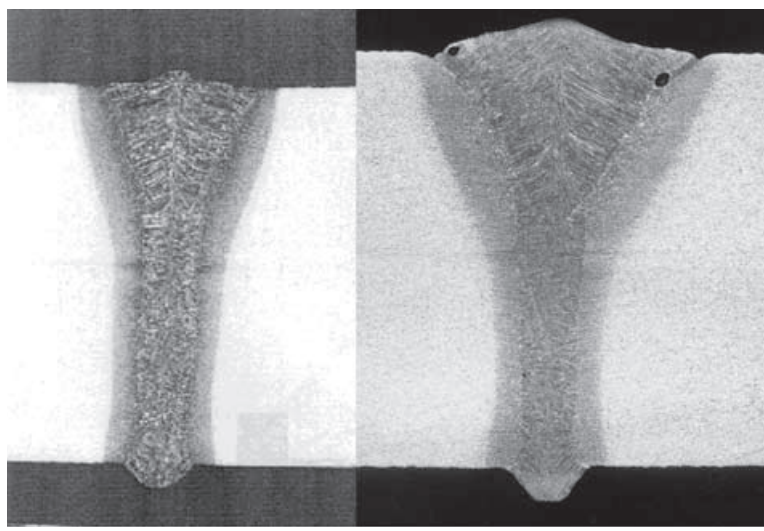

(a) (b)

5.1 Cross-section in 12 mm structural steel of: (a) a pure laser weld (laser peak power at wp 9 kW, speed 0.8 m/min and zero gap); and (b) a hybrid MAG–laser weld (laser power at 11 kW, arc power 7.0 kW, speed) 1.4 m min^{-1}, wire feed speed 15.8 m min^{-1} and gap 0.5 mm (Kristensen, 2007).

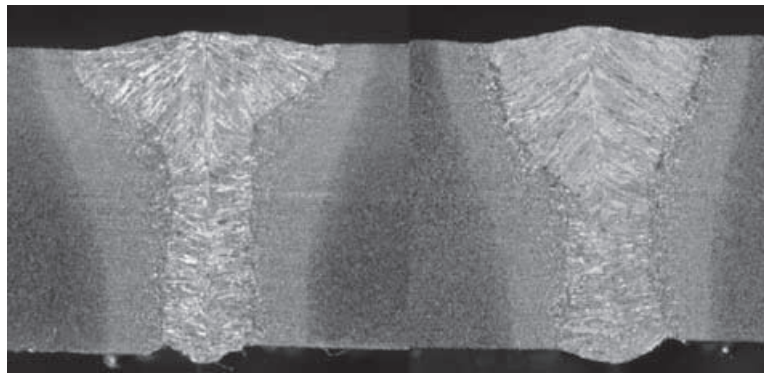

(a) (b)

5.2 The effect of the shielding gas CO_2 content on the width of the penetration profile: (a) 0%, (b) 10%. Air gap 0.8 mm (Fellman *et al.* 2003).

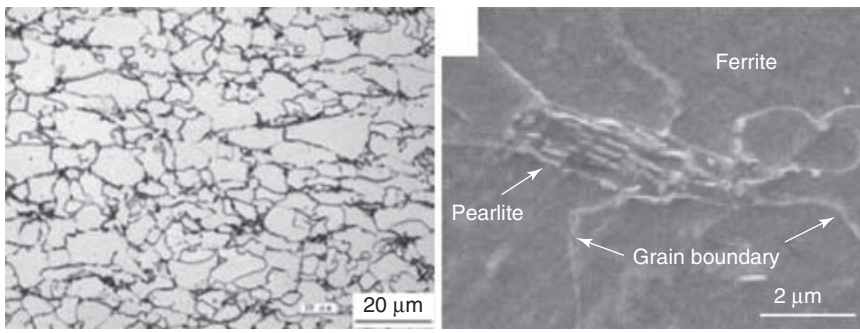

(a) (b)

5.3 Micrographs of base metal observed by (a) optical microscopy and (b) SEM (Liu *et al.* 2006).

coarse grain zone and weld metal. The microstructures of base metal, granular zone and fine grain zone are about the same in laser weld, GMA weld and laser–GMA hybrid weld.

The microstructure of base metal observed by optical microscopy and SEM are shown in Fig 5.3. The main microstructure is ferrite and pearlite. The white microstructure in Fig. 5.3(a) is ferrite. The average grain size of ferrite is about 8.2 μm. The white microstructure in Fig. 5.3(b) is cementite and the grey microstructure is ferrite. The ferrite is directed in Fig. 5.3(b).

The laser, GMA and laser–GMA hybrid welds were achieved under different welding processes and heat inputs. The microstructures of weld

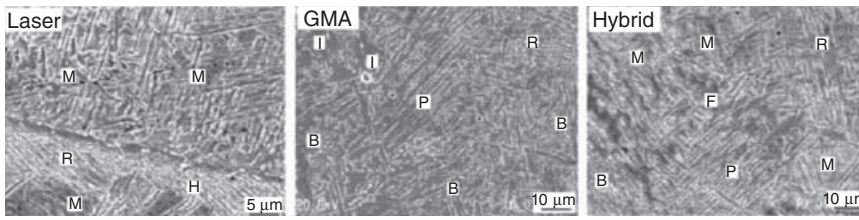

5.4 SEM images of laser weld metal, GMA weld metal and laser–GMA hybrid weld metal (Liu *et al.* 2006).

metals are very different as shown in Fig. 5.4. In laser weld metal, martensite was the main microstructure because of the low heat input. In GMA weld metal, the microstructures include ferrite, bainite, pearlite and a little amount of martensite because of the highest heat input in the three welding methods. The microstructures of hybrid weld metal include ferrite, bainite and martensite. The percentage of martensite is higher than that in GMA weld metal as shown in Fig. 5.4. (Liu *et al.* 2006).

In ultra-high strength steels (yield strength 960 MPa), microstructure is affected by cooling time. When $t_{7/3} > 2$ s ($t_{8/5} > 0.5$ s), fine lath bainitic–martensitic microstrucure is formed, which gives the best impact properties (see Fig. 5.4a), meanwhile, a shorter cooling time causes non-tempered martensitic microstructure with decreased toughness (Laitinen *et al.* 2007).

5.2.2 Stainless steels

In ordinary austenitic stainless steel, microstructure does not play an important role in affecting the mechanical properties, because of the absence of major phase transformations during cooling, except for the ferrite to austenite transformation, if solidification is primary ferritic. In laser welding, most austenitic stainless steels solidify primarily in the austenitic solidification mode, because of rapid cooling. This is also the case with hybrid laser welding, if a matching composition of filler metal is used. This causes ferrite content, which is quite minimal (≤1%). Figure 5.5 shows an example of a multi-pass hybrid weld, where a fully austenitic structure is formed (Jokinen *et al.* 2002).

In austenitic–ferritic stainless steels (duplex steels) the balance between austenite and ferrite guarantees the optimal mechanical and corrosion properties. They are somewhat problematic to weld with laser, because the cooling rate is so high that the ferrite–austenite transformation does not have time to occur and the microstructure has a very high ferrite content, almost 100%. This can be solved by adding nitrogen in the shielding gas to increase the tendency to austenite formation. Hybrid welding offers the

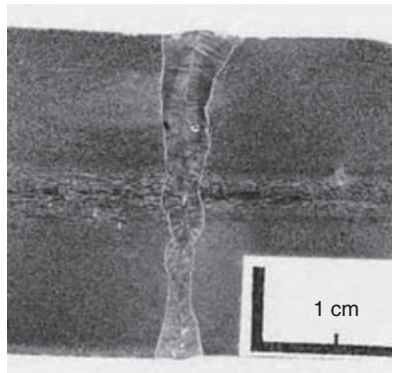

5.5 Cross-section of the hybrid weld with thickness of 20 mm filled with 4 passes. Groove angle 10°, welding speed 0.5–0.7 m min^{-1}, wire feeding rate 9.7 m min^{-1} (Jokinen *et al.* 2002).

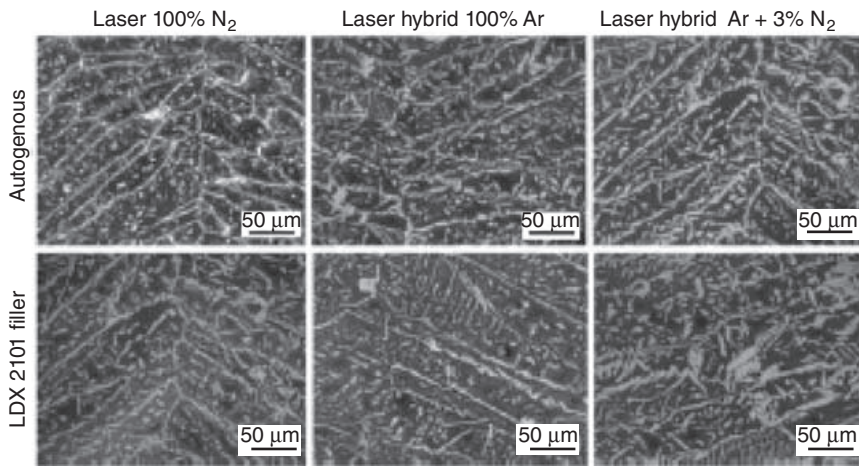

5.6 Lean duplex LDX2101 weld microstructure (Westin *et al.* 2007).

possibility of using filler metal and balancing ferrite content to the optimum (Vandewynckele *et al.* 2007). In Fig. 5.6, the effect of shielding gas and filler metal to the microstructure of autogenous and hybrid welding of duplex steels is shown.

5.2.3 Aluminium alloys

Laser and hybrid laser welding is used to join aluminium alloys in many different applications, e.g. car body and aircraft industries. Filler metal is often used in aluminium laser welding, either as cold-wire feeding or by

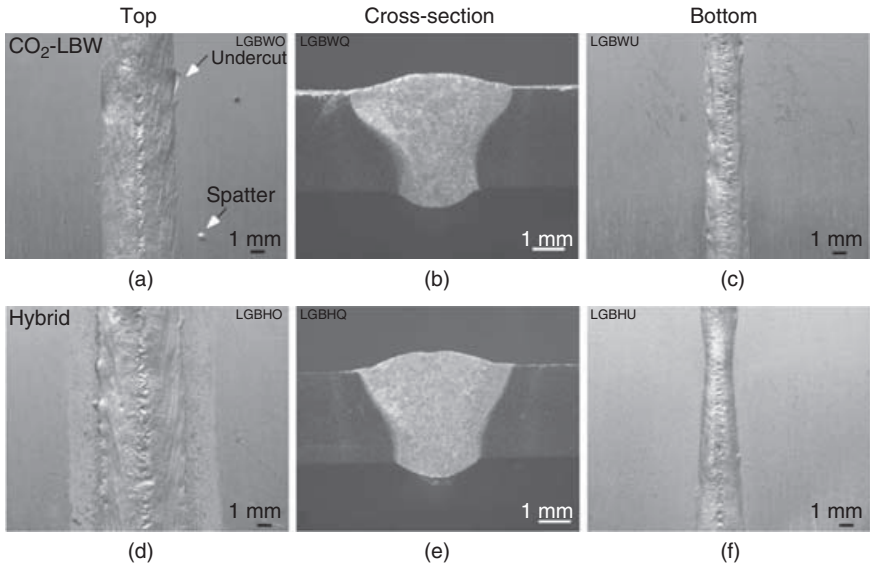

5.7 Surface appearance of the CO_2 laser beam weld (upper micrographs; a–c) and the hybrid weld (lower micrographs; d–e) in a 3.2 mm thick AA6013 sheet butt-welded in T6. The surface was cleaned, the cross-section was polished and lightly etched. Local height differences in the weld are seen as surface irregularities (Vaidyaa *et al.* 2006).

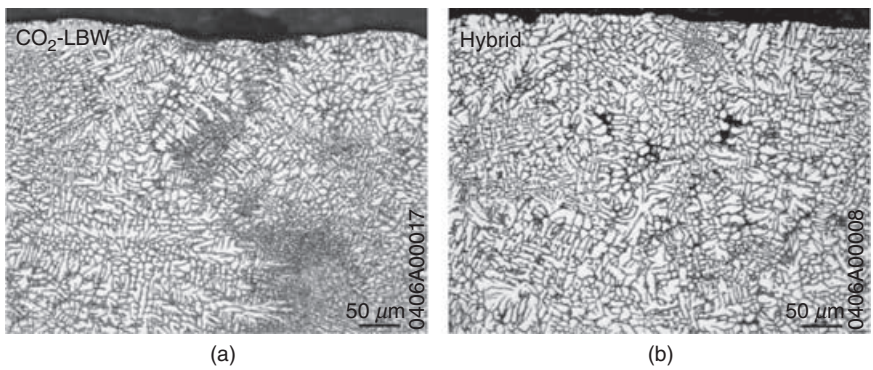

5.8 Typical dendritic structure in the upper section of the fusion zone in (a) CO_2 laser beam weld and (b) hybrid weld in a 3.2 mm thick AA6013 sheet butt-welded in T6 (Vaidyaa, 2006).

using hybrid laser welding. This is because autogenous laser welding often causes defect as pores, cracks and joint defects. In addition, an autogenous laser weld has a lowered mechanical properties.

In Fig. 5.7, an example of laser and hybrid welded cross section of an aluminium alloy is shown. A typical microstructure is shown in Fig. 5.8.

5.3 Hardness

Hardness is an important measure of mechanical properties and is used as a quality factor for applications where structural integrity is critical, e.g. shipbuilding and pressure vessels. Autogenous laser welding of high-strength steels may easily cause too high a hardness and hybrid laser welding can be helpful in decreasing hardness to an acceptable value. In aluminium alloys, hybrid laser welding offers the possibility of using filler metal to balance hardness closer to the level of the base metal.

5.3.1 Carbon steels

Comparing the heat input per unit length for typical arc and laser-based welds shows that the heat input in laser welds is typically almost an order of magnitude lower than in arc welds. It must therefore be taken into consideration that structural steels may become hard in both the weld metal (WM) and the heat-affected zone (HAZ) as a consequence of the fast thermal cycle inherently connected to the process. The resulting hardness depends, however, much on the composition of the steel and especially of the carbon content, as this controls the maximum possible hardness in a fully martensitic structure. (Kristensen 2007). Even in ordinary low-carbon steels, martensite can be formed but its hardness is low, because of low carbon content.

Figure 5.9 shows the hardness distributions of the laser weld, GMA weld and laser–GMA weld for 600 MPa grade steel. The hardness was evaluated along the line 0.8 mm below and parallel to the up surface of the substrate

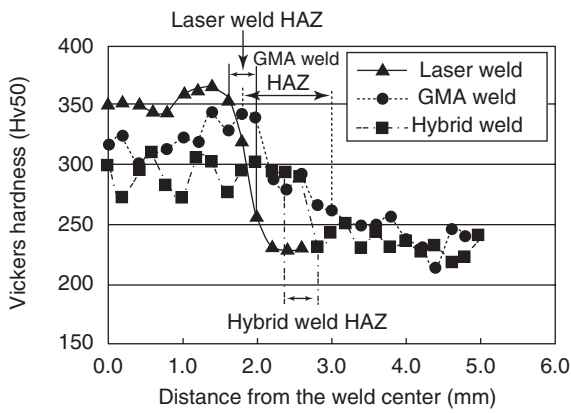

5.9 Hardness distribution in laser weld, GMA weld and laser–GMA hybrid weld (Liu *et al.* 2006).

plate. The distance between two trail points was 0.2 mm. The laser weld metal showed highest hardness about 350–370 HV. The hybrid weld metal showed the lowest hardness about 275–310 HV. The hardness of GMA weld metal in the middle level among the three kinds of weld metals. The hybrid weld metal had lower hardness than GMA weld metal because of the tested line in the laser and GMA arc welded zone in hybrid weld (Liu *et al.* 2006, Thomy *et al.* 2007).

Thus, it is shown that with hybrid laser welding, the hardness level can be more easily controlled than in autogenous laser welds. Hardness values are, however, sensible to parameters used and composition of the base and filler metal. Figure 5.10 shows an example of quenched and tempered HSLA S1100QL steel, where weldability is mainly determined by reaching the required strength and ductility value of the joint as well as by the

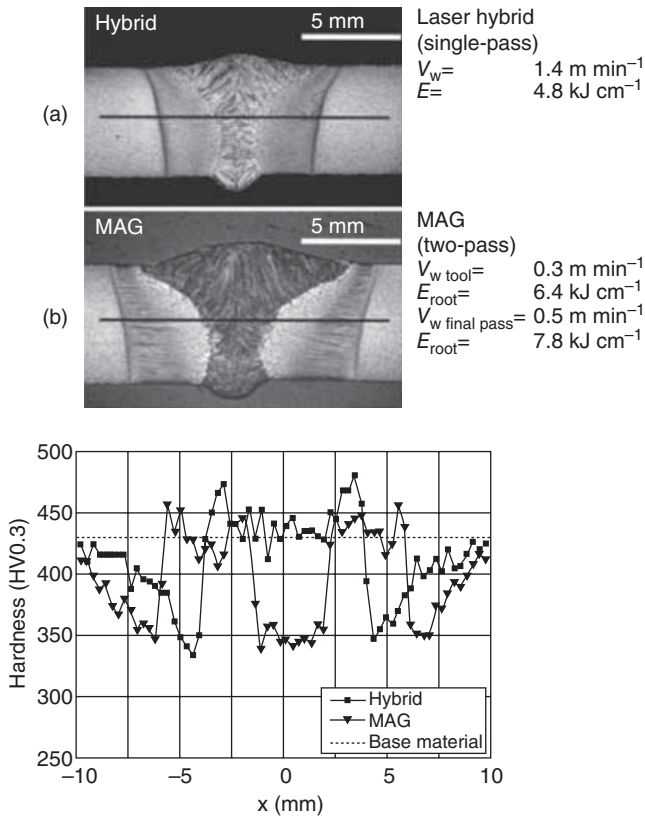

5.10 Micrographs and hardness distribution of (a) a hybrid weld and (b) a two-layer MAG weld, S1100QL (E = heat input per unit length) (Jahn *et al.* 2005).

evidence of the cold cracking resistance and brittle fracture resistance (Jahn *et al.* 2005). Owing to the quenched and tempered processes, the base material S1100QL consists of a tempered martensitic–bainitic structure with finely distributed carbide precipitates. The hardness of the base material is very high and amounts 420–450 HV0.3. Regardless of the welding technique, similar hardness distributions appeared in the HAZ. The welding heat causes a tempering of the base material in the outer HAZ. This effects a clear hardness reduction in this area. The maximum hardness appears on the line between outer and inside HAZ. This value is only insignificantly higher than that of the base material.

The lower heat input in the case of hybrid welding effects a higher maximum hardness value in the HAZ, compared with the metal active gas (MAG) seam. In spite of using the same filler material, the hybrid seam shows a visible increase of hardness in the weld metal. The reasons are a lower heat input, a higher content of base material in the weld metal because of the single-square-groove welding and no tempering process of a subsequent pass (Fig. 5.10) (Jahn *et al.* 2005). The same dependence of cooling rate, heat input and hardness is seen with all high-strength steels (Verwimp *et al.* 2007, Kristenset *et al.* 2007, Nielsen *et al.* 2007).

The mechanical properties of ultra-high strength steels are caused by the controlled rolling and tempering process during cooling. Therefore, a weld, which is basically a cast structure, has lower hardness than base material. Laser welding causes remarkably narrower melt and HAZ than arc welding and the soft zone is therefore also narrower, which makes laser welding a favourable process in many applications. Hybrid laser welding allows the possibility of using a filler metal which compensates for the decrease in softening. This is why hybrid laser welding is an especially promising process for joining of ultra-high strength steels (Laitinen *et al.* 2007, Leiviskä *et al.* 2007, Masato and Kyoyuki 2005).

In many applications, it is necessary to use position welding. According to Table 5.1, mechanical properties including hardness do not vary remarkably independently of welding position (Howse *et al.* 2005).

5.3.2 Aluminium alloys

Aluminium alloys, which are not heat treated do not show any major difference in hardness behaviour between base and weld metal. However, it is well known that hardness is decreased in welds of many aluminium alloys if filler metal is not used. This is especially the case when hardness is caused by heat treatment. This can be a problem in some applications of ordinary autogenous laser welding. By using filler metal as in hybrid welding, the difference in hardness can be minimized. If matching composition is used, hardness is similar as in autogenous laser welding, Fig. 5.11 (Vaidyaa *et al.*

Table 5.1 Mechanical testing results for Yb fibre laser–MAG hybrid welds made in X80 C–Mn line-pipe steel at a travel speed of 1.8 m min^{-1}. Charpy values quoted are actual values for sub size (7.5 × 10 mm) specimens tested at −10 °C (Howse *et al.* 2005)

Position	Charpy impact values at −10 °C (J)		Maximum hardness (HV10)		Cross-weld tensile tests (N mm^{-2})	Parent/ weld failure
	Average	Lowest	Weld metal	HAZ		
Overhead (4G)	73	64	380	380	700, 686, 696	Parent
Vertical up (3G)	78	70	394	387	732, 726, 728	Parent
Flat (1G)	69	65	357	413	722, 732, 689	Parent

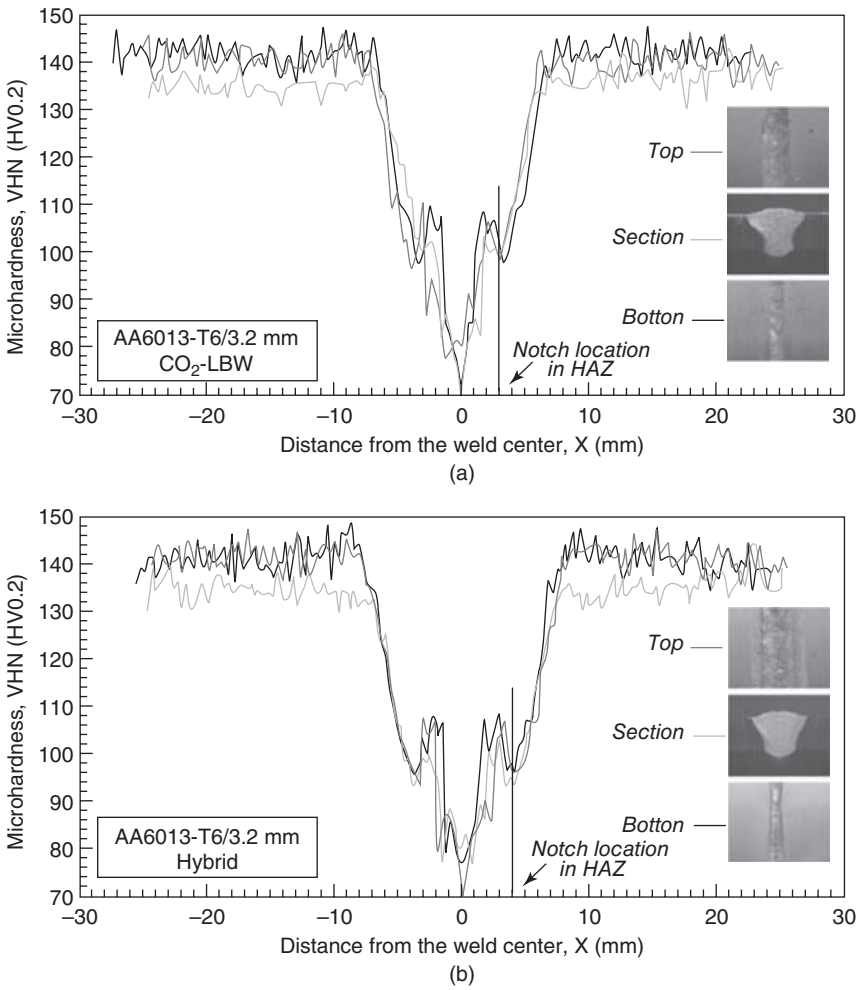

5.11 Microhardness gradient in (a) CO_2 laser beam weld and (b) hybrid weld in a 3.2 mm thick AA6013 sheet butt-welded in T6. Insets indicate the locations used for microhardness measurements. The notch location in the heat-affected zone (used for fatigue crack propagation tests) is shown in relation to the microhardness dip (Vaidyaa *et al.* 2006).

2006). A lowered hardness can be minimized by post-weld heat treatment (van Haver 2006).

5.4 Strength

5.4.1 Carbon steels

It is well known that ordinary low-strength carbon steels are easily welded by laser arc or hybrid welding. The strength of sound welds are the same or higher than that of base metals. So yield or tensile strength is not critical in hybrid welding of them.

In low-alloyed high-strength steels, the strength is partly caused by heat treatment during or after production of the steel. In these, the strength can be lowered if filler metal is not used. The difference seems to not to be critical in 600 MPa strength level (Liu *et al.* 2006). In ultra-high strength steels, the strength is much lower in autogenous laser welds. By using filler metal, the difference between the strength of base and weld metal can be remarkably diminished, Fig. 5.12 (Masato and Kiyoyuki 2006). It is, however, important that an inappropriate filler material in combination with low heat input can also lead to excessive metal hardness and strength leading to lowered toughness (Verwimp *et al.* 2007).

In Fig. 5.13, it is shown that yield and tensile strength of 1100 MPa steel hybrid welds can be maintained very close to the level of base metal with minimal softening (Jahn *et al.* 2005), unlike those of arc welds. Similar results are shown with CO_2-, fibre- and disc-laser welds, as well as with CO_2 and fibre-laser hybrid welds (Leiviskä *et al.* 2007, Laitinen *et al.* 2007).

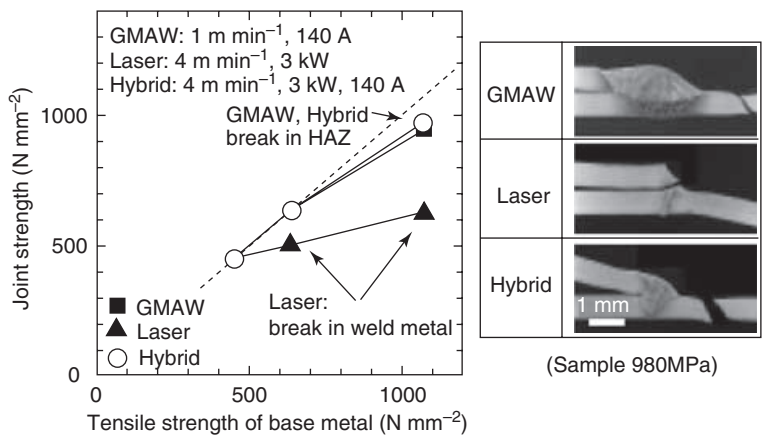

5.12 The tensile strength of welded joints of high-strength steel sheets with three different welding processes (Masato and Kiyoyuki, 2005).

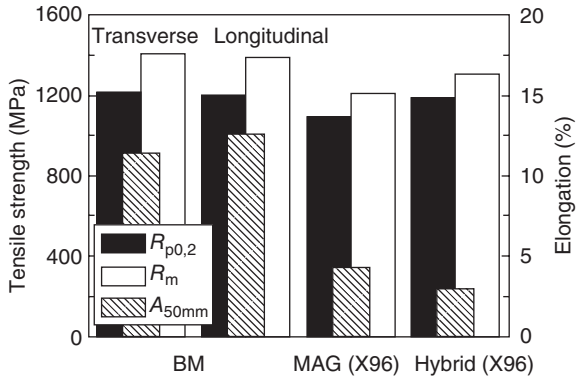

5.13 Strength and elongation of S1100QL, base metal, MAG and hybrid welds (Jahn *et al.* 2005).

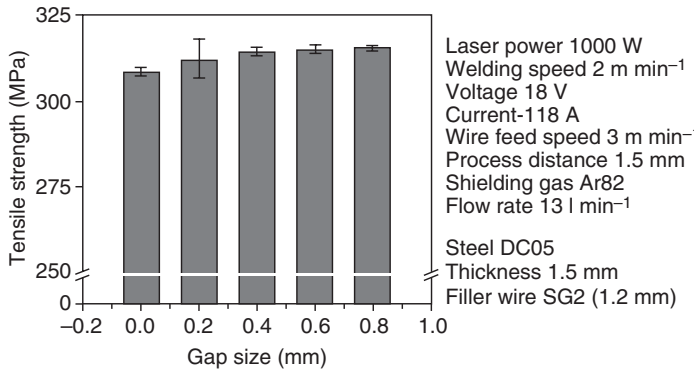

5.14 Effect of gap on tensile strength (Thomy *et al.* 2007).

Thomy *et al.* (2007) studied the effect of air gap on mechanical properties. It was found that the gap did not have a major effect on tensile strength or hardness at low strengths 310 MPa, Fig. 5.14.

5.4.2 Aluminium alloys

As for hardness, strength properties are also decreased in autogenous laser welding. With hybrid laser welding using a suitable filler metal, the decrease can be minimized. Van Haver *et al.* (2006) studied hybrid welding of 6056 aluminium alloy. According to the AIMS standard its tensile strength R_m in T4 heat treatment condition is >295 MPa and $R_{p0.2}$ >185 MPa. By using different filler metals, hybrid welds can reach $R_{p0.2}$ 220–240 MPa, and with T78

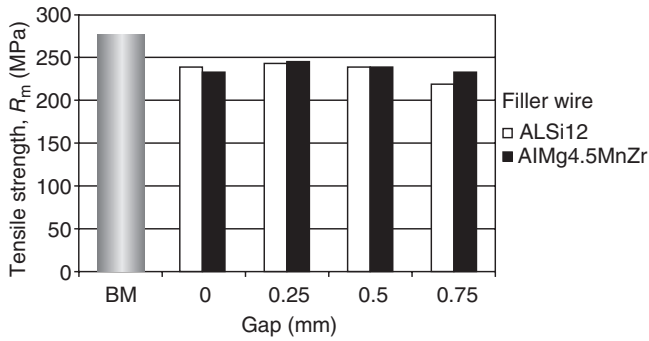

5.15 Tensile strength of square butt welds after artificial ageing on 3 mm AlMgSi1 with different gaps compared with the base material (BM), welded with filler wires AlSi12 and AlMg4.5MnZr (Dilthey *et al.* 2005).

post weld heat treatment this could be increased up to 280 MPa. In the test, the fracture occurred in the weld metal, which means that base metal enabled much higher strength than required.

The strength values which have been achieved with the hybrid process on materials with thicknesses from 2 to 5 mm correspond to the values that are to be expected after softening by the welding processes. In particular, the application of SG AlMg3 to Mg5 wires and with artificially aged joints, the method results in high strength values with a high uniformity, Fig. 5.15 (Dilthey *et al.* 2005).

5.5 Toughness

Toughness is an important property of base-centred cubic metals such as carbon steels because of transition temperature, under which toughness can be dramatically decreased. On the other hand, face-centred cubic metals such as austenitic stainless steels or aluminium alloys do not show this phenomenon of transition temperature and therefore they are more or less tough at all temperatures in static conditions.

5.5.1 Carbon steels

Kristensen (2007) has investigated the impact properties of thick plate S235 steel. Figure 5.16 shows as an example a full Charpy V-notch transition curve for a weld in the 12 mm S235 structural steel welded with an initial gap of 0.5 mm. As shown, the transition temperature is below –40 °C and, owing to the very tough structure, the level of the high temperature shoulder is significantly higher than the level of the base metal alone.

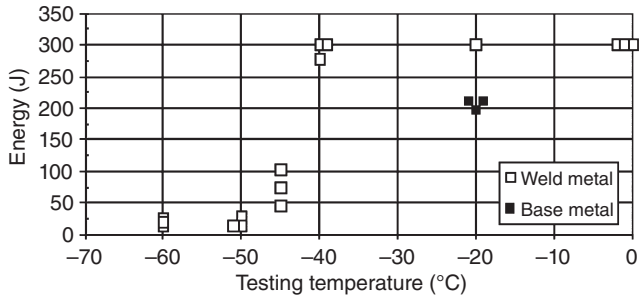

5.16 Charpy V-notch transition curve for the 0.5 mm gap weld made in 12 mm S235 structural steel. The maximum energy of the testing equipment is 300 J (Kristensen, 2007).

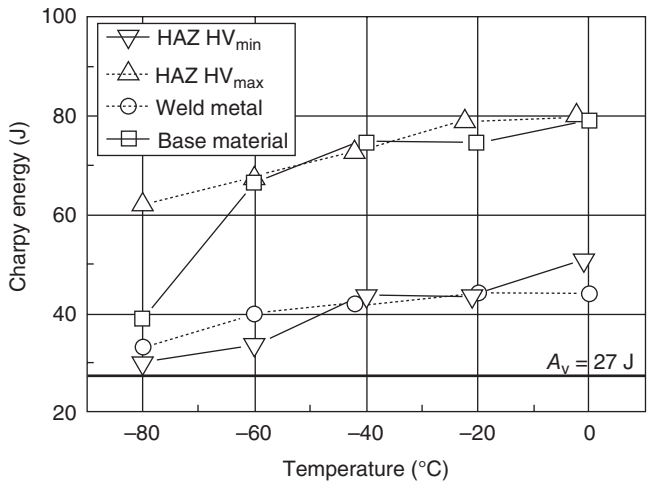

5.17 Charpy energy in dependence to the test temperature, S1100QL (Jahn *et al.* 2005).

Liu *et al*. (2006) studied Charpy V-notch toughness of weld metals of laser weld, GMA weld and laser-GMA hybrid weld in high-strength steels (600 MPa). It was found that the differences between processes were not very high. Laser welding showed lower impact energy in low temperatures. Jahn *et al.* (2005) showed that it is possible to have impact energy values of 30–40 J at 60 °C and yield strength 1100 MPa, Fig. 5.17. The fusion zone definitely revealed a lower Charpy energy than the base material, because of the fine acicular cast structure, rapidly cooled from the welding heat. The Charpy energy for the martensitic structure in the hardness maximum of

the HAZ is of the same level as of the base material. In the HAZ, the hardness minimum caused low impact energy values. The structure in this area consists of martensitic and ferritic grains as well as of partly quite coarse carbides.

Hybrid welding in different positions does not produce any remarkable effect on Charpy impact properties, as seen Table 5.1 (Howse *et al.* 2005).

5.6 Fatigue properties

To guarantee a high fatigue strength level in the welded joint is the outstanding challenge for industrial applications in fatigue-loaded constructions. Thus, the welding process and the quality of the welded joints have to meet the highest demands. The mechanical properties of the joints made in high-strength low-alloyed steels, are strongly dependent on the cooling time during the welding. Too short a cooling time causes a strong hardness increase in the welded joint closely connected with the danger of cracking. On the other hand, a loss of strength and ductility values have to be expected, for too long a cooling time (Jahn *et al.* 2005).

MAG welding is usually applied to weld high-strength steels. This process offers a high stability which is necessary for structural steel welding. However, a low practicable welding speed and the requirement of multi-pass welding at higher sheet thickness causes a low productivity and a high heat input in the welded structure. The consequences are a wide HAZ with reduced mechanical properties, e.g. decreased toughness and strength, as well as large distortion. In contrast to this, laser welding offers a deep penetration and a high welding speed. On the other hand, this welding process demands an exact beam positioning and a very low gap width. Laser–MAG hybrid welding techniques are excellent alternatives to overcome these disadvantages.

5.6.1 Constructional steels

The suitability of welded joints for fatigue loading is preliminary dependent on the seam design, metallurgical characteristics and the resulting properties of the diluted weld metal. In high-strength steels, it is also dependent on the reduction in the material properties in the HAZ. Experiences of studies on unwelded high-strength steels show the possibility of increasing the fatigue strength by using steel grades with higher tensile strength. However, this aim can only be reached by a reduction of stress concentrations. Consequently, the fatigue limit of unmachined welded joints is nearly independent on the base metal strength, owing to the notch effect (Jahn *et al.* 2005).

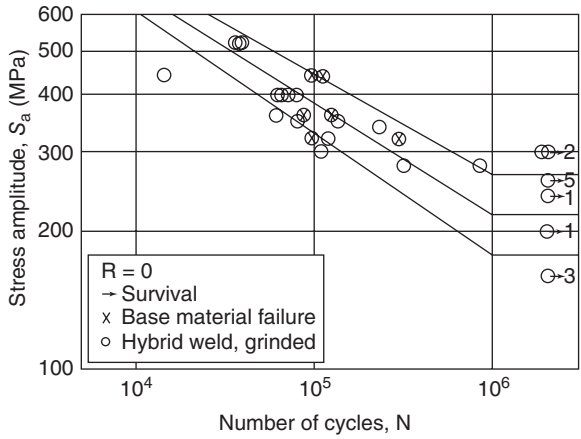

5.18 S–N curve of laser hybrid welds, $R = 0$, S1100QL, $S_{A\ 50\%}$ = 218 MPa (Jahn *et al.* 2005).

Figure 5.18 shows the results of the fatigue tests made at the laser hybrid welded joints. The fatigue limit $S_{A\ 50\%} = 218$ MPa ($P = 50\%$), gained at the stress ratio $R = 0$, exceeds the known fatigue limit values for unmachined welds with a factor of 2 to 3. Shot peening or TIG welding is used as post treatment.

The fatigue limit of $S_{A\ 50\%} = 328$ MPa was determined for a stress ratio of $R = -1$. It is about a factor of 3 above the reversed fatigue limit of unmachined welds of S960QL. The finite life fatigue strength values were clearly higher than those of S 960QL. The analysis of the fracture in Fig. 5.18 revealed that the fatigue crack at stress amplitude values near the fatigue limit always occurred at pores in the weld metal. With increasing stress amplitudes, failures in the grinded base material have been found. The diameter of the pores, positioned on the fracture surface, was between 0.1 and 0.6 mm.

With suitable parameter combinations excellent fatigue properties can be produced for high-strength structural steel butt joints even with thick materials (12 and 25 mm), Fig. 5.19 (Petring *et al.* 2007).

The influence of weld geometry on the fatigue life of laser welded HSLA-65 structural shapes was studied by Caccese *et al.* (2004). Much better control of weld geometry is possible with laser welding compared with more conventional techniques such as SMAW and GMAW. This is especially true when laser is combined with GMAW and it was demonstrated that welds with a nearly circular profile could be achieved. Welds with a circular profile can result in much better fatigue life than the same size weld with other profiles. This implies that smaller weld sizes of a circular

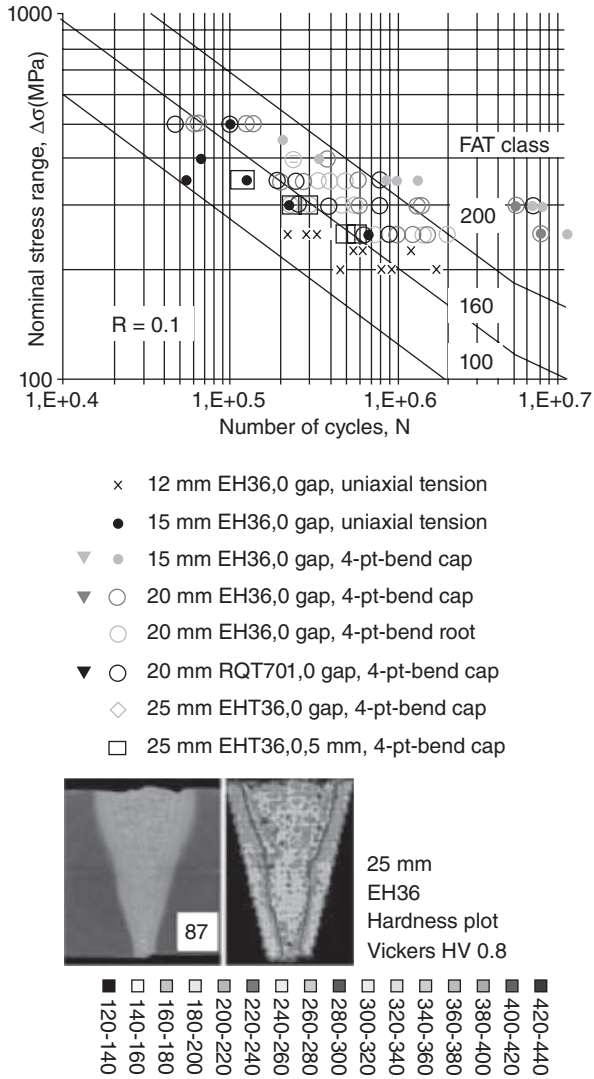

5.19 Excellent fatigue results of laser–MAG hybrid welds (V or Y-grooves) in high-strength structural steels up to 25 mm comply with high FAT classes according to design S–N curves of Eurocode 3 (tested by IEHK, RWTH Aachen) (Petring *et al.* 2007).

profile can be used to achieve the same fatigue life as larger conventional welds. This results in potentially higher processing speeds and a more efficient use of filler metal. (Caccese *et al.* 2004). Good fatigue properties for Nd:YAG-MAG and CO_2 hybrid welds of ordinary structural steel S235 are also achieved (Weldingh and Kristensen 2003, Remes *et al.* 2003).

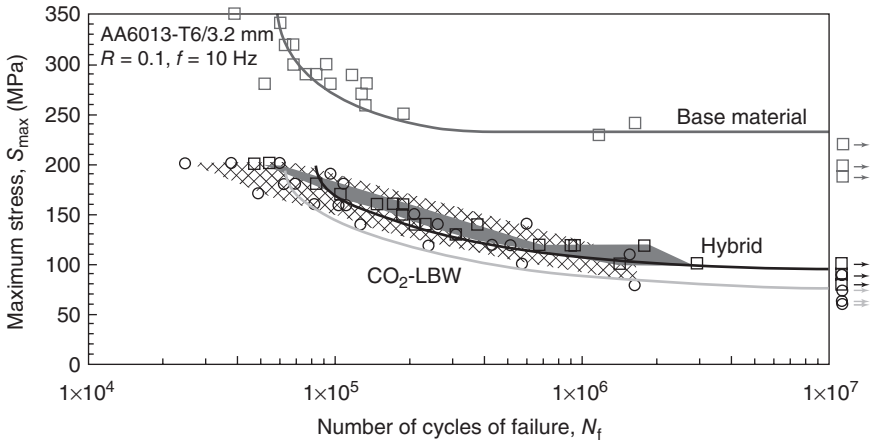

5.20 Comparative fatigue behaviour of the CO_2 laser beam weld and the hybrid weld in a 3.2 mm thick AA6013 sheet butt-welded in T6. Run-outs (i.e., unbroken specimens) are indicated by arrows (Vaidyaa, 2006).

5.6.2 Aluminium alloys

Fatigue is sensitive to defects, and it is therefore a more critical evaluation parameter than the tensile strength, since surface defects may not necessarily affect the latter. The major surface defects present are occasional undercuts and spatter in autogenous laser welding, whereas the hybrid weld is more free from such defects.

The fatigue behaviour of aluminium alloy AA 6013 is shown in Fig. 5.20 (Vaidyaa 2006). The base material data were obtained on finely milled surface (roughness, $Ra < 1$ μm) and should represent the uppermost limit that can be achieved by a fusion weld. Both the laser and hybrid welds had a fatigue resistance much lower than the base material. The hybrid welds are found to exhibit a better resistance to fatigue than laser welds.

Van Haver *et al.* (2006) compared the fatigue strength of hybrid laser and friction stir welds of aluminium alloy 6056 and found that FSW shows some higher fatigue strength compared to hybrid welds.

5.7 Corrosion properties

Corrosion properties are especially important when stainless steels are welded. In autogenous laser welding, it has previously been shown that pitting corrosion properties are better and critical pitting temperature (CPT) higher, compared with arc welding, e.g. TIG process (Kujanpää and

Table 5.2 CPT for pickled weld surface (cap) and root surfaces. LN and LFN are autogenous laser welds, the others are laser–TIG hybrid welds with various shielding gas mixtures (Ar_2–N_2) (Westin *et al.* 2007).

Test	CPT (°C)	
	Cap	Root
LN	17 ± 6	16 ± 7
LGA	22 ± 2	13 ± 5
LGN	21 ± 4	20 ± 5
LFN	18 ± 5	12 ± 6
LGFA	18 ± 5	16 ± 6
LGFN	21 ± 5	20 ± 5

David 1986). This is because of the higher cooling rate and therefore milder microsegregation of, in particular, molybdenum.

Studies on corrosion properties of hybrid welding of stainless steels are quite limited. Westin *et al.* (2007) studied pitting corrosion properties of laser and hybrid laser welding of lean duplex stainless steels, Table 5.2. It was found that the base metal had an average CPT of 26 ± 3°C; while the welds showed somewhat lower values. The surface had generally higher CPT than the root, but the scatter was rather large as is normal when corrosion testing laser welds. The difference in CPT between the different welding methods was small. The autogenous laser welds had the lowest average CPT and showed most pits in the weld metal on the surface side.

5.8 References

CACCESE V, BLOMQUIST P, OROZCO N, BERUBE K (2004) Fatigue life prediction of HSLA-65 welds made by laser/GMAW processes, *23th International Congress on Lasers and Electro-Optics (ICALEO 2004)*, Paper 709 Oct. 4th–7th, 2007, San Francisco, CA, USA, 93–102.

DILTHEY U, BRANDENBURG A, REICH F (2005) Investigation of the strength and quality of aluminium laser–MIG hybrid welded joints, International Institute of Welding, *IIW doc*. IV-882-05.

FELLMAN A, JERNSTRÖM P, KUJANPÄÄ V (2003) CO_2-GMA hybrid welding of carbon steel – the effect of shielding gas composition, *Proc Conf. Appl. Electro-Optics*, Jacksonville, FL, USA, 56–75.

HOWSE D, SCUDAMORE RJ, BOOTH G (2005) Yb fibre laser/MAG hybrid processing for welding of pipelines, International Institute of Welding, *IIW doc*. IV-880-05.

JAHN A, WINDERLICH B, ZWICK A, IMHOFF R, BRENNER B, TRÜMPER S (2005) Laser hybrid welding of fatigue loaded structural components made of the quenched and tempered HSLA steel S1100QL, International Institute of Welding, *IIW doc*. IV-886-05.

JOKINEN T, KARHU M, KUJANPÄÄ V (2002) Welding of thick austenitic stainless steel using Nd:YAG laser with filler wire and hybrid process, *21st Int. Congress on Appl. of Lasers and Electro-Optics (ICALEO2002)*, Oct. 14–17, 2002, Scottsdale, AZ, USA.

KRISTENSEN JK (2007) Thick plate hybrid CO_2-laser/MAG hybrid welding of steels, International Institute of Welding, *IIW doc*. IV-932-07.

KRISTENSEN JK, RASMUSSEN FR, NIELSEN SE (2007) Very thick plate hybrid CO_2-laser/MAG single and multi-pass welding of structural steels, *11th Conf. Nordic laser materials processing*, Lappeenranta, Finland, 589–601.

KUJANPÄÄ V, DAVID S (1986) Microsegregation in high-molybdenum austenitic stainless steel laser beam and gas tungsten arc welds, *Proc. 5th Int. Congress on Applications of Lasers and Electro-Optics ICALEO 1986*, 10–13 Nov. 1986, Arlington, VA, USA, 63–69.

LAITINEN R, KÖMI J, KESKITALO M, MÄKIKANGAS J (2007) Improvement of the strength of welded joints in ultra-high strength OPTIM 960 QC using autogenous Yb:YAG laser welding, *Nordic Laser Materials Processing Conference (NOLAMP 11)*, Lappeenranta, Finland, 204–215.

LEIVISKÄ P, FELLMAN A, LAITINEN R, VÄNSKÄ M (2007) Strength properties of laser and laser hybrid welds of low alloyed high-strength steels, *11th Conf. Nordic laser materials processing*, Lappeenranta, Finland, 173–184.

LIU Z, KUTSUNA M, XU G (2006) Properties of CO_2 laser-GMA hybrid welded high-strength steel joints, International Institute of Welding, *IIW doc*. IV-907-06.

LIU Z, KUTSUNA M (2005) Metallurgical study on laser-MAG hybrid welding of HSLA-590 steel, *24th International Congress on Lasers and Electro-Optics (ICALEO 2005)*, Paper 304, Oct. 31th–Nov. 3th, 2005, Miami, FL, USA, 127–134.

MASATO U, KIYOYUKI F (2005) Laser–arc hybrid welding of automotive high strength steel sheets, International Institute of Welding, *IIW doc*. XII-1854-05.

NIELSEN JS, ACCORSI M, OLSEN F (2007) Studies on induction assisted laser–hybrid welding, *11th Conf. Nordic Laser Materials Processing*, Lappeenranta, Finland, 602–613.

PETRING D, FUHRMANN C, WOLF N, POPRAWE R (2007) Progress in laser-MAG hybrid welding of high-strength steels up to 30 mm thickness, *26th International Congress on Lasers and Electro-Optics (ICALEO 2007)*, Paper 604, Oct. 29th–Nov. 1st, 2007, Orlando, FL, USA, 300–307.

REMES H, KUJALA P, LAITINEN R (2003) Fatigue characteristics of CO_2-laser MAG welded joints of laser RAEX Steel, *9th Conf. on Laser Materials Processing in the Nordic Countries*, 4–6 Aug., 2003, Trondheim, Norway, 37–48.

THOMY C, SEEFELD T, VOLLERTSEN F (2007) Fibre laser GMA hybrid welding of thin sheet material, *26th International Congress on Lasers and Electro-Optics (ICALEO 2007)*, Paper 1608, Oct. 29th–Nov. 1st, 2007, Orlando, FL, USA, 896–902.

VAIDYAA WV, ANGAMUTHUA K, KOÇAKA M, GRUBEB R, HACKIUSC J (2006) Strength and fatigue resistance of laser-MIG hybrid butt-welds of an airframe aluminium alloy AA6013, International Institute of Welding, *IIW doc*. IX-2222-06.

VAN HAVER W, STASSART X, VERWIMP J, DE MEESTER B, DHOOGE A (2006) Friction stir welding and hybrid laser welding applied to 6056 alloy, *IIW doc*. IX-NF-10-06/IX-2209-06.

VANDEWYNCKÈLE A, COUSO EV, OTERO JA, DE LAMA MP, QUINTÁNS G (2007), Laser–arc welding of duplex stainless steel, *Int. Conf. Lasers and Electro-Optics*, Orlando, FL, USA, 293–299.

VERWIMP J, GEDOPT J, GEERINCKX E, VAN HAVER W, DHOOGE A, CRIEL D (2007) Hybrid laser welding of dual phase steel DP600: Microstructural and mechanical properties, *Int. Conf. Applications of Lasers and Electro-optics*, Orlando, FL, USA, 325–334.

WELDINGH J, KRISTENSEN J (2003) Hybrid YAG-laser/MAG welding, quality and stability, *9th Conf. on Laser Materials Processing in the Nordic Countries*, 4–6 Aug., 2003, Trondheim, Norway, 15–24.

WESTIN E, KEEHAN E, STRÖM M, VON BRÖMSSEN B (2007), Laser welding of a lean duplex stainless steel, *Int. Conf. Lasers and Electro-Optics*, Orlando, FL, USA, 335–344.

6

Quality control and assessing weld quality in hybrid laser–arc welding

J. K. KRISTENSEN, FORCE Technology, Denmark

Abstract: Quality control and assessment of weld quality is examined for structural steels, aluminium alloys and stainless steels. Hybrid laser–arc welding shows a great potential in many structural applications and therefore evaluation of the mechanical properties as well as non-destructive testing are crucial issues to consider, that however involve a number of challenges. The challenges may be grouped into equipment-related challenges, process and quality monitoring, destructive and non-destructive testing as well as materials related problems.

Key words: laser arc welding, laser hybrid welding, quality control, non-destructive evaluation, steel, aluminium alloys.

6.1 Introduction

Hybrid laser–arc welding of structural materials has been the subject of intensive research and development for almost two decades. The challenges which have been dealt with may be grouped into equipment, process, quality, monitoring, non-destructive evaluation (NDE) and materials-related issues. In this chapter, the focus will be on quality control and assessing weld quality and, firstly, the weldability of some typical structural materials will be reviewed.

6.2 Weldability of typical structural materials

6.2.1 Structural steels

Structural steels are ferritic steels typically strengthened by C, Mn and various amounts of microalloying element as e.g. Ti, V or Nb. Small amounts of Cu, Cr and/or Ni may also be contained in the steels especially if they are scrap based. Different production routes (e.g. as-rolled, normalised, normalised rolled, controlled rolled, accelerated cooled, TMCP or QT delivery condition) are used depending on the demands to the steels (typically strength and toughness) and the available techniques at a given steel work.

Silicon and normally also Al is used for killing (deoxidising) the steels. Important impurity elements are S and P which may adversely influence the weld results. The guaranteed yield strength of structural steels typically falls in the range 235–700 MPa, but higher grades also exist.

The introduction of laser and hybrid laser–arc welding meant that it became of paramount importance that a number of general problems related to the properties of welded steel structures were solved. Developments during the last 3–4 decades in materials and their response to welding had to be reconsidered in the light of this new technology. Below a few of the major challenges and their possible solutions will be dealt with.

Self-quenching

Comparing the heat input per unit length for typical arc and laser welds (for the same penetration or throat thickness, respectively) shows that the heat input in laser welds is typically almost an order of magnitude lower than for arc welds. It must therefore be taken into consideration that structural steels may become fully martensitic in both the weld metal (WM) and the heat-affected zone (HAZ) as a consequence of the fast thermal cycle inherently connected to high-power, high-speed laser welding. This immediately gives rise to concerns related to e.g. hardness, ductility, toughness, fatigue and corrosion properties. Three principally different approaches to solve these challenges may be identified, namely:

- **Scenario 1:** Limitations to the weld speed so that the microstructure and consequently also the mechanical properties become acceptable for the relevant steels.
- **Scenario 2:** Preheating in order to decrease the cooling time and thus the hardness. It is primarily the cooling rate in the temperature interval 800–500 °C which influences the hardness in steels.
- **Scenario 3:** Limitations to the steel composition so that the mechanical properties become acceptable for all welding speeds, i.e. also for a fully martensitic microstructure.

In scenario 3, advantage is taken of the fact that the maximum hardness of a fully martensitic structure is determined to a good approximation by the carbon content only. Important consequences of scenario 1 are limitations to productivity as well as a need to use welding parameters dependent on the composition of the steel and scenario 2 is of course difficult to use on large structures. This argues in favour of scenario 3, but it must be taken into account that a consequence of this scenario is the limitation in carbon content to e.g. approximately 0.12% in order to limit the maximum hardness to roughly 380 HV, and this limitation in composition causes further limitations in the manufacturing of the steels.

Fracture path deviation in impact and toughness testing

As an other example, the impact toughness of the weld metal was in the beginning very challenging to measure by the standard Charpy V-notch test technique owing to fracture path deviation into the softer base metal. Originally, these test results therefore were disregarded, but based on a large amount of wide plate and other large scale tests as well as numerical simulation, the traditional Charpy test is now considered valid even in the presence of fracture path deviation.

Solidification flaws

Solidification flaws constitute a type of weld imperfection that is occasionally found in laser welds in structural steels. The imperfection is a solidification defect, but unlike usual solidification cracks (or hot cracks), solidification flaws are generally small, isolated imperfections occurring with a certain regularity along the weld. The flaws normally are embedded and seen in the weld centre-line only. The causes of the flaws are manifold and complexly interacting, but control of this phenomenon is a key challenge to thick plate structural steel laser welding. Figure 6.1 shows examples of the flaws.

Traditional types of solidification cracking tests are all characterised by the testing that is performed at one set of welding variables only, and normally also by a fixed mechanical constraint. They are thus good for evaluating the tendency for solidification flaw formation at this particular point in the weld parameter space, but not so suitable for determining the influence of e.g. the steel composition. In earlier research related to laser welding of

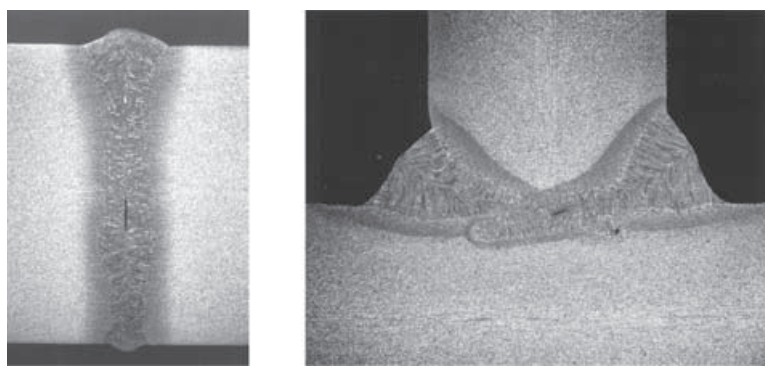

(a) (b)

6.1 Solidification flaws in hybrid laser–arc welded structural steels: (a) an I-butt 15 mm butt weld and (b) a T-joint in 12 mm plate thickness.

structural steels, these types of test have nevertheless also been used in the form of rigid butt welds and wedge type test specimens.[1] The research has been only partly successful, as a correlation of the cracking tendency with a compositional parameter (e.g. S/Mn + P) has been found, but the experimental scatter seems very high.

If total freedom from solidification flaws is demanded in addition to the control of the steel composition the welding parameters have also to be controlled. In particular, it seems beneficial to use excess laser power (relative to just penetrating) in order to stabilise the keyhole cavity geometry and dynamics. Figure 6.2 shows as a typical example a so-called weldability lobe: the welds are evaluated with respect to EN ISO 13919-1:1996, level C which is also the specified acceptance level.[2,3]

One approach has been to correlate the steel composition with the volume of the weld parameter tolerance box. In this way, the steel is tested by a range of weld parameters and the size of the obtained weld parameter box, i.e. the area in the weldability lobe plot that ensures acceptable welds, is taken as a measure of the weldability with respect to solidification flaw formation of the actual steel. By this approach a correlation like the one shown in Figure 6.3 may be found. The graph covers a large number of steel compositions and it is seen, that a welding parameter window of a reasonable size is achievable by controlling the steel composition. This approach

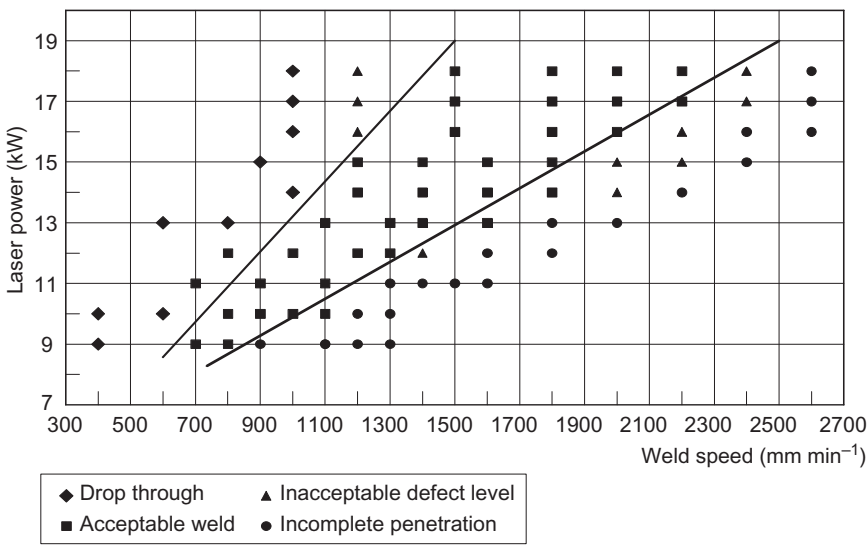

6.2 Weldability lobe for a 0.10%C–1.5%Mn–0.004%S–0.011%P grade S 355 TMCR steel. The welds are evaluated with respect to EN ISO 13919-1:1996, level C.

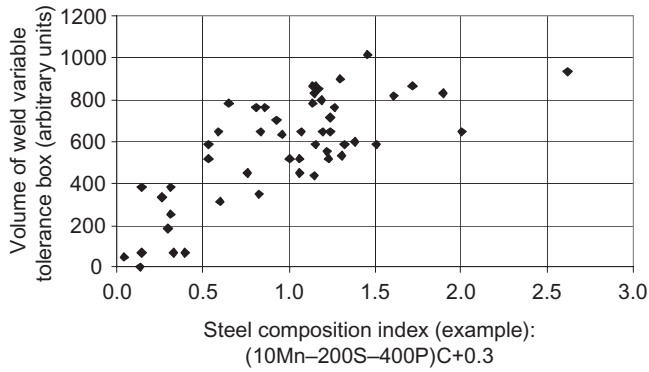

6.3 Weldability with respect to solidification flaw formation as a function of an index developed from the steel composition. The steel composition index shown is one example on a correlation, only.

has, since 1996, been adopted in many classification society rules for ship building.[3]

6.2.2 Aluminium alloys

Pure aluminium is soft and weak and for most applications one or more strengthening mechanisms are taken advantage of in order to improve strength and hardness. When discussing weldable wrought aluminium alloys for structural use, the main materials groups are as follows:

- pure aluminium and AlMn solid solution hardened types,
- AlMg and AlMgMn, solid solution hardened types,
- AlMgSi age (and solid solution) hardened types, and
- AlZnMg(Cu) age (and solid solution) hardened types.

Furthermore, Cu(MnMgSi)- and Li(MgCuZr)-alloyed types may achieve very high strengths, but for the first group the weldability is in general low while the latter group of alloys is still under development. In addition, cast types and, in particular, the very common AlSi-group may be mentioned.

The materials may be delivered in various stages of heat treatment and often deformation hardening (cold working) possibly in combination with annealing or partly re-crystallisation is used for optimising the mechanical properties further.

In relation to welding in general, aluminium alloys exhibit the following characteristics:

- low melting temperature,
- large thermal conductivity,

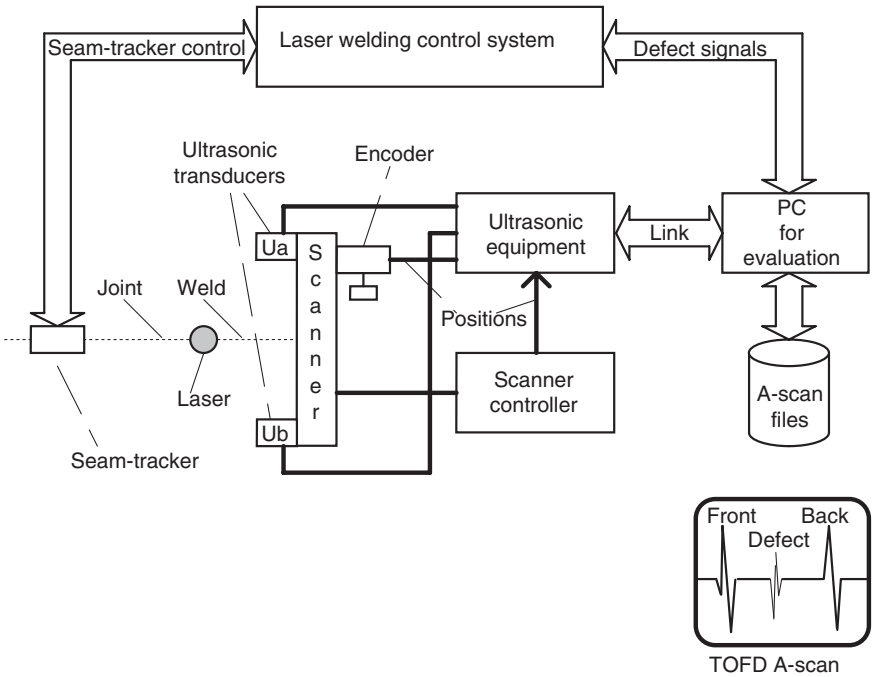

6.4 Defect detection using ultrasonic NDT.

- large solidification interval and therefore tendency to solidification cracking,
- liquid aluminium may dissolve more than an order of magnitude more hydrogen than solid which results in a tendency for porosity formation,
- Liquid aluminium has a low surface tension (roughly half that of steel) which means a poor ability to support the molten pool in fully penetrating welds.
- Opposed to welds in steel, a significant reduction in strength in the weld metal and/or the HAZ is, in general, observed for welds in aluminium. Possible exceptions are purely solution hardened and non-cold-worked alloys.

With special relation to laser welding it may in addition be mentioned that

- Although aluminium has a low melting temperature, it does not exhibit a correspondingly high vapour pressure. This means that key-hole type laser welding will be performed at a relatively high temperature owing to the coupling between the cavity internal pressure and temperature.

Many alloying elements (especially Mg) nevertheless have a high vapour pressure. This results in a pronounced tendency to pore formation.

- Aluminium alloys have a high surface reflectivity for light which means that it is difficult to absorb sufficient energy for creating the cavity. This effect is more pronounced the longer the wavelength of the laser light. Once the cavity is formed it will, however, to a large extent act as a black body to the radiation.

In general, the bead geometry and the ability of the surface tension of the liquid to support the molten pool constitute a big challenge in the welding of aluminium alloys. As mentioned, distortions owing to a reduction in strength are also to be expected. In addition to this, the main weld metal imperfections that must be dealt with are porosity and solidification flaws.

6.2.3 Stainless steels

Common to all stainless steels is a high chromium content that must exceed roughly 13% in order for the steels to become stainless. Many types of stainless steels exist, the characteristics of which are summarised in the following:

Austenitic stainless steels

- Intermediate strength, good ductility,
- Good general corrosion resistance, but susceptible to stress corrosion,
- No risk of brittle fracture,
- Generally good welding properties, but especially for the fully austenitic types susceptible to solidification cracking.

Ferritic stainless steels

- Good strength, intermediate ductility,
- Good resistance to stress corrosion,
- Risk of brittle fracture,
- Generally poor welding properties owing to grain growth in HAZ.

Martensitic stainless steels

- High strength, low ductility,
- Generally poor welding properties,
- Risk of brittle fracture.

Duplex stainless steel

- Fair strength,
- Fair general corrosion properties and good resistance to stress corrosion,
- Fair welding properties, but risk of brittle fracture and poor corrosion properties if the microstructure is changed e.g. by welding.

The microstructure of duplex stainless steels is roughly a 1:1 mixture of austenite and ferrite. Standard-type duplex stainless steels are optimised with respect to both mechanical and corrosion properties by having almost equal fractions of ferrite and austenite in the microstructure. In many respects duplex stainless steels have obtained the best properties from the austenitic and ferritic stainless steels, e.g. good mechanical properties, good general corrosion resistance and resistance towards stress corrosion cracking. The right balance between austenite and ferrite may be obtained by slow cooling from the melting temperature. At temperatures above 1200 °C, the microstructure will predominantly be ferritic and the solidification primarily will be ferritic thus suppressing solidification cracking. The formation of austenite from the ferrite-dominated area during cooling is slow, thus causing the weld metal to be predominantly ferritic at room temperature. The resulting microstructure is therefore highly depending on the thermal cycle involved and this problem is especially severe for laser-based welding as the low heat input of laser welding cause very high cooling rates. This also makes the resulting mechanical and corrosion properties difficult to control as they are intimately correlated with the microstructure. The situation may, however, be improved by the addition of nitrogen in the process gases or by using nickel-rich filler materials, or a by a combination of both.[4]

6.3 Weld quality

6.3.1 Weld imperfections and defects

Many physical imperfections and defects may be related to simple causes such as misalignment or poor joint preparation. Some are, however, caused by a complex interaction between many parameters such as steel composition, joint geometry and welding variables. Besides physical defects produced during welding, a structure may develop cracks or completely fail in service owing to:

- limited ductility,
- limited toughness (e.g. impact or quasi-static),
- environmentally assisted cracking (hydrogen cracking),
- general corrosion, and
- fatigue.

A number of mechanical tests have therefore been developed for assuring that the ductility and toughness is sufficient and that serious cracks do not develop during the lifetime of a product. For this reason, as part of a welding procedure testing, it is usually necessary to evaluate a number of the following mechanical properties by destructive testing:

- hardness,
- strength and possibly ductility,
- impact toughness, sometimes supplemented by CTOD values.

6.3.2 Classification of weld quality

Typical weld quality parameters describing possible deviations from the perfect weld may roughly be grouped as follows:

Surface defects

- underfill or overfill,
- vertical misalignment,
- angular misalignment,
- drop through, and
- undercut.

Internal imperfections and defects

- lack of binding,
- lack of penetration,
- solidification cracks or flaws, and
- porosity.

Cross sectional geometry

- WM width,
- HAZ width,
- bulging, etc.

Mechanical properties

- hardness,
- toughness (impact and quasi-stationary),
- ductility, and
- distortion data.

Penetration control – fillet welds only

- Penetration control.

6.4 Assessment of weld properties

6.4.1 Destructive testing

Visual inspection is of course the most obvious testing technique and combined with sectioning much information can be obtained in this way. In the weld cross-section also the hardness may be measured at various positions. Vickers hardness is the most appropriate method for establishing the hardness in the narrow laser welds, because the measurements may be performed at a range of indentation forces. Hardness and strength are relatively closely correlated whereas the correlation between hardness and ductility or toughness is not consistent but existing as a trend only e.g. for a well-defined group of materials.

Longitudinal and transverse tensile tests may be used to establish strength and ductility, but for overmatching welds (as e.g. welds in steels) the transverse tensile test will generally only test the weld up to the strength of the base metal. Bend testing may be used for evaluating the ductility.

The standard Charpy V-notch test may now be used to evaluate impact toughness even in the case of fracture path deviation in overmatching weldments. Although not commonly used, the fracture toughness tests (e.g. CTOD tests) have been demonstrated to work well for the laser-based welds. The sharper notch and the slower deformation speed is beneficial to avoid fracture path deviation and a further advantage of CTOD testing is that the results are applicable in fracture mechanics analysis approaches, but the acceptance value has to be agreed upon, although levels known e.g. from arc welding may be used.

6.4.2 Non-destructive evaluation

In this section, results are reported of non-destructive testing of laser welded I-butt and T-joints in structural steels performed with the aim of identifying the limits of the different inspection methods and to produce relevant procedures. A number of different non-destructive methods have been tested. These include normal and micro focus x-ray as well as ultrasonics in the forms of manual, automated pulse-echo, and time-of-flight diffraction (TOFD). The potential for off- and on-line use of NDE is also discussed. Direct on-line monitoring of the weld input variables is a relevant technique for substituting or complementing the NDE-investigations.

Radiography

Initially, the micro focus technique was applied in order to determine the sensitivity of the ultrasonic techniques without having to perform too many

destructive tests. The results show that small cracks and pores are easily interpreted. The size of the smallest pores visible in the radiographs is less than 0.5 mm in diameter. The size of the smallest cracks seen is about 1 mm. A standard x-ray method has also been used with a good result and a very considerable time saving. The sensitivity of the x-ray technique decreases with increase in material thickness but, at the same time, the critical defect size increases with increase in thickness. For I-shaped laser welded butt welds the orientation of the typical solidification flaw defects is ideal for the x-ray technique.

Ultrasonics

The ultrasonic inspections have been performed in two ways: both the standard pulse echo technique and TOFD have been used. The manual ultrasonic examinations show a good correlation with the automated ultrasonic examinations. The automated ultrasonic pulse–echo method is reasonably fast, it covers the entire volume, but the sensitivity is typically inferior to TOFD. However, the sensitivity of the pulse–echo technique is high enough to allow evaluation of welds to CEN/TC 121/SC 4/WG 8/N 15, intermediate quality level (C), if the proper reference level is used.

TOFD is the fastest examination method; it has a high sensitivity, but suffers from a 'dead zone' just below the scanning surface, where small, non-surface-breaking, defects cannot be detected. A full-volume examination requires scanning from both surfaces. The detection limit for internal defects has been found to be below 0.5 mm. A disadvantage of using TOFD for detection (production control) is that a classification of small defects is not possible at present and that the permanent high sensitivity reveals small, otherwise perfectly acceptable, solidification imperfections together with non-acceptable cracks. For larger cracks and pores, a classification may be possible with a signal recognition program but this will probably require off-line signal processing. Destructive tests made at selected representative positions have shown a good correlation between indications in TOFD results and defects found in the fracture surfaces.

For off-line ultrasonic examination of laser welds a pulse–echo technique with the evaluation based on the amplitude of the signals is believed to be the best choice. For on-line examination of butt welds, TOFD is probably the only technique that can show sufficient speed.

Process monitoring

Direct on-line monitoring of the weld input variables is a relevant technique for substituting or complementing NDE investigations. By real-time

monitoring, critical input variables as for example laser power, welding speed, arc current, wire feed speed, beam angle as well as the seam tracking system, confidence can be obtained that the welding process is reproducible and reliable. In combination with a certain amount of standard off-line NDE, the amount of weld imperfections or weld defects may be safely determined. The required amount of penetration in, for instance, a partly penetrating T-butt joint can also be checked using a combination of process monitoring and off-line NDT.

The ultrasonic equipment will be looking for defects in the solidification zone using the two transducers, Ua and Ub, working in the TOFD mode. This results in A scans where a defect will show up as an echo between the 'front' and the 'back' echoes that may act as gate limits. The results of these scannings show that inclusions and lack of penetration are detected and placed at the right positions compared with post-welding scannings and it was possible to determine the depth positions of a defect. The experiments were made with laser speeds from 500 to 2000 mm min^{-1}, and no defects were missing at the highest speed which means that it should be possible to get reliable inspection results welding faster. All scannings were performed with water as couplant with good results; no other couplants have been tested.

6.5 Conclusions

Hybrid laser–arc welding shows a great potential in the welding of many structural materials, but NDE as well as evaluation of the mechanical properties are crucial and does involve a number of challenges. Regarding the mechanical properties, small scale tests have been developed and/or modified to suit the demands which must be fulfilled when evaluating hybrid laser–arc welds in structural materials. In addition, large-scale fracture and fatigue tests have been performed and, in all cases, the findings were in accordance with the results of the small scale tests.

The weld imperfections most likely to occur are pores and solidification cracks or flaws, the latter being more critical owing to their flat and sharp character. Solidification flaws are prone to occur in e.g. heavy section structural steel welding. An understanding of the influence of the steel composition and weld parameters on the occurrence of solidification flaws has been achieved and a solidification flaw steel index for structural steels proposed. From the proposed index, it may also be seen that the demands in the steel composition are fairly easy and cheap to obtain.

The standard off-line NDE techniques have been shown to work satisfactorily with laser welds. In addition, on-line NDE using the TODF technique seems possible, although a certain dead-zone near the upper surface must be accepted. A combination of process input parameter monitoring

and off-line NDT is also an attractive combination for testing of laser welds in shipyards and related areas.

6.6 Acknowledgements

It is a pleasure for me to acknowledge the significant and important contribution to this chapter by my colleague, Peter Krarup of FORCE Technology.

6.7 References

1 KRISTENSEN J K, *Materials Aspects – Control of Weld Imperfections, Proc. of the Conf.: Exploitation of Laser Processing in Shipyards and Structural Steelwork*, Glasgow, UK, May 1996.
2 *Laser Welding in Ship Construction – Classification Society Unified Guidelines for the Approval of CO_2-Laser Welding* (1996).
3 *Classification Guidelines for the Approval of Autogenous Laser Welding and Hybrid Laser Welding*, May 2004.
4 KLÆSTRUP KRISTENSEN J, HANSEN L E and BORGGREEN K, *High Power Laser Welding of Duplex Stainless Steels – Process, Microstructure and Mechanical Properties*, *Proc. of Ninth International Conference on the Joining of Materials (JOM-9)*, Elsinore, Denmark (May 1999).

7

Hybrid welding of magnesium alloys

L. LIU, Dalian University of Technology, China

Abstract: The weldability of magnesium alloys is introduced and low-power laser–arc hybrid welding of magnesium alloys is discussed in detail. The advantage of the hybrid welding process and the interaction between laser beam and arc plasma are discussed. Some practical applications of hybrid welding process are presented.

Key words: magnesium alloy, laser–arc hybrid welding, mechanical property, porosity.

7.1 Introduction

Magnesium is the sixth most abundant element on the Earth's surface and the third most plentiful element dissolved in seawater, with an approximate concentration of 0.14%.[1] Being extremely lightweight, magnesium alloys have excellent specific strength,[2] excellent sound damping capabilities,[3,4] good castability,[5] hot formability,[6] excellent machinability,[7] good electromagnetic interference shielding,[8] and recyclability.[9] As the lightest structural material available so far,[2,10] magnesium alloys have been used widely in aerospace, aircraft, automotive, electronics and other fields, and have the potential to replace steel and aluminum in many structural applications.[3,4] As one of most important processes in the application of magnesium alloys, the welding and joining process of the magnesium alloys has attracted more and more attention all over the world.

In this chapter, the research and progress in laser–arc hybrid welding of magnesium alloys are critically reviewed. Section 7.2 describes the welding ability of magnesium alloys and the common welding defects in the welding processes. Section 7.3 introduces low-power laser–arc hybrid welding of magnesium alloys in detail, including the welding technology, microstructure, mechanical properties, porosity and plasma behaviors. Sections 7.4 and 7.5 investigate the numerical simulation and infrared temperature measurement of hybrid welding, respectively. Section 7.6 estimates the electron temperature and electron density of the welding plasma by spectral diagnosis. Section 7.7 discusses the interaction between laser beam and TIG arc in hybrid welding. Section 7.8 introduces some magnesium alloy products

welded by low-power laser–arc hybrid process. Section 7.9 depicts the existing problems in hybrid welding of magnesium alloys and views the developing trend of hybrid welding process.

7.2 Weldability of magnesium alloys

The crystal structure of magnesium is a close-packed hexagonal lattice. The physical properties of Mg, Al and Fe are listed in Table 7.1.[11] In the welding of the magnesium alloys, the distortion of the magnesium structure is serious owing to its high coefficient of thermal expansion and thermal conductivity. Solid magnesium starts to oxidize quite readily at 450 °C.[12] Oxidation is intensified at elevated temperature, so shielding gas or flux material are usually used to prevent the oxidation of magnesium alloys in the welding process. The defects, such as evaporation, grain coarsening, hot cracks, porosity and thermal stress, readily appear in the welding of magnesium alloys. In addition, it is easy to induce other defects, slag, incomplete penetration and overburning, in the welding process.

The wide applications of magnesium alloys needs reliable welding processes. Magnesium alloys can be joined by a variety of welding methods including tungsten-arc inert gas (TIG) welding,[13,14] metal-arc inert gas (MIG) welding,[15] plasma arc welding,[16] electron beam welding,[17] laser welding,[11,18] friction stir welding[19] and spot welding.[20] There are many disadvantages in TIG welding, such as the small depth-to-width ratio of welded joint, a large heat-affected zone (HAZ), big crystal grains and low welding efficiency. With the increase of requirements for high precision, reliability

Table 7.1 Physical parameters of Mg, Al and Fe at their melting points[11]

Properties	Mg	Al	Fe
Ionization energy (eV)	7.6	6	7.8
Specific heat (J kg^{-1} K^{-1})	1360	1080	795
Specific heat of fusion (J kg^{-1})	3.7×10^5	4×10^5	2.7×10^5
Melting point (°C)	650	660	1536
Boiling point (°C)	1090	2520	2860
Viscosity (kg m^{-1} s^{-1})	0.00125	0.0013	0.0055
Surface tension (N m^{-1})	0.559	0.914	1.872
Thermal conductivity (W m^{-1} K^{-1})	78	94.03	38
Thermal diffusivity (m^2 s^{-1})	3.73×10^{-5}	3.65×10^{-5}	6.80×10^{-6}
Coefficient of thermal expansion (1/K)	2.5×10^{-5}	2.4×10^{-5}	1.0×10^{-5}
Density (kg m^{-3})	1590	2385	7015
Elastic modulus (N m^{-3})	4.47×10^{10}	7.06×10^{10}	21×10^{10}
Electrical resistivity (μΩ m)	0.274	0.2425	1.386
Vapor pressure (Pa)	360	10^{-6}	2.3

and efficiency of modern products, the proportion of TIG welding in modern welding area has decreased gradually.

Laser welding is characterized by high energy density of laser beam (about 10^6 W/cm^2), high welding speed, high quality, small HAZ and low deformation. But the welding defects, e.g. gas porosity[21] and cracks,[22] appear easily and the fit-up gap and machining precision of base metal are required to be more exact in butt-welding due to the small dimension of the laser beam (about 0.1 mm~0.3 mm), which would increase the costs of preparation for welding.

Since laser–arc hybrid welding technology was propounded in 1978, it has attracted more and more attention for its various advantages. Nowadays, the laser–arc hybrid process is applied successfully in the welding of magnesium alloys.

7.3 Low-power laser–arc hybrid welding process

Laser–arc hybrid welding has been used widely in the welding of steel, Al and other alloys, in which typically more than 1.5 kW laser beams[23] are usually used. However, in the process of welding magnesium alloys, there is a serious problem of energy waste because of the low photoelectric transformation efficiency of the laser,[24] serious reflection of laser energy in the welding of non-ferrous metals,[25] and the absorption and defocusing effects of the laser beam when it penetrates through the arc plasma.[26] In studies of welding magnesium alloys, the author and co-workers have found that when a low-power laser beam is coupled with a TIG arc, the weld penetration of hybrid welding can double that of TIG welding and the weld joint shows good mechanical properties. Therefore, low-power laser–arc hybrid welding technology is propounded to weld magnesium alloys, in which the laser power used is less than 400 W. The schematic diagram of low-power laser–arc hybrid welding is shown in Fig. 7.1.[27] A device for TIG welding at currents of up to 300 A is used as the arc power supply. In the hybrid welding process, the TIG arc acts first to melt the surface metal and the laser beam follows behind. Argon gas is fed through the laser head nozzle and the TIG torch to the work zone as a shielding gas. The tilt angle of the TIG torch remains at about 45° during the whole welding process.

7.3.1 Morphology of the welded seam

AZ31B magnesium plates were welded by TIG, laser and low-power laser–arc hybrid welding separately under the same welding parameters. The weld appearances and macro-sections are illustrated in Fig. 7.2.[28] The welded seam by laser welding alone was narrow without any defects (Fig. 7.2a) and that of TIG welding alone was wide with the low depth-to-width ratio

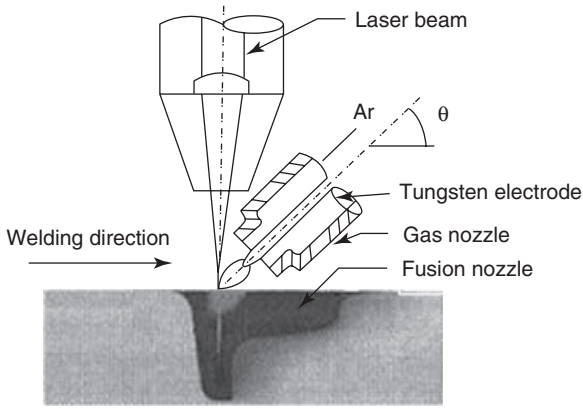

7.1 Schematic diagram of low-power laser–arc hybrid welding.[27]

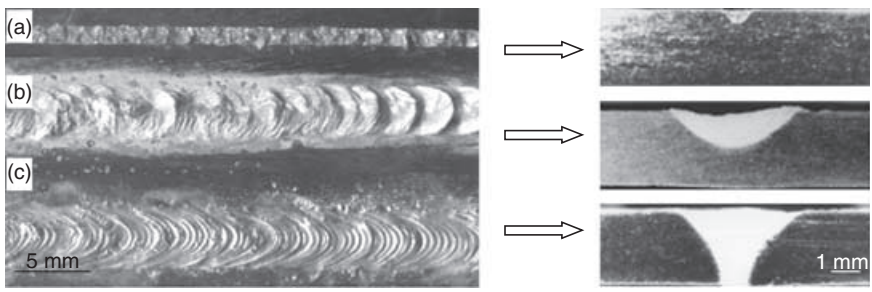

7.2 Comparison of welded joints and macrosections[28] (a) laser welding (b) TIG welding (c) hybrid welding.

(Fig. 7.2b), whereas in hybrid welding, the depth-to-width ratio was larger and the welded seam had a wavy appearance (Fig. 7.2c). The penetration of the hybrid welding seam was the deepest, four times deeper than that of laser welding and twice as deep as that of the TIG welding under the same conditions, thus proving the synergic characteristics of low-power laser–arc hybrid welding.

The typical appearance of magnesium alloys joints AZ31 to AZ31 and AZ31 to AZ91 welded by laser–TIG hybrid welding process are shown in Fig. 7.3.[29] The continuous weld seams without crack and surface pore were obtained. It found that the joint between identical alloys AZ31 to AZ31 took on a ripple effect just like scale, whereas the joints between different alloys, AZ31 to AZ61 and AZ91 were smooth. In addition, macroscopic cross-sections of dissimilar welds showed a large HAZ in the side of AZ61

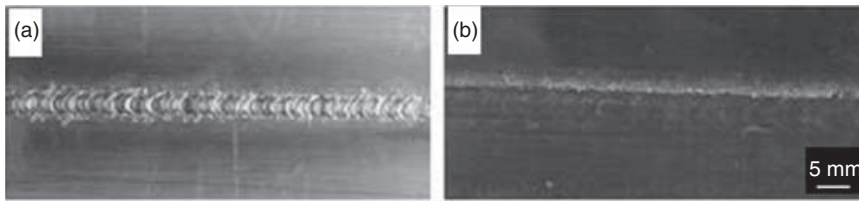

7.3 Appearance of joints of AZ31 to AZ31 and AZ31 to AZ91[29] (a) AZ31 to AZ31; (b) AZ31 to AZ91.

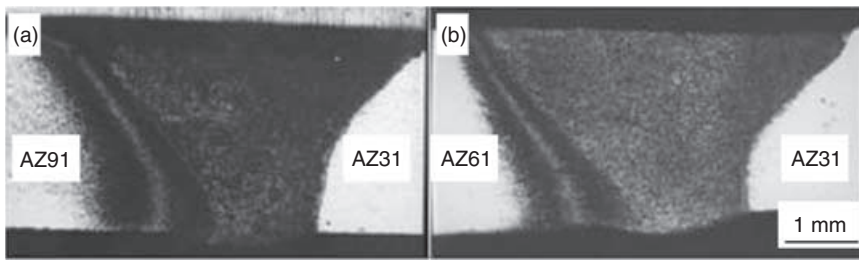

7.4 Cross-section of laser–TIG hybrid welded magnesium alloys[29] (a) dissimilar weld of AZ91 to AZ31; (b) dissimilar weld of AZ61 to AZ31.

and AZ91, but a narrow HAZ in the side of AZ31, as shown in Fig. 7.4.[29] The reason for this is the difference in surface tension and thermoconductivity of the magnesium alloys with increasing Al content.

7.3.2 Influence of welding parameters

Arc power

In low-power laser–arc hybrid welding, arc power is an important parameter to achieve good welding quality. Figure 7.5[30] shows the effect of arc power on weld penetration in hybrid welding, in which the laser power is kept constant at 300 W. The penetration of hybrid welding joint is much deeper than the sum of that of TIG welding and laser welding, even two times deeper than the sum when arc power increases to a specific value. The arc power necessary to achieve the deepest penetration in hybrid welding is 1500 W at the speed of 500 mm min^{-1} and 2500 W at the speed of 1000 mm min^{-1}.

Figure 7.6[31] shows the stability of hybrid laser–TIG welding and TIG only at various travel speeds as a function of TIG current. At some TIG currents,

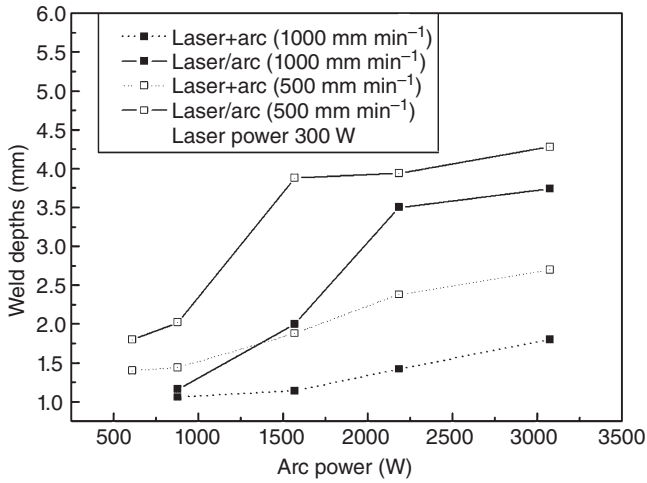

7.5 Variation of weld depths as a function of arc power in AZ31B.[30]

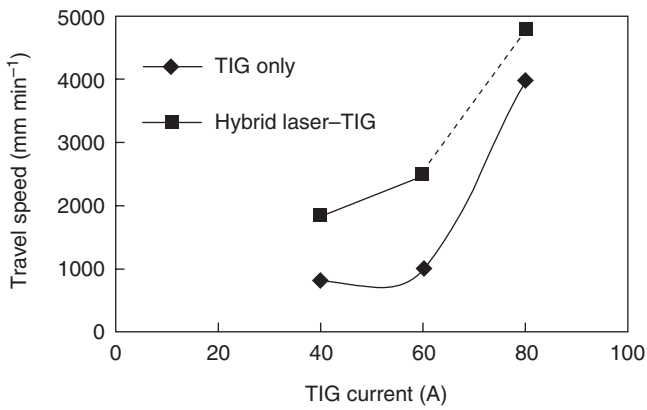

7.6 Stability of hybrid laser–TIG welding and TIG at various travel speed as a function of TIG current.[31]

welds are made with hybrid and TIG at increasing travel speed until instability was observed. The arc is clearly more stability at the presence of the laser beam in hybrid laser–TIG, especially at low TIG current. This is because laser generated plasma has a greater electron density which reduces arc resistance, and thermionic emission takes place very readily when a laser is present.

Defocusing value

The defocusing value characterises the position of laser focus relative to the surface of workpiece and influences the power density of the laser beam reaching the surface of the base metal and the flow of molten pool. As is shown in Fig. 7.7, when the defocusing value is within –0.8 mm~0.8 mm, the penetration of hybrid welding joint is the deepest and the formation of the weld seam is the best.[32] When the defocusing value exceeds –1.2 mm, the cross-section of the hybrid weld seam is the same as that of TIG welding and the effect of laser beam to weld penetration disappears. It is therefore, important to choose the optimal defocusing value in low-power laser–arc hybrid welding process.

Welding speed

As shown in Fig. 7.8, the influence of welding speed to weld seam is simple. With an increase in welding speed, both weld width and penetration decrease sharply. This is because the thermal input to the base metal decreases with an increase in welding speed. In low-power laser–arc hybrid welding of magnesium alloys, the welding arc is still stable at high welding speed, even at the speed of 1500 to ~2000 mm min^{-1}.[32]

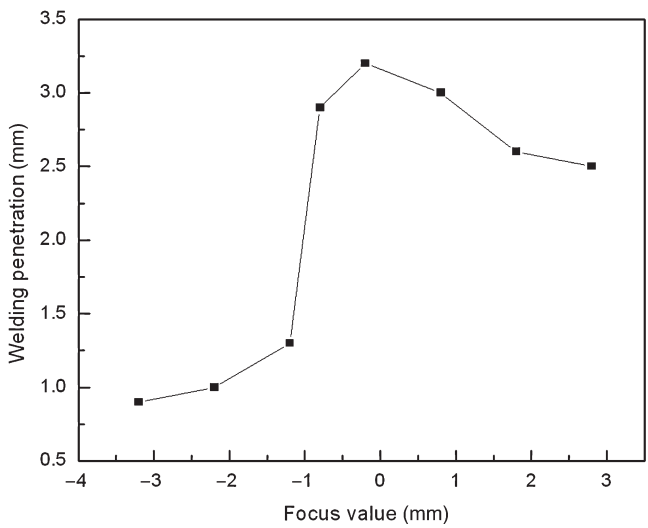

7.7 Influence of focus value on the welding penetration[32] (P = 400 W, f_d = –0.8 mm, I = 100 A, h = 2 mm, D_{LA} = 2.0 mm, V = 1200 mm min^{-1}, argon 10 L min^{-1}).

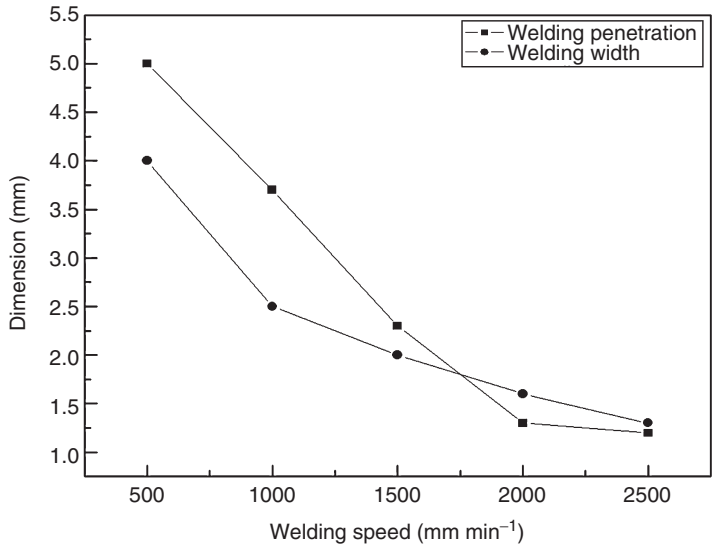

7.8 Influence of welding speed on welding quality (I = 120 A, P = 300 W).

Distance between laser and arc (D_{LA}*)*

D_{LA}, the distance between laser beam and tungsten electrode, is the most important parameter to effect the interaction of laser beam and arc plasma. Figure 7.9 shows the effect of D_{LA} in the formation of weld seam and penetration. It is found that the weld penetration increases remarkably with the decrease of D_{LA}, but the penetration decreases when D_{LA} is less than 0.5 mm. When D_{LA} is too short, the tungsten electrode will be burnt by the laser beam and it will increase the instability of arc plasma and induce defects such as spatter and tungsten inclusion. Therefore, in low-power laser–arc hybrid welding of magnesium alloys, the preferred D_{LA} is between 1.0~1.5 mm.[32]

7.3.3 Microstructure

As is shown in Fig. 7.10a, the microstructure of the base metal AZ31B is equiaxed grain. The transition region between the HAZ and welded zone is revealed in Fig. 7.10b, in which the fusion-line is marked by the arrow. It is found that the transition region combines well with the other two adjacent zones and the microstructure is homogeneous.[28]

Owing to welding thermal cycles, the crystal grains became uniform and nearly the same size as the grains of base metal. Because of the high speeds

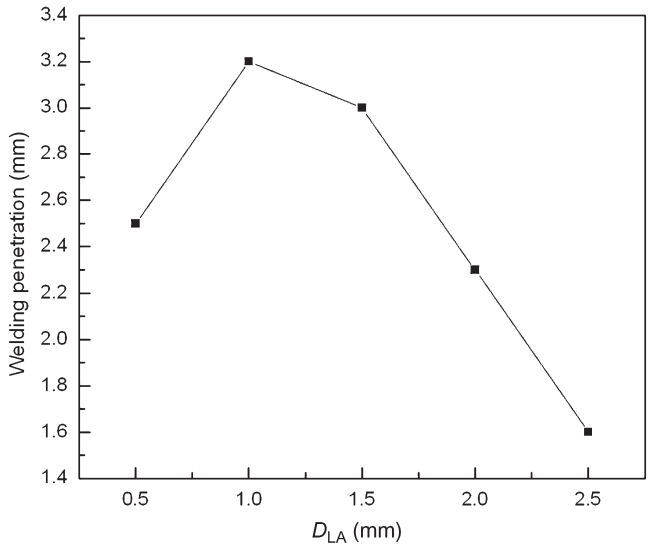

7.9 Influence of D_{LA} on weld penetration[32] (P = 400 W, I = 100 A, v = 1500 mm min^{-1}, Z = –0.8 mm).

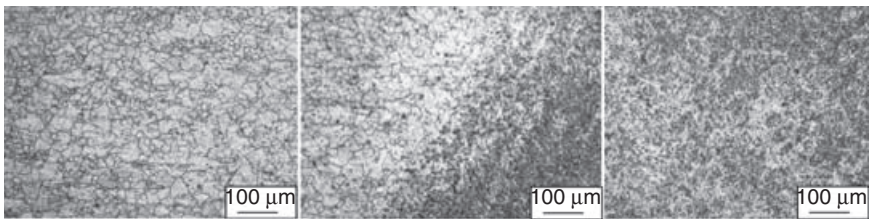

7.10 Microstructure of welded joint by hybrid welding[28] (a) base metal, (b) transition zone, (c) bond area.

of welding and heat transmission of magnesium alloys, there was cast quenching structure in the fusion zone (Fig. 7.10c), which was made up of exiguous equiaxed grains. When welded by TIG, the crystal grain in the HAZ was large (Fig. 7.11), which did harm to the capability of welded seam.

The microstructures of AZ61 and AZ91 are shown in Fig. 7.12.[29] The fibred microstructure was found in AZ31 base metal. The AZ61 Mg alloy showed equiaxed structure and the average grain size was about 30~50 μm. The microstructure of AZ91 was composed of primary α phase and $Mg_{17}Al_{12}$(β phase).

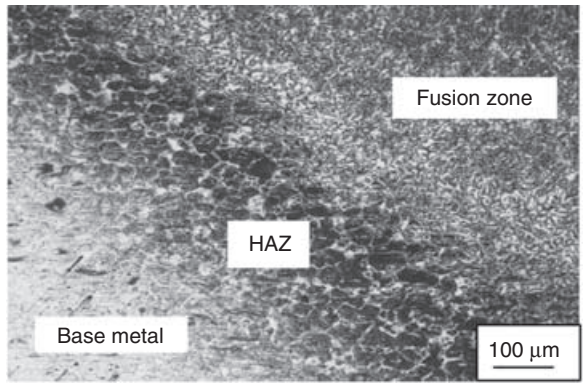

7.11 Microstructure of welded joint by TIG[28] (I_{arc} = 60 A, V = 500 mm min^{-1}).

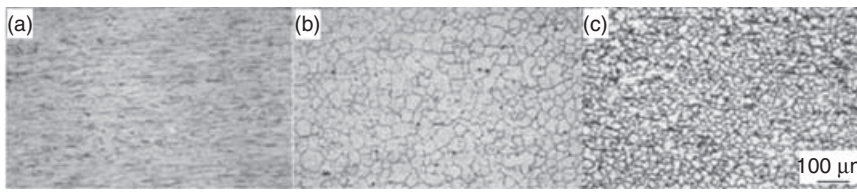

7.12 Microstructure of magnesium alloys[29] (a) AZ31; (b) AZ61; (c) AZ91.

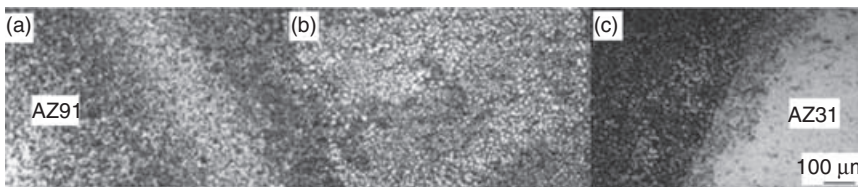

7.13 Microstructure of AZ31 to AZ91 joint.[29]

The microstructures of AZ31 welded to AZ61 and AZ31 welded to AZ91 are similar: Fig. 7.13 shows the typical microstructure of the dissimilar joint of AZ31 to AZ91.[29] Fig. 7.13a shows a large HAZ on the side of AZ91 in dissimilar joints, in which no grain coarsening was found. A cellular solidification structure was observed in the fusion zone, which showed a more globular grain shape, as shown in Fig. 7.13b. This cellular structure was a

typical cast structure, resulting from increased segregation effects during the rapid chill of the melt. The rapid cooling during laser–TIG hybrid welding also leads to a significant grain refinement compared with the initial structure shown in Fig. 7.12c. In addition, Fig. 7.13c shows the HAZ on the side of AZ31 in dissimilar joints, which is narrow. Figure 7.14[29] shows the back scattering electron image of AZ31 to AZ61 and AZ91 weld fusion and found that abundant β phase occurs at the boundary of grain; this appears as white strips as shown by the black arrows, and is composed of 75.02wt%Mg and 20.35wt%Al by EPMA.

To observe the element distribution of weld metal, the main elements, such as Mg, Al, Zn and O, were analyzed using EPMA. The results are shown in Fig. 7.15.[32] Al and Zn presented enrichment at the crystal boundary, especially in white spot marked by arrows. The white spot was a kind of Mg–Al–Zn intermediate compound. In addition, the O content within weld metal was very high and mainly distributed around the white spot. In overlap welding, argon gas can not provide effective shielding to prevent O between the sheets from invading the welding area. Both Mg and Al are active elements, which can be readily oxidized.

7.3.4 Mechanical properties

Table 7.2[33] shows the results of the tensile tests, in which the joint efficiency was defined as the ratio of tensile strength of the joint to that of the base metal. The tensile strength of joints of hybrid welding is better than that of TIG welding. The strength of AZ31B in similar joints of hybrid welding could approach or even exceed that of the base metal, which are fractured most in base metal owing to the narrow heat-affected zone (HAZ) and grain refinement in fusion zone. In addition, the tensile specimens of AZ31B to AZ61 joints are fractured at the side of AZ31B base metal, while that of AZ31B to AZ91D and AZ61 to AZ91D are fractured at the weld fusion

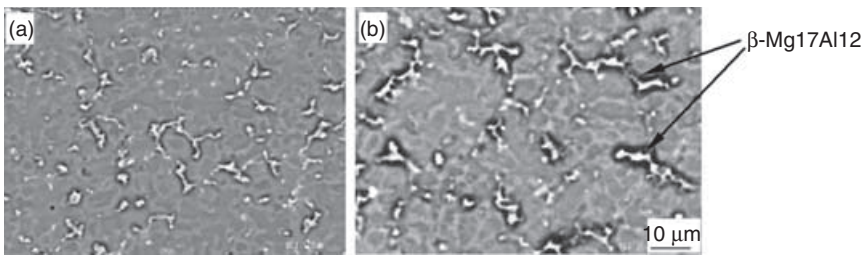

7.14 Back scattering electron image of weld metal[29] (a) dissimilar weld of AZ61 to AZ31, (b) dissimilar weld of AZ91 to AZ31.

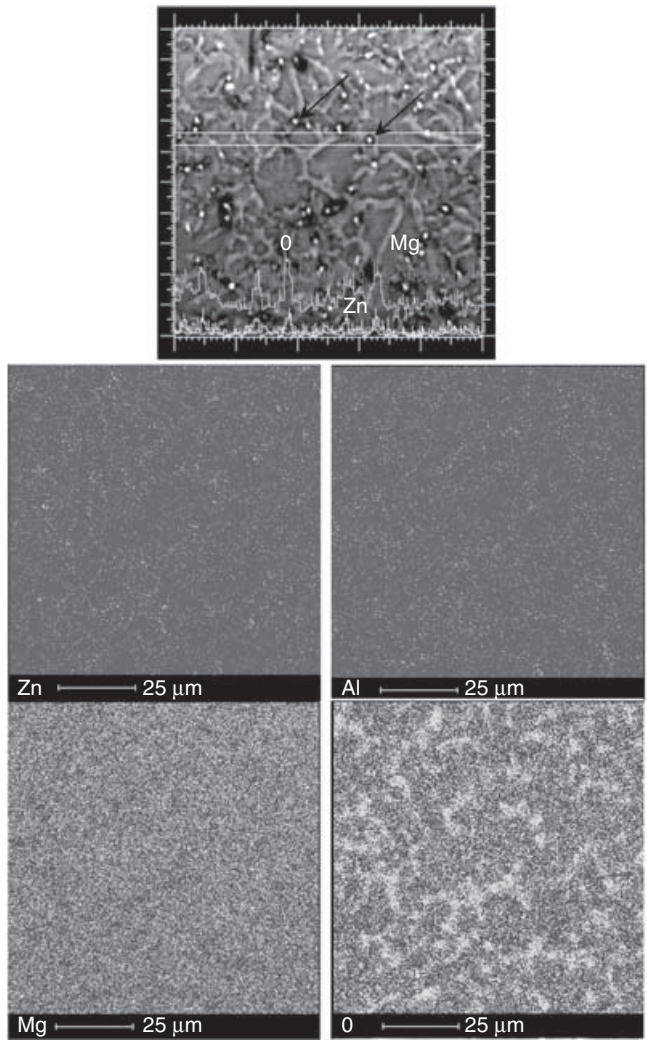

7.15 EPMA patterns obtained from AZ31B after hybrid overlaps welding.[32] (a) Backscattered electron image of fusion zone; (b), (c), (d), (e) show the distributions of Zn, Al, Mg, O, respectively, within fusion zone.

zone. Additionally, the impact ductility of the joint welded by hybrid welding attained 113% of that of base metal, much higher than that of TIG welding.

Figure 7.16[34] shows the results of fatigue test of AZ31B joints and base metal. It found the fatigue property of AZ31B welded by LTHW was lower than that of base metal in a different stress level, and the joint was

Table 7.2 Selected data obtained from the base metal and as-welded tensile specimens of Mg alloys produced by hybrid welding and TIG welding[32]

Materials	Welding style	Welding process	Tensile strength (MPa)	Joint efficiency (%)	Fracture position
AZ31B	Base	–	253	–	–
AZ61	Base	–	295	–	–
AZ91D	Base	–	325	–	–
AZ31B	Similar	Laser–arc	250	99	BM
AZ31B	Similar	Laser–arc	248	98	BM
AZ31B	Similar	Laser–arc	253	100	BM
AZ31B	Similar	TIG	236	93	HAZ
AZ31B	Similar	TIG	241	95	HAZ
AZ31B	Similar	TIG	234	92	HAZ
AZ31B to AZ61	Dissimilar	Laser–arc	255	101	BM (AZ31B)
AZ31B to AZ61	Dissimilar	Laser–arc	259	102	BM (AZ31B)
AZ31B to AZ61	Dissimilar	Laser–arc	257	102	BM (AZ31B)
AZ31B to AZ91D	Dissimilar	Laser–arc	261	103	FZ
AZ31B to AZ91D	Dissimilar	Laser–arc	259	102	FZ
AZ31B to AZ91D	Dissimilar	Laser–arc	254	100	FZ
AZ61 to AZ91D	Dissimilar	Laser–arc	252	85	FZ
AZ61 to AZ91D	Dissimilar	Laser–arc	234	79	FZ
AZ61 to AZ91D	Dissimilar	Laser–arc	237	80	FZ

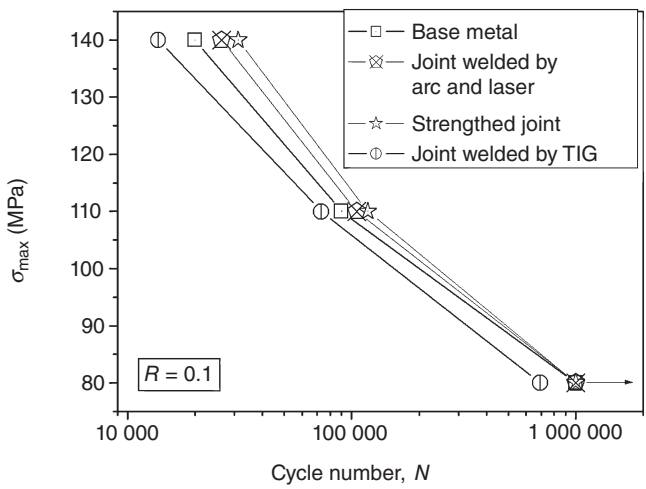

7.16 Tensile results of the welded joints.[34]

strengthened. However, the fatigue property of AZ31B welded by TIG was evidently lower than that of AZ31B welded by LTHW and base metal. Based on the curve of Strength-cycle Number (S-N), the cycle number of the joint welded by LTHW is 128% of base metal at stress level 140 MPa, 120% at 110 MPa and 100% at 80 MPa. While the cycle number of the joint welded by TIG is only 71% of base metal at stress level 140 MPa, 83% at 110 MPa and <72% at 80 MPa. This was because, when compared with TIG welding of magnesium alloys, the HAZ was narrower and the crystal grains were exiguous in hybrid welding. In addition, defects such as gas porosities and cracks could be avoided effectively in hybrid welding.

Measurements of microhardness were conducted to detect submicroscopic changes in the structure, especially in the HAZ. The results were used to evaluate the influence of the laser-TIG welding process on the mechanical properties of the joints. The hardness in the fusion zone (FZ) and in the HAZ of AZ61 and AZ91 is greatly changed relative to the base metal owing to the existance of the β phase, whereas there is no change relative to the base metal for AZ31, as shown in Fig. 7.17, 7.18 and 7.19.[35]

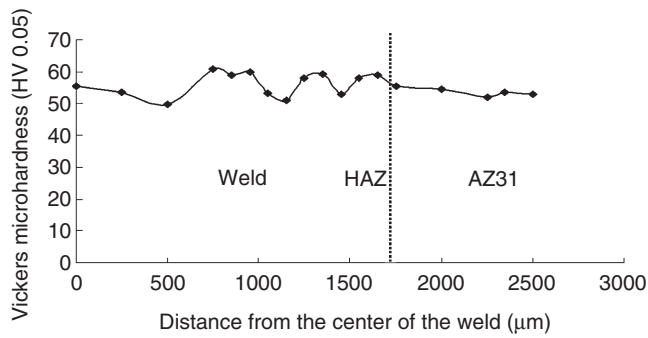

7.17 Hardness profile across weld in AZ31.[35]

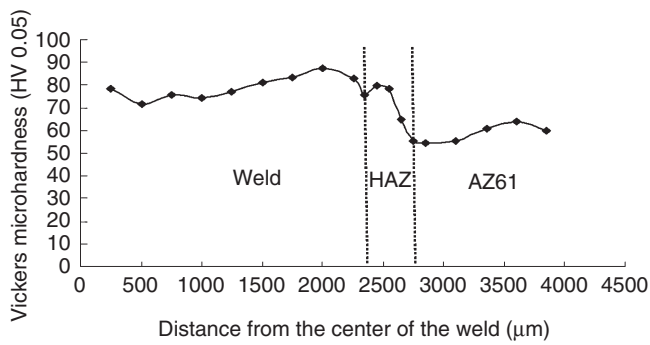

7.18 Hardness profile across weld in AZ61.[35]

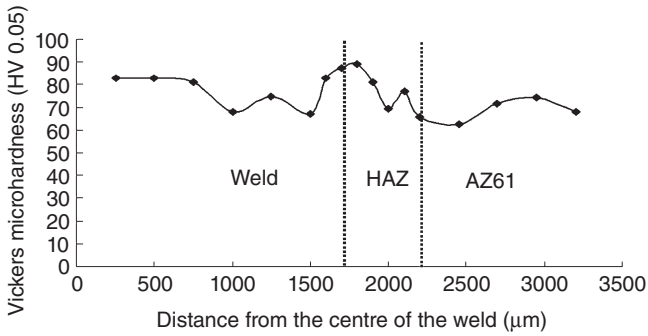

7.19 Hardness profile across weld in AZ91.[35]

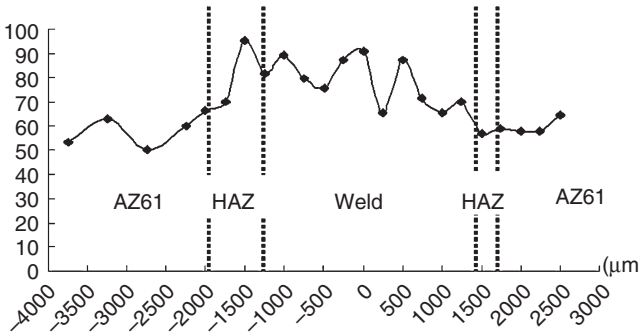

7.20 Hardness profile in the weld of AZ61 to AZ31.[29]

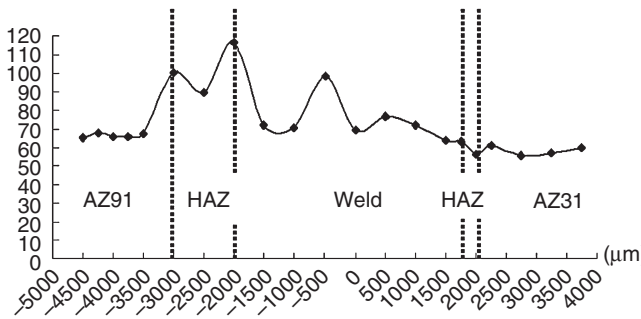

7.21 Hardness profile in the weld of AZ91 to AZ31.[29]

Figures 7.20 and 7.21 show the hardness of both dissimilar joints.[29] It was found that the hardness in the weld zone was obviously higher than that of each base metal in both dissimilar joints, and fluctuated due to the existence of β phase ($Mg_{17}Al_{12}$) distributed along the boundary of grain. In addition, the HAZ hardness augmentation at the side of AZ61 and AZ91 was found

in both dissimilar joints, whereas that on the side of AZ31 was unchanged compared with the hardness of the AZ31 base metal.

7.3.5 Porosity

One of the major concerns during high-speed welding of magnesium alloys is the presence of porosity in the weld metal that can cause a deterioration in mechanical properties. Two types of porosity are commonly produced when welding non-ferrous metals: pores with diameters >0.2 mm, observed by radiography, are called macropores, and pores with diameters of several micrometers, which can only be observed by optical microscopy or SEM, are called micropores.

Figure 7.22[27] shows the top-face of a hybrid welding joint treated by milling machine. Many pores are found explicitly in the weld metal and most of them are on the center of weld metal arranged in a line. The cross-section of a pore is shown in Fig. 7.23,[27] from which it is found that the wall of a pore is not smooth, and some reactants accumulate there. The dimension of pores is >0.5 mm and most of them are found in the under-part of the weld metal. It is a characteristic of laser–TIG hybrid welding with high welding speed and high cooling rate, that it is difficult to produce micropores induced by hydrogen.

The element profile of a pore is analyzed by EMPA. The contents of O and N in pores are excessive, up to 24.8 and 9.4%, respectively. It can safely be concluded that the air enters into the molten pool during the welding process. Magnesium is so active that it can react easily with oxygen and nitrogen at high temperatures resulting in the formation of oxide and nitride.

The pore formation is analyzed in Fig. 7.24.[27] During laser–TIG hybrid welding, the molten pool is shielded by argon gas through the TIG torch

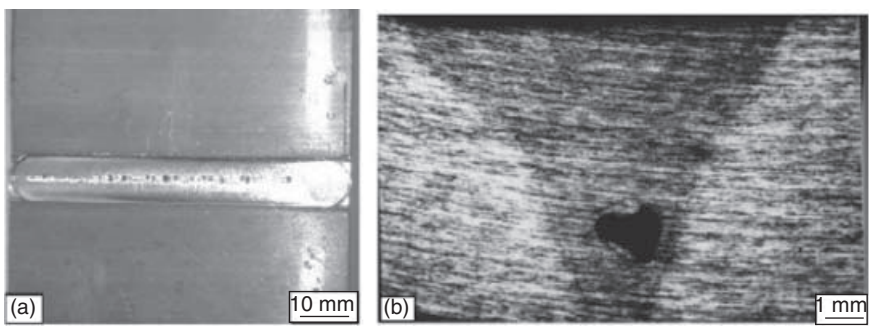

7.22 Micrographs of AZ31B weld joint:[27] (a) the top view of weld; (b) the cross-section of weld.

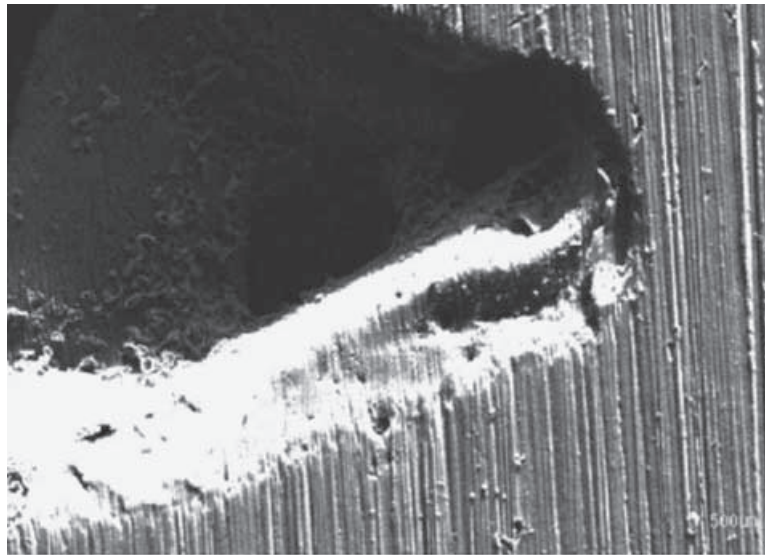

* Ratio [Correction = ZAF1]

No.	ELE.	Crystal	W.L. (A)	FKI-861	STD(I)	I-Ratio	WT(X)	Hol(X)	ELE.
1	Mg Ka	RAP	9.8900	31284.24	3178.48	9.8425	63.359	51.762	Mg
2	N Ka	PBST	31.6000	62.60	29.83	2.0948	24.852	35.230	N
3	O Ka	RAP	23.6200	27.39	41.75	0.6560	9.435	11.710	O
4	Al Ka	RAP	8.3333	488.60	3725.88	0.1298	1.330	0.878	Al
5	Zn La	RAP	12.2540	88.43	703.22	0.1186	0.890	0.270	Zn
6	Mn Ka	LIF	2.1018	13.29	633.54	0.0210	0.135	0.049	Mn
TOTAL							100.000		

7.23 Element distribution in pore by EMPA.[27]

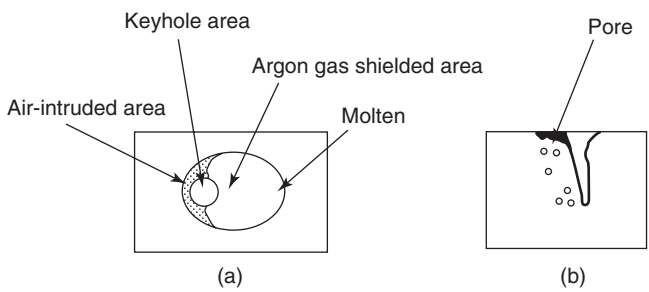

7.24 Pore formation sketch map.[27]

alone. When the workpiece plate is thin enough (<1.2 mm), the size of the molten pool is small, about 2 mm in diameter, especially at high welding speed. Under these conditions, the molten pool can be shielded soundly using the TIG torch alone. When the thickness of plate exceeds 1.2 mm, e.g. 2.5 or 5 mm, the increase in weld current results in a molten pool commonly between 5 and 8 mm in diameter. It is found that passing the shielding gas through TIG torch could not satisfy the practical demand. Figure 7.24a shows that the molten pool consists of an air-intruded area, a keyhole area and an argon gas shielded area. If the laser beam cannot be shielded by argon, the air is readily intruded into the molten pool and pores are formed. It is found that there is a film on the air-intruded area during welding, which displays as darkness, but the display was bright in the argon gas-shielding area. It can be concluded that the air-intruded area was the main source of gas inducing to form pores. In addition, during welding, the laser beams first come into contact with the air, forcing the air and even the shielding gas into the bottom of the molten pool. This causes the pores to form a line because the laser–TIG welding process has such a high welding speed and high cooling rate in the weld metal that the air does not have enough time to overflow and thus remains in the weld. However, the microstructure of magnesium alloy AZ31B by laser–TIG welding in Fig. 7.10 shows that there are no micropores in the weld metal because the gas dissolved cannot separate out and form pores because of the high speed of the welding and the high cooling rate in hybrid welding.

The weld surface produced by hybrid laser–TIG welding, which utilizes laser shielding coaxial gas and different TIG currents, is shown in Fig. 7.25.[27] In this experiment, the weld surface formed is rougher and darker when the TIG current is lower than 120 A with other parameters kept constant, whereas when the current is more than 120 A, the formation of the weld surface begins to level up. All this points to the fact that adding laser coaxial shielding gas has a strong effect on the arc, the direction of adding shielding

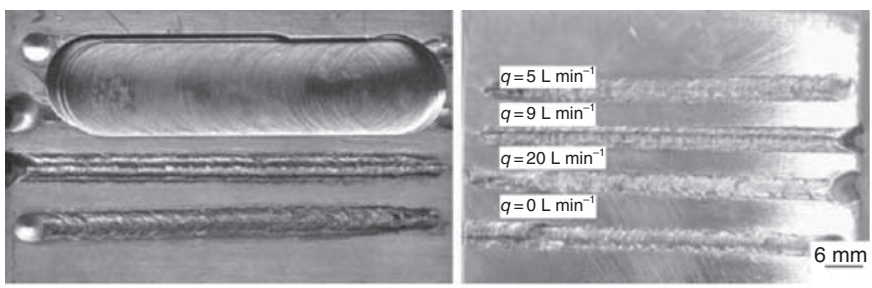

7.25 Number of pores in weld metal using laser coaxial shielding.[27]

gas can prevent the arc from rooting to the laser impinge spot, thus leading, in part, to the arc instability. Only when the arc current is high enough and the stiffness of arc is strong enough, can the arc be rooted to the laser impinge spot. It was found that there were various threshold values under various welding conditions. Using the coaxial shielding gas, a high arc current is needed to get high quality joints, whereas an advantage of the hybrid laser–TIG welding lies in the low current and high speed welding. Because of this, the application of this welding process will be limited.

Figure 7.25[27] shows the pore amount of the weld metal after adding coaxial shielding gas. The pore amount is evidently less than that without shielding and the formation of weld becomes worse with an increase in flux of the laser shielding gas. In addition, as the shielding gas is not optimal, a channel and surface pore appeared. Moreover, the flux of laser shielding gas has a strong effect on weld arc stability.

Figure 7.26[27] shows the pore amount of the weld added by the lateral shielding gas. It is found that the weld is continuous and bright. The pores have been restrained.

7.3.6 Plasma behavior

In the study of hybrid welding, arc behaviors in TIG welding with alternating current mode and low-power laser–arc hybrid welding were observed by a high-speed camera, as shown in Fig. 7.27.[33] And large differences between them were found. During TIG welding alone, in the positive wave of arc, the tungsten electrode was negative (ACEN) and the arc was used to heat the base metal; in the negative wave of arc, the electrode is positive (ACEP) and the arc mainly contributed to clear the oxidation film. Thus, the shape of arc in ACEP was divergent and the energy density was low,

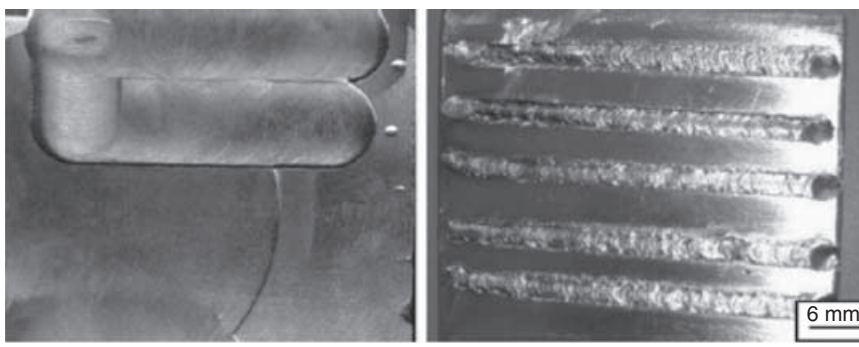

7.26 Number of pores in weld metal using laser lateral shielding.[27]

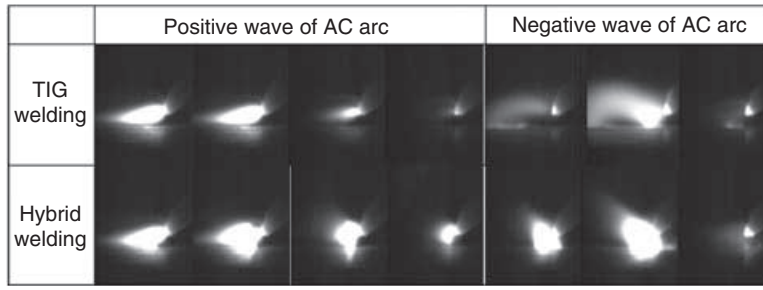

7.27 Plasma behavior in the welding process of magnesium alloy.[33]

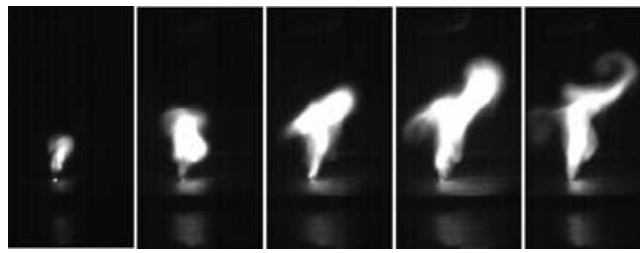

7.28 High-speed photographs of laser-induced plume/plasma of Mg alloy AZ31B during laser welding alone.[33]

which decreased the instability of arc, especially in high-speed welding. In hybrid welding, the frequencies of laser pulses and AC arc were different, so the laser could act on both positive wave and negative wave of the AC arc. Through the comparison of two cases, it was found that the synergic effect of laser beam and the arc was more obvious during ACEP, in which both the discharge capability and energy output of arc increased, and the negative wave was used to not only clear the oxidation film but also heat the metal, which had the benefit of heating the base metal and increasing the penetration depth. In addition, the laser-induced plasma is extended backwards during laser–arc welding, which is different from that in laser welding alone as shown in Fig. 7.28.[33]

7.4 Numerical simulation

Figure 7.29[36] shows a new heat source model, the Rotary–Gauss body heat source model, for high-energy beam welding, in which the keyhole effect, energy transmission of the wall of keyhole and the narrow heating area of laser are considered. The model satisfies the following conditions: (a) the

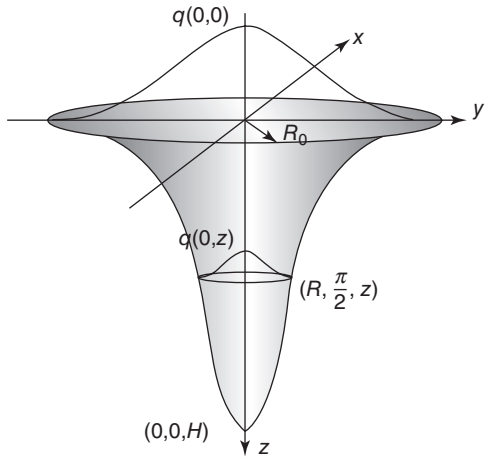

7.29 Rotary–Gauss body heat source model.[36]

sections in the 'z' direction of the model are circularity, in which the heat-flow density has a Gaussian distribution and $q(0,z)$, the heat-flow density at the center of circle, is the maximum; (b) the heat-flow density in axis 'z' is stationary, therefore $q(0,z)$ is constant. The heat-flow density in the acting region of heat source is the function of the height of heat source, effectual power of laser beam and radius of heat source. The mathematic equation of this heat source model is written as equation (7.1).

$$q(x,y,z)=\frac{9P}{\pi R_0^2 H\left(1-e^3\right)}\exp\left[\frac{-9}{\ln\left(\frac{H}{z}\right)R_0^2}\left(x^2+y^2\right)\right] \tag{7.1}$$

where H is the height of the heat source, P is effectual power of laser, R_0 is the radius of the heat source and x,y,z are the coordinates.

The Gauss area heat source model is used in numerical simulation of TIG welding.[37] In this model, the heat source distributes in two dimensions over a certain range based on the Gaussian function. The mathematic equation of this heat source model is written as follows:

$$q(x,y)=\frac{3Q}{\pi r_0^2}\exp\left[-\frac{3}{r_0^2}\left(x^2+y^2\right)\right] \tag{7.2}$$

$$Q=\eta U I_{\text{arc}} \tag{7.3}$$

where r_0 is the effectual radius of the heat source, Q is the effectual power of the heat source, η is the thermal efficiency of welding, U is the arc voltage

and I_{arc} is the welding current. The heat-flow density beyond r_0 is defined as 0. TIG welding can be simulated exactly by this model owing to the high welding speed of hybrid welding.

The heat source model of YAG laser–TIG hybrid welding is based on the two models mentioned above, but the hybrid model is not simply the addition of the two models because of the existence of some physical mechanism between the laser and the arc in hybrid welding. The utilization ratio of the arc increases owing to the introduction of the laser beam and therefore, the thermal efficiency η in the Gauss area heat source model of the TIG arc in hybrid welding increases accordingly. For AZ31B magnesium alloy, hybrid welding η should be increased by 0.1 in the simulation. At the same time, the laser compresses the arc and the radius r_0 in the model decreases, so the effective radius r_0 of the TIG arc is usually decreased by 0.5 mm in the simulation of hybrid welding compared with TIG welding alone. In hybrid welding, the TIG arc increases the utilization ratio of laser beam energy markedly and the effective power P in the Rotary–Gauss body heat source model increases correspondingly; thus, for magnesium alloy with a high reflectance ratio, the utilization ratio of laser should be increased to 75% in simulation. All the adjustments of parameters in the model are obtained by comparison with the practical experiments. The illustration of the heat source model of the magnesium alloy hybrid welding from the numerical simulation is shown in Fig. 7.30a. However, there is another heat source model in Fig. 7.30b, in which the enhanced effect between the laser and the arc is not considered.[36]

Figure 7.31,[36] shows the simulation results of TIG welding, laser welding and hybrid welding at the same welding speed. The results indicate that the hybrid heat source model is not simply the addition of the two but that the physical characteristics of hybrid welding are also considered.

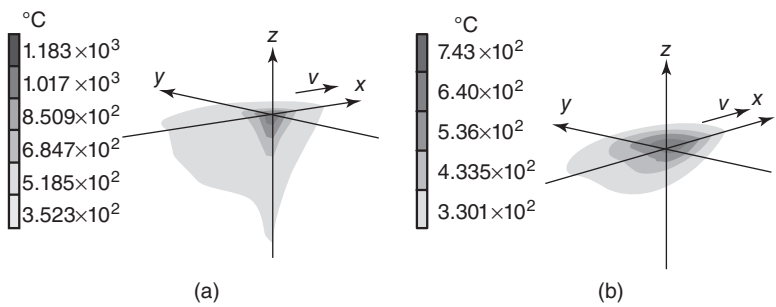

7.30 Heat source model of hybrid welding.[36] (a) The effect between laser and arc is considered; (b) The effect between laser and arc is not considered.

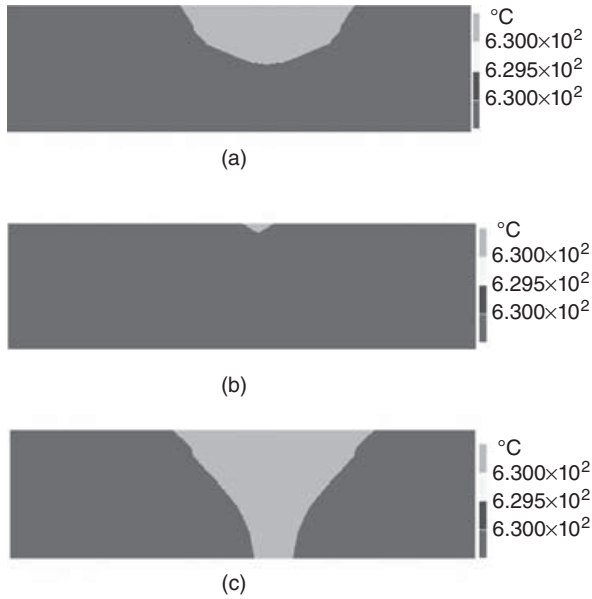

7.31 Numerical simulation of weld joints. (a) TIG welding alone; (b) Laser welding alone; and (c) Hybrid welding.

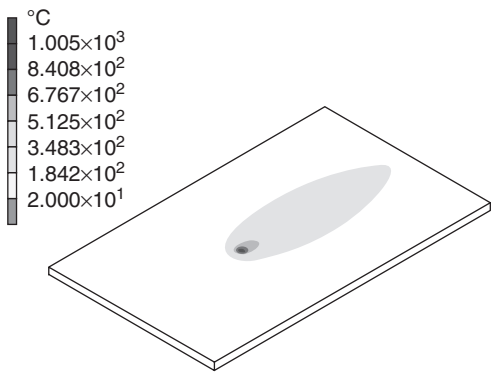

7.32 Temperature distribution of hybrid butt-welding at quasi-stable state.[36]

Distribution nephograms of temperature at the same position of weldments in hybrid welding and TIG welding alone show when the welding process has stabilized. As is shown in Figs 7.32 and 7.33, the isothermal range of hybrid welding is narrower than that of TIG welding alone, so the HAZ of hybrid welding is much narrower than the latter. This is because

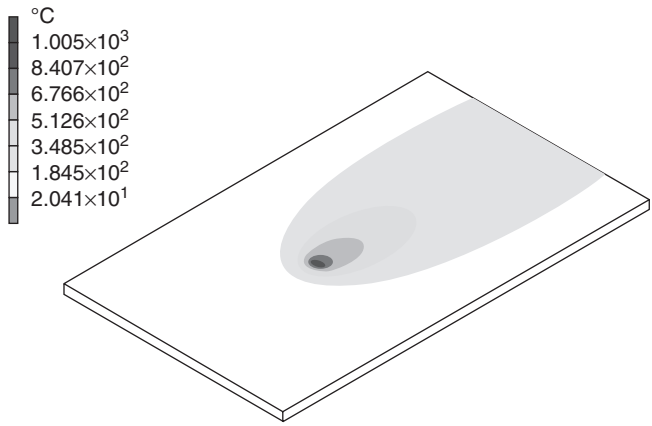

7.33 Temperature distribution of TIG butt-welding alone at quasi-stable state.[36]

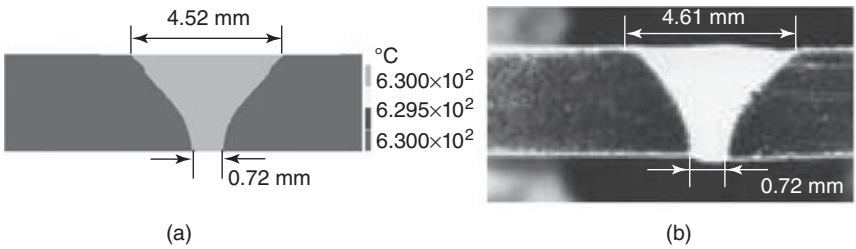

7.34 Comparison of experimental butt-welding joint and simulative result.[36] (a) Simulative weld joint of hybrid welding; (b) Experimental weld joint of hybrid welding.

the thermal diffusivity [thermal conductivity/(specific heat × density)], of magnesium alloy is high and, therefore, a large energy input is required to get satisfying penetration. In TIG welding, the energy input can be enhanced only by increasing welding current or decreasing welding speed and all of these produce a wide HAZ. In hybrid welding, the laser can enhance the longitudinal energy, improve the thermal efficiency of welding and increase the welding speed, so the heat input is low and the HAZ is narrow. The simulation results show that the welding speed in hybrid welding is twice that of TIG welding.[36]

The simulated weld joint is compared with the experimental result in Fig. 7.34.[36] It is found that there are few differences between them, which indicates that the simulation of the high-temperature region is correct.

7.5 Infrared temperature measurement

In infrared temperature measurement, the TIG tungsten electrode, TIG ceramic nozzle, arc light and laser nozzle influence the results. The validation system of infrared measuring is designed to avoid these interferences, as shown in Fig. 7.35.[38] The workpiece surface sensing point is located outside the area covered by the arc. The thermocouple is attached to a sensing point, from which the signal is transmitted to the screen where temperature is displayed. At the same time, infrared thermography also determined the sensing point by point measurement, this temperature value is also displayed on the screen real-time. For each sensing point in the infrared image taken by infrared thermography, its temperature t_i altered when its emissivity ε_i altered. Through data analysis based on t_i and ε_i, the relational expression was validated such that:

$$\sqrt[4]{\varepsilon_i}\,(t_i + 273.15) \approx \mathrm{C} = \mathrm{Constant} \tag{7.4}$$

which indicates that, for each infrared sensor, its output is able to reflect the Stefan–Boltzmann law of grey-body radiation accurately. By the combined use of infrared thermography and thermocouple, AZ31B Mg alloy plates, the surface emissivity ε and its corresponding temperature t were found, as shown in Table 7.3.[38] Thus, it is obvious that:

$$\sqrt[4]{\varepsilon}\,(t + 273.15) = \mathrm{C} \tag{7.5}$$

From equation (7.5), the relationship between t and C, based on the data shown in Table 7.3, is that:

$$t = 2.2979C - 478.67 \tag{7.6}$$

For each infrared image caught by infrared thermography during bead-on-plate hybrid laser–TIG welding process of AZ31B magnesium alloys, as

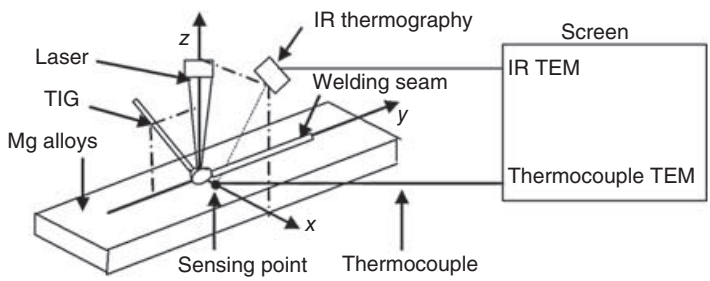

7.35 Sketch image of the infrared temperature measuring system.[38]

Table 7.3 AZ31B Mg alloy plates, surface emissivity and corresponding temperature[38]

E	*t* (°C)	*E*	*t* (°C)
0.08	584	0.16	180
0.09	497	0.17	151
0.1	433	0.18	130
0.11	395	0.19	112
0.12	338	0.2	93
0.13	291	0.21	88
0.14	258	0.24	67
0.15	220	0.3	26

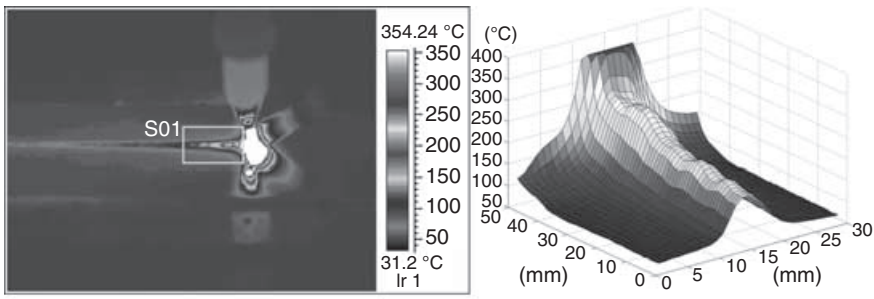

7.36 Infrared image and the zone analysis of S01 in hybrid welding.[38]

shown in Fig. 7.36a, with the combining use of equation (7.4) and equation (7.6), the welding infrared temperature distribution outside the area covered by arc was obtained, as shown in Fig. 7.36b, and the infrared temperature distribution data were reliable.[38]

7.6 Spectral diagnosis

7.6.1 Acquisition of welding plasma spectra

The plasma spectra from 200 to 1000 nm in the stable processes of TIG welding and hybrid welding are acquired by use of a 300 g mm^{-1} grating, as is shown in Fig. 7.37. It is found that the plasma spectrum includes both continuous and line spectra. The continuous spectrum is generated by bremsstrahlung of thermoelectrons (free-to-free transitions) and recombi-

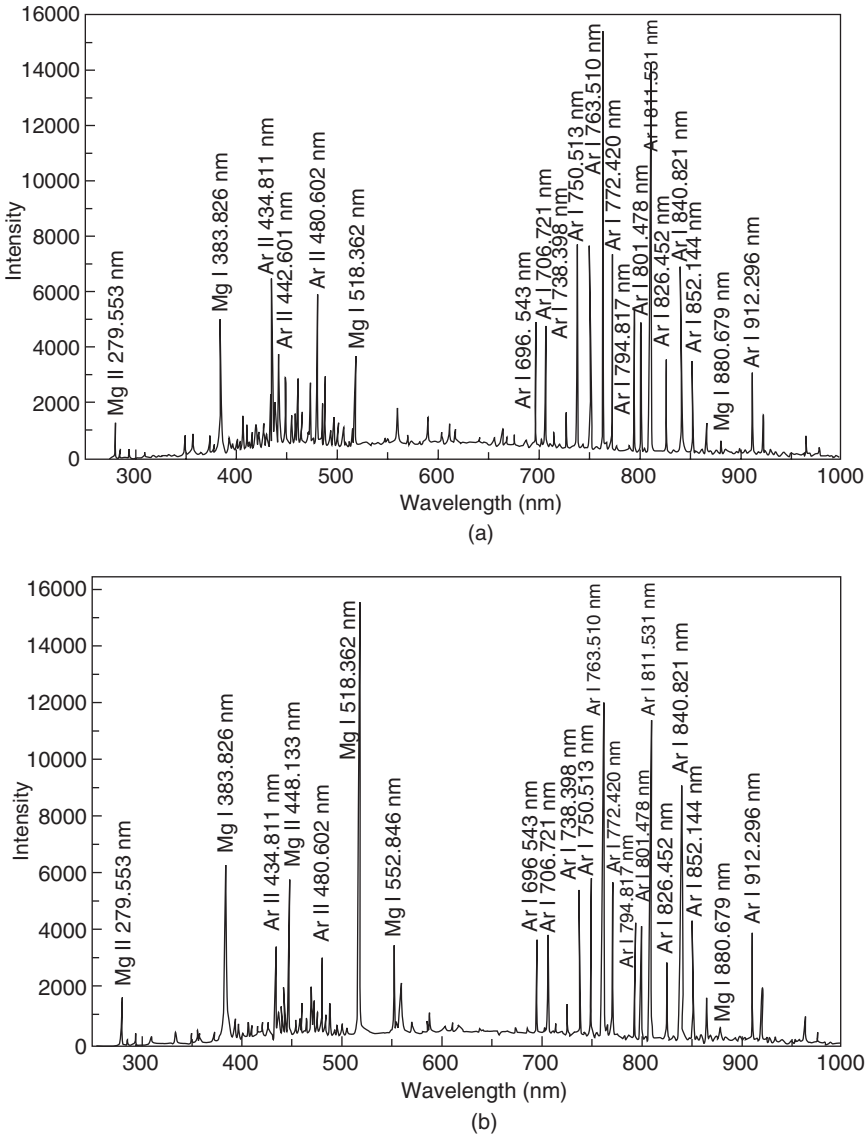

7.37 Spectra of (a) TIG welding plasma and (b) hybrid welding plasma.

nation radiation of electrons and ions (free-to-bounded transitions). The line spectrum consists of atomic spectra and ionic spectra. Referring to reference 39, it is confirmed that there are emission lines of Mg I, Mg II, Ar I and Ar II in the welding plasma, but no spectral lines of other alloy elements such as Al, Zn and Mn owing to their low concentrations.

Through the comparison of plasma spectra between TIG welding and hybrid welding under the same welding conditions, it is found that the intensities of emission spectra of Mg I and Mg II in hybrid welding are much stronger than that in TIG welding, whereas the intensities of the emission spectra of Ar I and Ar II in hybrid welding are a little weaker than that in TIG welding. Mg I 518.362 nm and Mg II 279.553 nm are the sensitive lines of Mg atom and Mg^+ ion. Ar I 811.531 nm and Ar II 480.602 nm are the sensitive lines of Ar atom and Ar^+ ion.[39] In hybrid welding, the intensity of Mg I 518.362 nm ($4s^3S_1 - 3p^3P_2^0$) is three times of that in TIG welding and the intensity of Mg II 279.553 nm ($3p^2P_{3/2}^0 - 3s^2S_{1/2}$) increases by about 30% of that in TIG welding, while the intensities of Ar I 811.531 nm ($4p^2[5/2]_3 - 4s^2[3/2]_2^0$) and Ar II 480.602 nm ($4p^4P_{5/2}^0 - 4s^4P_{5/2}$)[40] are only about 80 and 60%, respectively, of that in TIG welding, respectively.

The spectra of plasmas in TIG welding and hybrid welding are acquired under the same acquiring parameters of the spectrograph, so the influence of the spectrograph on the intensity of the spectral line is neglected. The changes above are induced by the addition of laser pulses. In TIG welding, argon gas is ionized to conduct electricity, so the emission spectra of Ar element are clear and strong. However, in hybrid welding, Mg alloy vaporizes rapidly owing to its low melting point and boiling point under the action of the laser beam after the surface of base metal is melted by the TIG arc. The ionization energy of Mg is much lower than that of Ar, so Mg atoms are ionized first instead of Ar atoms. A large number of Mg^+ ions and electrons are supplied to stabilize the arc and Ar plasma in the arc column is diluted. Thus, the spectral lines of Mg plasma intensify and those of Ar weaken in hybrid welding owing to the evaporation and ionization of Mg alloy.

7.6.2 Electron temperature and density

In order to study the interactions between laser pulse and arc plasma, the electron temperature is estimated by the Boltzmann plot method. If we consider the weld plasma to be in local thermodynamic equilibrium (LTE), the electron temperature is approximate to the excitation temperature. The excitation levels within the plasma are populated according to the Boltzmann distribution and the ratio of the line intensities can be described by:

$$\frac{I_1}{I_2} = \frac{A_1 g_1 \lambda_2}{A_2 g_2 \lambda_1} \exp\left(-\frac{E_1 - E_2}{kT_e}\right) \tag{7.7}$$

where λ and I are the wavelength and intensity of the spectral line, E and g are the excitation energy and statistical weight of the upper transition level, A is transition probability of the electron from the upper level to the

lower level, k is the Boltzmann constant and T_e is the electron temperature.

In the Boltzmann plot method to calculate the electron temperature, the spectral lines of the same atomic or ion are usually selected and they should fulfill the criterion

$$E_1 - E_2 > kT_e \tag{7.8}$$

on the upper energy levels.[41] The calculation result shows that the electron temperature of the plasma near the target metal in TIG welding is about 12 200 K ± 1000 K; when the laser beam is added, the electron temperature decreases to 8500 K ± 800 K.

The profile of an emission line can be affected by different mechanisms of broadening: natural broadening, thermal Doppler broadening, Stark broadening and instrumental broadening.[42] In the welding process, Stark and Doppler broadening mechanisms have a large effect on the profile of the spectral line. The Doppler broadening can be calculated from equation (7.9)

$$\Delta\lambda_D = 7.16 \times 10^{-7} \lambda \left(\frac{T_e}{M}\right)^{1/2} \tag{7.9}$$

where T_e is the electron temperature of plasma, M is the atomic mass and λ is the wavelength of spectral line. When the electron temperature is 20 000 K, the Doppler line width of Mg I 516.732 nm is about 0.015 nm. In this experiment, the line width of Mg I 516.732 nm is larger than 0.06 nm, so the Doppler broadening of the spectral line profile is neglected and Stark broadening is the main factor that affects the profile of the spectral line. The electron density of the welding arc plasma can be estimated from the Stark broadening effect.

$$N_e \approx \frac{\Delta\lambda_{1/2}^S}{2w} \times 10^{16} \tag{7.10}$$

where N_e is the electron density (cm^{-3}), $\Delta\lambda_{1/2}^S$ is the full width at half-maximum intensity of the spectral lines and w is the electron collision broadening parameter.[42] In this experiment, Mg I 516.732 nm is used to calculate the electron density of arc plasma. Corresponding to the change in electron temperature, the electron density of the plasma increases from 8.13×10^{16} cm^{-3} to 1.05×10^{17} cm^{-3}.

The increase in electron density of the plasma is caused by the ionization of magnesium alloy and the contraction of the arc column. In hybrid welding, owing to the increased evaporation of magnesium alloy, the magnesium

vapor covers the arc. On one hand, the ionization energy of magnesium atom is only 7.6 eV, magnesium atoms are ionized easily and cumulative ionization occurs owing to the collision. On the other hand, for the high thermal conductivity and radiation of magnesium atom, the temperature at the edge of the arc plasma decreases and it causes a contraction of the arc plasma owing to the thermal pinch effect. It makes the arc column concentrate with high temperature, so the electron density in the column of arc plasma increases.

7.6.3 Local thermal equilibrium (LTE) analyses

In the spectral analysis of plasma, the most important assumption of local thermal equilibrium involves use of the Boltzmann plot method. The assumption of LTE is fulfilled when the electron density is high enough so that:

$$N_e \geq 1.6 \times 10^{12} T_e^{1/2} (\Delta E)^3 \quad (\mathrm{cm}^{-3}) \tag{7.11}$$

where ΔE (ev) is the largest energy gap in the atomic energy level system and T_e (K) is the electron temperature of plasma.[43] When the electron temperature is 20 000 K, the threshold value of electron density to fulfil the LTE assumption is about 4.14×10^{15} cm^{-3}. In this experiment, the electron densities of both TIG welding plasma and hybrid welding plasma are higher than the threshold value, so the welding plasma satisfies the assumption of LTE and the electron temperature and density estimated by the Boltzmann plot method and the Stark broadening effect reflect the characteristics of the plasma correctly.

7.7 Interaction between laser beam and arc plasma

The welding penetration of hybrid welding indicates that it is not the simple addition of laser beam and arc plasma, but there are complicated physical interactions between the two thermal resources. On the one hand, in laser welding of magnesium alloys, the laser energy is reflected seriously. The absorptivity for a Nd:YAG laser beam is only about 8 to 20% at room temperature.[25] In hybrid welding process, TIG arc is used to melt the base metal ahead and the absorptivity of the magnesium alloy for the laser beam shoots up to 90%, which improves the thermal input remarkably. For magnesium alloy, the melting point and boiling point of magnesium alloy are low and the ionization energy of magnesium atoms is much lower than argon atoms, magnesium alloy vaporizes rapidly and ionizes instead of argon gas under the action of the laser beam. There are many magnesium atoms in the plasma column. The electrons with high energy transfer this energy to

magnesium atoms or ions by collision, thus leading to the cumulative ionization of magnesium atoms. Then the electron density increases and both the average energy of electrons and electron temperature decrease. In addition, because of the high thermal conductivity and radiation of magnesium alloys, the temperature of the arc plasma decreases and this leads to a contraction of the arc giving thermal pinch effect. It also causes an enhancement of electron density.

On the other hand, laser welding changes from the thermal-conduction mode to the keyhole mode by the use of TIG arc. In low-power laser welding alone, the laser power density is insufficient to ionize the magnesium atoms adequately, so the welding process is performed in thermal-conduction mode. When the TIG arc is coupled with a laser beam, the surface material is melted by the action of TIG arc ahead. When laser pulses irradiate on the fusion metal, the magnesium atoms will be vaporized and ionized rapidly because of the low melting point and boiling point of magnesium alloy. The free electrons can be accelerated by the electric field induced by the TIG arc. The electrons with high energy impact the base metal and a small depression in the workpiece forms. As the depression deepens, a keyhole forms and the laser light is scattered repeatedly within it, then laser energy can penetrate deeply into the workpiece by means of Fresnel absorption on the keyhole wall and inverse bremsstrahlung absorption in the partially ionized plume of vapor in the keyhole until the laser energy is absorbed completely. In this case, the power of the pulse laser is absorbed at greater depths, not just at the surface, so the welding penetration is much deeper than in conduction mode.

In addition, solid magnesium starts to oxidize quite readily at 450 °C.[12] In the welding process, the natural surface of magnesium alloys is usually covered with an oxide film (MgO) owing to its high reactivity with oxygen. The melting point and boiling point of MgO are 2800 °C and 3600 °C, respectively, and it will waste a great deal of energy to be melted in the welding process. In hybrid welding, an AC arc is used to clear the oxide film in the negative wave, so the efficiency of the thermal input is improved.

These studies indicate that the interaction between laser beam and arc plasma improves the thermal input in the welding process, so magnesium alloys can be welded with good quality by low-power laser–arc hybrid welding.

7.8 Practical application

Laser–arc hybrid welding joints of magnesium alloy have the same capability as base metal under both steady loads and dynamic loads. The hybrid method has been successfully applied in the bicycle and automotive industries; some samples and products are show in Fig. 7.38 and Fig. 7.39. Batch

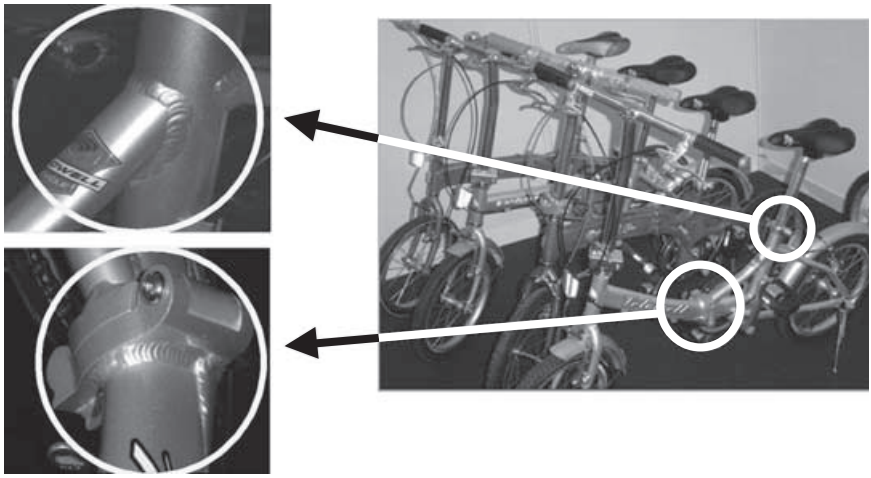

7.38 Products of magnesium alloy bicycle.

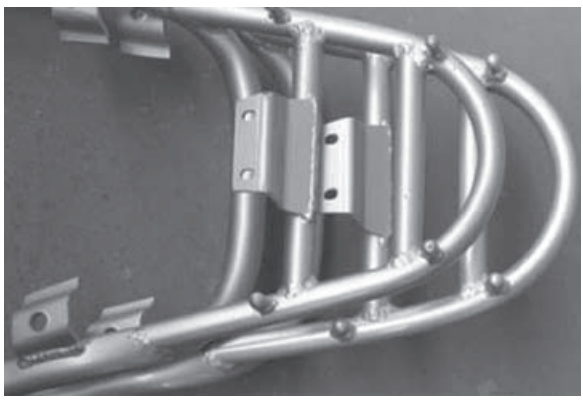

(a)

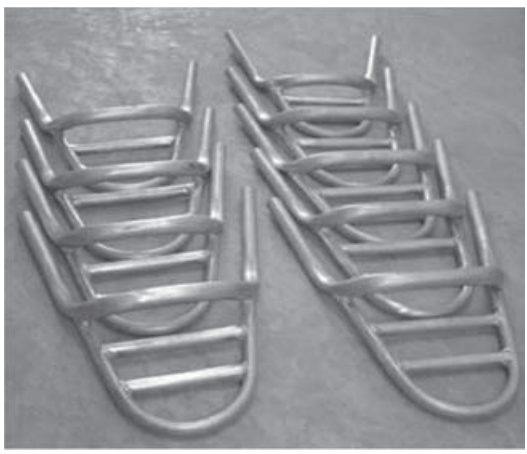

(b)

7.39 Products of magnesium alloy autocycle.

production of these magnesium alloy products has been achieved. The low-power laser–arc hybrid welding process has shown excellent economic and social performance.

7.9 Conclusions and future trends

Low-power laser–arc hybrid welding has been applied to weld magnesium alloys at high speeds successfully. The hybrid weld joint has deep penetration and excellent mechanical properties both under dynamic and steady load, thus expanding its application in industry. An investigation of the plasma behavior, numerical simulation and infrared temperature distribution showed the interaction between laser beam and arc plasma. However, the interaction in hybrid welding has not been explained systematically. It still needs more research to identify the physical effects between low-power laser beam and arc plasma. In addition, it is necessary to develop laser–MIG hybrid welding to meet the needs of joining thick magnesium plates. Many problems result from the physical properties of magnesium, for instance its narrow interval between melting point and vaporization point. The energy input into the filler material has to be regulated in such a way that the wire will melt but not vaporize. It is difficult to achieve this result except by using a special power source. So far, only German workers[15] weld magnesium alloys by the MIG welding process and are examining and optimizing the special power source characteristics. The butt weld joints reveals a tensile strength from about 80 to 100% of the base metal, but the fatigue strength of the weld joints only reaches 50% of that of base metal and 75% of the base metal after reinforcement, which cannot meet the dynamic load request of the structure.

7.10 References

1 M.M. AVEDESIAN, H. BAKER, *Magnesium and Magnesium Alloys, ASM Specialty Handbook*, 1999.

2 H. HAFERKAMP, M. NIEMEYER, U. DILTHEY, G. TREGER, Laser and electron beam welding of magnesium materials, *Weld. Cutt.* 2000 **52**(8) 178–180.

3 P.G. SANDERS, J.S. KESKE, K.H. LEGNG, G. KOMECKI, High power Nd:YAG and CO_2 laser welding of magnesium, *J. Laser Appl.* 1999 **11**(2) 96–103.

4 K.H. LEONG, G. KOMECKI, P.G. SANDERS, J.S. KESKE, Laser beam welding of AZ31B-H24 alloy, *ICALEO 98: Laser Materials Processing Conference*, Orlando, FL, 1998 **16–19** 28–36.

5 B.L. MORDIKE, T. EBERT, Magnesium: properties – applications – potential, *Mater. Sci. Eng. A*. 2001 **302** 37–45.

6 M. MARYA, D.L. OLSON, G.R. EDWARDS, Welding of magnesium alloys for transportation applications, in: Proceedings from Materials Solution'00 on Joining of Advanced and Specialty Materials, St. Louis, Missouri, 2000 **9–11** 122–128.

7 M. PASTOR, H. ZHAO, T. DEBROY, Continuous wave Nd: yttrium–aluminium–garnet laser welding of AM60B magnesium alloys, *J. Laser Appl.* 2000 **12**(3) 91–100.

8 E. AGHION, B. BRONFIN, Magnesium alloys development towards the 21st century, *Mater. Sci. Forum* 2000 **350–351** 19–28.

9 M. MARYA, G. EDWARDS, S. MARYA, D.L. OLSON, Fundamentals in the fusion welding of magnesium and its alloys, in: *Proceedings of the Seventh JWS International Symposium*, Kobe, 2001 **20–22** 597–602.

10 C. LEHNER, G. REINHART, L. SCHALLER, Welding of die cast magnesium alloys for production, *J. Laser Appl.* 1999 **11**(5) 206–210.

11 X. CAO, M. JAHAZI, J.P. IMMARIGEON, W. WALLACE, A review of laser welding techniques for magnesium alloys, *J. Mater. Process. Technol.* 2006 **171** 188–204.

12 J. WEGRZYN, M. MAZUR, A. SZYMANSKI, B. BALCEROWSKA, Development of a filler for welding magnesium alloy GA8, *Weld. Int.* 1987 **2** 146–150.

13 L.M. LIU, D.H. CAI, Z.D. ZHANG, Gas tungsten arc welding of magnesium alloy using activated flux-coated wire, *Script. Mater.* 2007 **8** 695–698.

14 A. MUNITZ, C. COTLER, A. STERN, G. KOHN, Mechanical properties and microstructure of gas tungsten arc welded magnesium AZ91D plates, *Mater. Sci. Eng.* 2001 **1** 68–73.

15 M. RETHMEIER, B. KLEINPETER, H. WOHLFAHRT, MIG welding of magnesium alloys metallographic aspects, *Weld. World* 2004 **48** 28–33.

16 E. CRAIG, The plasma arc process-a review[J]. *Weld J.* 1988 **67**(2) 19–25.

17 C.T. CHI, C.G. CHAO, T.F. LIU, C.C WANG, A study of weldability and fracture modes in electron beam weldments of AZ series magnesium alloys. *Mater. Sci. Eng. A* 2006 **5** 672–680.

18 A. WEISHEIT, R. GALUN, B.L. MORDIKE, CO_2 laser beam welding of magnesium based alloys. *Weld. J.* 1998 **77**(4) 148–154.

19 X.H. WANG, K.S. WANG, Microstructure and properties of friction stir butt-welded AZ31 magnesium alloy, *Mater. Sci. Eng. A* 2006 **1–2** 114–117.

20 D.Q. SUN, B. LANG, D.X. SUN, J.B. LI, Microstructures and mechanical properties of resistance spot welded magnesium alloy joints, *Mater. Sci. Eng. A* 2007 **15** 494–498.

21 H. ZHAO, T. DEBROY, Pore formation during laser beam welding of die-cast magnesium alloy AM60B mechanism and remedy. *Weld. J.* 2001 **8**(80) 204–210.

22 M. MARYA, G.R. EDWARDS, The laser welding of magnesium alloy AZ91, *Weld. World* 2000 **44**(2) 31–37.

23 A. MAHRLE, E. BEYER, Hybrid laser beam welding – classification, characteristics, and applications. *J. Laser Appl.* 2006 **18**(3) 169–180.

24 T. GRAF, H. STAUFER, *Weld. J.* 2003 **82** 42–48.

25 H. HAFERKAMP, M. GOEDE, A. BORMANN, P. CORDINI, Laser beam welding of magnesium alloys – new possibilities using filler wire and arc welding, *Proc. LANE: Laser Assist. Net Shape Eng.* 2001 **3** 333–338.

26 Y.B. CHEN, L.Q. LI, L. WU, Quantitative measurement of absorption and defocusing of laser beam by electric arc. *Trans. China Weld. Inst.* 2003 **24** 56–58.

27 L.M. LIU, G. SONG, G.L. LIANG, J.F. WANG, Pore formation during hybrid laser-tungsten inert gas arc welding of magnesium alloy AZ31B-mechanism and remedy. *Mater. Sci. Eng. A* 2005 **390** 76–80.

28 L.M. LIU, X.F. HAO, G. SONG, A new laser–arc hybrid welding technique based on energy conservation, *Mater. Trans.* 2006 **47** 1611–1614.
29 L.M. LIU, G. SONG, M.S. CHI, Laser–tungsten inert gas hybrid welding of dissimilar AZ based magnesium alloys, *Mater. Sci. Technol.* 2005 **21** 1078–1082.
30 G. SONG, Research on low-power laser–tungsten inert gas (TIG) hybrid welding technology of Mg alloy. PhD thesis, *Dalian University of Technology*, 2006.
31 L.M. LIU, J.F. WANG, G. SONG, Hybrid laser–TIG welding, laser beam welding and gas tungsten arc welding of AZ31B magnesium alloy. *Mater. Sci. Eng. A* 2004 **381**(1–2) 129–133.
32 G. SONG, L.M. LIU, P.C. WANG, Overlap welding of magnesium AZ31B sheets using laser–arc hybrid welding process, *Mater. Sci. Eng. A* 2006 **429** 312–319.
33 X. HAO, S. GANG, Low-power YAG laser–arc hybrid welding of AZ-based Mg alloy, *Rare Metal* 2007 **26** 67–72.
34 G. SONG, L.M. LIU, M.S. CHI, Laser–TIG hybrid weldability of AZ-based magnesium alloys, *Proceedings of International Conference on Advanced Welding and Joining Technology*, Dalian, China, 2005 B69–B74.
35 G. SONG, L.M. LIU, M.S. CHI, J.F. WANG, Investigations on laser–TIG hybrid welding of magnesium alloys. *Mater. Sci. Forum* 2005 **488–489** 371–376.
36 L.M. LIU, M.S. CHI, G. SONG, A new heat source model in numerical simulation of AZ31B magnesium alloy laser–TIG hybrid welding, *Chin. J. Mech. Eng.* 2006 **42(2)** 82–85.
37 L.M. CHONG, Predicting Welding Hardness. Thesis. Ottawa, Canada: Caleton University, 1982.
38 R.S. HUANG, L.M. LIU, G. SONG, Infrared temperature measurement and interference analysis of magnesium alloys in hybrid laser–TIG welding process. *Mater. Sci. Eng. A* 2007 **447**(1–2) 239–243.
39 Wavelength list of spectral lines, *Industry Press of China*, 1971.
40 *National Institute of Standards and Technology database*. http://physics.nist.gov/PhysRefData/ASD/lines_form.html
41 J. SABBAGHZADEH, S. DADRAS, M.J. TORKAMANY, Comparison of pulsed Nd:YAG laser welding qualitative features with plasma plume thermal characteristics. *J. Phys. D: Appl. Phys.* 2007 **40** 1047–1051.
42 H. R. GRIEM, *Plasma Spectroscopy*. New York: McGraw–Hill, 1964.
43 C. COLON, A. ALONSO-MEDINA, Application of a laser produced plasma: experiment Stark widths of single ionized lead lines. *Spectrochim. Acta Part B* 2006 **61** 856–863.

8

Shipbuilding applications of hybrid laser–arc welding

J. K. KRISTENSEN, FORCE Technology, Denmark

Abstract: A review is presented of laser welding and especially hybrid MIG–laser welding, which shows attractive properties such as e.g. low distortion, high welding speed and easy automation, and thus shows a great potential in the welding of structural steels used in the shipbuilding industry. Particular emphasis is placed on the introduction of high power laser and laser-hybrid welding for structural applications to reduce distortion. The challenges related to the process itself, the microstructure and the mechanical properties, which had, however, to be dealt with before the processes could introduced into production are reviewed and the typical mechanical properties achieved are discussed. The current, quite extensive, use of laser-based welding in European yards is also reviewed.

Key words: laser welding, laser arc welding, mechanical properties, Classification society guidelines, shipbuilding.

8.1 Introduction

Laser hybrid welding owing to its higher power density offers many advantages over traditional welding processes. The advantages include high-speed seam welding, low distortion, and single-pass welding in large thickness, easy automation and positive effects on the working environment. For these reasons, laser-based welding has also experienced a dramatic increase in use within structural applications in heavier sections. In the fully synergetic hybrid processes, the plasma formed at the interaction point of the laser on the work-piece surface controls the arc-root by reducing the cathode voltage drop, so that the interaction point becomes the same for the laser and the arc. When welding thick parts and/or in the presence of a gap, hybrid laser using the MAG process is most advantageous as, integrated in the process, it offers easy addition of filler material. Roughly speaking, in heavy section laser–arc welding, the weld penetration is determined by the laser beam action alone. However, owing to the arc, the welding speed may be maintained at a high level even in the case of a relatively large gap. Thus, an increased ability to bridge a gap as well as a significant increase in speed

8.1 Typical arc welded deck panels for a passenger ship; note the distortions.

may be taken advantage of by using the hybrid process as compared with the traditional high-power laser welding process and, furthermore, the heat input per unit length (and therefore also the distortions) is typically not increased significantly.

Laser and especially laser–hybrid welding are now making an important impact on the medium and heavy section welding industry. The shipbuilding industry is leading in the introduction of high-power laser and laser–hybrid welding, but, for example, pipe and boiler manufacturing are also highly relevant. Many concrete initiatives have been taken during the last one and a half decades and several European shipyards have now introduced the process. The major motivation for this is reduced distortion as it is estimated that between 20 and 30% of the man-hours used in shipbuilding is due to reworking caused by welding distortions. Figure 8.1 illustrates this very convincingly.

8.2 The approval of laser-based welding in shipbuilding

8.2.1 General

In addition to physical defects produced during welding, a structure may develop flaws or completely fail in service owing to:

- limited strength or ductility;
- limited toughness (e.g. impact or quasi-static);
- environmentally assisted cracking (hydrogen cracking);
- general corrosion;
- fatigue.

For traditional arc welding, a number of mechanical tests have been developed for assuring that the ductility and toughness is sufficient and that serious cracks do not develop during the lifetime of a product. As part of a welding procedure testing, it is for this reason usually recommended that a number of the following mechanical properties are evaluated:

- hardness,
- strength and ductility,
- impact toughness, sometimes supplemented by CTOD values,
- weld defects like geometrical defects, cracks or pores.

The introduction of the new welding process in shipbuilding involved a number of challenges to be solved. Firstly, the actual measurement of the properties was difficult as the established techniques cannot be applied without modifications and, secondly, the acceptance criteria should be reconsidered thereby making it difficult directly to build on the decades of experience connected to these criteria.

8.2.2 The main challenges

For the introduction of firstly pure laser welding and later hybrid laser–arc welding it therefore became of paramount importance that a number of general problems related to the properties of welded structures were solved. Developments during the previous three to four decades within materials and their response to welding had to be reconsidered in the light of this new technology.

The ductility of the weld could thus no longer be measured by the standard tensile testing techniques owing to the narrow weld and the hard and strong weld metal. Impact and toughness testing showed fracture path deviation making the evaluation of the tests difficult. Solidification cracking also turned out to be a challenge when welding thicker sections and also the techniques for performing non-destructive evaluation of the welds had to be reconsidered. Related to fatigue, concern was raised about the potential sharpness of the geometrical stress concentration imperfections in, e.g., the weld toe region, and similarly the fatigue crack growth rate in the potentially martensitic weld metal was questioned, as was also the general and stress corrosion properties of the weldments. In Chapter 6 of this volume some of the main challenges are discussed, e.g. the self-quenching of the weld metal (WM) and heat-affected zone (HAZ), fracture path deviation in impact and toughness testing and solidification flaw control.

8.2.3 Mechanical properties

Shipbuilding steels are typically ferritic steels strengthened by C, Mn and various numbers of microalloying elements, e.g. Ti, V or Nb. Different

production routes are used depending on the demands on the steels and the available techniques at the given steel works. Carbon typically is in the range 0.05–0.18% (weight), Mn in the range 0.5–1.5% and S and P in the range 0.005–0.03%. The guaranteed yield strength of structural steels for shipbuilding typically is 235–460 MPa, but higher grades also exist. In Chapter 6, the above is discussed in more details.

Comparing the heat input per unit length for typical arc and laser-based (pure or hybrid) welds (for the same penetration or throat thickness, respectively) shows that the heat input in laser welds is typically almost an order of magnitude lower than in arc welds. It must therefore be taken into consideration that structural steels may become hard in both the WM and HAZ as a consequence of the fast thermal cycle inherently connected to processes. The resulting hardness does, however, depend very much on the composition of the steel which determines the hardenability as well as on the carbon content alone, as this controls the maximum possible hardness in a fully martensitic structure. Figure 8.2 shows three examples of hardness traverses in three different steels using an EN 440-G3Si1 (SG2) solid wire.

The impact properties are also interesting and, as an example, Figure 8.3 shows a full Charpy V-notch transition curve for a weld in the 12 mm S235 structural steel welded with an initial gap of 0.5 mm. As shown, the transition temperature is below –40 °C and, owing to the very tough structure, the level of the high temperature shoulder is significantly higher than the

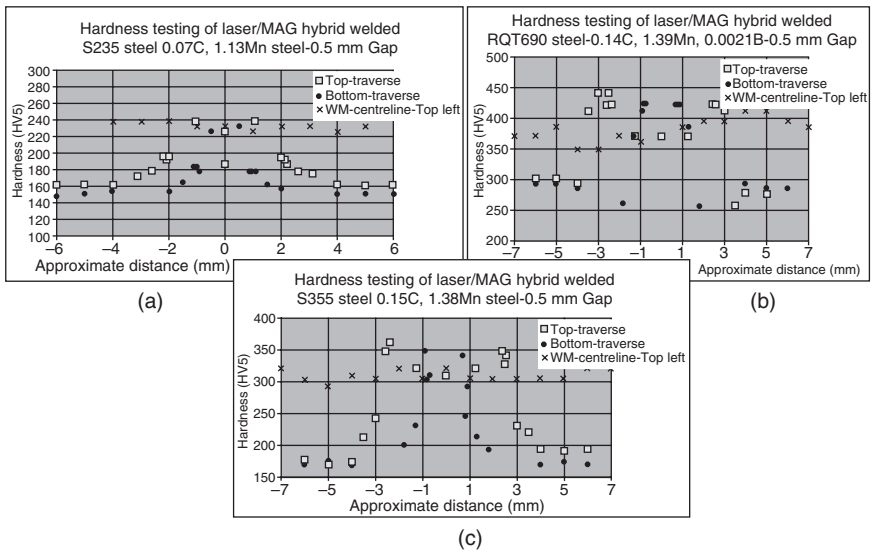

8.2 Hardness profiles for welds in (a) S235 (0.07C, 1.13Mn), (b) RQT 690 (0.14C, 1.39Mn, 0.0021B) and (c) S355 (0.15C, 1.38Mn) steels.

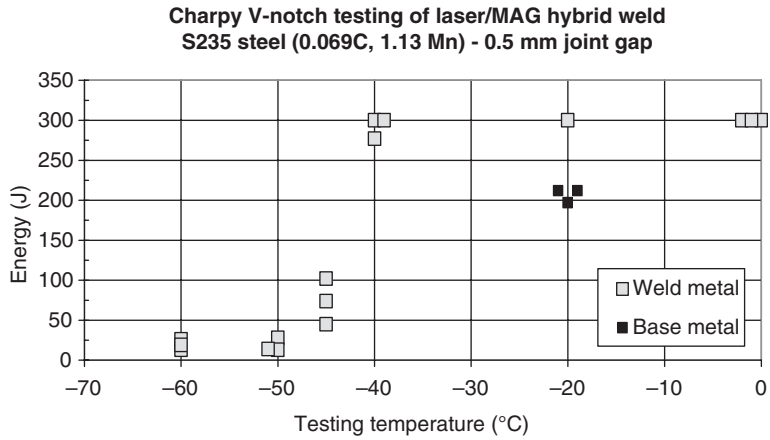

8.3 Charpy V-notch transition curve for the 0.5 mm gap weld made in 12 mm S235 structural steel. The maximum energy of the testing equipment is 300 J.

level of the base metal alone. The fatigue behavior has also been extensively investigated using e.g. four-point bending or uniaxial loading. Typically tests show results in excess of the FAT100 line.

8.2.4 The effects of mismatching

Compared with traditional arc welding techniques, many advantages can be gained from the low distortion and high speed characteristic of deep penetration laser welding. On the other hand, a major challenge is encountered with regard to the mechanical properties of the weldment. This is partly because of the fast thermal cycle and partly to the very narrow (typically 1–3 mm) weld and correspondingly abrupt changes in properties across the weld.

Opposed to arc welds where HAZ properties often control the performance of a welded joint, in laser welds the WM is dominating the properties. Furthermore, the possibility of influencing the composition of the WM by the filler material is very limited as the zero gap situation must normally also be accepted. In general, a high degree of overmatching in strength will occur and an overmatch by a factor of two is not unusual. The high level of overmatching combined with the aforementioned narrowness of the weld make laser welds of structural steels an extreme example upon a mismatching joint of the 'sandwich-type'. It is, however, generally found that weld metal notched wide-plate tests under transverse loading conditions show a beneficial effects of WM strength overmatching by promoting failure in the

lower strength, but higher toughness base plate. In contrast, undermatched welds require a high straining capacity in the soft weld metal owing to the deformation being localised here. It may also be noted that crack propagation preferably take place in the softer zones, i.e. the fracture path for a crack initiated in the WM of an overmatched weld normally deviates into the softer and more tough base metal. These conclusions are supported by experimental and numerical investigations on laser welds using as well smaller specimens as wide plates.[1–4]

8.2.5 Unified guidelines

Developments during the last three to four decades within materials and their response to welding had to be reconsidered in the light of this new technology. The challenge of getting the new welding approach approved by the ship classification societies was tremendous and could not be overcome by one shipyard or one country alone. For over two decades, a large number of tests have therefore been performed in various European collaboration projects involving several shipyards and classification societies as well as many institutes and universities.

The work performed involved:

- Process development (incl filler metal addition),
- Sensor based seam tracking and real time adaptive control,
- Mechanical properties:
  - Hardness and strength,
  - Ductility,
  - Toughness (impact and quasi-static),
  - Fatigue,
- Corrosion properties:
  - Stress corrosion,
  - General corrosion,
- Weld imperfections and defects:
  - Surface defects,
  - Hydrogen introduced cracking (cold cracking),
  - Solidification cracking (hot cracking),
  - Porosity,
- Health and safety aspects:
  - Working environment,
  - External environment,
- NDT:
  - On-line and off-line,
- Wide-plate and large-scale testing,
- Repair welding.

The European ship classification societies issued in 1996 their first unified guidelines for the approval of pure CO_2-laser welding.[5] These guidelines considered only pure CO_2-laser welding, and, as solidification cracking was still a problem in thicker sections, 100% non-destructive testing was typically demanded here, thus still made it unfavourable to the shipyards to apply laser welding on a larger scale. Only in 2004 were normal NDT shipyard practice allowed as were also other laser sources as well as hybrid laser/MAG welding.[6]

8.3 Industrial examples

The shipbuilding industry was, as mentioned, a pioneer in being first to adopt pure laser and later hybrid laser welding. In particular, cruise and passenger ships are well suited for this application as the steel work is dominated by the large amount of deck-structures needed, which typically are made in 5–8 mm plate thickness. Figure 8.4 shows as an example the world's biggest, at present, (2008) cruise ships that are built at Aker Yard in Turku (Finland).

8.3.1 Meyer Wertft, Germany

By 1995 Meyer Werft had included the first simple sandwich panels in ship structures of minor structural importance and, from 1998, the panels were also used for passenger decks. The panels were of the type shown in Fig. 8.5.

Meyer Werft has furthermore in 2001 invested in a new and technically very ambitious panel manufacturing line, which is equipped with a total of four high power laser (12 kW) hybrid welding machines. As 20-m long plates were not available on the market for the entire range of required plate thicknesses (4.5 to 30 mm) and structural optimisation called for a high flexibility in plate thickness and materials used within one section ('tailored decks'), a butt welding station was needed to produce plate 'strips', being up to 20 m long and 4 m wide.[7] These 20-m long strips delivered from the

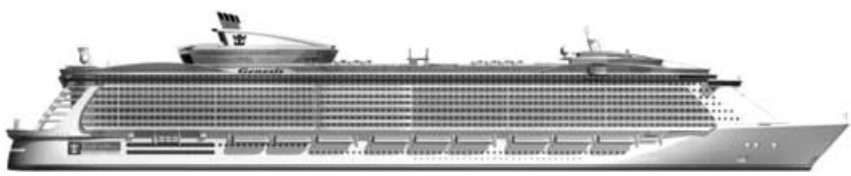

8.4 The world's biggest (2008) cruise ships built at Aker Yard in Turku, Finland. (Courtesy: Kari Laiho, Aker Yard, Turku).

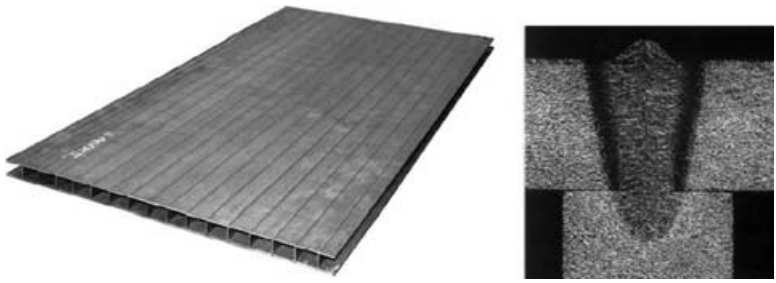

8.5 First laser welded sandwich panels produced at Meyer Werft, Germany (Courtesy: Guido Pethan, Meyer Werft).

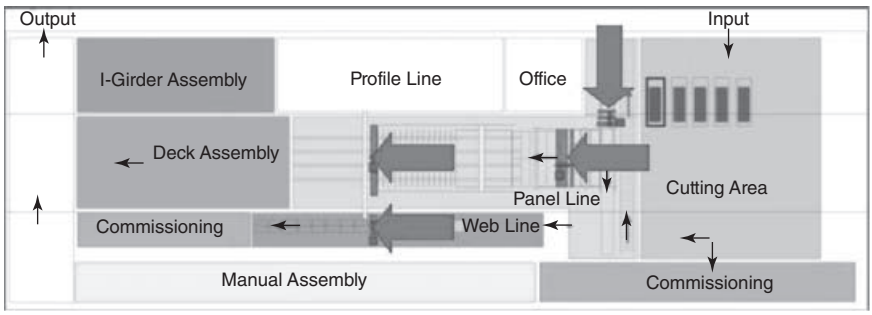

8.6 Layout of new pre-manufacturing workshop at Meyer Werft, red arrows indicate laser hybrid welding positions (Courtesy: Guido Pethan, Meyer Werft).

first butt welding station were then joined to each other and strengthened with stiffeners etc. in order to form deck panels, up to 20 m × 20 m. In order to reduce man hours, a fully automated operation including material handling, edge preparation by grinding/milling and welding is used at the entire panel line.[7] The resulting principal layout of the steel pre-manufacturing workshop is shown in Fig. 8.6 and 8.7 show the installation as well as a stiffener welding head and clamping tools.

In early 2002, the conventional panel line was removed and all flat sections for the ships produced at Meyer Werft were now coming from the new pre-manufacturing workshop. The amount of laser hybrid welds in a large cruise ship was now approx. 50% of the total weld length which may be of the order of 400 km. The majority of the plates welded are 'thin' plates, i.e. of the order of 5–8 mm.[7]

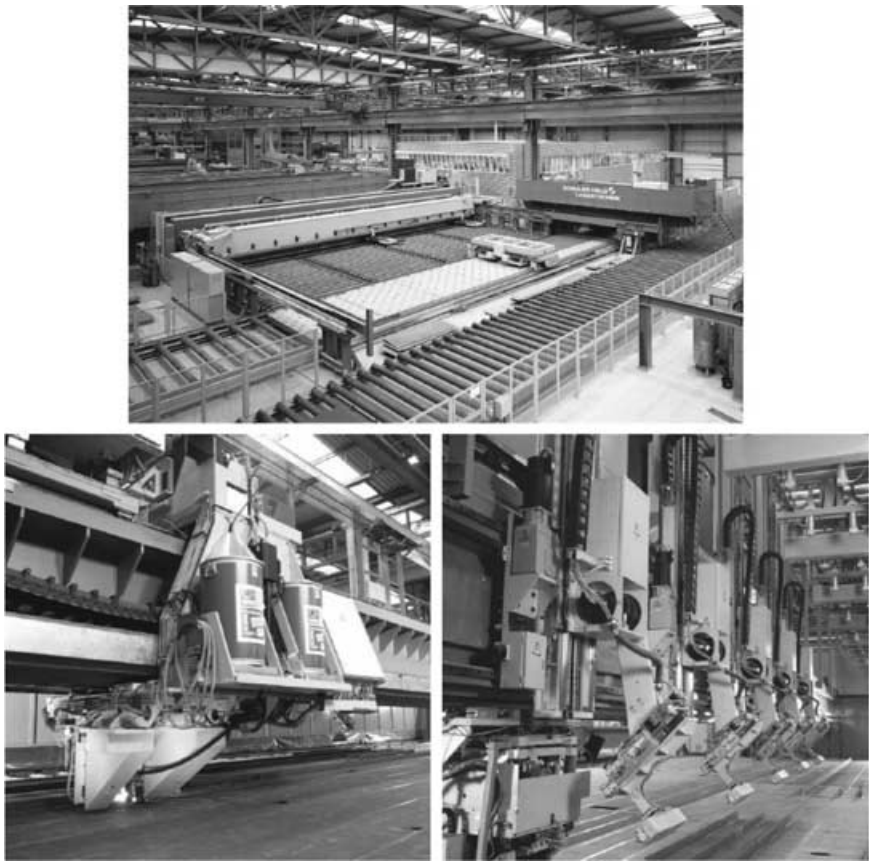

8.7 Photos of the installation as well as of a stiffener welding head and clamping tools (Courtesy: Guido Pethan, Meyer Werft).

8.3.2 Blohm & Voss, Germany

Blohm & Voss GmbH is part of a group with six European shipyards which belong to ThyssenKruppMarine Systems. B&V is the centre for frigates, corvettes and mega–yachts. Blohm & Voss GmbH has used laser technology for more than ten years for manufacturing of complete decks parts (including frames, longitudinal and transversal stiffeners). These welds are typically T-joints in the plate thickness range t = 3–12 mm that are welded with two 12-kW CO_2 lasers simultaneously without additional wire and using nitrogen laser cutting for the edge preparation.[8] Figure 8.8 show an overview of the installation as well as a T-joint welding head and cross-section.

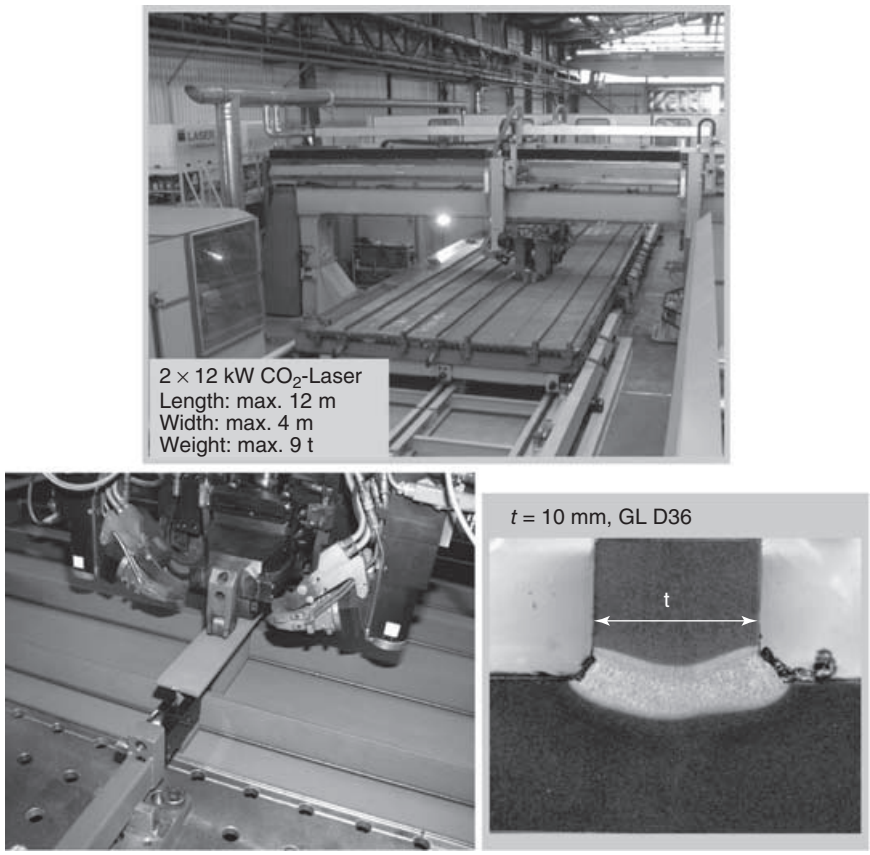

8.8 An overview of the installation as well as a T-joint welding head and cross section (Courtesy: Jens Keil, Blohm + Voss).

8.3.3 Aker Yard, Finland

Aker Yards has three shipyards in Finland. The yards are mainly building cruise ships and ferries. The biggest of the three yards is the one located in Turku in south west of Finland.

Aker Yards has implemented laser hybrid welding into production in December 2006. The laser technology is installed to the existing panel line which reduced the total cost of the investment. At this stage, laser hybrid is used for welding butt welds in panel fabrication. Interestingly, the laser beam is a 6-kW fibre laser.[9] Figure 8.9 show an overview of the installation as well as various elements of it.

(a)

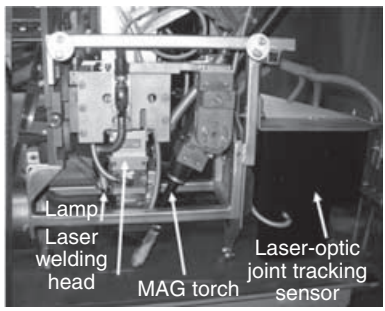

(b)

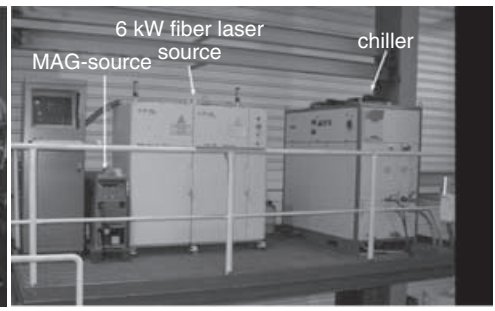

(c)

8.9 (a) An overview of the installation, (b) the laser head and (c) the laser-source and MAG power supply. Owing to the laser light wavelength the installation is encapsulated. (Courtesy: Kari Laiho, Aker Yard).

Aker Yards intends to develop the laser hybrid technique further and the next step will be with material thicknesses over 10 mm. To utilize all the benefits that laser hybrid welding offers for deck panel fabrication, also profiles and transverse elements will in the future be welded with laser hybrid.[9]

8.3.4 Fincantieri, Italy

This yard also has had a laser installation since roughly 1996. The installation is for butt welding of plates for deck structures and uses a 17 kW laser source in combination with an advanced clamping system. This installation has mainly been used for development work. Recently, the yard has, however, invested in a new highly automated panel line installation in which the butt welding is performed using a 10-kW fibre laser for hybrid

welding. This installation may produce panels up to 16 × 40 m and was installed in 2008.[10]

8.3.5 Odense steel shipyard, Denmark

Unlike the other yards mentioned, Odense Steel Shipyard mainly builds very large commercial ships, in particular, very large container ships as for example shown in Fig. 8.10.

At Odense steel shipyard, a combined laser welding and cutting installation was installed in 1997. Interestingly, the same 12-kW CO_2-laser source is used for both purposes. The first production of ship elements with laser welding took place in January 1998 followed by various demonstrations of laser welding in production. In August 2000, the first trials using CO_2-laser/MAG hybrid welding was performed followed by the production of parts for different blocks with laser hybrid welding.[12] Today, however, the installation is mainly used for development work. Figure 8.11 shows the installation together with a welding head.

8.3.6 Future applications

Many joint European projects have been carried out in the last two decades and recently also laser sources that allow fibre delivery of the laser light have been investigated. Today, the fibre laser seems to have a large potential for robotised welding as well as welding in the dock area.

8.10 11 000 twenty foot equivalent (TEU) container vessel at Odense Steel Shipyard. With 11 000 TEU containers including 1000 forty foot equivalent (FEU) reefers. The ship is today (2008) the world's greatest container carrier and reefer vessel.[11] (Courtesy Odense Steel Shipyard).

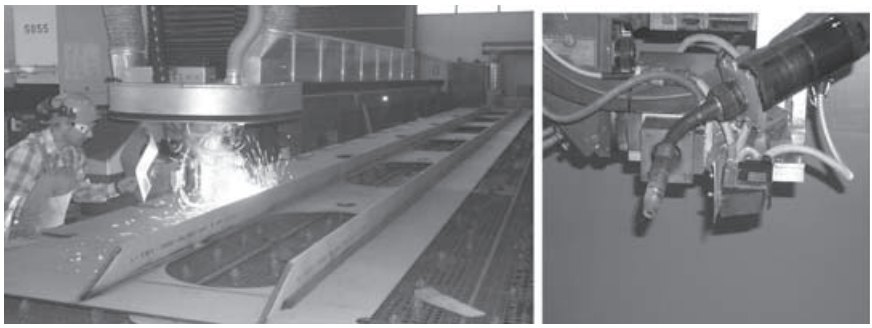

(a) (b)

8.11 (a) Laser installation at Odense Steel Shipyard and (b) the T-joint hybrid welding head (Courtesy: Mads Elvang, Odense Steel Shipyard).

8.4 Conclusions

Laser welding shows a great potential in the welding of structural steels in general and in shipbuilding in particular. This is because of its attractive properties such as high welding speed, low distortion and easy automation. Hybrid MIG–laser welding has the advantages of an increased ability to bridge a gap as well as a significant increase in speed when welding a wide gap.

As a result of intensive work over the last two decades small-scale tests have been modified to suit the demands of laser welds. Furthermore, relevant standards and Classification Societies guide-lines have been made allowing the use of laser hybrid welding in ship production.

Wide-plate and other large-scale tests have been performed. The findings of the large-scale tests are in accordance with the results of the small-scale tests and it may be concluded that laser welds behave at least as good as arc welds. In all cases, the fracture did deviate into the base metal immediately after initiation. In the narrow zone of a laser weld, overmatching seems to be beneficial in preventing flaws from developing in transverse loading conditions.

With regard to mechanical properties, pure and hybrid laser–MAG welding are very similar owing to their similar weld geometries and degree of overmatching obtained. The resulting hardness does, owing to the fast thermal cycle inherently connected to the processes, depend very much on the composition of the steel determining the hardenability as well as on the carbon content alone. The impact properties also generally show acceptable results as does the ductility. In addition, the fatigue behaviour has been extensively investigated and typically tests show results in excess of the FAT100 line.

The weld imperfections most likely to occur are pores and solidification flaws of which the latter are more critical owing to their flat and sharp character. The flaws tend to occur in higher thicknesses when welding at a combination of power and speed close to the limit where full penetration is just achieved. An understanding of the influence of the steel composition and weld parameters on the occurrence of solidification flaws have been achieved, and it seems possible totally to avoid solidification flaws in laser-based welding of structural steels by a combined control of the composition of the steels and the welding parameters.

Laser-based welding is used extensively in European yards and, regarding future development, the fibre laser, in particular, seems to have a large potential for robotised welding as well as welding in the dock area.

8.5 References

1 KOÇAK M, KIM Y-J, CAM G, DOS SANTOS J, RIEKEHR S, TOTSTER F, INSTRAN A, CARDIANL N, WEBSTER S KLÆSTRUP KRISTENSEN, J and BORGGREEN K, *Recommendations on Tensile and Fracture Toughness Testing Procedures for Power Beam Welds*, *Proc. of European Symposium on Assessment of Power Beam Welds*, Geesthacht, Germany (February 1999).

2 KIM Y-C, KOÇAK M and SCHWALBE K-H, *Defect Assessment Procedures for Power Beam Welds*, *Proc. of European Symposium on Assessment of Power Beam Welds*, Geesthacht, Germany (February 1999).

3 KOÇAK M, RIEKEHR S, DOS SANTOS J, CARDINAL N, WEBSTER S, KLÆSTRUP KRISTENSEN J, BORGGREEN K, KLEIN R and FISCHER R, Analysis of Fracture Behavior of Laser Beam Welded Wide Plates, *Proc. of European Symposium on Assessment of Power Beam Welds*, Geesthacht, Germany (February 1999).

4 SENOGLES D J, HARRISON P L and CARDINAL N, *Analysis of Wide Plate Behavior of Steel Laser Welds*, *Proc. of European Symposium on Assessment of Power Beam Welds*, Geesthacht, Germany (February 1999).

5 *Laser Welding in Ship Construction – Classification Society Unified Guidelines for the Approval of CO_2-Laser Welding* (1996).

6 *Classification Guidelines for the Approval of Autogenous Laser Welding and Hybrid Laser Welding* (May 2004).

7 GUIDO PETHAN, Meyer Werft, personal communication (January 2008).

8 JENS KEIL, Blohm + Voss, personal communication (January 2008).

9 KARI LAIHO, Aker Yard, Turku, personal communication (January 2008).

10 PETER SEYFFARTH and RAINER GAEDE, The world-first combined system of powerful hybrid fiberlaser and SAW-tandem welding gantry for the shipbuilding industry, *Proc. of 3rd European Conf. on Production Technologies in Shipbuilding*, p. 127, Stralsund, Germany (October 2008).

11 The website of Odense Steel Shipyard, www.oss.dk.

12 MADS ELVANG, Odense Steel Shipyard, personal communication (2006).

9

Industrial robotic application of laser-hybrid and laser-hybrid-tandem welding

H. STAUFER, Fronius International GmbH, Austria

Abstract: The application of a robotic hybrid process in laser-hybrid and laser-hybrid-tandem welding is described. Laser beam welding and GMA welding are long established in welding technology and both processes allow a wide field of application in joining technology. New possibilities and synergetic effects, however, are based on the combination of both processes. Laser radiation causes a very narrow thermally affected zone with a high ratio between welding depth and seam width. For laser welding, the gap bridging ability is very low owing to the small focus diameter, but very high welding speeds can be achieved. The GMA or tandem welding process features a significantly lower energy density, has a larger focused spot on the material surface, and is characterised by its good gap bridging ability.

Key words: robots, laser-hybrid welding, GMAW, tandem welding.

9.1 Introduction

The combination of laser light and arc in one welding process has been known since the 1970s, however, it has not been developed any further.[1,2] This technology was taken up again recently. The current aim is to combine the benefits of the arc with those of the laser in one hybrid welding process.[3,4] At the beginning, the laser beam sources had to prove their suitability for industrial use, now they already form part of the conventional technology employed in the automotive industry.

The combination of laser welding with any other welding process is called the laser-hybrid welding process. This means that both a laser beam and an arc simultaneously act on the welding zone and that they affect and support each other. Here, fantasy knows no bounds. As a recent example, technological examinations of CO_2 laser beam welding with filler wire and in combination with the GMAW process have been carried out.[5]

LaserHybrid (trade name of the company Fronius) welding does not only require a high laser power but also a high beam quality in order to be able to achieve the so-called deep-weld effect.[6]

Thanks to the good beam quality, the CO_2 laser has conquered the area of cutting and will certainly remain there, but it has to be considered that fibre or disc lasers will nowadays have approximately the same beam parameter product. It seems as if the slab laser and the diode-pumped laser were of special interest only for the future, as the CO_2 laser is perfectly suitable for cutting and welding of aluminium owing to the good focusing ability, the high beam quality and the resultant high intensity that can be achieved. However, the use is limited owing to the low jointing cross-section – as a direct consequence of the high intensity – especially in the case of square butt welds on the lap joint. Owing to the fact that Nd:YAG solid lasers with an ever-increasing power are being offered on the market, these are used for welding more frequently. As the solid laser is operated with flexible light cables, they are considerably more advantageous compared to the rigid beam arms used for guiding the CO_2 laser light. A flexible beam manipulation allows welding jobs to be carried out inside passenger compartments, trunks, doors, opening hoods or body front ends.[7] The CO_2 laser, however, is still in demand when it comes to two-dimensional or to simple three-dimensional applications on the outside. The compact high-duty diode laser is starting to establish a market. It is already employed for LaserBrazing (Trade name of company Fronius) and will be able to carry out the first welding jobs for thin sheets before long. However, this makes further development necessary with regards to increasing the power with an optimised focusing of the laser beam, in order to get from high conduction welding to deep penetration welding. Today, the diode laser costs as much (€/kW) as other high-duty lasers, however, the price for this kind of laser will certainly be reduced with the decreasing costs of the diodes.

Up to a power density of 10^6 W cm^{-2} we speak of high conduction welding. If the intensity is increased, the welding depth increases erratically. If the intensity is further increased, the welding depth also increases significantly. A cavity, formed in the workpiece owing to the high power densities, remains open owing to the vapour pressure of the evaporating material. The laser beam profoundly penetrates the workpiece through this cavity and the condensing vapour flows around the cavity, solidifies and forms a slim weld seam.[8] This is an advantage over most of the conventional welding processes where the seam depth is a function of the heat conduction, so that a relatively wide seam with a low welding depth is formed.[9]

9.2 Laser-hybrid process for industrial applications

For the welding of metal workpieces, the Nd:YAG laser beam is focused on intensities above 10^6 W cm^{-2}. As soon as the laser beam impinges on the material surface, the surface is heated on this spot to evaporating

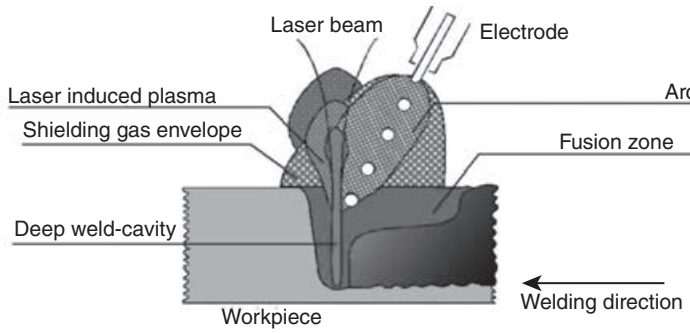

9.1 Schematic representation: laser-hybrid welding.

temperature and, owing to the flowing metal vapour, a cavity forms in the weld metal. The weld seam features a high ratio between depth and width. The energy flow density of the free arc is slightly above 10^4 W cm^{-2}. Fig. 9.1 shows the principle of LaserHybrid welding. The laser beam inputs additional heat to the weld metal in the upper weld region in addition to the arc. In contrast to a series-connected arrangement, hybrid welding is the combination of both welding processes in one process zone. The resultant mutual influence of the processes can have different intensity and characteristics depending on the arc and the laser process used and on the process parameters applied.

Compared with the individual processes the welding depth and the welding speed are increased together with the realisation of the laser process and the arc heat. The metal vapour evaporating from the cavity reacts with the arc plasma. The absorption of the Nd:YAG laser radiation in the working plasma remains negligibly low. Depending on the selected ratio of the powers either the laser or the arc character prevail.

The temperature of the workpiece is a decisive factor for the absorption of laser radiation. To start the laser welding process, it is necessary to overcome the starting reflection – especially in the case of aluminium surfaces. After the evaporating temperature has been reached, the cavity forms so that almost the whole radiation energy can be input into the workpiece. The energy required for this is also determined by the temperature-specific absorption and the energy output owing to the heat conduction in the workpiece. With the LaserHybrid welding not only the workpiece surface evaporates but also the filler wire so that there is more metal vapour available and the input of the laser radiation is facilitated. This also prevents process interruptions. Figure 9.2 shows the metal transfer in case of the LaserHybrid process.

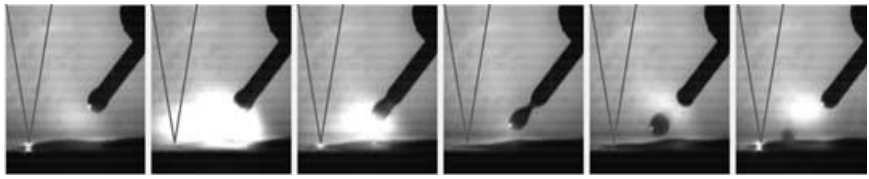

9.2 Metal transfer (background current phase, current rise phase, high current phase, necking, droplet detachment, dipping in molten pool).

9.2.1 Weld seam geometry

To compare the penetration characteristic of laser, MIG and LaserHybrid, it shows that the laser weld seam has weld concavity, while the MIG weld seam has an extreme weld reinforcement and a high weld seam width with the same penetration depth and the same welding speed. In order to be able to achieve the same penetration with the LaserHybrid process, you only need half the wire feed speed, thus 5.5 m min^{-1} instead of the 11 m min^{-1} that would be required for the MIG process. If you once consider the LaserHybrid weld seam, you will notice that a slight weld reinforcement is reached with the same penetration depth.

9.3 Applications and case studies in the automotive industry

The GMA welding process convinces by its high gap bridging ability and the minimum groove preparation required. The benefits of the laser welding can be found in the concentrated heat input, the high welding depths and the high speed. For welding the doors of the Volkswagen Phaeton, the LaserHybrid process is applied in addition to MIG welding and laser welding, Fig. 9.3. One door includes seven MIG seams, 11 laser seams and 48 LaserHybrid seams. The seven MIG seams comprise 380 mm, the 11 laser seams comprise 1030 mm and the 48 hybrid seams are 3570 mm long. The LaserHybrid welding is used for welding the extruded sections, castings and sheets made from aluminium in the doors of the Phaeton. The seams are mainly fillet seams on the lap joint, partially also butt seams.

To be able to meet the rigidity requirements of the doors and to save weight at the same time, it would be necessary to have a tailor-made combination of sheet, casting and extruded material. At different spots, these parts can only be jointed by the LaserHybrid process owing to the required speeds and the tolerances given. Without the hybrid process, VW would have had to use heavy casting material.

(a)

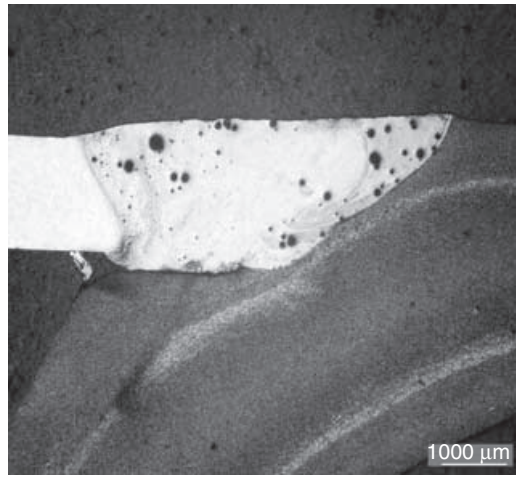

(b)

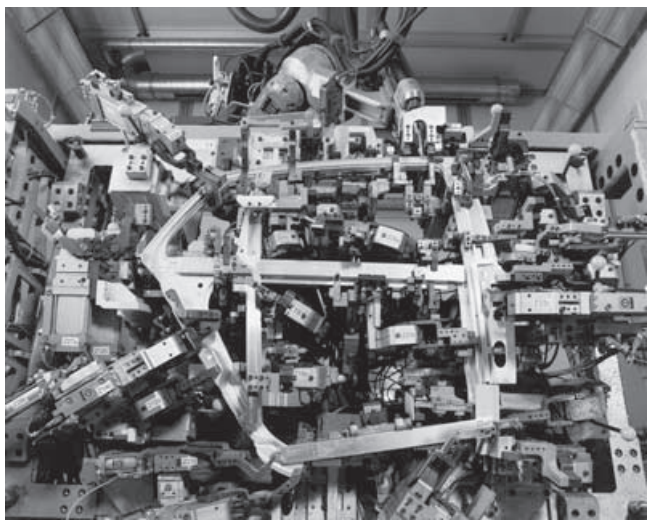

(c)

9.3 Laser-hybrid welded door, macro section and clamping device of the VW Phaeton.

The fact that the hybrid process is not applied to the entire 4980 mm length of weld seams in the Phaeton door, can be put down to the characteristic feature of the respective seams: if the gap width is excessive, the laser of the LaserHybrid process will not be useful either, in this case the pure MIG process is advantageous. Vice versa: for very small gap widths,

the pure laser process with its low heat input and high welding speed can be considered the best possible solution. However, the LaserHybrid process is extremely versatile. By varying the share of laser welding and MIG welding, the process can be adapted to the different welding requirements. This means that it is possible to carry out a pure laser process or a pure MIG process by means of the LaserHybrid system, but one part of the processes would have to be switched off. The speeds can also vary considerably depending on the welding job. For example for a butt weld in the Phaeton door, the range is as follows: speeds between 1.2 and 4.8 m min^{-1} are possible, wire feed speeds of 4–9 m min^{-1} and laser powers on the workpiece of 2–4 kW. The process was finally optimised for a welding speed of 4.2 m min^{-1}, for a wire feed speed of 6.5 m min^{-1} and a laser power of 2.9 kW.

A LaserHybrid system is also employed in the case of the new Audi A8, Fig. 9.4. Each vehicle comprises a total of 4.5 m of weld seams. In the case of the A8, the LaserHybrid welding is used in the area of the lateral roof frame that is equipped with various functional sheets.

(a)

(b)

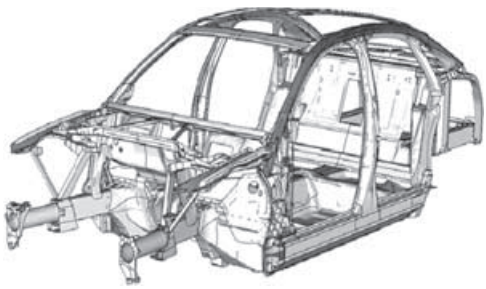

(c)

9.4 Laser beam hybrid welding at Audi: OEM in Ingolstadt applies the process for 4.5 m of weld seams in the roof area of the new A8 and thus achieves higher welding speeds and stronger seams.

(a)

(b)

9.5 Axle component from the Daimler C-Class: welding speed: 4.5 m min^{-1}, wire feed rate: 6.0 m min^{-1}; Courtesy: Steinmetz–Daimler.

9.3.1 LaserHybrid welding at Daimler

For the power train production plant at Daimler in Mettingen it can be said that the features of LaserHybrid welding are a high welding speed, a low heat input and a good fusion penetration. On this industrial application, the welding speed is increased by approximately 30% compared with the GMAW-Tandem process. Furthermore, on the shop floor space is reduced and wire consumption is minimized. Figure 9.5 shows an axle component from Daimler, welded with LaserHybrid.

9.3.2 Further applications in the automotive industry

The following figure gives an impression of a further application of an aluminium panel as case study in the automotive industry. The welding speed in this situation is 4.5 m min^{-1}, while the material thickness is 1.5 mm for each part. Most important in this case, is the good penetration behaviour and the rounded edge of welded seam. Both can be easily achieved by using the LaserHybrid welding process. The high energy density of the laser and the higher diameter of the arc ensures a given cross-section as shown in Fig.

9.6 Application in the automotive industry: side panel in front of the driver's cabin.

Table 9.1 Outstanding performance by using the LaserHybrid process

Welding speed		+30%
Shopfloor space		–50%
Wire consumption		–80%
Shopfloor staff		–30%
Cost reduction on material		up to 7€
Full penetration	→	Reduced number of variants
No quality control needed	→	Absolutely stable process

9.6. Such a welding process has been running for several years in the automotive supplying industry.

Table 9.1 shows the economic advantages of a welded component from the automotive industry.

9.4 Applications in shipbuilding

The high quantum efficiency of the CO_2 laser, which enabled efficiency factors up to 20%, relatively simple technical possibilities for implementation and their scalability are the reasons that this is the most important laser for industrial material machining. CO_2 lasers are characterised by a high power output and offered commercially in capacity ranges up to 50 kW.

With the CO_2 laser (12 kW) from Trumpf Laser technology and Fronius TPS digital power source equipment, the following results are given from Meyer Werft. Jos. L. Meyer GmbH (Papenburg, Germany) is revolutionising shipbuilding using laser technology to improve quality, speed and effi-

ciency, because the only way this manufacturer of the largest cruise ships in the world can hold its place against competition from the Far East, is by leading-edge technology. Laser systems from Schuld Held Lasertechnik and Fronius now play a role in increasing Meyer's technological lead in keeping European shipbuilding on course. These ships are the floating cities of the high seas with up to 4000 inhabitants at one time. On these ships the journey is the destination and the trip is nothing more than being underway. Worldwide, between 2004 and 2007, approximately two dozen ships were built, and currently more than 60 of the giant cruise ships are on order. In the following, the welding process will be described in more detail.

Just as in the automotive industry, shipbuilding tries to reduce material consumption and weight in order to keep operating costs as low as possible. In shipbuilding, they also make use of the technique known as 'tailor-welded blanks', that is, joining panels made of plates of varying thickness as required by the specifications and static calculations of the ship's hull.

The working area on this laboratory set up is 4.5 m × 13 m. Within the clamping device used, it was possible to weld samples with the geometry of 2000 mm × 300 mm. The material used was the shipbuilding steel Grad A, with the usual primer (Lindokote Shopprimer). The welding tests were carried out with a butt joint and fillet joint preparation, in the position PA and PB and without backing support.

The investigation covers the mentioned butt welds with a material thickness up to 15 mm. The Submerged-, the LaserHybrid- and the laser with filler wire processes were compared with each other. The Submerged Arc welding process allows a gap bridging ability from 2 to 5 mm up to a thickness of 12 mm. With the Laser Hybrid process, it is possible to reach a gap bridging ability up to 1 mm for a material thickness up to 15 mm, but the welding speed is three times faster than in comparison to Submerged Arc welding and twice as fast as the laser with filler wire process. With the laser plus filler wire process, it is possible to reach a gap bridging ability up to 0.4 mm and a material thickness up to 15 mm. Four different material thicknesses of 5, 8, 12 and 15 mm were investigated in order to evaluate the maximal welding speed at maximal gap. The influence of the shielding gas helium and argon on the laser–arc welding process was studied by fundamental investigations. A shielding gas which is predominantly He is necessary for welding with high-power CO_2 lasers. Meyer uses a laser hybrid process that the company itself perfected. With the aid of MIG welding, the filler metal and the seam edge are fusion-welded while the focused spot of the laser, which is following directly behind the arc, ensures fusion into the root of the seam by means of deep-penetration welding effect. In this way the laser produces a weld that is as good as a conventional root penetration even though it is processing from just one side and with a very low angle of beam spread.

Stiffening elements required to reinforce the deck are then fillet-welded onto the panels using the same welding procedure and, again, only from one side. During the process, the profiles are welded over the entire thickness of the cross-section.

Meyer has experienced significant benefits from this new installation. The panels no longer have to be machined for the root penetration weld, a process that becomes more and more difficult as the prefabricated blocks and panels get bigger. Welding rates are much higher than pure MIG welding, but also higher than pure laser welding. Because of the deep penetration, the side angle can be reduced to six degrees, which helps to make dramatic reductions in the quantity of extra wire needed compared with conventional welding processes. Reducing the side angle also makes for reductions in the cutting volume when preparing the weld.

Narrowing the area affected by heat also reduces the energy input applied per unit length, resulting in tangible reductions in panel distortion. The distortion in LaserHybrid welding is 0.2 mm min^{-1}, and in submerged arc welding 1.5 mm m^{-1}. This ensures that the welding process can be automated. Moreover, costly and time-intensive reworking is reduced and the assembly of the blocks in the dock simplified. By using a MIG welding source to apply energy in areas near the surface, the laser is available solely for deep penetration welding, for example, for the process is urgently dependent on the laser's qualities. Energy costs are almost halved compared with pure laser welding.

Prefabrication decks are manufactured fully automatically by means of the technology developed by the shipyard. Because of the quality of this welding method it is possible to manufacture 20 times 20 m long sections without turn-over of the panel. There are two butt welding stations installed in the prefabrication area. A plate thickness up to 15 mm can be welded by a welding speed of up to 3.0 m min^{-1}. Further on two fillet welding stations are installed. Stiffeners up to a length of 20 m and a thickness of up to 12 mm for decks and walls are welded. The welding speed that can be achieved is 2.5 m min^{-1}.[8–10]

Table 9.2 shows the comparison between the submerged arc, laser hybrid and laser plus filler wire welding. The speed in laser hybrid welding is three times higher, than in submerged arc welding. One of the disadvantage of the laser hybrid process is that the gap bridging ability is much lower than it is in submerged arc welding.

9.4.1 Equipment for LaserHybrid welding in shipbuilding

At the heart of the system are two butt-joint welding machines for the production of panels and two fillet-joint welding machines with appropriate automation for placement of the reinforcement elements. Whereas the butt

Table 9.2 Comparison of LaserHybrid welding to alternative processes[1]

Process	Submerged arc	LaserHybrid	Laser + filler
Speed	100%	300%	150%
Thickness	<12 mm	<15 mm	<15 mm
Gap	2–5 mm	0–1 mm	0–0.4
Distortion	<1.5 mm m^{-1}	<0.2 mm m^{-1}	<0.1 mm m^{-1}
Metallurgy	Not critical	Not critical	Critical
Fatigue	Good	Excellent	Critical

joint-welding machines join individual plates to form the deck panels, the fillet-joint welding machines equip the panels with reinforcing elements that extend around the ship in a longitudinal direction. Here, for the first time anywhere, butt-welded seams and fillet-welded seams are applied continuously over the full length. The huge fillet-joint welding machine with its length of 29 m has a total weight of about 160 tonne, by far the most ambitious laser system ever built. It also represents a milestone in laser welding technology because it is the first to supply an entire deck panel with reinforcing elements of various shapes, sizes and kinds in a fully automated mode with a manual preparation.

The data loading takes place as a closed processing chain from the CAD program to the machine. The geometry of the deck is transformed into the operating plan, the working sequences along with the appropriate geometrical information are transferred to the lead calculation unit of the machines.

The welding machine contains 27 CNC axes and three hydraulic axes that are controlled by two CNC units. One of the CNC units controls the five handling functions that serve to place and position the reinforcing elements on the panel. The special challenge for control technology here is that these handling units must be perfectly synchronized in order to work together to process reinforcing elements up to 20 m long and that require all five handling procedures for reliable transport. Because the welding head and the handling devices are operated by different controls, it is only by precise synchronization of the movements of the head and each individual handling unit that collisions can be avoided. The welding carriage consists of a positioning head, which is responsible for clamping and orienting of the reinforcing elements.

The LaserHybrid process perfected by Meyer Shipyard offers the following advantages:

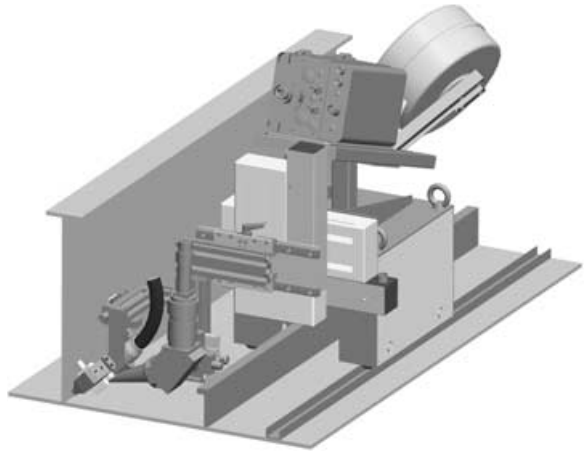

9.7 Welding system of a fillet weld.

- The process is fully automated despite the different configurations of the panels.
- The size of the system and the quality of the welds permit prefabrication of sections as large as 20 m × 20 m without ever having to turn the panel over.

9.4.2 Sensorik

Three sensors are employed for adjustment of the laser and MIG axis in order to position the laser focal point and the MIG torch to an accuracy of +/– 0.1 mm relative to the reinforcing element and the plate. The butt weld machines use a light section sensor to trace the weld deviation or tramping. The axes of the MIG and laser head are subsequently adjusted, in accordance with the sensor signal. Depending on the size of the deviation, the technology parameter records are modified to comply with the programmed functions of this deviation.

Investigations of coupling a 7 kW fibre laser with an arc process shows, that it is possible to weld in a single pass unalloyed and high alloyed steels with a thickness up to 8 mm and more depending on the welding speed. The welding tests were carried out at the LaserHybrid laboratory at the R&D department at Fronius-Wels. Figure 9.8 illustrates the macro section and the lab set up of LaserHybrid in combination with a fiber laser from IPG.

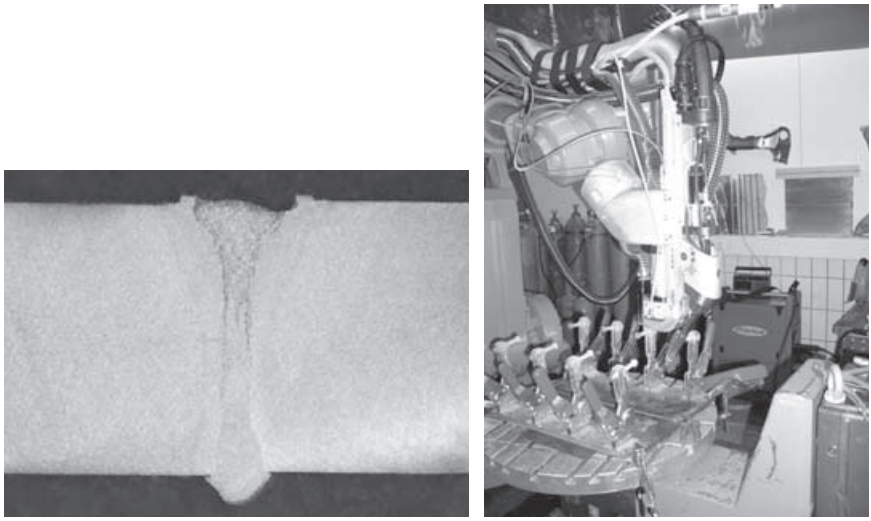

(a) (b)

9.8 LaserHybrid welding with a fibre laser (P_l 6.9 kW, V_s, 2.4 m min^{-1}, s 8 mm, base material S235JR, Filler wire G3Si1)

9.5 Synergies by LaserHybrid

The following benefits can be achieved by combining the arc and the laser beam: Compared with the laser welding process the LaserHybrid process features the following advantages: high gap bridging ability in the case of a gap existing for a short period, wider and deeper penetration, significantly wider range of applications, lower investment costs by saving laser power, and increased toughness. LaserHybrid advantages compared with MIG are higher welding speeds, deeper penetration at higher speeds, lower heat input, higher strength and narrower seam.

By combining the laser beam and the arc a larger molten pool is formed compared with the laser beam welding process. Consequently, components with larger gaps can be welded. The arc welding process is characterised by a low-cost energy source, a good gap bridging ability and a microstructure that can be influenced by the filler material added. The laser beam process features a high penetration depth, a high welding speed, a low thermal load and a narrow seam. In the case of metal workpieces, the laser light produces the so-called deep-weld effect as of a determined beam density, so that components with an increased wall thickness can be welded providing the laser power is sufficient.

LaserHybrid welding therefore allows higher welding speeds, a process stabilisation owing to the interaction between arc and laser light, and a

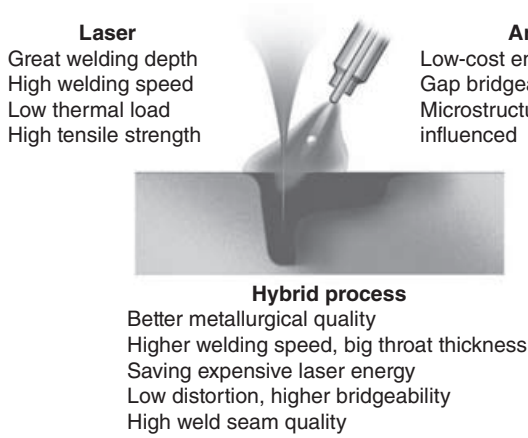

9.9 Advantages of combining the processes.

neutralisation of tolerances. The smaller molten pool compared with the MIG process results in a lower heat input and thus in a smaller heat-affected zone (HAZ), which reduces distortion and consequently the subsequent straightening work. In the event that two separated molten pools are available, the laser-beam-welded area – especially in the case of steel – is tempered owing to the subsequent heat input via the arc and it is also possible to reduce hardness peaks. Figure 9.9 shows a summary of the advantages of combining the processes. The higher welding speeds allow fabrication times and hence fabrication costs to be reduced.

9.6 The laser-hybrid-tandem welding process in the automotive industry

The leading laser beam is used to reach a large penetration depth for a given welding speed, and the trailing tandem process for increasing the gap bridgeability and the throat thickness. One significant aspect of the process as a whole is its high flexibility, for example, three different power outputs can be set, depending on what welding result is desired. In this way, the user can select a suitable power output for the tandem process with reference to the weld-seam geometry, the desired weld overfill and the welding speed. The depth of the root can be adjusted in the course of the bevel preparation, as necessitated by the laser power, focus diameter and welding speed. What is more, two different filler metals, with various different wires, can be used to achieve desired metallurgical effects. The laser beam is set at an approximately rectangular angle to the workpiece. All the other arcs have a leading tilt angle. The principle of laser-hybrid-tandem welding is outlined in Fig. 9.10.

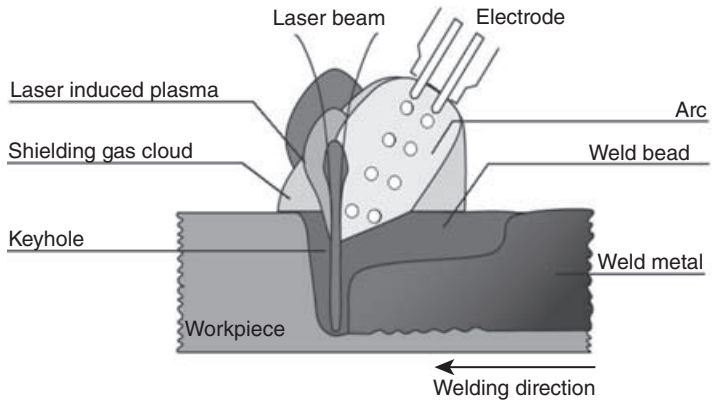

9.10 Schematic outline: laser-hybrid-tandem welding.

9.11 Case study: component from the automotive industry, welding speed 4.2 m min^{-1}.

9.12 LaserTandem welding on a steel component, material thickness 4 mm, welding speed 3.5 m min^{-1}.

With this process it is possible to increase the welding speed in case of steel by 100% in comparison to LaserHybrid welding. Also the gap bridgeability can be increased by about 50%. The LaserTandem (trade name of Fronius) welding process enables separate control of the laser power and the power and the arc length of both arcs. This results in a perfect drop detachment, stable arcs and fewer spatters. High deposition efficiencies and high welding speeds can be achieved. Furthermore, laser-single-wire welding with one arc only is also possible, which may be useful in the case of large gaps if the two electrodes are not guided exactly one after the other, but if there is a lateral displacement of the electrodes from the weld direction. A major advantage of combining processes in this way is that the arc pressure generated as the filler metal melts off does not act on the workpiece and the melt at just one arc root, but is distributed across separate arc roots.

With the LaserTandem process it is possible, especially for industrial applications, to increase not only the welding speed but also the gap bridging ability compared with the conventional laser-single-wire welding. The examples in Fig. 9.11 and Fig. 9.12 show two components from the automotive industry, where higher gaps between the two parts are given.

9.7 Application of LaserTandem welding in the pipeline industry

Currently land and sea pipelines are fabricated using mechanised metal active gas (MAG) welding for the girth welds that join the pipe sections, and a number of arc welding passes are required to complete each joint. In an attempt to control the high cost of pipeline construction and enhance safety through implementation of innovative technology, pipeline owners and operators have been pursuing a number of next-generation pipeline technologies including higher-strength pipeline steels and fittings, multiwire mechanized welding and ultrasonic inspection, advanced coating systems, and alternative integrity-validation processes.

Almost all the work reported in the literature relates to CO_2 laser welding, since high power Nd:YAG lasers are a recent development. The following provides a good indication of the likely response of pipeline steels to Nd:YAG laser welding, since welding speeds and weld size will be similar. Some of the earliest work on high power CO_2 laser welding included an evaluation of welding pipeline steels. In the investigation, an experimental X80 steel of 13 mm thickness was welded, performing autogenous full penetration welds with a power level of 12 kW, at welding speeds of 0.75 m min^{-1} for single-pass welds, and 1.65 m min^{-1} for double-sided welds. They

performed conventional mechanical property tests, and reported good results for strength, ductility, and toughness.[11,12]

The construction cost for a pipeline represents approximately half the total project costs. The welding costs are a major component of the overall construction costs, and industry continues to seek future-generation pipeline welding technologies to achieve additional improvements in productivity and significant cost savings. The economics of pipeline construction are primarily determined by two aspects of the pipeline welding method. The root pass welding speed governs the overall productivity of the pipeline construction spread, and fill pass welding deposition governs the number of welding stations needed to maintain pace with the root pass. Dual-tandem welding pulsed gas metal arc welding is currently considered the most efficient method, as it improves the efficiency of fill and cap processes and lowers welding costs by reducing the number of fill stations required in a pipeline welding spread.

Laser–hybrid welding, whereby one or two arcs and a laser beam are combined in the same molten pool, is attractive for these pipeline steels since this new process has the potential to complete the girth weld in only one or two passes; removing several welding stages in the pipe-laying process and the costs of reducing pipe laying.[13] Hybrid welding processes are also becoming increasingly attractive for more widespread industrial fabrication, since the benefits of each individual process should be obtained when combining the two processes. It is desired that the fast travel speed and deep penetration of the laser weld are retained when combined with the fit-up tolerance, filler addition control and good mechanical properties of the arc process. Already combinations of CO_2 lasers and plasma welding, TIG or MAG welding have been used to obtain good quality welds at fast travel speeds. In this chapter, hybrid welding using a Nd:YAG laser and MAG tandem welding process is described. Generally, it can be said, that the LaserTandem welding process has a very low hydrogen potential and produces significantly lower residual tensile stresses compared with conventional welding methods, the risk of hydrogen-induced cracking is reduced. In addition, rework of the weld joints, normally a manual operation, would be greatly reduced. In this investigation, the pipe was welded without any weld support and in two passes with a very high process stability.

The following investigation shows a 8 mm thick root bead, which can be deposited at a travel speed up to 1 m min^{-1} with a 4 kW Nd:YAG laser, Fig. 9.13. The root pass is welded without backing, while the second layer with three runs has a travel speed of 1.4 m min^{-1}. The material thickness of this sample is 12 mm and the diameter of the pipe has a dimension of 190 mm. The t8/5 time in the root pass was measured with an average value in the root of 10.1 s.

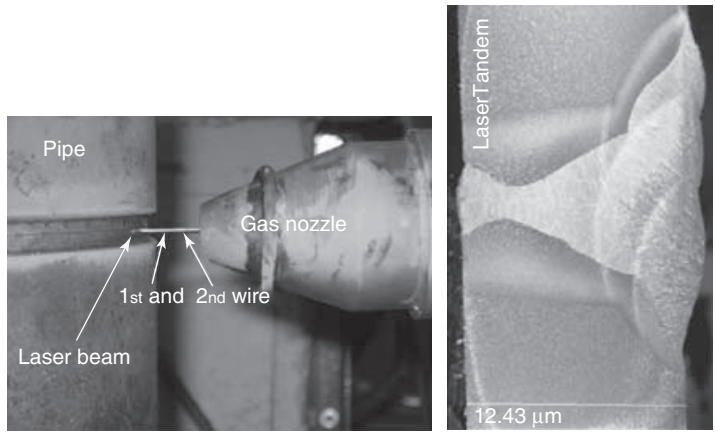

9.13 (a) Welding of a pipe in the position 2G with LaserTandem and (b) macrosection of the welded pipe (Courtesy: Fronius).

9.8 LaserTandem welding system

For the above mentioned investigation, a LaserTandem welding head was developed. The laser beam and the welding wires are located one behind the other. The integrated adjustment device with a meter reading unit allows the first and the second wire to be varied *vis-à-vis* the laser beam in all Cartesian directions.

The geometrical arrangement of the individual components in relation to one another is of central importance. Additional, previously hard-to-imagine advantages and as a result, solution possibilities for a multitude of demanding welding assignments present themselves alongside those of the hybrid process mentioned before. An important boundary condition for the basic research on the use of laser tandem welding process was the development and design of a welding head. The integration of the tandem torch in the experimental set-up along with the laser beam focusing unit had to be considered. The following requirements had to be taken into account in the development and design of the welding head:

- Separate adjustability of the processes on their own
- The design of the welding head has to be modular
- Good accessibility and compact dimensions
- Protection of the optics system by a strong crossjet
- Reproducibility through scaled axial adjustment
- Shielding gas input via the gas nozzle of the tandem torch

The LaserTandem welding head makes it possible to reproducibly position the tandem torch relative to the laser beam. Each wire is connected to

its own wire feed system and power source. The arcs from the tandem process together with the laser beam generate, at closed distance, a shared plasma and molten pool. The LaserTandem equipment combines commercially available laser and newly developed arc welding equipment for resolving a multitude of demanding welding jobs.

The spattering taking place during the joining process leads to increasing soiling of the protective glass. The quartz glass, consisting on both sides of anti-reflection coated material, is intended to protect the laser optical system against damage. Depending on the degree of soiling, the spatter deposits on the glass may stop as much as 10% of the power from reaching the workpiece. If the degree of soiling is more severe than this, this will generally lead to the destruction of the protective glass, as this then absorbs a high proportion of the radiant energy, leading to thermal stresses in the glass. In order to stop all this happening, an integrated cross-jet is used. This is designed to ensure that the welding spatter is deflected by up to 90° and then vacuumed off before it can hit the protective glass. The cross-jet nozzle has been designed in such a way that the jet is discharged with sufficiently increased velocity to obtain a supersonic flow, which enables the welding spatter to be deflected even more effectively. In order to prevent the air flow from the nozzle flowing into the welding zone, it is vacuumed off through an enclosed air exit duct. Another advantage of this is that the processing cell is not soiled by welding fumes and spatter, with the result that work can always take place in a clean environment.

Moreover, the tandem precision torch in the welding system is equipped with a built-in collision protection feature, so that in the event of a crash, neither optical nor mechanical components can be damaged and work can continue without any prolonged downtime. Wire feeders are also part of the high-performance welding systems, in such a way that the wire feeder is used to overcome the resistance in the hose pack. The wire feeder is equipped with a central connection and with a quick-action coupling for the wire.

Both power sources, which are shown in Fig. 9.14 are synchronised and operate in two arcs. Hence, there are two separate welding processes. This also requires two remote controls and balanced inductance on the ground lines is no longer necessary. Furthermore, two wire feeders are used. The synchronisation of the two power sources is again carried out via the so-called Local High Speed Bus.

In the best case, an automatised welding system is completed by a gas nozzle cleaning system that makes use of the time the robot stands still for cleaning the gas nozzle. Conventional systems operate with a mill that remove spatter from the gas nozzle. However, this technique is disadvantageous as the gas nozzle, contact tube and nozzle stock get damaged; furthermore, spatter adheres more easily on the milled spots. Therefore, a touchless gas nozzle cleaning unit was developed, which operates in two

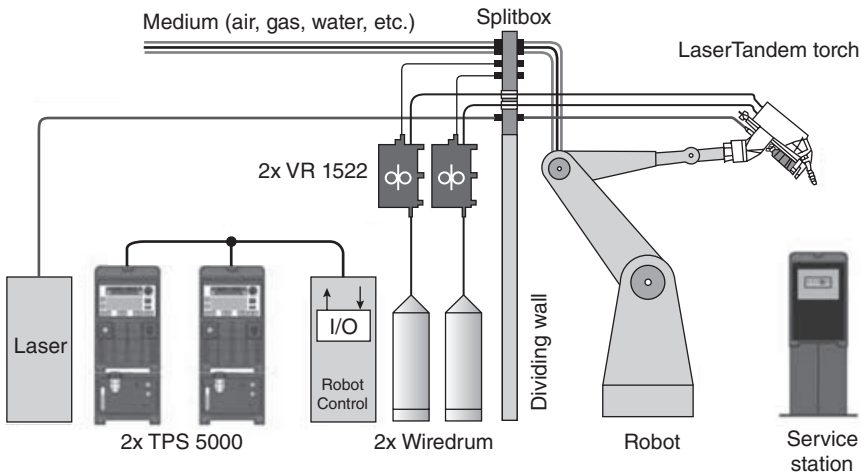

9.14 LaserTandem welding system including laser, power sources, wire feeder, welding head, dividing wall and service station.

steps: first the torch is submerged in a coolant to loosen the spatter ring by thermal tensions. In a second step, the spatter ring is removed electromagnetically. However, there is a certain restriction placed on this process as the gas nozzle cleaning mode is limited to the steel area. In the laser tandem concept, there is also a diving wall foreseen to separate the components that have to be used inside the robot cell from the components that can stay outside the cell. For maintenance of the power source it is not necessary to go inside the welding cell.

9.9 Laser-hybrid welding with three arcs: principles of laser-hybrid-tandem welding process

One significant aspect of the process as a whole is its high flexibility: for example, four different power outputs can be set, depending on what welding result is desired. In this way, the user can select a suitable power output for the tandem process with reference to the weld-seam geometry, the desired weld overfill and the welding speed. What is more, two or three different filler metals, with various different wire diameters, can be used to achieve desired metallurgical effects. The laser beam is set at an angle of 30° to the first following arc. Like all the other arcs, the laser beam has a leading tilt angle. By varying the distance between the first and the second arc, the user can systematically influence the cooling speed of the root. If a high t8/5 time is desired, the arcs must be spaced further apart. The principle of laser-hybrid welding with three arcs is outlined in Fig. 9.15.

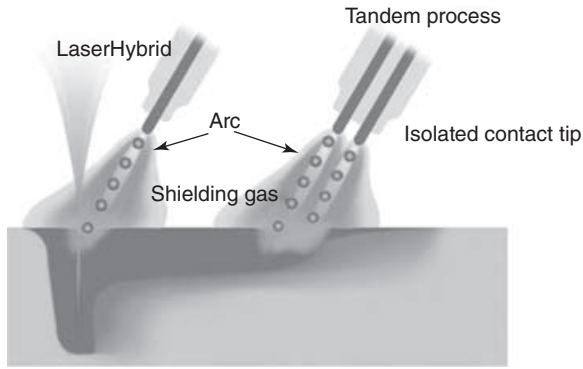

9.15 Schematic outline: LaserHybrid + tandem welding.

9.16 Welding-head system for fabricating thick-walled tubes and pipes.

A major advantage of combining processes in the way mentioned is the reduction of laser power. This welding process is based on the combination of the laser beam and three arcs. Apart from the fact that the first two welding heat sources act in one process zone and the other heat sources are acting in a second process zone.

9.9.1 Test procedure

A 4 kW HL4000D laser from Trumpf Laser was used for the investigations. The specimens were prepared by mechanical milling and butt-welded under

M22 shielding gas to EN 439 with no gap and without any weld-pool backing support. The depth of the root was 3.5 mm and an included angle of 55° was chosen. When optimising the process parameters, a welding speed of 1 m min^{-1} was aimed at. Following this, parameters such as the focal position, the spacing between the laser beam and arcs, the arc power, the stick-out lengths, the depth of the root and the included angle were all optimised at the maximum possible laser power of 4 kW so as to ascertain the maximum possible welding speed. In all the welding trials, t8/5 measurements were performed and documented. The distance between the first two arcs in this investigation was 104 mm. The metal welded was 8 mm thick ALFORM700M® produced by voestalpine Stahl.

9.9.2 Test results

The macro sections of the various specimens can be seen in Fig. 9.3. The left-hand specimen was welded with the laser GMA hybrid process only (root weld). All the other specimens were welded with laser GMA + tandem.

Owing to its short t8/5 cooling times, laser welding makes very demanding requirements in respect of the cold cracking resistance of the HAZ of the base metal. Owing to its low carbon equivalent (CE_{IIW}~0.34), the micro-alloyed and thermomechanically rolled fine-grained ALFORM700M® structural steel grade made by voestalpine Stahl has superb cold cracking resistance and was able to be processed without preheating. Measurement of the t8/5 time on the laser GMA hybrid welded root yielded a value of 2.2 s. The hardness in the Böhler X 70-IG weld metal (Re > 690 N/mm^2) is ~270HV1 in this case, and is only slightly higher than that of the base metal (~265HV1). The minimum hardness in the very narrow hardness dip of the HAZ is ~245HV1. The failure in the root weld in the quasistatic tensile test is located in the non-heat-affected base metal, the yield stress being 717 ± 9 N mm^{-2} and the tensile strength 781 ± 27 N mm^{-2}. A closer look at the laser GMA + tandem weld illustrated in Fig. 9.5, with t8/5 cooling times of up to 14.5 s, shows that a non-critical widening of the hardening dip occurs in the HAZ, the minimum hardness being ~220HV1.

The notch-impact requirements (27 J at –40 °C) in the coarse-grained zone of the HAZ were amply achieved on account of the low carbon equivalent and the titanium and niobium stabilisation of the ALFORM700M® made by voestalpine Stahl. In quasistatic tensile testing, failure in the weld metal starts to occur from a t8/5 time of 13.7 s upwards, the yield stress being 690 ± 2 N mm^{-2} and the tensile strength 727 ± 16 N mm^2. The reason for this is that with t8/5 times from 13.7 s upwards, the hardness of the weld metal used here (~250HV1) is substantially below the hardness of the base metal (~265HV1). Consequently, the filler metal Böhler X 90-IG (Re > 890 N mm^{-2}) may be regarded as the optimum choice for this type of joint.

9.9.3 Synergies

The arc-welding processes are characterised by low-cost energy sources, good gap bridgeability, and the scope they offer for influencing the microstructure by introducing filler metals. The laser-beam process stands out for its great weld penetration depth, high welding speed, low thermal stressing and narrow weld seams. The higher the proportion of the energy input provided by the arcs, the lower the proportion from the laser beam will be. By requiring less laser power, this permits considerable savings to be made in the necessary investment outlays. Quite apart from this factor, it is now for the first time possible to weld thick-walled pipes (with a wall thickness of 8 mm) using a 4 kW solid-state laser. Without this technology, the same welding task would require a laser with an output power of between 6 and 10 kW. The higher welding speed enables both the fabrication times and the manufacturing costs to be reduced. Although this completely novel welding process does necessitate a somewhat greater investment in technical equipment, it offers significantly higher performance and efficiency than the conventional hybrid welding process using only one arc. Investigation of this potential is the object of the collaborative venture currently underway with voestalpine Stahl.[14]

9.10 Conclusions

The synergetic effects achieved by the absolutely new laser-hybrid technology open up a wide field of application in jointing technology, especially where the tolerances of the jointing parts required for laser beam welding cannot be met or can only be met incurring high costs. Thanks to a considerable extension of the field of application and the efficiency of the combined process it is possible to reduce investment costs, fabrication time and fabrication costs as well as to increase productivity. An increase in competitiveness is the result. The design is being offered new possibilities through narrower joint geometries.

The employment of a stable process, however, has only recently been made possible thanks to the availability of the higher output power of the solid laser. Numerous examinations were carried out in the past with basic process information on laser-hybrid welding processes. The laser-hybrid and laser-hybrid-tandem welding processes are combinations of laser beam welding and the arc processes with only one single process zone (plasma and weld pool). By selecting favourable process parameters, seam properties such as geometry and structural constitution can be purposefully influenced. The arc welding processes increases the gap bridging ability owing to the filler material added and determines the seam width and thus

decreases the weld seam preparations. Process efficiency can be considerably increased by the interactions of the processes.

9.11 References

1 MATSUDA, J.; UTSUMI, A.; KATSUMURA, M.; HAMASAKI, M.; NAGATA, S.: TIG or MIG arc augmented laser welding of thick mild steel plate. *Joining & Materials* 1988, 31–34.

2 STEEN *et al.*: Arc-augmented laser welding. *4th Int. Conf. on Advances in Welding Processes*, Paper No. 17 (1978) pp. 257–265.

3 CUI, H.: Untersuchung der Wechselwirkungen zwischen Schweisslichtbogen und fokussiertem Laserstrahl und der Anwendungsmöglichkeiten kombinierter Laser-Lichtbogentechnik. TU Braunschweig, Dissertation, 1991.

4 MAIER, C.; BEERSIEK, J.; NEUENHAHN, K.: Kombiniertes Lichtbogen-Laserstrahl-Schweißverfahren On-line-Prozessüberwachung. DVS 170 (1995) S.45–51.

5 HABERLING, C.: Prozesstechnische Untersuchungen des CO_2-Laserstrahlschweissens mit Zusatzdraht und in Kombination mit dem MIG-Schweissverfahren. Diplomarbeit, RWTH, Lehrstuhl für Lasertechnik, 1994.

6 DAUSINGER, F.: Hohe Prozesssicherheit beim Aluminiumschweissen mit Nd: YAG-Lasern. *Bleche und Profile* **42** (1995) 9, 544–547.

7 TREUSCH, H.-G.; JUNGE, H.: *Laser in der Materialbearbeitung, Schweißen mit Festkörperlasern*, Band 2, VDI-Verlag, 1995.

8 BEYER, E.: *Schweißen mit Laser*: Grundlagen, Springer–Verlag, 1997.

9 STEEN: *Laser Material Processing*, Springer–Verlag, 1996.

10 WEGENER, K.: Shipbuilding experiences a revolution. *Industrial Laser Solutions*, December 2002, 8–12.

11 YAPP, D.; DENNEY, J.; EASTMAN, J.; JOHNSON, M.: Nd:YAG laser welding of high strength pipeline steels, *Pipeline Welding and Technology, Proceedings*, KAWT'99 International Conference on Advances in Welding Technology, Session 5, Paper 5.

12 BREINAN, E.M.; BANAS, C.M.: Preliminary evaluation of laser welding of X80 Arctic pipeline steel. *Welding Research Council Bulletin* **201**, Dec. 1974, 47–57.

13 DILTHEY, U.; WIESCHEMANN, A.: Prospects by combining and coupling laser beam and arc welding processes. *IIW* Doc. XII-1565-99.

14 STAUFER, H.; SCHMARANZER, C.; RAUCH, R.: Laser-MSG-Hybridschweißen mit drei Lichtbögen, ein Hochleistungsschweiß-verfahren zum Fügen von dickwandigen Rohren aus hochfestem Stahl. *GST Essen* 2005, 395.

10

Hybrid laser–arc welding of aluminium

C. THOMY, BIAS – Bremer Institut für angewandte Strahltechnik GmbH, Germany

Abstract: Based on an overview on aluminium properties, applications and state-of-the-art fusion welding processes, specific features of hybrid welding of aluminium are discussed, focusing also on the effect of major process parameters. After briefly reporting recent studies on properties of hybrid welds in aluminium, results of an extended investigation performed on alloy EN AW-6XXX are reported, comparing them with properties of laser welds in the same material. Moreover, case studies on the application of hybrid welding of aluminium in automotive and railway car production are included, before an assessment of potential future trends is attempted.

Key words: hybrid welding, aluminium alloy, laser–arc welding, microstructure, mechanical properties.

10.1 Introduction

In this chapter, the process of hybrid welding of aluminium alloys is discussed. After a short introduction into the properties of aluminium and its alloys as well as into the main areas of application (section 10.2), special challenges characteristic of all fusion welding processes for aluminium alloys (such as hot cracking) as well as state-of-the-art automated welding processes and the potential of hybrid welding are briefly discussed in section 10.3. After a survey of recent research carried out to investigate the hybrid welding process for aluminium alloys, specific features of hybrid welding are discussed with respect to such aspects as heat input and gap bridging (section 10.4). Then, after an overview on the variety of governing parameters that have to be optimised to implement the advantages of hybrid welding for a given application, the effect of major parameters is discussed in detail. In particular, parameters such as type of laser source, laser power, spot size, arc parameters and geometrical parameters (e.g. distance laser–arc) as well as gap are investigated in detail for the case of laser–MIG hybrid welding (section 10.4). Section 10.5 deals with properties of hybrid welds. After briefly reporting recent studies, the focus is on an extended investigation into the properties of laser–MIG hybrid welds in

alloy EN AW-6XXX, comparing them to properties of laser welds in the same material. Moreover, some comments on the properties of laser–MIG hybrid welds in other alloys as well as on properties obtained with other state-of-the-art welding processes are included. In section 10.6, typical applications and application studies from the transportation industries are reported, and requirements associated with these applications are discussed. Potential future trends for development and application will be addressed in section 10.7. All references are given in section 10.8.

10.2 Aluminium and its alloys

For slightly more than 100 years, aluminium has developed from a speciality material to the second most used metal, surpassed only by steel (Ostermann, 1998; Schoer, 2002). This success story started with the development of a process to produce aluminium electrolytically from aluminium oxide (alumina) by C M Hall and P L T Héroult in 1886 (Cock, 1999). This process made aluminium available at a competitive price for the first time. Since then, the annual production of primary and secondary (from scrap) aluminium has increased from slightly more than 5000 tons a year in 1900 to 31 million tons in 1999. It is generally expected that this number will grow at a rate of two to three per cent until 2010 (Cock, 1999).

The reason for this rapid growth in the use of aluminium is to be found in its remarkable properties (Table 10.1, for further data see Ostermann, 1998). In particular, aluminium and its alloys are lightweight, non-magnetic, relatively corrosion-resistant, ductile because of their cubic-face-centred (cfc) structure and can be easily formed and machined (Schulze *et al.*, 1996). This makes them the optimum choice for a wide variety of applications in most major industries (Cock, 1999; Schoer, 2002). As an example, in the transportation industry their low density (only one third of the density of steel) contributes to reducing deadweight and energy consumption whilst increasing load capacity. Consequently, more than 50% of all rolled and extruded aluminium products are used in this industry (Cock, 1999).

Although more than 120 standard wrought and cast alloys are commercially available today, it is relatively easy to get a good overview on their properties, as most of them are binary or ternary systems with the five principal alloying elements copper (Cu), magnesium (Mg), manganese (Mn), silicon (Si) and zinc (Zn). According to DIN EN 573 T3, wrought alloys are then classified as follows (Schulze *et al.*, 1996):

- 1xxx: Al (with Al ≥ 99.00%);
- 2xxx: AlCu(Mg, Pb) alloys;

Table 10.1 Properties of pure aluminium Al99.99 at 20 °C

	Value	Unit
Symbol	Al	
Atomic number	13	
Lattice structure	cfc*	
Lattice constant	0.40496	nm
Density	2.6989×10^{6}	kg m^{-3}
Average linear coefficient of thermal expansion between 20 and 100 °C	23.6×10^{-6}	1/K
Modulus of elasticity	6.66×10^{-4}	MPa
Modulus of shear	2.5×10^{-4}	MPa
Poisson number	0.35	–
Melting temperature	660.2	°C
Heat of fusion	390	kJ kg^{-1}
Heat of evaporation	11.4	MJ kg^{-1}
Specific heat C_p	0.89	kJ kg^{-1}
Electric conductivity	37.67	m Ω^{-1} mm^{-1}
Thermal conductivity	235	W m^{-1} K^{-1}
Magnetic susceptibility	0.62×10^{-9}	m^3 kg^{-1}

* cubic face centred. Source: Schoer (2002) and Ostermann (1998).

- 3xxx: AlMn(Mg) alloys;
- 4xxx: AlSi alloys;
- 5xxx: AlMg(Mn) alloys;
- 6xxx: AlMgSi alloys;
- 7xxx: AlZn(Mg, Cu) alloys;
- 8xxx: Al(Fe, Li, other elements) alloys.

These wrought alloys, which typically come as rolled plates or extruded profiles (Ostermann, 1996), are divided into two main groups: the work hardening alloys EN AW-1xxxx, EN AW-3xxx, EN AW-5xxx and EN AW-8xxx where strength is related to the amount of 'cold work' applied by rolling or forming, and heat treatable or precipitation hardening alloys (EN AW-2xxx, EN AW-6xxx, EN AW-7xxx and EN AW-8xxx). With the latter, strength and other properties can be enhanced by various heat treatment processes. As, depending on the condition of the alloy, the mechanical properties may greatly differ, it is mandatory to give the condition in order to be able to fully compare properties reported. In general, it is possible to distinguish between the conditions:

- annealed (EN AW-XXXX-O);
- tempered (EN AW-XXXX-T) for precipitation hardening alloys;
- work-hardened (EN AW-XXXX-H) for work-hardening alloys.

Table 10.2 Mechanical properties of selected wrought alloys

EN AW-	Yield strength strength $R_{p0,2}$ (MPa)	Ultimate tensile strength R_m (MPa)	Elongation to fracture A_{50} (%)	Vickers hardness HV (–)
2024-T4	330	460	20	125
5052-O	90	195	24	50
5083-O	145	300	22	75
5754-O	100	215	24	55
6005-T4	110	210	16 (A_5)	–
6005-T6	260	285	12 (A_5)	95
6060-T4	90	160	20	55
6060-T6	215	245	12	90
6082-T4	170	260	19	75
6082-T6	310	340	11	100
7075-T6	505	570	10	160

Source: Ostermann (1998).

In order to give all the required information on the condition, further designators are used according to DIN EN 515, of which T4 (solution annealed, quenched and naturally aged) and T6 (solution annealed, quenched and artificially aged) are often encountered in base materials used for fusion welding. Throughout chapter 10, all alloy designations will be in accordance with DIN EN 515, except in cases where the original work of other authors using different designation systems is cited.

Table 10.2 gives an overview of the basic properties of some wrought alloys of the groups EN AW-2XXX, EN AW-5XXX, EN AW-6XXX and EN-AW-7XXX, focusing on those alloys which have already been considered in depth for hybrid welding processes and are of significant industrial relevance especially in the transportation industry. In addition to wrought alloys, which make the basis for the larger part of all semi-finished products, cast alloys are also widely used.

10.3 Fusion welding of aluminium alloys

Fusion welding is one of the key technologies in the production of aluminium parts and structures. As an example, the development of MIG (metal inert gas) welding in combination with the use of extruded profiles from aluminium has enabled the success of modern lightweight structures in rail vehicles (Ostermann, 1998). Other examples where fusion welding of aluminium is used to promote lightweight concepts are the car industry (Dilthey, 2006; Furrer 2007), yacht construction (Aichele, 2003) and the aircraft industries (Vollertsen, 2004).

10.3.1 Effect of the basic properties of aluminium in fusion welding

The physical and chemical properties of aluminium have a great influence on its weldability. Therefore, their effects have to be acknowledged in order to understand the peculiarities associated with all fusion welding processes for aluminium. In particular, the following key points have to be considered (Schulze *et al.*, 1996).

High heat conductivity

The high heat conductivity of aluminium, as shown in Table 10.1, approximately three times the heat conductivity of steel (Ostermann, 1998), requires welding processes with a higher energy density such as plasma, metal inert gas (MIG) or laser beam (LB) welding. The higher the energy density, the less is the loss of strength in the heat-affected zone (HAZ) of wrought alloys (section 10.3.2) and less distortion has to be expected (Schulze *et al.*, 1996).

High coefficient of thermal expansion

The coefficient of thermal expansion of aluminium (Table 10.1) is approximately twice the coefficient of thermal expansion of low-alloy steel (Schulze *et al.*, 1996). In combination with the lower modulus of elasticity, distortion may be significantly higher than with steel.

Surface layer of natural aluminium oxide

Owing to the high affinity of aluminium for oxygen, the surface of aluminium is coated by a natural, chemically and thermally stable and non-conductive oxide layer mainly consisting of Al_2O_3. In fusion welding, this oxide layer is normally not dissolved owing to its high melting point ($T_m = 2050\,°C$) and may therefore contribute to weld defects such as incomplete fusion. To avoid this, it has to be removed completely from the joint zone before welding, preferably by pickling or dry machining, if higher requirements are to be met (Schulze *et al.*, 1996).

Hydrogen solubility of solid and liquid aluminium

Hydrogen is a primary source of porosity in the welding of aluminium, as it is highly soluble in aluminium melt, but not in solid aluminium. Quite typically, the solubility is reduced to one twentieth within the solidification range (Ostermann, 1998). Whereas in slow processes such as casting, the

hydrogen can normally evaporate the solidifying melt, this is often not the case for rapid solidification associated with most fusion welding processes. Therefore, hydrogen is segregated in gaseous form in spherical pores with a typical diameter of 5 to 10 μm (Ostermann, 1998). These pores are regularly distributed in the weld and may be associated with crack initiation, lowering both static and dynamic strength (Beckert, 1997). This makes it desirable to suppress such porosity.

In most cases, hydrogen originates from humidity and organic contaminations on the surface of the base material or the filler wire and, therefore, a cleaning process is often applied before welding (Schulze *et al.*, 1996). Other sources of hydrogen are the hydrogen content in the base or filler material (especially with die-cast aluminium alloys (Schulze *et al.*, 1996)) or incomplete gas shielding resulting in humidity close to the melt pool.

The above key aspects are relevant for all fusion welding processes of aluminium. Moreover, there are some aspects that are of importance only for some processes, e.g., electrical conductivity (Table 10.1) is rather high, reaching approximately 60% of the electrical conductivity of copper. This influences the selection of process parameters in all arc welding processes (Schulze *et al.*, 1996). Another example is the high reflectivity of aluminium for most wavelengths, which is especially relevant for laser beam welding (e.g. Diebold *et al.*, 1984).

10.3.2 Effect of fusion welding on joint properties

Owing to the application of a fusion welding process, the microstructure in the joining zone is significantly affected. Figure 10.1 gives the typical temperature profiles and the resulting microstructural zones in the aluminium alloy. Three regions can be discerned: melt zone (MZ), heat-affected zone (HAZ) and base material (BM). The melt zone or melt pool consists of molten base material or a mixture of molten base material and filler material. Depending on the heat flow conditions (i.e. the temperature gradient), a solidification structure is formed. Typically, this structure consists of dendrites growing against the direction of heat dissipation into the base material. The grains in the melt zone are typically much larger than in the base material and are covered by a thin film of a eutectic phase with lower melting temperature. The MZ and the HAZ are separated by the fusion line, which is determined by the position of the liquidus line (Ostermann, 1998; Schubert, 2003). In the HAZ, the material is subject to temperatures between the melting point and a characteristic lower temperature (approximately 150 °C for aluminium). Close to the fusion line, there is a small zone in which, owing to the high temperatures, a melting of the eutectic at the grain boundaries can occur (partially melted zone (PMZ)) (Kou, 2003). Depending on heat input and heat flow conditions as well as on the base

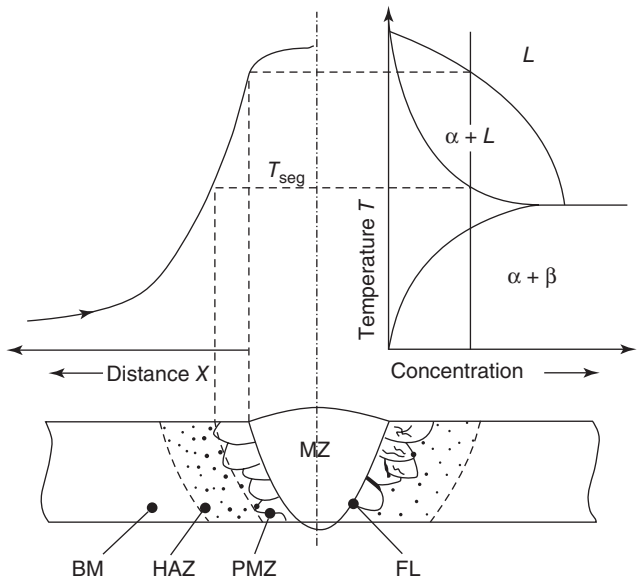

10.1 Schematic illustration of temperature profile, phase diagram and resulting microstructural zones in fusion welding of aluminium alloys: BM base material; HAZ heat-affected zone, PMZ partially melted zone; MZ molten zone; FL fusion line; T_{seg} temperature region for the dissolution of precipitates (Schubert, 2003).

metal alloy and filler material composition, different microstructural changes can occur, which result in differences in the mechanical and technological properties of the joint.

The two most important issues in this context are the reduction of strength due to crystal regeneration, and the susceptibility of some alloys to hot-cracking (solidification cracking). Considering the first aspect, it is necessary to distinguish between work-hardening and heat-treatable alloys. Work-hardening alloys (e.g. EN AW-5XXX) only suffer a deterioration of their properties if a work-hardening process has already been applied. In such a case, depending on the alloy, its condition and the heat input, a reduction of strength down to a minimum equalling the strength of the annealed alloy may occur (Ostermann, 1998). Heat-treatable alloys are also subject to a decrease in strength and hardness in the joint zone (Fig. 10.2). In this case, it is necessary to distinguish between EN AW-6XXX (AlMgSi) and EN AW-7XXX (AlZnMg) alloys. Alloys of the group EN AW-6XXX can only be restored to their properties before welding if they are solution annealed and quenched again, a procedure that, in most cases, may be prohibitive owing to part size and the potentially resulting distortion. Artificial ageing can yield a strength increase up to a strength of 70 to 80% of the base

material, but at the penalty of a reduction in elongation to fracture (Ostermann, 1998). In contrast, e.g. the alloy EN AW-7020 almost reaches its full strength again after a period of 90 days of natural ageing at ambient temperature. This is due to the large temperature region for solution heat treatment (350–500 °C), which makes the welding process a short solution heat treatment with subsequent self-quenching (Ostermann, 1998). However, as for all alloys, the strength decrease also depends on the heat input (more exactly, the time-temperature cycle of the welding process), there is a good opportunity to reduce the strength decrease by minimising heat input and using more concentrated heat sources (Fig. 10.2).

The second problem, the susceptibility of an aluminium alloy to hot-cracking is mainly influenced by its composition, the welding process and its parameters (i.e. heat input and heat flow) as well as the clamping conditions (Ostermann, 1998). Hot cracks are formed during cooling in the interval between solidus and liquidus temperature during the action of residual tensile stresses, if the amount of the eutectic at the grain boundary is insufficient. With increasing solidification interval and increasing residual tensile stresses, the probability of hot-cracking increases. The high coefficient of thermal expansion (Table 10.1) and a significant shrinkage of aluminium alloys promote the occurrence of these residual tensile stresses. This can be influenced by optimising heat input and heat flow e.g. by reducing welding speed to decrease cooling rate and residual tensile stresses. Moreover, the

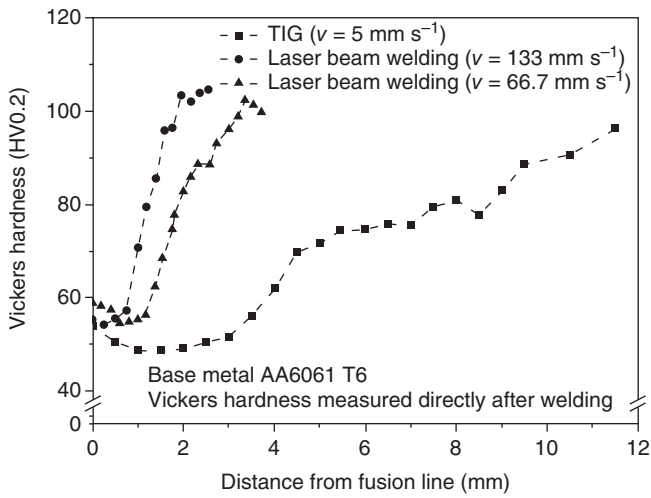

10.2 Hardness distributions in welded specimens of alloy AA 6061 T6 directly after welding for laser beam welding and TIG welding at different welding speeds (Hirose, 1999).

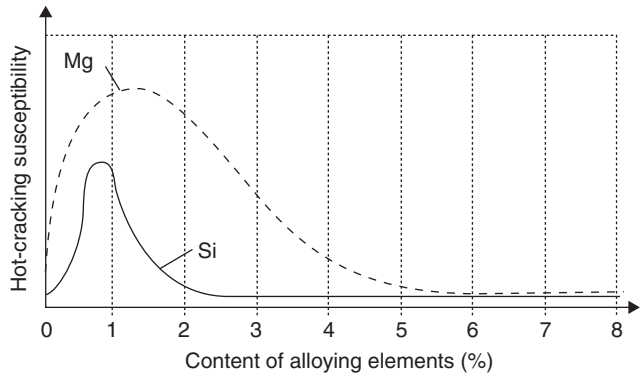

10.3 Hot-cracking susceptibility of EN AW-6XXX alloys depending on the content of Si and Mg (Kou, 2003).

hot-cracking susceptibility depends on the concentration of alloying elements in the melt pool and can be influenced by introducing appropriate filler materials. In particular, the elements silicon and manganese have an influence on the hot-cracking susceptibility (Fig. 10.3). As an example, EN AW-6XXX alloys exhibit the highest hot-cracking susceptibility at a silicon content of approximately 0.75% and of manganese of approximately 1.3% (Kou, 2003). The reason for this behaviour is that the size of the solidification interval and, consequently, the hot-cracking susceptibility are small for small contents of alloying elements. An increase in these contents yields an increase in this solidification interval, in turn increasing the hot-cracking susceptibility of the material. A further increase in Si and Mn contents shifts the ratio between solid and liquid phase (eutectic) during solidification of the melt pool and, using appropriate filler material, may additionally result in the formation of a dendritic solidification structure. This eutectic then provides a sufficient amount of melt to fill the cavities between the solid phases. Moreover, dendritic structures exhibit a high ductility, thus reducing residual stresses during cooling. This further contributes to a reduction of the hot-cracking susceptibility (Kou, 2003; Schubert, 2003).

In summary, the following two main influences govern the properties of aluminium joints.

Heat input and heat flow

Both heat input and heat flow influence the time–temperature cycle during welding, thus influencing the development of the microstructure and the resulting mechanical properties of a given alloy. Consequently, tailoring the

process to optimise the time–temperature cycle has a significant potential to improve joint properties.

Base metal and filler composition

Both base metal and filler material composition as well as heat input and heat flow influence the hot-cracking susceptibility. Consequently, both the appropriate selection of filler materials (e.g. Schulze *et al.*, 1996; Schoer, 2002) as well as an optimisation of the process with respect to the time–temperature cycle may contribute to improved joint properties.

10.3.3 State-of-the-art processes for fusion welding and the potential of hybrid welding

Aluminium and aluminium alloys can be joined by most welding processes (Ostermann, 1998; Johannessen, 1994). For fully automated welding, the following fusion welding methods are most common (Schulze *et al.*, 1996):

- Metal inert gas (MIG), preferably as pulsed MIG welding;
- Tungsten inert gas (TIG) welding;
- Laser beam welding.

Other state-of-the-art fusion welding processes are e.g. plasma MIG and electron beam welding (Johannessen, 1995; Ostermann, 1998). However, these methods have a limited range of use, mostly in connection with the manufacture of special products (Johannessen, 1995). More recently, modified MIG processes such as Cold Arc (Goecke, 2005) or CMT (Bruckner *et al.*, 2004) have been suggested and are increasingly applied industrially. Each of the common methods MIG, TIG and laser beam welding have their specific properties and areas of application. A valuable overview on these and further processes with respect to welding of aluminium is given by Baumann (1999). As MIG welding is used predominately as one of the subprocesses in hybrid welding of aluminium and its alloys, both MIG welding and laser beam welding will be examined more closely in the following. Based on an assessment of their specific advantages and disadvantages, the potentials of a hybrid combination of the two processes are highlighted (Fig. 10.4).

In MIG welding, an electric arc is ignited and maintained between the base material and a wire electrode, which is continuously fed through a welding torch. The wire is molten and transferred in the form of liquid droplets (in case of pulsed arc welding) into the melt pool created in the base material. Considering the advantages of MIG welding for the welding of aluminium alloys (Fig. 10.4), a proven system technology in combination with low investment and operating costs (partly because of a considerable

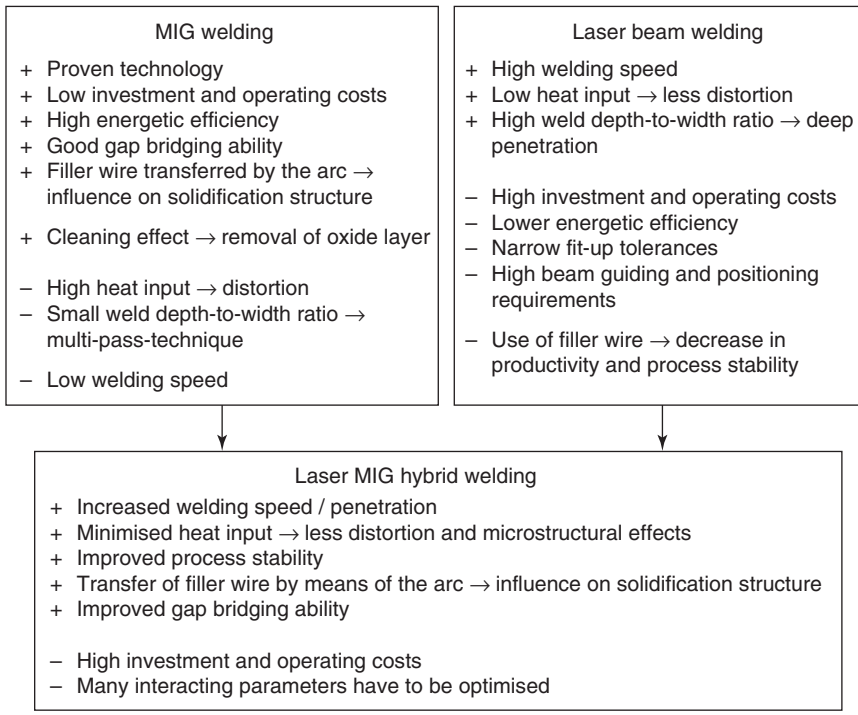
MIG welding
+ Proven technology
+ Low investment and operating costs
+ High energetic efficiency
+ Good gap bridging ability
+ Filler wire transferred by the arc → influence on solidification structure
+ Cleaning effect → removal of oxide layer
– High heat input → distortion
– Small weld depth-to-width ratio → multi-pass-technique
– Low welding speed
Laser beam welding
+ High welding speed
+ Low heat input → less distortion
+ High weld depth-to-width ratio → deep penetration
– High investment and operating costs
– Lower energetic efficiency
– Narrow fit-up tolerances
– High beam guiding and positioning requirements
– Use of filler wire → decrease in productivity and process stability
Laser MIG hybrid welding
+ Increased welding speed / penetration
+ Minimised heat input → less distortion and microstructural effects
+ Improved process stability
+ Transfer of filler wire by means of the arc → influence on solidification structure
+ Improved gap bridging ability
– High investment and operating costs
– Many interacting parameters have to be optimised

10.4 Advantages and disadvantages of MIG welding, laser beam welding and laser MIG hybrid welding of aluminium alloys.

energetic efficiency of up to 80%) are the most striking arguments (Sepold *et al.*, 2003). Among the technological advantages, there are a good gap bridging ability owing to the use of filler wire transferred by means of the arc (Andersen, 2001) as well as the possibility of influencing the solidification structure (by weld metal alloying by the help of the filler wire or by an optimised heat input). Finally, as in all arc welding processes, the so-called cleaning effect contributes to a dissolution of the oxide layer on the aluminium surface, which is beneficial for weld quality. However, these advantages are balanced by some disadvantages such as a relatively high heat input and a low energy density (typically around 10^4 W cm^{-2} (Diebold *et al.*, 1984; Staufer, 2003)), resulting in a small depth-to-width ratio of the weld, a wide HAZ and sometimes remarkable distortion. In particular, the comparably low penetration may require multi-pass welding with special seam preparation for thicker sections. In view of cost, a considerable drawback for MIG welding (as well as for all arc welding techniques) is the relatively low typical welding speed (<2 m min^{-1} (Ueyama *et al.*, 2004; Tong

et al., 2003)). For applications where the pure welding time has a significant impact on the total production time (such as welding of extruded profiles in railway car production (section 10.6)), this is a particular disadvantage (Sepold *et al.*, 2003).

Laser beam welding, on the other hand, is characterised by its high power density focused on a relatively small area. If this power density exceeds approximately 10^6 W cm^{-2}, base metal is evaporated, and a so-called keyhole penetrating deep into the material is formed (e.g. Duley, 1999). This results in a higher depth-to-width ratio of the weld, enables a higher welding speed, and leads to a comparably lower heat input and a smaller HAZ, thus lowering distortion (Thomy *et al.*, 2005a) (Fig. 10.4). Because of these advantages laser beam welding has found numerous industrial applications despite its lower energetic efficiency (less than 30% for modern solid-state lasers and less than 50% for high-power diode lasers (Kohn *et al.*, 2004)) and considerable investment requirements and operating cost. Moreover, the small melt pool requires seam preparation within narrow tolerances and exact beam positioning and guiding to avoid weld imperfections such as lack of fusion or undercuts (Sepold *et al.*, 2003). A particular aspect is the use of filler wire required for various aluminium alloys (section 10.3.2). Aside from process stability issues in laser beam welding with cold wire feeding (Binroth, 1995), the amount of heat used for melting the filler wire is not available for base metal fusion. Thus penetration or welding speed are decreased for a given laser power. A typical decrease in achievable welding speed is around 20% (Shi *et al.*, 2004).

Consequently, the primary aim of introducing laser–arc hybrid welding (as a combination of arc and laser beam in one common process zone) is to overcome the disadvantages associated with arc welding in general and MIG welding in particular as well as with laser beam welding whilst maintaining their respective advantages (Fig. 10.4). For the case of laser MIG hybrid welding, this means that the sub-process MIG welding supplies the filler wire, enlarges the melt pool and thus compensates for poor fit-up tolerances and beam positioning (Petring *et al.*, 2003; Uchiumi *et al.*, 2004), whereas the sub-process laser beam welding increases penetration, welding speed and process stability (Sepold *et al.*, 2003). The overall expectations associated with hybrid welding are an increase in the quality of the weldments by minimising thermal effects such as distortion and microstructural impairment by reducing heat input, and an increase in productivity by increasing welding speed and reducing the amount of rework (straightening) required (Thomy *et al.*, 2004).

However, the high investment and operating costs associated with laser-based processes have to be balanced carefully for each specific application against the potential advantages of hybrid welding (Rasmussen and Dubourg, 1995). Moreover, the problem of optimising a wide variety of

interacting parameters for a given application has to be dealt with (Sepold *et al.*, 2003) (section 10.4.3).

10.4 Hybrid laser–arc welding processes for aluminium alloys

10.4.1 Overview of hybrid welding processes investigated

For an overview of research into hybrid welding in general and parameter effects in hybrid welding of aluminium in particular, the recent review articles of Bagger and Olsen (2005) as well as Rasmussen and Dubourg (1995) should be consulted. Moreover, the PhD thesis of Maier (1999), Hackius (2003), Helten (2003) and Reich (2005) are valuable sources of information. Readers interested in a comparison of hybrid welding with laser, electron beam and arc welding processes are particularly referred to Baumann (1999) for a concise overview on processing conditions and gap bridging.

Table 10.3 includes a fully referenced overview on research work carried out in the field of hybrid welding of aluminium alloys over recent decades. Whereas in the 1980s and early 1990s, only CO_2 lasers were available at sufficient power and therefore the primary laser source for hybrid welding investigations (Diebold and Albright, 1984; Decker *et al.*, 1995; Maier, 1996; Fuerschbach, 1999), interest has shifted more towards solid-state laser systems. Although some work is still carried out using CO_2 lasers (Hackius *et al.*, 2000 and 2001; Vollertsen *et al.*, 2004; Casalino and Lobifaro, 2005; Casalino *et al.*, 2005; Shonin *et al.*, 2006; Casalino, 2007; Dilthey, 2007), approximately 80% of all research work on hybrid welding of aluminium was performed using solid-state laser systems such as the Nd:YAG laser (Aalderink *et al.*, 2007; Allen *et al.*, 2006; Andersen and Jensen, 2001; Anon., 2002; Dilthey *et al.*, 2007; Fuerschbach, 1999; Hu and Richardson, 2006a, 2006b, and 2007; Jasnau *et al.*, 2003; Ji *et al.*, 2007a, 2007b, 2007c, and 2007d; Jokinen *et al.*, 2003; Katayama *et al.*, 2005, 2006a, 2006b, 2006c, 2007a, and 2007b; Kling *et al.*, 2007; Lee and Park, 2003; Ema and Sasabe, 2003; Pinto *et al.*, 2006; Pries *et al.*, 2002; Schilf *et al.*, 2003; Shibata *et al.*, 2006; Thomy and Seefeld, 2005; Thomy *et al.*, 2004a, 2004b, 2005a; Thomy *et al.*, 2005b, and 2008; Traupe *et al.*, 2002; Trommer and Staufer, 2004; Uchiumi *et al.*, 2004; Vaidya *et al.*, 2006; Verwimp *et al.*, 2006; Vewimp and Gedopt, 2007; Vewimp *et al.*, 2007; Vollertsen *et al.*, 2004; Wagner *et al.*, 2006; Wang *et al.*, 2007a and 2007b) and, more recently, the high-power fibre laser (Allen *et al.*, 2006; Kohn *et al.*, 2005; Thomy *et al.*, 2005a; Thomy and Seefeld, 2005b; Thomy *et al.*, 2005b, 2005c, 2005d, 2005e, and 2006; Verhaeghe *et al.*, 2007; Verhaeghe *et al.*, 2007; Vollertsen and Thomy, 2005; Wagner *et al.*, 2006). A particular approach was presented by Ueyama *et al.* (Tong *et al.*, 2003;

Table 10.3 Overview of hybrid welding processes investigated

	Arc source		
Laser source	TIG	MIG	Plasma
CO_2	Diebold and Albright (1984) Decker *et al.* (1995) Hackius *et al.* (2001)	Casalino and Lobifaro (2005) Casalino *et al.* (2005) Casalino (2007) Dilthey *et al.* (2007) Hackius *et al.* (2001) Maier *et al.* (1996) Shonin *et al.* (2006) Vollertsen *et al.* (2004)	Fuerschbach (1999) Hackius *et al.* (2000) Hackius *et al.* (2001)
Nd:YAG	Katayama *et al.* (2005) Katayama *et al.* (2006c) Kling *et al.* (2007) Pries *et al.* (2002)	Aalderink *et al.* (2007) Allen *et al.* (2006) Andersen and Jensen (2001) Dilthey *et al.* (2007) Ema and Sasabe (2003) Fuerschbach (1999) Hu and Richardson (2006a) Hu and Richardson (2006b) Hu and Richardson (2007) Jasnau *et al.* (2003) Ji *et al.* (2007a) Ji *et al.* (2007b) Ji *et al.* (2007c) Ji *et al.* (2007d) Jokinen *et al.* (2003) Katayama *et al.* (2005) Katayama *et al.* (2006a) Katayama *et al.* (2006b) Katayama *et al.* (2006c) Katayama *et al.* (2007a) Katayama *et al.* (2007b) Kling *et al.* (2007) Lee and Park (2003) Pinto *et al.* (2006) Pries *et al.* (2002) Schubert *et al.* (2002) Schilf *et al.* (2003) Shibata *et al.* (2006)	Thomy *et al.* (2008)

Table 10.3 Continued

	Arc source		
Laser source	TIG	MIG	Plasma
		Thomy and Seefeld (2005) Thomy *et al.* (2004a) Thomy *et al.* (2004b) Thomy *et al.* (2005a) Thomy *et al.* (2005b) Thomy *et al.* (2008) Traupe *et al.* (2002) Trommer and Staufer (2004) Uchiumi *et al.* (2004) Vaidya *et al.* (2006) Verwimp *et al.* (2006) Verwimp and Gedopt (2007) Verwimp *et al.* (2007) Vollertsen *et al.* (2004) Wagner *et al.* (2006) Wang *et al.* (2007a) Wang *et al.* (2007b)	
High-power fibre		Allen *et al.* (2006) Kohn *et al.* (2005) Thomy and Seefeld (2005) Thomy *et al.* (2004b) Thomy *et al.* (2005a) Thomy *et al.* (2005b) Thomy *et al.* (2005c) Thomy *et al.* (2005d) Thomy *et al.* (2005e) Verhaeghe (2007) Verhaeghe *et al.* (2007) Vollertsen and Thomy (2005) Wagner *et al.* (2006)	
High-power diode		Löhr *et al.* (2005) Tomita *et al.* (2004) Wang *et al.* (2007b)	

Tomita *et al.*, 2004; Löhr *et al.*, 2005) and investigated by Wang *et al.* (2007a), who are using a defocused high-power diode laser beam. Hybrid welding of aluminium alloys using the disc laser as a laser source was not reported widely so far.

With regard to the arc source, again the situation is quite clear. Whereas more then 80% of the investigations were carried out using a (in most cases pulsed) MIG arc (Aalderink *et al.*, 2007; Allen *et al.*, 2006; Andersen and Jensen, 2001; Anon., 2002; Casalino and Lobifaro, 2005; Casalino *et al.*, 2005b, Casalino, 2007; Dilthey *et al.*, 2007; Ema and Sasabe, 2003; Hackius *et al.*, 2001; Hu and Richardson, 2006a, 2006b, and 2007; Jasnau *et al.*, 2003; Ji *et al.*, 2007a, 2007b, 2007c, and 2007d; Jokinen *et al.*, 2003; Katayama *et al.*, 2005, 2006a, 2006b, 2006c, 2007a, and 2007b; Kling *et al.*, 2007; Kohn *et al.*, 2005; Lee and Park, 2003; Maier *et al.*, 1996; Pinto *et al.*, 2006; Schubert *et al.*, 2002; Schilf *et al.*, 2003; Shibata *et al.*, 2006; Shonin *et al.*, 2006; Thomy and Seefeld, 2005; Thomy *et al.*, 2004a, 2004b, 2005a, 2005b, 2005c, 2005d, and 2005e; Traupe *et al.*, 2002; Trommer and Staufer, 2004; Uchiumi *et al.*, 2004; Vaidya *et al.*, 2006; Verwimp *et al.*, 2006; Verhaeghe *et al.*, 2007; Verwimp and Gedopt, 2007a; Verwimp *et al.*, 2007b; Verhaeghe, 2007; Vollertsen *et al.*, 2004; Vollertsen and Thomy, 2005; Wagner *et al.*, 2006; Wang *et al.*, 2007a and 2007b), a TIG arc was in most cases only used for basic investigations on parameter effects and interactions (Diebold and Albright, 1984; Decker *et al.*, 1995; Hackius *et al.*, 2001; Katayama *et al.*, 2005; Katayama *et al.*, 2006c; Kling *et al.*, 2007) or for other special investigations such as welding of cast aluminium (Decker *et al.*, 1995; Pries *et al.*, 2002; Wiesner *et al.*, 2001; Wiesner *et al.*, 2005). Ueyama *et al.* applied an AC MIG arc in combination with a high-power diode laser (Tomita *et al.*, 2004; Löhr *et al.*, 2005), and some basic investigations were carried out using a plasma arc (Fuerschbach, 1999; Hackius *et al.*, 2000; Hackius *et al.*, 2001; Thomy *et al.*, 2008).

It may be concluded that the state-of-the-art hybrid welding process for aluminium alloys is Nd:YAG laser MIG welding, with a slight trend towards a replacement of the Nd:YAG laser by other types of solid state lasers (such as the high-power fibre laser). Therefore, the following comments and explanations will focus on this process, only briefly commenting on the features of other processes, where appropriate.

10.4.2 Specific features of hybrid welding of aluminium alloys

In the following, a closer look at the specific features associated with the potential advantages and disadvantages of laser MIG hybrid welding (section 10.3.3) is taken. The feasibility of these advantages, which are generally attributed to a synergistic interaction between the two sub-processes combined in one process zone (Sepold *et al.*, 2003; Thomy *et al.*, 2004a), strongly depends on the individual application and its challenges (Rasmussen *et al.*, 2005).

In general, most researchers report an increase in welding speed (e.g. Staufer *et al.*, 2003; Vollertsen *et al.*, 2004; Aichele, 2003; Petring, 2001;

Petring *et al.*, 2003 and Uchiumi *et al.*, 2004). As an example, in butt joining of EN AW-6XXX aluminium extrusions with a thickness of 2 mm, the welding speed was increased from 0.95 m min^{-1} for MIG welding or 3 m min^{-1} for laser beam welding (at a Nd:YAG laser power of 4 kW) to 5 m min^{-1} using hybrid laser arc welding (at a Nd:YAG laser power of only 2 kW) (Sasabe, 2004). In view of improving weld penetration at a given welding speed, typical increases mentioned for common parameter settings are 10 to 20% compared with laser beam welding (Vollertsen *et al.*, 2004) and 20 to 50% compared with MIG welding (Page *et al.*, 2002). However, the recent development of high-power fibre lasers (and potentially, disc lasers) has changed this, and single-pass hybrid welds exceeding a penetration of 8 mm in aluminium alloys as well as welding speeds exceeding 8 m min^{-1} seem now within reach (Thomy *et al.*, 2005a; Vollertsen and Thomy, 2005). One of the reasons for the stability of a welding arc at such high speeds is assumed in an enhancement of the stability of the welding process compared with the use of either of the sub-processes alone. This effect was demonstrated in many studies and attributed to beneficial interactions between the two sub-processes (Page *et al.*, 2002; Petring, 2001; Petring *et al.*, 2003; Schilf *et al.*, 2003; Seyffarth and Krivtsun, 2002; Thomy *et al.*, 2004a and 2008; Vollertsen *et al.*, 2004).

Moreover, for typical applications such as welding of extruded aluminium profiles, the heat input can indeed be drastically reduced (up to 85% compared with MIG welding) for typical applications (Thomy *et al.*, 2004b). Figure 10.5 displays the energy input per volume of molten material for

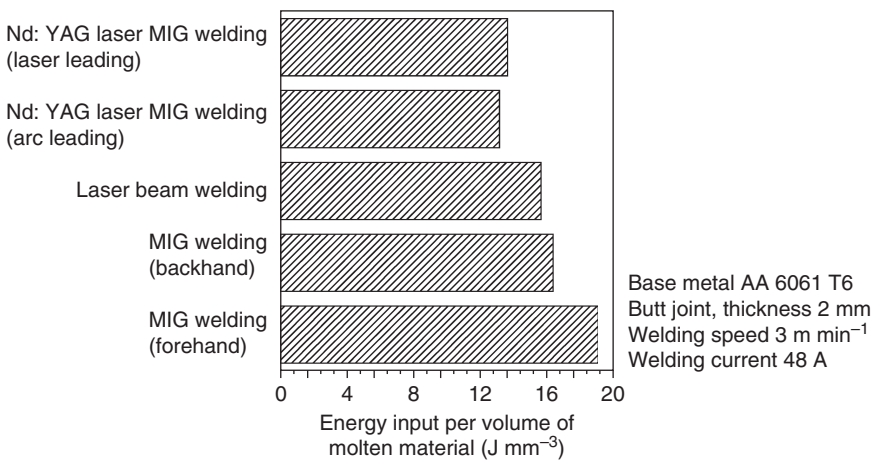

10.5 Energy input per volume of molten material for various welding processes for a given joint configuration and welding speed (Lee and Park, 2003).

laser welding, MIG welding (backhand and forehand) and Nd:YAG laser MIG hybrid welding (laser leading / arc leading). Compared with forehand MIG welding, the input energy per volume of molten material is reduced by about one third, demonstrating a drastic increase in the melting efficiency. For the case of a leading arc, a slightly higher melting efficiency (13.1 J mm^{-3}) than for the case of a leading laser (13.6 J mm^{-3}) is observed. This is explained by Lee and Park (2003) as being due to the cleaning effect of the leading arc and counts among the synergistic effects characteristic for hybrid welding. The overall reduction in heat input is explained by the high energy density and high typical speed of hybrid welding processes (Aichele, 2001; Andersen and Jensen, 2001; Seyffarth and Krivtsun, 2002). As a consequence of lowering the heat input, the distortion of welded components can be significantly decreased (Aichele, 2001; Andersen and Jensen, 2001; Seyffarth and Krivtsun, 2002; Thomy *et al.*, 2004b).

Another feature often demonstrated for hybrid welding of aluminium alloys is the gap bridging potential when using a MIG arc. Since the subprocess MIG welding produces a wider melt pool, hybrid welding generally allows a better gap bridging than laser beam welding (Aalderink *et al.*, 2007; Andersen and Jensen, 2001; Baumann, 1999; Diltehy *et al.*, 2006; Dilthey *et al.*, 2007; Ji *et al.*, 2007a; Löhr *et al.*, 2005; Shibata *et al.*, 2006; Tomita *et al.*, 2004; Tong *et al.*, 2003; Ueyama *et al.*, 2004; Wang *et al.*, 2007b). This, in turn, will mean less effort for clamping, seam preparation and positioning. Depending on the application, gaps up to approximately 50% of sheet thickness can be bridged at an acceptable weld quality (Lee and Park, 2003). Figure 10.6 illustrates this situation for Nd:YAG laser MIG hybrid

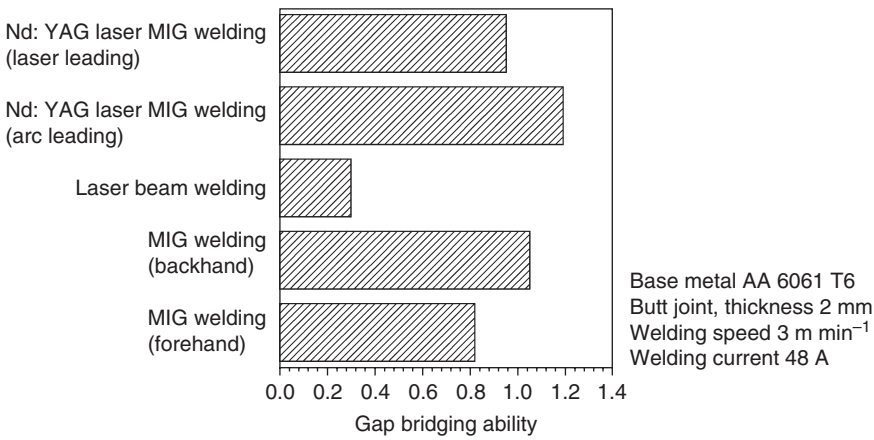
Nd: YAG laser MIG welding (laser leading)
Nd: YAG laser MIG welding (arc leading)
Laser beam welding
MIG welding (backhand)
MIG welding (forehand)
Base metal AA 6061 T6
Butt joint, thickness 2 mm
Welding speed 3 m min−1
Welding current 48 A
0.0 0.2 0.4 0.6 0.8 1.0 1.2 1.4
Gap bridging ability

10.6 Gap bridging ability of various welding processes for given process parameters and joint configuration (Lee and Park, 2003).

welding of alloy AA6061 with a thickness of 2 mm in butt-joint configuration at a welding speed of 3 m min^{-1}. Compared with laser beam welding with a gap bridging potential of around 0.3 mm (provided exact beam positioning relative to the gap is guaranteed), gap bridging is increased by a factor of 4. Depending on the arrangement of the processes, in some cases gap bridging in hybrid welding can even exceed gap bridging for pure MIG welding (Lee and Park, 2003). A gap bridging of around 1 mm for a similar application was also found by Aalderink *et al.* (2007) and Baumann (1999), and for thicker materials of 5 mm by Andersen and Jensen (2001) and Ji *et al.* (2007a). For fillet welds in overlap configuration, gap bridging was also found to be around 1 mm (Shibata *et al.*, 2006). However, for thicker materials in butt joint configuration, where the lower part of the seam is narrower and bears typical characteristics of a laser weld (section 10.6), the relative gap bridging potential is less, and typical gap bridging in industrial production will normally not exceed 1 mm.

Related to the issue of gap bridging is the issue of wire feed misalignment, which is a major challenge in laser beam welding with cold wire (Binroth, 1995; Petring *et al.*, 2003; Uchiumi *et al.*, 2004). Since in laser–MIG hybrid welding the wire is molten by means of the arc, the wire does not have to intersect the laser beam and the small weld pool, which makes the addition of filler material (which is often mandatory in welding of aluminium alloys, section 10.3) significantly easier (Vollertsen *et al.*, 2004).

Finally, from the metallurgical point of view (which will be treated in-depth in section 10.5), the high energy density and high welding speed result in a low heat input and can beneficially influence the microstructure and, as a consequence, the mechanical properties of the welded components.

However, there are also some specific challenges in hybrid welding of aluminium alloys. First, since the molten zone on the weld top is increased by the arc process, the MZ and HAZ are larger in hybrid welding than in laser beam welding (Page *et al.*, 2002). This may cause metallurgical concerns in some alloys and will be looked at more closely in section 10.6. Second, as the melt pool is increased, it may become more difficult to shield the weld surface effectively. In combination with the high melt pool temperatures in hybrid welding, this can result in a higher hydrogen absorption and thus porosity (Rasmussen *et al.*, 2005). Third, volatile alloying elements (such as Mg in EN AW-5XXX alloys) can evaporate from the keyhole, which is normally generated. This can be partially compensated by suitable filler selection (Duley, 1999). Fourth, owing to the low surface tension (see section 10.3), aluminium and its alloys have a poor ability to support the root side of the melt pool, which may lead to difficulties in full penetration welding especially of thicker butt joints (Andersen and Jensen, 2001) and may require special measures such as integrated backings in extruded profiles. Finally – and this is the central challenge – the number of welding

parameters in hybrid welding that cannot be chosen independently because of their interactions is significantly increased compared with MIG or laser beam welding and, together with the metallurgical challenges in fusion welding of aluminium, makes hybrid welding of these alloys one of the most complex processes to design and operate (Sepold *et al.*, 2003). The successful implementation of hybrid laser arc welding requires an understanding of the governing parameters and their effects (Rasmussen *et al.*, 2005) and interactions in order to be able to fully exploit the advantages of hybrid welding and obtain a robust industrial process (Sepold *et al.*, 2003).

10.4.3 Parameters in hybrid welding

Governing parameters

To be able to fully exploit the potential benefits arising from the combination of an arc and a laser beam in a hybrid welding process, a wide variety of parameters have to be understood and optimized (Fig. 10.7). The main parameters significantly influencing the process result can be grouped in process parameters (parameters of the combined process, parameters of the sub-process laser beam welding and parameters of the sub-process arc welding), material parameters and design parameters.

The main parameters of the combined process are welding speed, process gas (quantity, composition, method of delivery) and the relative spatial

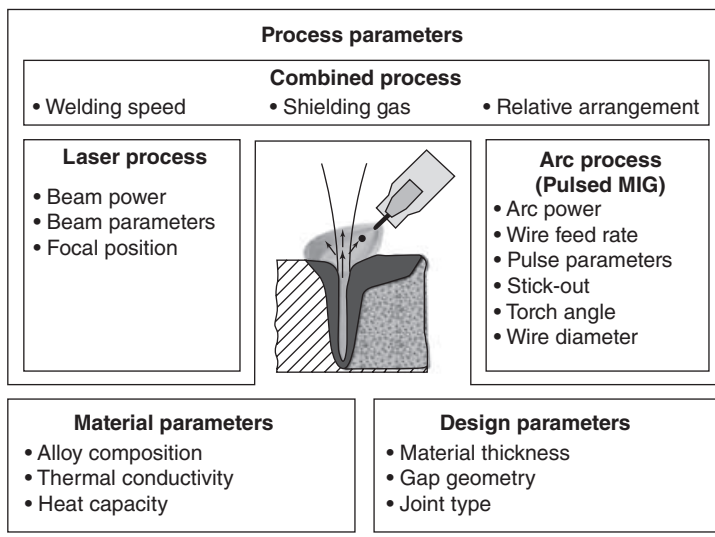

10.7 Governing parameters in Nd:YAG laser MIG hybrid welding (not exhaustive).

arrangement of the two sub-processes. For the latter, angle and distance between laser beam and arc and the welding direction (leading laser vs. leading arc) are of special importance. The sub-process laser beam welding is mainly characterised by the beam power as well as by the beam parameters and the focal position relative to the sheet surface. Among the beam parameters are the wavelength (i.e. type of laser source), the spot diameter and the beam quality. The sub-process arc welding is mostly governed by the arc parameters, in particular by the arc type. In the case of pulsed MIG welding, which is most common in hybrid welding of aluminium alloys, the most important parameters are arc power and wire feed rate as well as pulse parameters such as pulse frequency and pulse duration. Moreover, wire diameter, wire stick-out and torch angle relative to sheet surface are relevant. Considering material parameters, alloy composition and the associated thermophysical properties thermal conductivity and heat capacity are of special importance. Moreover, design parameters such as material thickness, joint type and gap geometry have to be taken into account. However, the central challenge in developing hybrid welding processes for aluminium alloys lies with the process parameters, most of which cannot be chosen independently from each other, as they tend to interact (e.g. Kling *et al.*, 2007; Thomy *et al.*, 2004a; Thomy *et al.*, 2008; Diebold and Albright, 1984). Therefore, the effect of some of the process parameters of hybrid welding will be considered more closely in the following, focusing on Nd:YAG laser MIG hybrid welding.

Effect of parameters of the sub-process laser beam welding

Considering the effect of the parameters of the sub-process laser welding, aside from discussing the effect of the use of various laser sources, research on the effect of laser power (Casalino and Lobifaro, 2005; Casalino, 2007; Decker *et al.*, 1995; Ji *et al.*, 2007a, 2007b and 2007c; Thomy *et al.*, 2004a and 2008; Wang *et al.*, 2007a) and focal position / spot size (Ji *et al.*, 2007a; Jokinen *et al.*, 2003; Löhr *et al.*, 2005; Tong *et al.*, 2003; Ueyama *et al.*, 2004; Wang *et al.*, 2007a) will be reported.

The type of laser source used in laser–arc hybrid welding of aluminium alloys can greatly affect the process. As pointed out above, the CO_2 laser, the high-power diode laser and the solid-state lasers Nd:YAG laser and high-power fibre laser have been investigated for hybrid welding of aluminium alloys so far. Table 10.4 gives an overview on some of the typical properties of commercially available types of these laser sources. Owing to its moderate beam quality, the high-power diode laser currently only provides spot sizes which yield intensities that do not allow stable keyhole welding. The three other laser types are mainly operated in keyhole welding mode

Table 10.4 Properties of laser sources used in hybrid welding of aluminium alloys

Property	Value	Laser source			
		CO_2	Nd:YAG	Fibre	Diode
Wavelength	μm	10.6	1.064	1.070	0.78–0.94
Maximum output power	kW	20	5	20	10
Efficiency	%	10	3–10	>20	35–50
Beam quality	mm × mrad	3–8	15–25	4–12	>50
Spot size	μm	200–600	400–600	200–500	>1000
Keyhole welding	–	+	+	+	–
Beam delivery	–	Mirror	Fibre	Fibre	Fibre

Source: Kohn *et al.* (2004), Rath (2006), Vollertsen and Thomy (2005), Thomy *et al.* (2004b).

for hybrid welding. As the keyhole welding condition is preferred except for very thin parts, high-power diode lasers are not used frequently in hybrid welding.

The major laser source applied for hybrid welding today is the Nd:YAG laser. There are several reasons for this. First, the absorptivity of aluminium strongly depends on the wavelength of the laser beam and is approximately twice for the Nd:YAG-laser compared with the CO_2 laser (Diebold and Albright, 1984), which in turn reduces the intensity required for keyhole welding (Duley, 1999). Second, owing to the wavelength of the Nd:YAG laser, a shielding of the laser beam by the process plasma (arc plasma and laser-induced metal vapour) is not to be expected, as might be the case in hybrid welding with a CO_2 laser. Third, the Nd:YAG laser beam can be delivered by fibres, which greatly increases the processing flexibility compared with a CO_2 laser (Duley, 1999), allowing the use of robot systems. All this also holds true for the high-power fibre laser with its wavelength similar to that of the Nd:YAG laser. The disadvantages of the Nd:YAG laser are its limitations in power and beam quality compared with the CO_2 laser, which can be a drawback especially if thicker materials have to be joined. Moreover, the efficiency is lower. However, the high-power fibre laser can overcome these drawbacks with its high available power and its excellent beam quality and efficiency. A potential alternative to the high-power fibre laser in that respect may also be the disc laser (Rath, 2006). Consequently, owing to their advantages, it is to be expected that the high-power fibre laser and potentially the disc laser will be used increasingly in laser MIG hybrid welding of aluminium alloys.

The power of the laser beam has two main influences. The first influence is, of course, on seam geometry. As soon as the penetration of the laser beam exceeds the penetration of the MIG arc, a characteristic seam with the cross-section shaped like a wine glass is formed, and the penetration expectedly increases with increasing power (Ji *et al.*, 2007a). Moreover, compared with pure MIG welding with otherwise unchanged parameters, the width of the top bead is also slightly increased, which can be attributed to the heat input of the laser beam 'pre-heating' the base material for the arc process (Ji *et al.*, 2007a).

The second influence is related to the characteristic interaction effects associated with hybrid welding. For the case of CO_2 laser TIG hybrid welding of EN AW-5XXX, Diebold *et al.* (1984) as well as Cui (1991) found a sensitive response of the pulsed arc with small variations in laser parameters. Thomy *et al.* (2004a) have demonstrated for the case of Nd:YAG laser MIG welding (pulsed mode) of EN AW-6082 that, with increasing arc power, a slight deviation of the arc occurs at smaller process distances. This resulted in an increase in arc length and, as a consequence, a decrease in pulse current. Therefore, it takes more time to provide the energy to detach the droplet, and, consequently, droplet detachment time relative to the rising edge of the pulse is delayed. This has to be taken into account in developing and optimising power source characteristics for hybrid welding. To further investigate interaction effects in hybrid welding of aluminium alloys, a coaxial Nd:YAG laser plasma hybrid welding head was developed by Thomy *et al.* (2008). When switching on the laser beam in bead-on-plate welding of EN AW-6082 with this welding head, it was observed for most parameter combinations that the seam was stabilized. Whereas the plasma arc without laser beam produced only irregular traces on the aluminium surface, switching on the laser resulted in the formation of a weld bead significantly narrower than the arc traces observed without a laser beam. A typical example for this effect is given in Fig. 10.8. The observation of the arc for a laser power of 0 kW and a laser power of 3 kW revealed that, without laser beam, the arc was relatively wide, with its foot point irregularly moving over the sheet surface. In contrast, for a laser power of 3 kW the arc foot point was more stable, tending to move towards the melt pool generated by the laser process. As a result, the arc zone was significantly constricted. Moreover, depending on the arc current, at a spot size of 0.6 mm at workpiece a significant influence of laser power on arc voltage was observed (for a plasma arc power source with constant current characteristics), Fig. 10.9 and 10.10. For an increase in spot size to 0.8 mm at workpiece, this effect was still observed. However, a further increase to 1.2 mm at workpiece did no longer produce an effect on arc voltage. This may be related to the fact that for this processing condition, no keyhole is formed. Thomy *et al.* (2008) assume

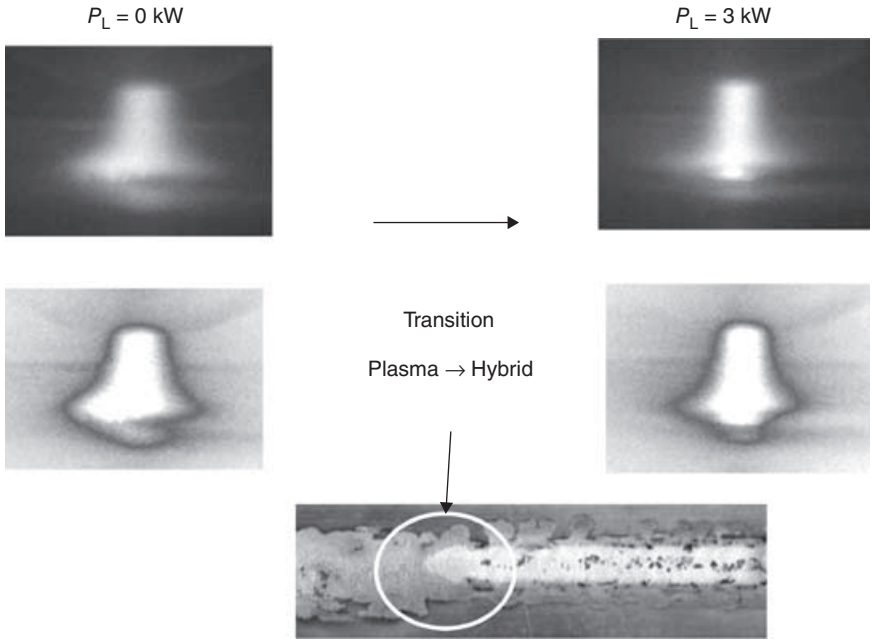

10.8 Example for the effect of laser power P_L on top bead appearance and arc zone geometry in coaxial Nd:YAG laser plasma arc welding of EN AW-6082 (spot size 0.6 mm, current 50 A, bead-on-plate weld) (Thomy *et al.*, 2008).

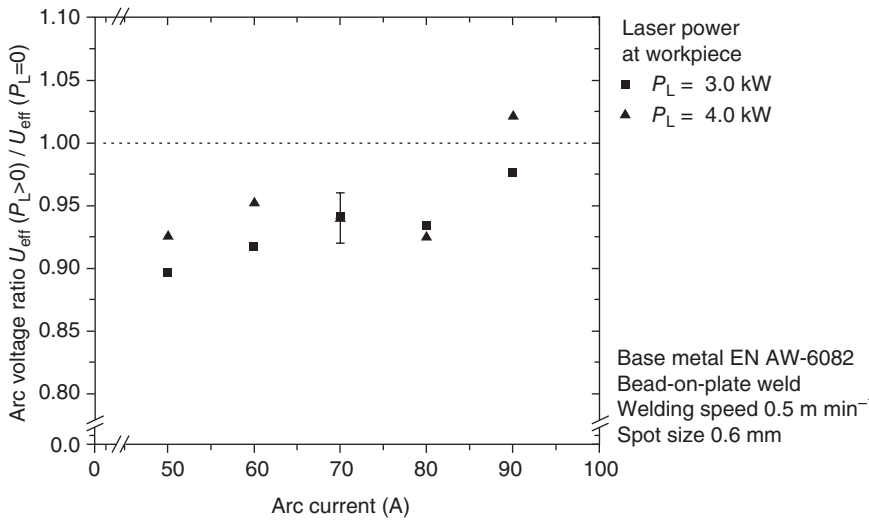

10.9 Effect of arc current and laser power at workpiece on the effective arc voltage ratio in coaxial Nd:YAG laser plasma arc welding of EN AW-6082 (Thomy *et al.*, 2008).

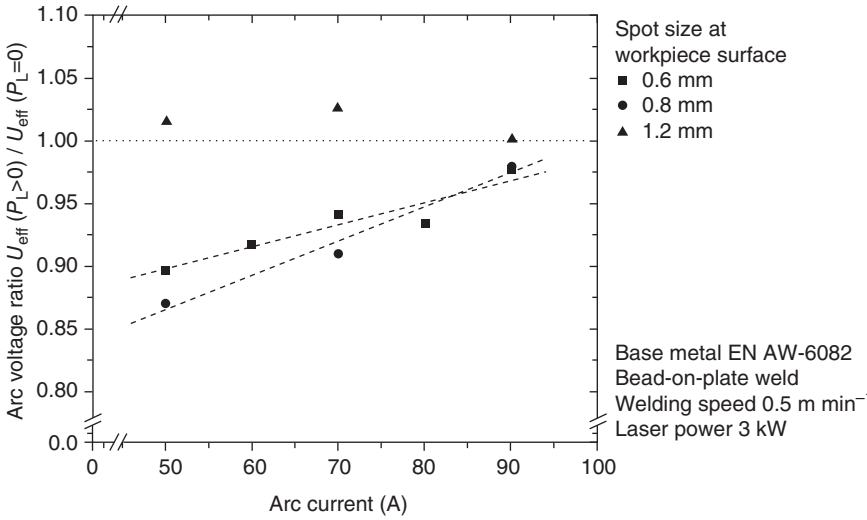

10.10 Effect of arc current and spot diameter at workpiece on the effective arc voltage ratio in coaxial Nd:YAG laser plasma arc welding of EN AW-6082 (Thomy *et al.,* 2008).

that the formation of a significant amount of metal vapour in the process zone over the keyhole is the main factor to explain the reduction of the effective arc voltage ratio. As already very small amounts of metal vapour in an arc plasma can affect plasma properties by providing a component with lower ionisation energy, electrical conductivity and – for constant current characteristics – voltage can be greatly influenced. This was substantiated by the high-speed videos, which showed that the arc zone was more concentrated over the keyhole (Fig. 10.8). However, this effect was less pronounced for a higher arc current, as the relative amount of metal vapour is then lower.

Although there is strong supporting data that in the generally preferred keyhole welding mode e.g. placing the spot at the workpiece surface (Jokinen *et al.*, 2002) or slightly below (Ji *et al.*, 2007a), there is a significant and mostly beneficial effect of the laser beam on the arc, some researchers have also found the application of a diode laser in hybrid welding of thinner aluminium sheets (<2 mm) useful (Tong *et al.*, 2003). They argue that, with an increase of the beam spot diameter an increase in the possible torch aiming deviation is obtained. This improvement is explained by the increase of deposit metal wettability with the increase in spot diameter in their AC arc welding process. Moreover, in conduction mode welding they observed less porosity, which can occur owing to sporadic closure of the keyhole

(Duley, 1999) for inappropriate processing conditions. Even with a large beam diameter >6 mm, a synergistic phenomenon was found, and Tong *et al.* (2003) stated that the laser beam diameter had only little effect on the heat input in conduction condition. Wang *et al.* (2007a) have substantiated this, finding only marginal differences to Nd:YAG laser MIG hybrid welding. Jokinen *et al.* (2003) also found that a smoother weld bead was achieved when the power density was decreased. However, the welding speed was decreased as well (Jokinen *et al.*, 2003).

Effect of parameters of the sub-process arc welding

Considering the effect of the parameters of the sub-process arc welding, work on the effect of arc mode and power (Ji *et al.*, 2007a; Katayama *et al.*, 2005, 2006a, 2006b, 2006c, 2007a, and 2007b; Löhr *et al.*, 2005; Shibata *et al.*, 2006; Uchiumi *et al.*, 2004; Wang *et al.*, 2007a) is reported.

The most common MIG arc mode used in hybrid welding of aluminium alloys is pulsed MIG welding with positive polarity of the electrode. The positive polarity is useful to remove the non-conductive oxide layer on the aluminium base material and gives a more stable arc than negative polarity (Mathers, 2002). Moreover, with the pulsed arc, the average heat input can be reduced, and the metal transfer is usually more defined and regular. Recently, MIG welding in AC mode was also used for hybrid welding of aluminium sheets with a thickness <3 mm (Tong *et al.*, 2003; Ueyama *et al.*, 2004) to further reduce heat input and improve process stability.

The power of the arc has a significant influence on process stability and bead formation. With respect to process stability, excessive arc voltage should be avoided. As Jokinen *et al.* (2002) observed, there is a disturbance of the keyhole for such conditions in Nd:YAG laser MIG hybrid welding. With increasing arc current (and wire feed rate in MIG welding), both seam width and penetration tend to be increased (Ji *et al.*, 2007a; Uchiumi *et al.*, 2004), especially for shallower welds at lower welding speed (Uchiumi *et al.*, 2004), Fig. 10.11. For a small distance between laser and arc (of 2 mm), this effect is nearly independent from welding direction, i.e. whether the laser or the arc is leading (as described in the following subsection). For higher arc current, the melt pool is slightly depressed, which contributes to the increase in penetration (Ji *et al.*, 2007a; Uchiumi *et al.*, 2004) as well as to a reduction in porosity (Uchiumi *et al.*, 2004; Katayama *et al.*, 2006a) (section 10.5.2). The latter is attributed to an improved degassing of the melt pool, as bubbles formed at the keyhole bottom in bead-on-plate welding evaporated more readily before solidification of the melt pool, as the distance to the surface of the melt pool is reduced by the depression (Katayama *et al.*, 2006a; Uchiumi *et al.*, 2004).

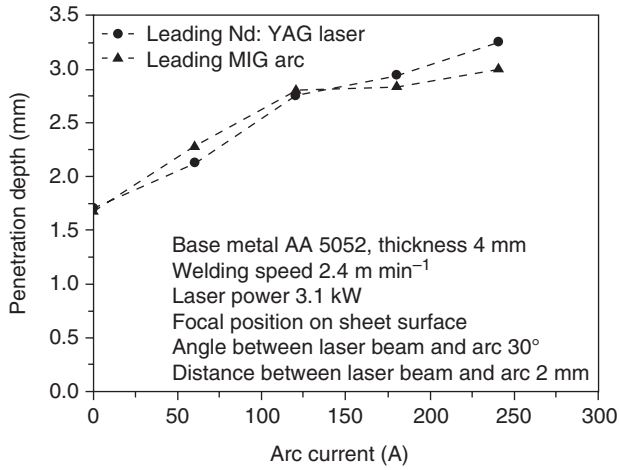

10.11 Effect of arc current on penetration in Nd:YAG laser MIG hybrid welding of aluminium (Uchiumi *et al.,* 2004).

Effect of parameters of the hybrid process

The most significant parameters of the process combination are welding speed (Andersen and Jensen, 2001; Casalino and Lobifaro, 2005; Hu and Richardson, 2006a; Ji *et al.*, 2007c, 2007b, and 2007d; Jokinen *et al.*, 2003; Katayama *et al.*, 2006a; Shibata *et al.*, 2006; Uchiumi *et al.*, 2004; Wang *et al.*, 2007a; Wang *et al.*, 2007b), the relative arrangement of laser beam and arc and welding direction (Casalino and Lobifaro, 2005; Casalino, 2007; Jokinen *et al.*, 2003; Katayama *et al.*, 2006a, 2006b, 2007a, and 2007b; Uchiumi *et al.*, 2004; Wang *et al.*, 2007b) as well as shielding gas composition and flow rate (Schubert *et al.*, 2002).

Most researchers have observed that, contrary to laser beam welding, welding speed can be increased with increasing gap in laser MIG hybrid welding of aluminium alloys (Andersen and Jensen, 2001). However, it is necessary that the gap, which should not be excessive (section 10.4.2), is maintained precisely in order to obtain a sufficient root quality. Moreover, through its influence on heat flow and, consequently, the time–temperature cycle, welding speed also influences microstructure (Ji *et al.*, 2007d; Hu and Richardson, 2006a). As welding speed also influences melt pool dynamics, the formation of process pores can be affected (Jasnau *et al.*, 2003). The latter two aspects will be dealt with in detail in section 10.5.

The relative arrangement of laser beam and arc is of significant importance in laser MIG hybrid welding. In particular, the incidence angle of the laser beam, the relative angle between the laser beam and the arc (torch)

and the distance between laser beam and arc (typically defined as the distance between the laser spot and the projection of the MIG wire on the sheet surface). The incidence angle is normally selected to be perpendicular to the sheet surface or at a slight angle of approx. 5° to avoid potential damage of the optical system owing to back-reflection as a result of the high reflectivity of aluminium alloys (section 10.2). Moreover, the angle of torch and laser beam relative to sheet surface should not be chosen in such a way that potential back-reflection of the laser beam is directed onto the torch, causing potential overheating of the torch and disturbing the arc process (Ueyama *et al.*, 2004) by excessive heating of the wire. The optimum angle between laser beam and arc is generally assumed to be between 20° and 30° (Uchiumi *et al.*, 2004; Petring, 2001), which is also the angle implemented in most industrial systems for Nd:YAG laser MIG hybrid welding. However, if the beam incidence greatly differs from rectangular to sheet surface, other angles between laser beam and arc might be useful (Ueyama *et al.*, 2004).

Katayama *et al.* (Uchiumi *et al.*, 2004; Katayama *et al.*, 2006b) have investigated the effect of laser beam angle and distance between laser and arc on penetration (Fig. 10.12). If the laser beam was leading or tilted by approximately 30° from the surface normal to the welding direction, the highest penetration was observed for a distance of 2 to 4 mm. For a leading MIG arc at rectangular laser beam incidence, the highest penetration was

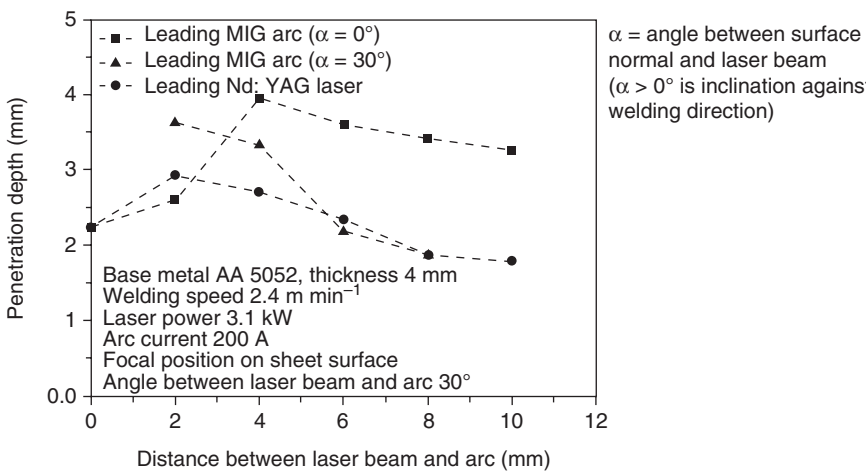

10.12 Effect of the distance between laser beam and arc on penetration in Nd:YAG laser MIG hybrid welding of aluminium (Uchiumi *et al.,* 2004).

observed at a distance of 4 mm. If the coupling between the laser beam and the arc is too close, the arc can disturb the stability of the keyhole, which then decreases penetration (Andersen and Jensen, 2001; Uchiumi *et al.*, 2004; Jokinen *et al.*, 2002; Ishide *et al.*, 2002). On the other hand, if the distance is increased to such an extent that each process has its own melt pool, the penetration also decreases owing to the decrease in synergistic action (Andersen and Jensen, 2001; Uchiumi *et al.*, 2004; Jokinen *et al.*, 2002; Ishide *et al.*, 2002). In particular, Uchiumi *et al.* have demonstrated in bead-on-plate welding in an aluminium sheet of 3 mm thickness that, if the distance between laser beam and arc is increased to more than 4 mm, the penetration again is decreased to the level of autogenous laser welding (Uchiumi *et al.*, 2004). As a consequence, the optimum distance should be between 2 and 4 mm for most applications.

The welding direction or the process leading (laser or arc, Fig. 10.9) does not greatly affect the hybrid process, and for a close coupling with a distance between laser and arc of less than 4 mm, there is virtually no effect on penetration (see Figs 10.11 and 10.12), irrespective of arc current (Uchiumi *et al.*, 2004). However, melting efficiency is slightly affected, as was demonstrated by Lee and Park (2003), Fig. 10.5. With respect to weld quality, Lee and Park (2003) suggest a way to improve dilution (i.e. the mixing of filler material with base material in the melt pool) by using a leading arc in order to allow the laser to import the filler material all around the keyhole. The same authors also found that the porosity level was decreased in the case of leading arc and explained this by the cleaning effect of the arc (Lee and Park, 2003). However, Katayama *et al.* (2006b) have found a decrease in surface quality of the weld for a leading MIG arc. Therefore, it seems that the decision on the welding direction depends on the requirements of the specific application.

Finally, shielding gas is an important issue in hybrid welding of aluminium, as it has a significant effect on arc voltage and stability. Typically, argon-based shielding gases are used. Whereas argon (Ar) tends to stabilise a welding arc owing to its lower breakdown voltage, helium (He) can increase the arc voltage by 20%, thus destabilising the arc but increasing heat input and penetration (Schubert *et al.*, 2002). Moreover, an increase in He-content is also suggested to reduce porosity (Dilthey *et al.*, 2007) (section 10.5.2). Finally, if a CO_2 laser is used, the use of helium may be mandatory in order to avoid a shielding of the laser beam by the process plasma (see the previous subsection) (Ishide *et al.*, 2002).

10.4.4 Conclusions

The following conclusions can be drawn on the present status in process development in hybrid welding of aluminium alloys:

- Nd:YAG laser MIG welding is the current state-of-the-art hybrid welding process.
- The specific advantages demonstrated for Nd:YAG laser MIG hybrid welding are an increase in welding speed and penetration, a stabilisation of the process, a reduction in heat input and distortion compared with pure MIG welding, a gap bridging ability of around 1 mm and an improved tolerance against wire feed misalignment.
- The main challenge in hybrid welding is to optimise the variety of interacting parameters which influence the process result.
- There is a strong influence of the laser beam on the arc which is attributed to metal evaporation in keyhole welding mode.
- The laser beam incidence angle is typically perpendicular or slightly inclined, with a relative angle between laser beam and arc of approximately 30° and a distance between laser beam and arc preferably 4 mm or less.
- In most cases, an Ar-based shielding gas is used.
- Recent developments in industrial lasers (such as the high-power fibre laser or the disc laser) may enhance the application potentials for laser MIG hybrid welding of aluminium alloys.

10.5 Properties of hybrid laser–arc welds

10.5.1 Overview of base materials, joint types and properties investigated

Table 10.5 gives an overview of base materials, joint types and properties investigated. Nearly all investigations were carried out on wrought alloys, the research efforts being nearly equally distributed between alloys from the work hardening group EN AW-5XXX (Aalderink *et al.*, 2007; Andersen and Jensen, 2001; Baumann, 1999; Casalino and Lobifaro, 2005; Casalino, 2007; Diebold and Albright, 1984; Hackius *et al.*, 2000; Hackius *et al.*, 2001; Jasnau *et al.*, 2003; Ji *et al.*, 2007b and 2007c; Jokinen *et al.*, 2003; Katayama *et al.*, 2005, 2006a, 2006b, 2006c, 2007a, and 2007b; Löhr *et al.*, 2005; Maier *et al.*, 1996; Pinto *et al.*, 2006; Schubert *et al.*, 2002; Uchiumi *et al.*, 2004; Wang *et al.*, 2007a; Wang *et al.*, 2007b) and alloys from the heat treatable group EN AW-6XXX (Decker *et al.*, 1995; Diltehy *et al.*, 2006; Dilthey *et al.*, 2007; Ema and Sasabe, 2003; Fuerschbach, 1999; Hackius *et al.*, 2001; Kohn *et al.*, 2005; Lee and Park, 2003; Maier *et al.*, 1996; Petring, 2001; Schubert *et al.*, 2002; Schilf *et al.*, 2003; Shibata *et al.*, 2006; Shonin *et al.*, 2006; Thomy *et al.*, 2004a and 2008; Tomita *et al.*, 2004; Tong *et al.*, 2003; Traupe *et al.*, 2002; Ueyama *et al.*, 2004; Vaidya *et al.*, 2006; Verwimp and Gedopt, 2007; Verwimp *et al.*, 2006 and 2007; Vollertsen *et al.*, 2004; Vollertsen and Thomy, 2005; Wagner *et al.*, 2006; Wiesner *et al.*, 2001; Wiesner

Table 10.5 Overview of base materials, joint types and properties investigated

	References
Alloy	
EN AW-2XXX	Vollertsen *et al.*, 2004
EN AW-5XXX	Aalderink *et al.*, 2007; Andersen and Jensen, 2001; Baumann, 1999; Casalino and Lobifaro, 2005; Casalino, 2007; Diebold and Albright, 1984; Hackius *et al.*, 2000; Hackius *et al.*, 2001; Jasnau *et al.*, 2003; Ji *et al.*, 2007b; Ji *et al.*, 2007c; Jokinen *et al.*, 2003; Katayama *et al.*, 2005; Katayama *et al.*, 2006a; Katayama *et al.*, 2006b; Katayama *et al.*, 2006c; Katayama *et al.*, 2007a; Katayama *et al.*, 2007b; Löhr *et al.*, 2005; Maier *et al.*, 1996; Pinto *et al.*, 2006; Schubert *et al.*, 2002; Uchiumi *et al.*, 2004; Wang *et al.*, 2007a; Wang *et al.*, 2007b
EN AW-6XXX	Decker *et al.*, 1995; Diltehy *et al.*, 2006; Dilthey *et al.*, 2007; Ema and Sasabe, 2003; Fuerschbach, 1999; Hackius *et al.*, 2001; Kohn *et al.*, 2005; Lee and Park, 2003; Maier *et al.*, 1996; Petring, 2001; Schubert *et al.*, 2002; Schilf *et al.*, 2003; Shibata *et al.*, 2006; Shonin *et al.*, 2006; Thomy *et al.*, 2004a; Thomy *et al.*, 2008; Tomita *et al.*, 2004; Tong *et al.*, 2003; Traupe *et al.*, 2002; Ueyama *et al.*, 2004; Vaidya *et al.*, 2006; Verwimp *et al.*, 2006; Verwimp and Gedopt, 2007; Verwimp *et al.*, 2007; Vollertsen *et al.*, 2004; Vollertsen and Thomy, 2005; Wagner *et al.*, 2006; Wiesner *et al.*, 2001; Wiesner *et al.*, 2005
EW AW-7XXX	Allen *et al.*, 2006; Hu and Richardson, 2006a; Hu and Richardson, 2006b; Hu and Richardson, 2007; Verhaeghe, 2007; Verhaeghe *et al.*, 2007
Joint type	
Butt weld	Aalderink *et al.*, 2007; Allen *et al.*, 2006; Andersen and Jensen, 2001; Baumann, 1999; Decker *et al.*, 1995; Diebold and Albright, 1984; Diltehy *et al.*, 2006; Dilthey *et al.*, 2007; Hackius *et al.*, 2000; Hackius *et al.*, 2001; Hu and Richardson, 2006a; Hu and Richardson, 2006b; Hu and Richardson, 2007; Jasnau *et al.*, 2003; Ji *et al.*, 2007a; Ji *et al.*, 2007b; Ji *et al.*, 2007c; Ji *et al.*, 2007d; Jokinen *et al.*, 2003; Kohn *et al.*, 2005; Lee and Park, 2003; Maier *et al.*, 1996; Petring, 2001; Pinto *et al.*, 2006; Schubert *et al.*, 2002; Shonin *et al.*, 2006; Thomy *et al.*, 2004a; Vaidya *et al.*, 2006; Verwimp *et al.*, 2006; Verhaeghe *et al.*, 2007; Verwimp and Gedopt, 2007; Verwimp *et al.*, 2007; Verhaeghe, 2007; Vollertsen *et al.*, 2004; Vollertsen and Thomy, 2005; Wagner *et al.*, 2006; Wiesner *et al.*, 2001; Wiesner *et al.*, 2005
Overlap, fillet weld	Löhr *et al.*, 2005; Schubert *et al.*, 2002; Shibata *et al.*, 2006; Tomita *et al.*, 2004; Tong *et al.*, 2003; Ueyama *et al.*, 2004
Overlap, penetration weld	Dilthey *et al.*, 2006; Shibata *et al.*, 2006
T-joint	Jasnau *et al.*, 2003; Traupe *et al.*, 2002

Table 10.5 Continued

	References
Bead-on-plate weld	Casalino and Lobifaro, 2005; Casalino *et al.*, 2005; Casalino, 2007; Fuerschbach, 1999; Hackius *et al.*, 2000; Hu and Richardson, 2006a; Hu and Richardson, 2006b; Hu and Richardson, 2007; Katayama *et al.*, 2005; Katayama *et al.*, 2006a; Katayama *et al.*, 2006b; Katayama *et al.*, 2006c; Katayama *et al.*, 2007a; Katayama *et al.*, 2007b, Lee and Park, 2003; Schubert *et al.*, 2002; Schilf *et al.*, 2003; Thomy *et al.*, 2004a; Thomy *et al.*, 2008; Tomita *et al.*, 2004; Uchiumi *et al.*, 2004; Wang *et al.*, 2007a
Properties	
Bead appearance and seam geometry	Andersen and Jensen, 2001; Baumann, 1999; Casalino and Lobifaro, 2005; Casalino, 2007; Decker *et al.*, 1995; Diebold and Albright, 1984; Fuerschbach, 1999; Hackius *et al.*, 2000; Hu and Richardson, 2006a; Hu and Richardson, 2006b; Jasnau *et al.*, 2003; Ji *et al.*, 2007a; Jokinen *et al.*, 2003; Katayama *et al.*, 2005; Katayama *et al.*, 2006a; Katayama *et al.*, 2006b; Katayama *et al.*, 2006c; Katayama *et al.*, 2007a; Katayama *et al.*, 2007b; Kohn *et al.*, 2005; Löhr *et al.*, 2005; Maier *et al.*, 1996; Shibata *et al.*, 2006; Thomy *et al.*, 2008; Uchiumi *et al.*, 2004; Vaidya *et al.*, 2006; Verwimp and Gedopt, 2007; Verwimp *et al.*, 2006; Verwimp *et al.*, 2007; Vollertsen and Thomy, 2005; Wagner *et al.*, 2006; Wang *et al.*, 2007b
Porosity and cracking	Allen *et al.*, 2006; Andersen and Jensen, 2001; Decker *et al.*, 1995; Dilthey *et al.*, 2007; Hackius *et al.*, 2000; Hackius *et al.*, 2001; Hu and Richardson, 2006a; Jasnau *et al.*, 2003; Ji *et al.*, 2007b; Ji *et al.*, 2007c; Katayama *et al.*, 2005; Katayama *et al.*, 2006a; Katayama *et al.*, 2006b; Katayama *et al.*, 2006c; Katayama *et al.*, 2007a; Katayama *et al.*, 2007b; Kohn *et al.*, 2005; Uchiumi *et al.*, 2004; Vaidya *et al.*, 2006; Verwimp *et al.*, 2006; Verhaeghe, 2007; Verhaeghe *et al.*, 2007; Verwimp and Gedopt, 2007; Verwimp *et al.*, 2007; Vollertsen and Thomy, 2005; Wagner *et al.*, 2006; Wiesner *et al.*, 2001; Wiesner *et al.*, 2005
Hardness	Allen *et al.*, 2006; Baumann, 1999; Dilthey *et al.*, 2007; Ema and Sasabe, 2003; Hackius *et al.*, 2000; Hackius *et al.*, 2001; Hu and Richardson, 2006a; Hu and Richardson, 2007; Jasnau *et al.*, 2003; Ji *et al.*, 2007d; Maier *et al.*, 1996; Pinto *et al.*, 2006; Vaidya *et al.*, 2006; Verhaeghe, 2007; Verhaeghe *et al.*, 2007; Verwimp and Gedopt, 2007; Verwimp *et al.*, 2006; Verwimp *et al.*, 2007
Strength	Allen *et al.*, 2006; Baumann, 1999; Casalino *et al.*, 2005; Ema and Sasabe, 2003; Hackius *et al.*, 2000; Hu and Richardson, 2007; Jasnau *et al.*, 2003; Maier *et al.*, 1996; Shibata *et al.*, 2006; Vaidya *et al.*, 2006; Verwimp *et al.*, 2006; Verwimp and Gedopt, 2007; Verwimp *et al.*, 2007
Microstructure	Allen *et al.*, 2006; Casalino *et al.*, 2005; Hu and Richardson, 2006a; Hu and Richardson, 2006b; Hu and Richardson, 2007; Ji *et al.*, 2007d; Maier *et al.*, 1996; Pinto *et al.*, 2006; Vaidya *et al.*, 2006
Fatigue	Maier *et al.*, 1996; Traupe *et al.*, 2002; Vaidya *et al.*, 2006; Verwimp and Gedopt, 2007
Residual stresses	Pinto *et al.*, 2006; Shonin *et al.*, 2006
Formability	Hackius *et al.*, 2001

et al., 2005). So far, only minor efforts were dedicated to alloys EN AW-2XXX (Vollertsen *et al.*, 2004) and EN AW-7XXX (Allen *et al.*, 2006; Hu and Richardson, 2006a, 2006b, and 2007; Verhaeghe *et al.*, 2007; Verhaeghe, 2007), although these may be of increasing importance for advanced applications demanding higher strength. A special application is the joining of cast alloys to cast alloys and cast alloys to wrought alloys (Decker *et al.*, 1995; Dilthey *et al.*, 2006; Hackius *et al.*, 2001; Pries *et al.*, 2002; Wiesner *et al.*, 2001 and 2005), which was also given some minor attention, mainly using a CO_2 laser TIG process (Decker *et al.*, 1995; Pries *et al.*, 2002; Wiesner *et al.*, 2001 and 2005).

Considering joint type, a vast majority of work was carried out on butt welds (Aalderink *et al.*, 2007; Allen *et al.*, 2006; Andersen and Jensen, 2001; Baumann, 1999; Decker *et al.*, 1995; Diebold and Albright, 1984; Diltehy *et al.*, 2006 and 2007; Hackius *et al.*, 2000; Hackius *et al.*, 2001; Hu and Richardson, 2006a, 2006b, and 2007; Jasnau *et al.*, 2003; Ji *et al.*, 2007a, 2007b, 2007c, and 2007d; Jokinen *et al.*, 2003; Kohn *et al.*, 2005; Lee and Park, 2003; Maier *et al.*, 1996; Petring, 2001; Pinto *et al.*, 2006; Schubert *et al.*, 2002; Shonin *et al.*, 2006; Thomy *et al.*, 2004a; Vaidya *et al.*, 2006; Verhaeghe, 2007; Verhaeghe *et al.*, 2007; Verwimp *et al.*, 2006 and 2007; Verwimp and Gedopt, 2007a; Vollertsen *et al.*, 2004; Vollertsen and Thomy, 2005; Wagner *et al.*, 2006; Wiesner *et al.*, 2001 and 2005). Overlap configurations, whether as fillet welds (Löhr *et al.*, 2005; Schubert *et al.*, 2002; Shibata *et al.*, 2006; Tomita *et al.*, 2004; Tong *et al.*, 2003; Ueyama *et al.*, 2004) or as penetration welds (Dilthey *et al.*, 2006; Shibata *et al.*, 2006), were only considered by few researchers. The same is true for T-joints (Jasnau *et al.*, 2003; Traupe *et al.*, 2002). Bead-on-plate welds (Casalino and Lobifaro, 2005; Casalino *et al.*, 2005; Casalino, 2007; Fuerschbach, 1999; Hackius *et al.*, 2000; Hu and Richardson, 2006a, 2006b, and 2007; Katayama *et al.*, 2005, 2006a, 2006b, 2006c, 2007a, and 2007b, Lee and Park, 2003; Schubert *et al.*, 2002; Schilf *et al.*, 2003; Thomy *et al.*, 2004a and 2008; Tomita *et al.*, 2004; Uchiumi *et al.*, 2004; Wang *et al.*, 2007a) were considered predominantly by those researchers focusing on basic process investigations, rather than on properties of joints.

The properties most often investigated and commented on are the bead appearance and seam geometry in dependence of process parameters (Andersen and Jensen, 2001; Baumann, 1999; Casalino and Lobifaro, 2005; Casalino, 2007; Decker *et al.*, 1995; Diebold and Albright, 1984; Fuerschbach, 1999; Hackius *et al.*, 2000; Hu and Richardson, 2006a, and 2006b; Jasnau *et al.*, 2003; Ji *et al.*, 2007a; Jokinen *et al.*, 2003; Katayama *et al.*, 2005, 2006a, 2006b, 2006c, 2007a, and 2007b; Kohn *et al.*, 2005; Löhr *et al.*, 2005; Maier *et al.*, 1996; Shibata *et al.*, 2006; Thomy *et al.*, 2008; Uchiumi *et al.*, 2004; Vaidya *et al.*, 2006; Verwimp and Gedopt, 2007; Verwimp *et al.*, 2006 and 2007b; Vollertsen and Thomy, 2005; Wagner *et al.*, 2006; Wang

et al., 2007b), porosity and cracking (Allen *et al.*, 2006; Andersen and Jensen, 2001; Decker *et al.*, 1995; Dilthey *et al.*, 2007; Hackius *et al.*, 2000; Hackius *et al.*, 2001; Hu and Richardson, 2006a; Jasnau *et al.*, 2003; Ji *et al.*, 2007b and 2007c; Katayama *et al.*, 2005, 2006a, 2006b, 2006c, 2007a, and 2007b; Kohn *et al.*, 2005; Uchiumi *et al.*, 2004; Vaidya *et al.*, 2006; Verhaeghe, 2007; Verhaeghe *et al.*, 2007; Verwimp *et al.*, 2006; Verwimp and Gedopt, 2007; Verwimp *et al.*, 2007; Vollertsen and Thomy, 2005; Wagner *et al.*, 2006; Wiesner *et al.*, 2001; Wiesner *et al.*, 2005) and the mechanical properties hardness (Allen *et al.*, 2006; Baumann, 1999; Dilthey *et al.*, 2007; Ema and Sasabe, 2003; Hackius *et al.*, 2000 and 2001; Hu and Richardson, 2006a and 2007; Jasnau *et al.*, 2003; Ji *et al.*, 2007d; Maier *et al.*, 1996; Pinto *et al.*, 2006; Vaidya *et al.*, 2006; Verhaeghe, 2007; Verhaeghe *et al.*, 2007; Verwimp and Gedopt, 2007; Verwimp *et al.*, 2006 and 2007); and strength (Allen *et al.*, 2006; Baumann, 1999; Casalino *et al.*, 2005; Ema and Sasabe, 2003; Hackius *et al.*, 2000; Hu and Richardson, 2007; Jasnau *et al.*, 2003; Maier *et al.*, 1996; Shibata *et al.*, 2006; Vaidya *et al.*, 2006; Verwimp and Gedopt, 2007; Verwimp *et al.*, 2006 and 2007). Data on the microstructure of hybrid welds can be taken from Allen *et al.* (2006), Casalino *et al.* (2005), Hu and Richardson (2006a, 2006b, and 2007), Ji *et al.* (2007d), Maier *et al.* (1996), Pinto *et al.* (2006) and Vaidya *et al.* (2006). Fatigue properties were investigated by Maier *et al.* (1996), Traupe *et al.* (2002), Vaidya *et al.* (2006) and Verwimp and Gedopt (2007). Effects on residual stresses were subject of research work performed by Pinto *et al.* (2006) and Shonin *et al.* (2006). Finally, Hackius *et al.* (2001) presented data on the formability of laser MIG welded joints, using the Erichsen test.

In addition to the above references, the PhD theses of Maier (1999), Hackius (2003), Helten (2003) and Reich (2005) are rich sources of information on mechanical properties of hybrid welds in various aluminium alloys. Readers interested in a comparison of properties of hybrid welds to welds obtained with other processes are specially referred to Baumann (1999) for a concise overview in comparison with laser, electron beam and arc welding processes, to Verwimp and coworkers (Verwimp and Gedopt, 2007; Verwimp *et al.*, 2006 and 2007) for detailed data on hybrid and friction stir welds and to Vaidya *et al.* (2006) for detailed data on hybrid and laser welds.

The following comments will focus on a comprehensive study by Vaidya *et al.* (2006) on Nd:YAG laser MIG hybrid welding in comparison with CO_2 laser beam welding with AlSi12 filler material of the same base material, the latter process being a standard welding process in the aircraft industries today (Vollertsen *et al.*, 2004). The purpose of the work by Vaidya *et al.* (2006) was to verify the feasibility of hybrid welding for butt-joints of the airframe alloy AA6013 T6 (thickness 3.2 mm). Where appropriate, notes on other materials and processes are also included in the following sections.

10.5.2 Visual inspection, macrosections and the issue of porosity

The major obvious difference between a hybrid weld and a laser weld is in the weld appearance (Fig. 10.13). Whereas a laser weld generally shows typical weld ripples on the top side and can have occasional undercuts and spatter, a hybrid weld can be much smoother and shinier (Baumann, 1999; Vaidya *et al.*, 2006) and show less undercut especially in alloys difficult to weld (Hu and Richardson, 2006a). Although the width of the seam and the HAZ in a hybrid weld is typically larger on the top side, at the back side both laser and hybrid welds tend to have a similar width. This is especially true for hybrid welds in thicker materials, as, owing to the characteristics of the heat input of the process, the typical character of a laser weld will prevail in the bottom region of the weld. For systematically assessing the cross-sectional geometry in hybrid welds of aluminium alloys, Ji *et al.* (2007a) suggested a standardised procedure, prescribing which characteristic measures to extract.

Considering porosity, hydrogen-induced pores and process pores have to be distinguished. To achieve a minimum level of hydrogen-induced porosity, it is generally recommended to prepare the surface by dry-machining shortly before welding (Verhaeghe *et al.*, 2007; Verhaeghe, 2007), especially

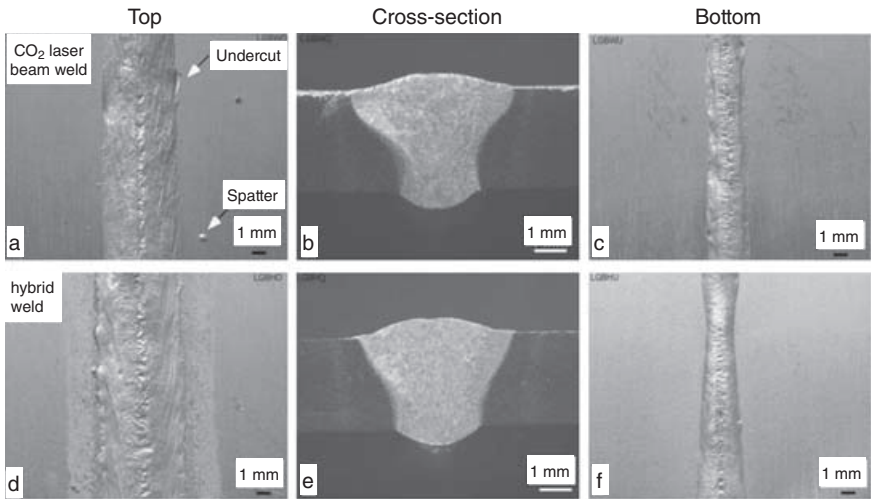

10.13 Surface appearance and cross-section of the CO_2 laser beam weld (upper micrographs; a–c) and the hybrid weld (lower micrographs; d–e) in a 3.2 mm thick AA6013 sheet butt-welded in T6 (Vaidya *et al.*, 2006).

if thicker materials are to be welded. To reduce process pores owing to instabilities in the laser-induced keyhole, Ji and coworkers (Ji *et al.*, 2007b and 2007c) have developed a strategy for parameter selection, suggesting that the laser power should be reduced as far as possible to get small keyhole aspect ratios, thus stabilizing the keyhole; that the MIG power should be increased in order to enlarge the melt pool and facilitate de-gassing of the melt pool by suppressing it by means of the arc pressure; and that the welding speed should be increased for given parameters, reducing welding depth.

Whereas the first three suggestions are in good agreement with the findings of other researchers looking at hybrid welding of thick-section aluminium alloys (Thomy and Seefeld, 2005; Thomy *et al.*, 2004a, 2004b, 2005a, 2005b, 2005c, 2005d, and 2005e; Vollertsen and Thomy, 2005; Wagner *et al.*, 2006) as well as x-ray measurements by Katayama *et al.* (2005, 2006a, 2006b, 2006c, 2007a, and 2007b) demonstrating the mechanisms of pore formation in dependence of process parameters and the spatial arrangement of the sub-processes, the latter seems not to be generally valid. Both Jasnau *et al.* (2003) and Thomy *et al.*, (e.g. Vollertsen and Thomy (2005), Wagner *et al.* (2006)) have demonstrated for wrought alloys with a thickness of 5 mm and above, that a reduction of welding speed will allow for an enlargement of the weld pool and, as a consequence, an improved de-gassing, in turn reducing the number and position of pores in the cross-section. Another suggestion is to tilt the beam incidence angle approximately 30° from the surface normal to the base material against welding direction, which is reported to reduce porosity, but with the disadvantage of impaired bead appearance (Katayama *et al.*, 2006b). Moreover, the selection of special welding positions such as vertical-up (PF) can support de-gassing and further reduce process pores, especially in thicker materials (Verhaeghe, 2007; Verhaeghe *et al.*, 2007). The same was found for the effect of gap condition, with welds with zero gap generally showing a larger amount of porosity at otherwise unchanged process parameters (Andersen and Jensen, 2001). Finally, shielding gas composition can have an effect on process stability and, thus, on porosity, with a higher He-content (75% He, 25% Ar) significantly reducing the number of pores in wrought alloys (Dilthey *et al.*, 2007). For the special application of welding die-cast to die-cast and die-cast to wrought alloys, laser TIG welding was suggested and found to be effective in reducing the number of pores, even without specifically removing the casting skin (Decker *et al.*, 1995; Hackius *et al.*, 2001; Wiesner *et al.*, 2001; Wiesner *et al.*, 2005).

10.5.3 Microstructure and cracking

With the additional heat input from the MIG arc on top during hybrid welding, major changes in microstructure can be expected in this region.

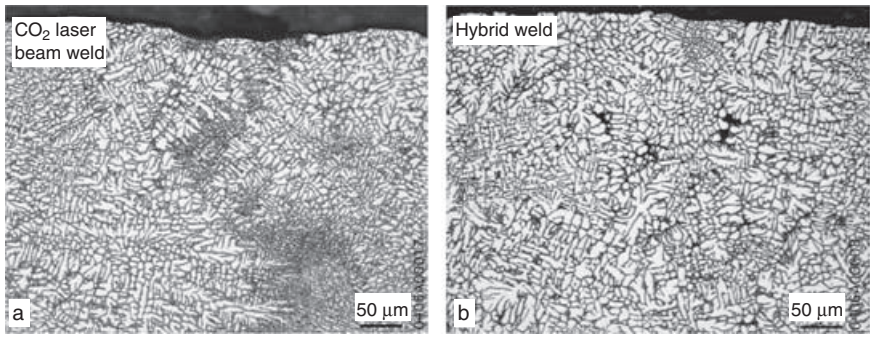

10.14 Difference in the dendritic structure in (a) CO_2 laser beam weld and (b) hybrid weld in a 3.2 mm thick AA6013 sheet butt-welded in T6 in the top centre region of the weld metal (Vaidya *et al.,* 2006).

Figure 10.14 gives an impression of the difference in the dendritic structure in the laser weld and the hybrid weld in the top centre region of the weld metal. In this region, dendrites in the hybrid weld tend to be marginally larger, whereas the other regions in the weld generally show a similar microstructure. A predominately dendritic microstructure is also found by Pinto *et al.* (2006) for EN AW-5XXX. Moreover, in the study of Vaidya *et al.* (2006), for both welds grain boundary liquation was limited to about two grains and did not show any cracking, neither within the fusion zone nor adjacent to the interface 'fusion zone-base material'.

Owing to the characteristic features of the heat source in hybrid welding, the width of the HAZ in a hybrid weld is, as expected, slightly larger, although with a similar microstructure. This was also found by Hu and Richardson (2006a) for EN AW-7XXX T6 alloys. The grain size in the HAZ of hybrid welds in AA6013 T6 tends to be finer and more mixed in the hybrid weld than in the laser weld with filler wire (for the processing conditions investigated by Vaidya *et al.* (2006)), Fig. 10.15. This indicates a generally higher temperature in the hybrid weld; in turn, the pancaked grains (partially recrystallised initially) undergo recrystallisation within the HAZ, which leads to various grain sizes.

As a conclusion, the marginal differences in the cell size in the fusion zone and the change in grain size in HAZ do indicate higher temperatures or slower cooling rates or both in the hybrid weld compared with the laser weld. This assumption is supported by data given by Ji *et al.* (2007d) for EN AW-5083 O, suggesting that a variation of heat input and heat flow can modify grain size and solidification structure in the weld metal significantly. In particular, it was found that, for a given heat input, an increase in the relative share of the heat input from the laser will lead to a refinement of

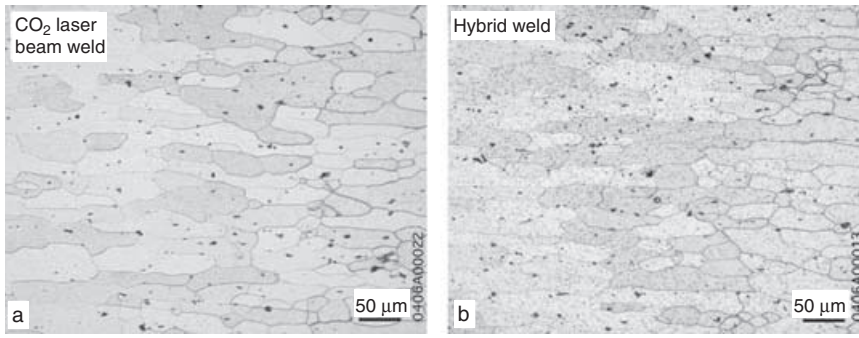

10.15 Change in the microstructure of the heat affected area close to the base material in (a) CO_2 laser beam weld and (b) hybrid weld in a 3.2 mm thick AA6013 sheet butt-welded in T6 (Vaidya *et al.,* 2006).

the grain size. For alloys of group EN AW-6XXX, this suggests that the grain refinement may result in a suppression of hot-cracking.

10.5.4 Hardness

As in all welding processes for aluminium, hardness in general and microhardness in particular is significantly affected, depending on the temper of the base metal alloys as well as on the composition of the filler material. Figure 10.16 gives the microhardness measurements for laser and laser MIG hybrid welds in AA6013 T6 (Vaidya *et al.*, 2006) taken along a trace across the weld in three locations (on specimens polished to metallographic quality): top, section and bottom (Fig. 10.13). The microhardness profiles are symmetrical to the weld centreline, and there is a drop in hardness, which is slightly larger for the hybrid weld. This drop in hardness is quite typical for aluminium alloys welded in the peak aged condition, whereby in addition to the dissolution and overageing of precipitates in HAZ, the filler wire used (AlSi12) causes dilution and change in the chemical composition of the fusion zone. Except for the difference in the width of the hardness drop, the hardness itself is similar in the fusion zone and in HAZ in both welds. In the base material, the top and the bottom exhibited similar curves, both in the trend and in the values. It is only in the cross-section of both the laser and the hybrid weld that the hardness level is decreased, and the decrease is more pronounced in the hybrid weld than in the laser weld. Here, two critical sites can be identified; the centre of the fusion zone and the HAZ. The softening in the HAZ should support that the temperature in the hybrid weld should have been higher and there was heat stagnation over the thickness for the given processing conditions. This was also found

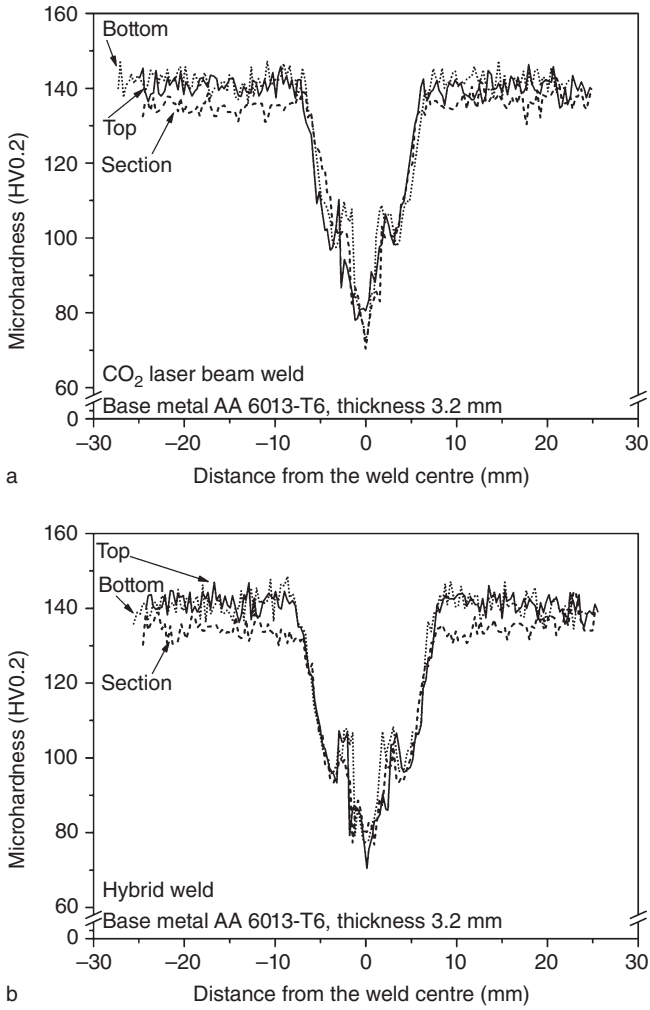

10.16 Microhardness gradient in (a) CO_2 laser beam weld and (b) hybrid weld in a 3.2 mm thick AA6013 sheet butt-welded in T6 (Vaidya *et al.,* 2006).

by other researchers, e.g. Hackius *et al.* (2001), Maier *et al.* (1996) and Pinto *et al.* (2006). Fortunately, the penalty in hardness (except for that characteristic of the fusion zone and HAZ) is not at all different or excessive for the hybrid weld. For welds on EX AW-6XXX alloys in T4 temper, post-weld heat treatment (T78) can remove this hardness drop, resulting in a similar hardness in base metal and HAZ (Verwimp and Gedopt, 2007; Verwimp *et al.*, 2007). Further data on hardness in EN-AW5XXX (Baumann, 1999)

and EN AW-7XXX (Allen *et al.*, 2006; Hu and Richardson, 2006a and 2007) alloys can be taken from the respective references.

10.5.5 Tensile strength

Although the penalty in the hardness value is not excessive for the hybrid weld in AA6013 T6 compared with the laser weld, HAZ and the zone of the hardness drop are broader by about 30% each in the hybrid weld than in the laser beam weld (Vaidya *et al.*, 2006) (Fig. 10.16). As this is the region of softening, this may cause a loss of strength. However, the penalty again is negligible as shown by the tensile curves in Fig. 10.17.

Certainly, compared with the base material, both welds exhibit a decrease in strength; the joint efficiency of the welds is about 72% and 82% in terms of yield strength and ultimate tensile strength, respectively. This effect, the so-called strength undermatching, is again characteristic for welded high-strength precipitation hardenable aluminium alloys. But when the welds are compared with each other, the hybrid process does not impair strength (Shibata *et al.*, 2006; Maier *et al.*, 1996). Maier *et al.* (1996) have even demonstrated an increase in yield strength for the hybrid weld compared with the pure laser weld, which they attributed to the lower porosity observed in the hybrid weld for their processing conditions.

The lower elongation of both laser and hybrid welds in the standard tensile test specimen is also common, and should be attributed to the strain

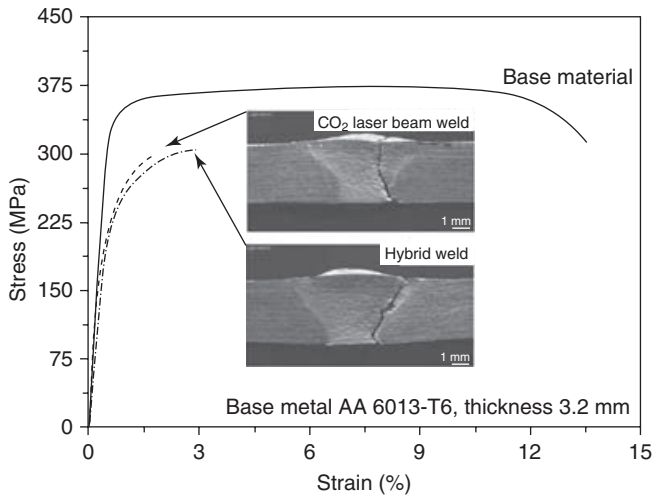

10.17 Tensile curves and the fracture location in the CO_2 laser beam weld and the hybrid weld in a 3.2 mm thick AA6013 sheet butt-welded in T6. The fracture is restricted to the weld (Vaidya *et al.,* 2006).

concentration within or adjacent to the weld. Moreover, the whole deformation is concentrated in a very short length (to the first approximation to the width of seam and HAZ) which, when measured over the standard gauge length (50 mm) turns out to be low, even when the weld itself is ductile. Nonetheless, the hybrid weld is found to possess a slightly higher elongation even in the standard specimen (Fig. 10.17).

Thus, although the width of the hardness drop as inferred from the microhardness gradient was higher (Fig. 10.16), the overall strength of the weld was not affected unfavourably by applying the hybrid welding process (Fig. 10.17). This was also established for EN AW-5XXX in comparison with a wider variety of arc welding processes (Baumann, 1999) and EN AW-7XXX alloys (Allen *et al.*, 2006; Hu and Richardson, 2007).

10.5.6 Fatigue behaviour

Fatigue, being sensitive to defects, is a more critical evaluation parameter than the tensile strength, since surface defects may not necessarily affect the latter. The major surface defects present in the study of Vaidya *et al.* (2006) on AA6013 were occasional undercuts and spatter in the laser welds, whereas the hybrid welds were free from such defects (Fig. 10.13). The resulting fatigue behaviour is given in Fig. 10.18 in comparison to base material, with the stress level calculated using base material plate thickness.

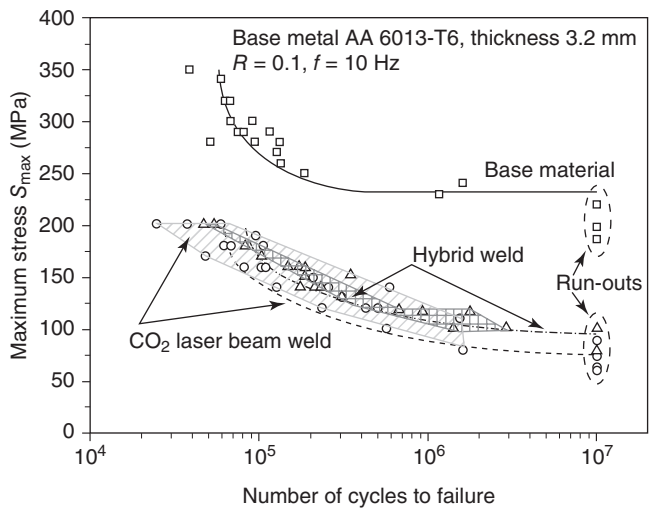

10.18 Comparative fatigue behaviour of the CO_2 laser beam weld and the hybrid weld in a 3.2 mm thick AA6013 sheet butt-welded in T6 (Vaidya *et al.*, 2006).

In order to elucidate potential detrimental effects of (surface) defects, the specimen surface of the welds was not processed before testing.

Both the laser and the hybrid welds exhibit a fatigue resistance much lower than the base material. It is remarkable that the laser welds are characterised by a larger scatter band than the hybrid welds. However, data for the latter welds is still within the scatter band of the laser weld. Assuming the lower bound curve shown as a basis for comparison, the hybrid weld is found to exhibit a better resistance to fatigue than the laser weld. This is confirmed particularly in the high cycle regime where the crack initiation phase dominates. With 10^7 life cycles as a technical definition of run-outs for the fatigue limit, the latter is higher by about 30% for the hybrid weld than for the laser weld. This is also the range in which the fatigue resistance was improved over the entire regime.

In the work of Vaidya *et al.* (2006), the major crack initiation site was at the top for the laser welds, whereas for the hybrid welds it was at the bottom. In the former, the weld defects were present at top, whereas in the latter, some instability in the root occured (Fig. 10.13). This seems to have induced a notch effect, which is in agreement with the observations by Maier *et al.* (1996). This assumption is further supported by the fact that, in case a laser welded specimen was defect-free, its fatigue response became better even in the high cycle regime Vaidya *et al.* (2006).

10.5.7 Conclusions

Based on the above details, the following general conclusions may be drawn on the properties of hybrid (butt-joint) welds in aluminium alloys, especially in comparison with laser welds:

- Hybrid welds tend to be wider and smoother in the top of the weld and show less spatter and undercut than laser welds. Such differences are less pronounced in the lower regions of the cross-section and in the root.
- Porosity can be controlled by applying an appropriate cleaning process, He-rich shielding gas mixtures and by optimising process parameters, especially arc power and welding speed.
- Although microstructural differences between optimised laser welds and hybrid welds are in most cases marginal, a specific adjustment of heat input and heat flow via the process parameters can be used to modify the microstructure especially in the upper part of the weld.
- Depending on the temper of the base material, the characteristic zone of hardness drop tends to be wider in hybrid welds than in laser welds, owing to the characteristic of the respective heat sources. Nonetheless, hardness values tend to be similar.

- Hybrid welds generally exhibit a strength undermatching (at least in the as-welded condition) with a joint efficiency between 60 and 90%. Whereas ultimate tensile strength is similar to that achieved in laser welds, elongation and – in some cases – yield strength can be slightly higher in hybrid welds.
- Fatigue resistance (particularly in the high cycle regime) tends to be improved in hybrid welds compared with laser welds, a behaviour which can be attributed to the reduction of surface defects in hybrid welds.

10.6 Applications

In general, laser hybrid welding is considered for those applications where the productivity of a laser process in joining of aluminium is desired, whilst poor fit-up tolerances yielding gap prohibit the use of pure laser beam welding. This is the case especially in the transportation industries, i.e. the automotive, railway and shipbuilding industry, where the base materials are processed as casts, extruded profiles or sheets. As the requirement 'gap-bridging' necessitates the use of filler materials, the sub-process arc welding is typically implemented using a MIG arc. Normally, the Nd:YAG laser is used for the sub-process laser beam welding (e.g. Anon., 2002), whereas high-power fibre lasers have been subject of recent application studies especially for thick-section welding of extruded profiles for the railway industries (Kohn *et al.*, 2005; Thomy and Seefeld, 2005; Thomy *et al.*, 2004b, 2005a, 2005b, 2005c, 2005d, and 2005e; Vollertsen and Thomy, 2005; Wagner *et al.*, 2006). A potential niche application is found in the aircraft industries, where for some difficult-to-weld alloys (EN AW-2XXX and EN AW-7XXX) the introduction of large quantities of filler material by the MIG arc and the possibility to exactly tailor heat input and heat flow by optimising the hybrid welding parameters are specially attractive (Allen *et al.*, 2006; Verhaeghe *et al.*, 2007; Verwimp and Gedopt, 2007; Vollertsen *et al.*, 2004).

In the automotive industry, where the demand for lightweight structures to reduce fuel consumption is one of the main incitements for the use of aluminium alloys in space-frame structures, laser–MIG hybrid welding of aluminium has already found some applications (Anon., 2004; Staufer, 2002, 2005, and 2006; Staufer and Helten, 2003; Staufer *et al.*, 2003; Trommer and Staufer, 2004). For these car body applications, which are characterised by (relatively) short weld lengths and high-volume production, the main challenge hybrid welding processes have to face is the need for gap-bridging and for joining extruded profiles, castings and sheets with each other to achieve optimum stiffness (Staufer and Helten, 2003). Typical joint geometries are fillet welds in overlap configuration and but welds (Staufer and Helten, 2003). Industrial applications implemented so far are the welding

of side doors in VW Phaeton and the Audi A8 roof rails (Staufer and Helten, 2003; Staufer, 2005 and 2006; Trommer and Staufer, 2004).

For the first application, the VW Phaeton side door consisting of sheet, cast and extruded components, 48 Nd:YAG laser MIG weldments are performed in one welding station (together with 7 MIG welds and 11 laser welds). The total weld length is 4980 mm (Larsson, 2003). Using AiSi12 with a diameter of 1.6 mm as filler wire and argon as shielding gas, the typical welding speed is 4.2 m min^{-1}. In the second application, the welding of the Audi A8 roof rail, the hybrid welding process is used for attaching smaller brackets and the roof rail inner parts (AA6181) to the main roof rail, which is a 4.0 mm thick hydroformed section of AA6014 quality (Larsson, 2003). One of the most important requirements is to have a smooth weld surface on the inside of the roof rail area. This requirement comes from the attachment of an inflatable curtain in this area, a safety device inflating at side impact. This device is stored in a textile bag, which could be sensitive to wear if subjected to contact with sharp edges. The solution was found in laser MIG hybrid welding using a 4.0 kW diode-pumped Nd:YAG laser with 600 μm fibre delivery system and a focal length of 250 mm, and a trailing MIG torch offering 250 A. In two steps, a total of 29 hybrid welds is performed for each side at a welding speed between 3.5 m min^{-1} and 5.5 m min^{-1}. The total hybrid weld length is 2300 mm for each side. Aside from achieving a smooth seam, process stability is increased owing to the ability to bridge gaps (maximum 0.4 mm) and allow for offset positioning (up to 0.4 mm). Finally, a special application for hybrid welding associated with the automotive industry is the welding of tailored blanks, which was investigated by Hackius *et al.* (2001).

In the railway industry, lightweight design to improve fuel efficiency is also one of the central issues. In lightweight train superstructures, especially in high-speed trains such as the German ICE train, customised extruded aluminium profiles with high stiffness and fastening possibilities for aggregates and interior fittings are used (Dilthey and Reich, 2003). These extruded profiles (typically of EN AW-6XXX alloys) are then welded together over the full length of one railway car (typically 26 m), which gives a total weld length exceeding 1 km (Dilthey and Reich, 2003). In these applications, the stability of the process over long weld lengths, the production of sound welds within narrow standards to achieve sufficient strength and fatigue properties and the reduction of distortion are the central challenges. In particular, the latter aspect should make hybrid welding an attractive process compared with MIG welding, which is the process currently used most widely. Consequently, application studies have been performed in that field.

Maier *et al.* (1996) have assessed the potential of Nd:YAG laser–MIG hybrid welding of extruded aluminium profiles as early as 1996, focusing on

microstructural and technological properties of the welds, demonstrating the superior fatigue behaviour of hybrid welds over laser and MIG welds. However, owing to restrictions in laser power at that time, welding speed was limited to approximately 2.4 m min^{-1} at a welding depth of less than 4 mm. In 2004, Thomy *et al.* (2004a) have published related research on extruded profiles, manufacturing prototype test panel sections from the roof segment of the ICE train (Fig. 10.19) using an Nd:YAG laser MIG hybrid welding process. The test panels consisted of six extruded profiles (thickness 3 mm, length 2 m) and were welded at a speed of 4 m min^{-1} without special clamping devices. Laser power at workpiece was 4 kW, and the power of the pulsed MIG was 3.65 kW. The process fulfilled all requirements considering weld quality and gap bridging. Moreover, compared with pure MIG welding, Nd:YAG-Laser MIG welding allowed a significant increase in welding speed, which is associated with a reduction of seam volume and total heat input (up to 85%), thus yielding a considerably lower distortion. With the industrial availability of high-power fibre lasers of the 10-kW class, this work was continued to further enhance productivity and the material thickness range, and a welding speed in the range of 6 to 8 m min^{-1} for a material thickness of up to 8 mm was successfully demonstrated in a laboratory environment (Kohn *et al.*, 2005, 2004b; Thomy and Seefeld, 2005; Thomy *et al.*, 2005a, 2005b, 2005c, 2005d, and 2005e; Vollertsen and Thomy, 2005; Wagner *et al.*, 2006). This would result in an increase in welding speed of more than six times that of MIG welding.

In shipbuilding in general and yacht and ferry construction in particular, lightweight design using aluminium alloys is an important issue, aiming at

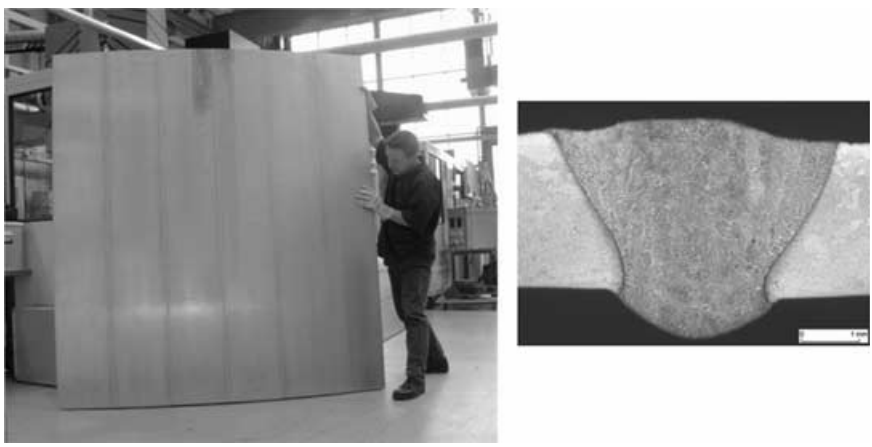

10.19 Roof segment of the ICE train/cross-section of the weld.

improving structural properties in view of capsize stability, but also of fuel efficiency (Dilthey and Reich, 2003). Taking into account again fit-up tolerance issues associated with all heavy-industry manufacturing as well as the large amount of welding to be performed, a gap-tolerant high-productivity hybrid welding process for aluminium alloys would be desirable. Consequently, based on the experiences with hybrid welding of steel structures in shipbuilding, first application studies were performed on aluminium alloys, also focusing on joint configurations such as T-joints (Jasnau *et al.*, 2003), which are typical for such types of structures.

In conclusion, the following general comments can be made:

- Hybrid welding processes (preferrably laser MIG hybrid welding) should be considered especially for those applications in aluminium welding which face poor fit-up conditions, but require a high productivity.
- So far, Nd:YAG laser MIG hybrid welding of aluminium alloys (sheet, extruded and cast material) has been successfully applied in production processes in various industrial car body applications.
- Potential further fields of application can be identified in the railway industry and in shipbuilding, especially since the availability of high-power solid-state lasers permits welding of thicker sections at a competitive processing speed.

10.7 Future trends

Based on the above review, a forecast of potential future trends in hybrid welding shall be attempted. With the increasing demand for lightweight design in the transportation industries in order to improve fuel efficiency, the demand for advanced aluminium structures is likely to increase (Furrer, 2007). As fusion welding is strongly linked to the success of such structures (Ostermann, 1998), the need for welding processes which are able to produce adequate quality at a high productivity is certain to rise. Hybrid welding, and especially laser MIG welding has excellent answers to this demand, as should be clear from the above.

Moreover, new laser sources being offered to the market (such as the disc or fibre laser) are combining the advantages of an Nd:YAG laser (so far the standard laser source in hybrid welding) such as fibre-guided beam delivery with the main technological advantages of the CO_2 laser (high beam power and quality). Consequently, together with their higher efficiency, they should have the potential to gradually replace the Nd:YAG laser in some existing hybrid welding applications as well as to open new applications to hybrid welding of aluminium alloys. Among these may be counted the welding of ship hull or railway car structures, where thicker

sections have to be joined at elevated speed. A special advantage for the latter applications might also lie in the reduction of distortion.

Another aspect might be the application of advanced arc welding processes such as cold arc (Goecke, 1996) or CMT (Bruckner, 2004), which allow very precise control of the heat input. Although this is certain to require additional research effort, the potential especially with respect to controlling distortion and microstructure by further optimising heat input and heat flow seem to be quite tempting.

For further research, many additional topics may arise. Aside from improving the understanding of the basic mechanisms underlying the synergistic interaction effects between laser beam and arc through experimental investigations, modelling efforts will have to continue in order to facilitate the optimisation of parameters in practical applications. Moreover, the development of advanced alloys with challenging weldability (such as those of group EN AW-7XXX) will stimulate additional research.

In conclusion, it should be quite clear that, although hybrid welding of aluminium alloys is a feasible process today, there is still considerable potential for future developments and applications.

10.8 References

AALDERINK B, AARTS R G K M and MEIJER J (2007), 'Increased gap bridging capabilities using twin spot and hybrid laser/GMA welding for AA5182', in Vollertsen F, Emmelmann C, Schmidt M and Otto A, *Proc. 4th International WLT-Conference on Lasers in Manufacturing 2007*, Stuttgart, AT-Fachverlag, 79–84.

AICHELE G (2003), 'Das Fügen von Aluminium bleibt ein spannendes Thema, Teil I', *Aluminium*, **79**(12), 1059–1068.

ALLEN C M, VERHAEGHE G, HILTON P A, HEASON C P and PRANGNELL P B (2006), 'Laser and hybrid laser–MIG welding of 6.35 and 12.7 mm thick aluminium aerospace alloy', *Materials Science Forum*, 519–521, 1139–1144.

ANDERSEN M and JENSEN A (2001), 'Hybrid Nd:YAG laser MIG welding in aluminium', in Olsen F and Kristensen J, *Proc. 8th Nordic Conferepce on Laser Materials Processing*, Lyngby, Denmark, 371–380.

ANON. (2002), 'Kombination aus Laser- und MIG-Schweißprozess ist praxisreif', *Aluminium*, **78**(1/2), 94–96.

ANON. (2004), 'Laser–MIG process for automotive industry', *Industrial Robot: An International Journal*, **31**(1), 82–86.

BAGGER C and OLSEN F (2005), 'Review of laser hybrid welding', *Journal of Laser Applications,* **17**(1), 2–14.

BAUMANN B (1999), 'Gegenüberstellung von Hochleistungsschweißverfahren für das Aluminiumschweißen irn Dünnblechbereich', in *DVS-Berichte* **199**, Düsseldorf, DVS Verlag, 52–57.

BECKERT M (1997), *Eignung metallischer Werkstoffe zum Schweißen,* Düsseldorf, DVS Verlag.

BINROTH S (1995), *Beitrag zur Prozeßstabilität beim CO_2-Laserstrahlschweißen von Aluminium mit Zusatzwerkstoff*, Bremen, BIAS Verlag.

BRUCKNER J, HIMMELBAUER K, and HACKL H (2004), '*Der CMT-Prozess und seine Möglichkeiten, im Speziellen das Fügen von Stahl mit Aluminium*', Düsseldorf, DVS Verlag, 201–204.

CASALINO G (2007), 'Statistical analysis of MIG–laser CO_2 hybrid welding of Al–Mg alloy' *Journal of Materials Processing Technology* **191**, 106–110.

CASALINO G and LOBIFARO F (2005) 'Process parameters effects on Al–Mg alloys MIG laser CO_2 welding', in Ostendorf A, *Proc. 24th International Congress on Applications of Lasers & Electro-Optics ICALEO 2005*, 1062–1068.

CASALINO G, LUDOVICO A and CHIECO G (2005) 'Characterisation of Al–Mg alloys MIG–laser CO_2 combined welding', in Ostendorf A, *Proc. 24th International Congress on Applications of Lasers & Electro-Optics ICALEO 2005*, 190–195.

COCK T (1999), *Aluminium – A Light Metal*, EAA – European Aluminium Association.

CUI H (1991), *Untersuchung der Wechselwirkung zwischen Schweißlichtbogen und fokussiertem Laserstrahl un der Anwendungsmöglichkeiten kombinierter Laser-Lichtbogentechnik*, Dissertation TU Darmstadt.

DECKER I, WENDELSTORF J and WOHLFAHRT H (1995), 'Laserstrahl-WIG-Schweißen von Aluminiumlegierungen', *Proc. Schweißen und Schneiden '95,* Düsseldorf, DVS Verlag, 96–99.

DIEBOLD T P and ALBRIGHT C E (1984), 'Laser GTA welding of aluminium alloy 5052', *Welding Journal* (June), 18–24.

DILTHEY U and REICH F (2003), 'Applications of the laser–GMA hybrid welding process in steel and aluminium vehicle construction', in Poprawe R and Otto A, *Proc. 2nd International WLT-Conference on Lasers in Manufacturing 2003*, Stuttgart, AT–Fachverlag, 157–163.

DILTHEY U and STEIN L (2006), 'Multimaterial car body design – a challenge for welding and joining', *Proc. IIW Congress: Welding and Related Inspection Technologies*, Stellenbosch, Paper 051.

DILTHEY U, WOESTE K and WAGNER N (2007), 'Laserstrahl-MIG-Hybridschweißen von Aluminium- und Magnesiumlegierungen', *Schweißen und Schneiden*, **59**(1), 16–22.

DULEY W W (1999), *Laser welding*, New Jersey, John Wiley & Sons.

EMA M and SASABE S (2003), 'Joint strength of Al–Mg–Si alloys for automobiles by advanced welding technologies', *Welding International*, **18**(1), 11–15.

FUERSCHBACH P (1999), 'Laser assisted plasma arc welding', in Christensen P, *Proc. 18th International Congress on Applications of Lasers & Electro-Optics ICALEO '99*, 102–109.

FURRER P (2007), 'Aluminium Applications in the Automotive Industry', Sato S and Katayama S, *Proc. 10th International Conference on Joints in Aluminium*, Osaka, 45–52.

GOECKE S F (2006), 'Energiereduziertes Lichtbogen-Fügeverfahren für wärmeempfindliche Werkstoffe', *Schweißen und Schneiden 2005*, **237**, Düsseldorf, DVS Verlag, 44–48.

HACKIUS J (2003), *Laserstahl-Hybridschweißen von Aluminiumlegierungen*, Stuttgart, IRB Verlag.

HACKIUS J, BRENNER B, WINDERLICH B, STANDFUß J, BEYER E and NÄGELER S (2001), 'Laserhybridschweißen von Aluminiumlegierungen', *LaserOpto*, **33**(2), 49–55.

HACKIUS J, NAEGELER A, BRENNER B and BEYER E (2000), 'Innovation in laser hybrid technology for aluminum welding', in Hügel H, Matsunawa A and Mazumder J,

Proc. 19th International Congress on Applications of Lasers & Electro-Optics ICALEO 2000, B8–B19.

HELTEN S (2003), *Qualifizierung des Nd:YAG-MIG-Hybridschweißverfahrens für den Aluminiumkarosseriebau*, Aachen, Shaker.

HIROSE A *et al.* (1999), 'Quantitative evaluation of softened regions in weld heat-affected zones of 6061-T6 aluminium alloy – characterizing of the laser beam welding process', *Metallurgical and Materials Trans. A.*, **30**, 2115–2120.

HU B and RICHARDSON I M (2006a), 'Hybrid laser/GMA welding aluminium alloy 7075', *Welding in the World*, **50**(7/8), 51–57.

HU B and RICHARDSON I M (2006b), 'Mechanism and possible solution for transverse solidification cracking in laser welding of high strength aluminium alloys', *Materials Science and Engineering*, **A429**, 287–294.

HU B and RICHARDSON I M (2007), 'Microstructure and mechanical properties of AA7075 (T6) hybrid laser/GMA welds', *Materials Science and Engineering*, **A459**, 94–100.

ISHIDE T, TSUBOTA S and WATANABE M (2002), 'Latest MIG, TIG arc–YAG laser hybrid welding systems for various welding products', in *Proc First International Symposium on High Power Laser Macroprocessing, SPIE* **4831**, 347–352.

JASNAU U, HOFFMANN J and SEYFFARTH P (2003), 'Nd:YAG-Laser-MSG-Hybridschweißen von Aluminiumlegierungen im Schiffbau', in *Schweißen und Schneiden 2003*, DVS–Berichte 225, Düsseldorf, DVS Verlag, 181–186.

JI J, JASNAU U and SEYFFARTH P (2007a), 'Nahtgeometrie beim Nd:YAG-Laserstrahl-MSG-Hybridschweißen von Aluminiumlegierungen', *Schweißen und Schneiden*, **59**(3), 130–137.

JI J, JASNAU U and SEYFFARTH P (2007b), 'Prozessporen beim Nd:YAG-Laserstrahl-MSG-Hybridschweißen von Aluminiumlegierungen. Teil 1: Parametereinflüsse', *Schweißen und Schneiden*, **59**(6), 334–337.

JI J, JASNAU U and SEYFFARTH P (2007c), 'Prozessporen beim Nd:YAG-Laserstrahl-MSG-Hybridschweißen von Aluminiumlegierungen. Teil 2: Strategie zu ihrer Vermeidung', *Schweißen und Schneiden*, **59**(10), 555–560.

JI J, JASNAU U and SEYFFARTH P (2007d), 'Gefügeverbesserung im Schweißgut beim Nd:YAG-Laserstrahl-MSG-Hybridschweißen von Aluminiumlegierungen', *Schweißen und Schneiden*, **59**(11), 608–612.

JOHANNESSEN J I (1994), Structural Materials Fabrication, AA – European Aluminium Association.

JOKINEN T, JERNSTRÖM P, KARHU M, VANTTAJA M and KUJANPÄÄ V (2003), 'Optimisation of parameters in hybrid welding of aluminium alloy', in Miyamoto I, Kobayashi K F, Sugioka K, Poprawe R and Helvajian H, *Proc. First International Symposium On High-power Laser Macroprocessing*, SPIE **4831**, 307–312.

KATAYAMA S, NAITO Y, UCHIUMI S and MIZUTANI M (2005), 'Penetration and porosity prevention mechanism in laser–arc hybrid welding', in Beyer E, Dausinger F, Ostendorf A and Otto A, *Proc. 3rd International WLT-Conference on Lasers in Manufacturing 2005*, Stuttgart, AT–Fachverlag, 193–198.

KATAYAMA S, UCHIUMI S, MIZUTANI M, WANG J and FUJII K (2006a), 'Penetration and porosity prevention mechanism in YAG laser–MIG hybrid welding', *Welding International*, **21**(1), 25–31.

KATAYAMA S, UCHIUMI S and BRIAND F (2006b), 'Production of sound deep-penetration hybrid weld in aluminum alloy with YAG laser and MIG arc', in Ostendorf A,

Proc. 25th International Congress on Applications of Lasers & Electro-Optics ICALEO 2006, 953–959.

KATAYAMA S, NAITO Y, UCHIUMI S and MIZUTANI M (2006c), 'Physical phenomena and porosity prevention mechanism in laser–arc hybrid welding', *Trans. JWRI*, **35**(1), 13–18.

KATAYAMA S, KAWAHITO Y and MIZUTANI M (2007a), 'Weld penetration, defect prevention and phenomena in laser and hybrid welding of aluminium alloys', in *Proc. 10th International Conference on Joints in Aluminium (INALCO 2007)*, 53–62.

KATAYAMA S, KAWAHITO Y and MIZUTANI M (2007b), 'Understanding of laser and hybrid welding phenomena', *IIW Doc. IV-943-07*.

KLING R, OTTE F, STAHLHUT C and HERMSDORF J (2007), 'Minimale Laserleistung mit Lasern angepasster Strahleigenschaften für das Laser/MSG-Hybrid-Schweißen in Fertigungssystemen für die Fahrzeugfertigung', in *Die Verbindungs Spezialisten 2007*, DVS–Berichte 244, Düsseldorf, DVS Verlag, 409–418.

KOHN H, THOMY C, GRUPP M and VOLLERTSEN F (2004), 'Neue Entwicklungen beim Laserstrahlschweißen von Rohren', in *Proc. 18. Oldenburger Rohrleitungsforum 2004*, Essen, Vulkan Verlag, 50–74.

KOHN H, THOMY C and VOLLERTSEN F (2005), 'Schweißtechnische Anwendungen mit einem 10 kW Faserlaser – Erste Ergebnisse', in *Proc. EALA European Automotive Laser Application 2005*, 291–303.

KOU S (2003), *Welding Metallurgy*, New Jersey, Wiley & Sons.

LARSSON J K (2003), 'Recent laser trends and applications in the automotive industry', in Halmoy E, *Proc. 9th Conference on Laser Materials Processing in the Nordic Countries (NOLAMP)*, 167–179.

LEE K and PARK K (2003), 'A study on the process robustness of Nd:YAG laser-MIG hybrid welding of aluminum alloy 6061-T6', in Chen X and Duley W W, *Proc. 22nd International Congress on Applications of Lasers & Electro-Optics ICALEO 2003*, 48–55.

LÖHR M, UEYAMA T and TONG H (2005), 'Verschweißen von Aluminiumwerkstoffen mit gepulsten AC/MIG Laser Hybridverfahren', *Schweißen und Schneiden 2005*, DVS-Berichte 237, Düsseldorf, DVS Verlag, 194–199.

MAIER C (1999), *Laserstrahl-Lichtbogen-Hybridschweißen von Aluminiumwerkstoffen*, Aachen, Shaker.

MAIER C, REINHOLD P, MALY H, BEHLER K, BEYER E and VON HEESEN N (1996), 'Aluminium-Strangpreßprofile im Schienenfahrzeugbau, geschweißt mit dem Hybridverfahren Nd:VAG-Laser MIG', in *Schweißen und Schneiden '96*, DVS–Berichte 176, Düsseldorf, DVS Verlag, 198–202.

MATHERS G (2002), *The Welding of Aluminium and its Alloys*, Abington, Woodhead Publishing Ltd.

OSTERMANN F (1998), *Anwendungstechnologie Aluminium*, Berlin, Springer.

PAGE C J, DEVERMANN T, BIFIN J and BLUNDELL N (2002), 'Plasma augmented laser welding and its applications', *Science and Technology of Welding and Joining*, **7**, 1–10.

PETRING D (2001), 'Hybrid laser welding', *Industrial Laser Solutions*, (12), 12–16.

PETRING D, FUHRMANN C, WOLF N and POPRAWE R (2003), 'Investigations and applications of laser–arc hybrid welding from thin sheets up to heavy section components', in Chen X and Duley W W, *Proc. 22nd International Congress on Applications of Lasers & Electro-Optics ICALEO 2003*, 1–10.

PINTO H, PYZALLA A, HACKL H and BRUCKNER J (2006), 'A comparative study of microstructure and residual stresses of CMT-, MIG- and laser-hybrid welds', *Materials Science Forum*, **524–525**, 627–632.

PRIES H, RETHMEIER M, WIESNER S and WOHLFAHRT H (2002), 'Laser- und Elektronenstrahlschweißen von Aluminium-Druckguss', in *Schweißen und Schneiden 2002*, DVS–Berichte 220, Düsseldorf, DVS Verlag, 219–223.

RASMUSSEN D and DUBOURG L (2005), 'Hybrid laser–GMAW welding of aluminium alloys: a review', in David S, DebRoy T, Lippold J C, Smartt H B and Vitak J M, *Proc. 7th International Conference on Trends in Welding Research*, 133–152.

RATH W (2006), 'Laser hoher Strahlqualität: Technik und Anwendungen', in Vollertsen F and Seefeld T, *Proc. 5. Laser-Anwenderforum 2006*, 153–158.

REICH J F (2005), *Untersuchungen zu Festigkeit und Qualität von Laser-MIG-Hybridgeschweißten Aluminiumverbindungen*, Aachen, Shaker Verlag.

SASABE S (2004), 'Welding propertics of aluminum alloys for automotive structures', *Welding in the World*, 48 (Special Issue), 53–64.

SCHILF M, THOMY C, SEEFELD T and VOLLERTSEN F (2003), 'Some aspects of arc stability in GMA-laser-hybrid welding', in Poprawe R and Otto A, *Proc. 2nd International WLT-Conference on Lasers in Manufacturing 2003*, Stuttgart, AT–Fachverlag, 171–175.

SCHOER G (2002), *Schweißen und Hartlöten von Aluminiumwerkstoffen*, Düsseldorf, DVS Verlag.

SCHUBERT E (2003), *Untersuchungen zum Leichtbau mit Hilfe lasergestützter Mischbauweisen*, Bremen, BIAS Verlag.

SCHUBERT E, WEDEL B and KÖHLER G (2002), 'Influence of the process parameters on the welding result of laser-GMA welding', Beyer E and Patel R, *Proc. 21st International Congress on Applications of Lasers & Electro-Optics ICALEO 2002*, 48–55.

SCHULZE G, KRAFKA H and NEUMANN P (1996), *Schweißtechnik*, Düsseldorf, VDI Verlag.

SEPOLD G, THOMY C, SEEFELD T, SCHILF M, VOLLERTSEN F and HOFFMANN R (2003), 'CO_2-laser GMA hybrid welding – aspects of research and industrial application', in Poprawe R and Otto A, *Proc. 2nd International WLT-Conference on Lasers in Manufacturing 2003*, Stuttgart, AT–Fachverlag, 149–156.

SEYFFARTH P and KRIVTSUN I V (2002), *Laser–arc processes and their applications in welding and material treatment*, New York, Taylor & Francis.

SHI G, HILTON P, BOOTH G S and PUNSHON C (2004), 'Enhancements to power beam welding processes for land transport', *Welding in the World*, **48** (July, Special Issue), 43–52.

SHIBATA K, SAKAMOTO H and IWASE T (2006), 'Laser–MIG hybrid welding of aluminium alloys', *Welding in the World*, **50**(1/2), 28–34.

SHONIN V A, MASHIN V Y, KHASKIN V Y and NEDEJ T (2006), 'Residual stresses in butt joints of thin sheets from alloy AMg6 after arc and laser welding', *Paton Welding Journal*, **9**, 20–24.

STAUFER H (2002), 'Laserhybrid and laserhotwire: two processes with high joining speeds', in *50th WTlA Annual Conference and the l2th International TWI Computer Technology in Welding and Manufacturing Conference*, 26–30 August 2002, Sydney, New South Wales, Australia.

STAUFER H (2005), 'LaserHybrid welding and LaserBrazing: state of the art in technology and practice by the examples of the Audi A8 and VW-Phaeton', in Beyer E, Dausinger F, Ostendorf A and Otto A, *Proc. 3rd International WLT-Conference on Lasers in Manufacturing 2005*, Stuttgart, AT–Fachverlag, 203–208.

STAUFER H (2006), 'Laser hybrid welding and laser brazing at Audi and VW', *Welding in the World*, **50**(7/8), 44–50.

STAUFER H, RÜHRNÖßL M and MIESSBACHER G (2003), 'Hybrid welding for the automotive industry', *Industrial Laser Solutions*, **18**(2), 7–10.

STAUFER H and HELTEN S (2003), 'Laser-Hybridschweißen für neuartige Leichtbaukonzepte im Automobilbau', in *Schweißen und Schneiden 2003*, DVS–Berichte 225, Düsseldorf, DVS Verlag, 175–180.

THOMY C and SEEFELD T (2005), 'Basics and Applications of Laser GMA Hybrid Welding', in Paton B E and Kovalenko V S, *Proc. 2nd International Conference on Laser Technologies in Welding and Materials Processing (LTWMP 05)*, 203–206.

THOMY C, SCHILF M, SEEFELD T and VOLLERTSEN F (2004a), 'Nd:YAG-laser GMA hybrid welding of aluminium alloys', in Geiger M and Otto A, *Proc. LANE 2004: Laser Assisted Net-Shape Engineering*, Vol. 1, Bamberg, Meisenbach Verlag, 159–168.

THOMY C, SEEFELD T and VOLLERTSEN F (2004b), 'Grundlagen und Einsatzpotentiale des Laser-MSG-Hybridschweißens anhand von Beispielen für die industrielle Fertigung', in *Proc. Innovationsforum Hybridtechnologien – Fügetechnik für die Fertigung der Zukunft*, 26–34.

THOMY C, SEEFELD T and VOLLERTSEN F (2005a), 'Laser GMA hybrid welding with various laser systems', *IIW Doc. XII-1843-05*.

THOMY C, SCHILF M, SEEFELD T, KOHN H and VOLLERTSEN F (2005b), 'Laser and laser GMA welding of steel and aluminium alloys for heavy industry applications', *IIW Doc. XII-1856-05*.

THOMY C, KOHN H and VOLLERTSEN F (2005c), 'Application of high-power fibre lasers in laser and laser-MIG hybrid welding', in Paton B E and Kovalenko V S, *Proc. 2nd International Conference on Laser Technologies in Welding and Materials Processing (LTWMP 05)*, 46–48.

THOMY C, SEEFELD T and VOLLERTSEN F (2005d), 'Application of high-power fiber lasers for joining of steel and aluminium alloys', in Beyer E, Dausinger F, Ostendorf A and Otto A, *Proc. 3rd International WLT-Conference on Lasers in Manufacturing 2005*, Stuttgart, AT–Fachverlag, 27–32.

THOMY C, SEEFELD T and VOLLERTSEN F (2005e), 'Schweißen mit Hochleistungs-Faserlasern – Was sind die Vorteile, wo sind die Grenzen?', *Laser Technik Journal*, (3), 28–31.

THOMY C, SEEFELD T and VOLLERTSEN F (2006), 'Industrial potential for high power fibre laser welding', *The Industrial Laser User*, (42), 22–26.

THOMY C, MÖLLER F, SEPOLD G and VOLLERTSEN F (2008), 'Interaction between laser beam and arc in hybrid welding for dissimilar materials', *IIW Doc. IVI-961-08*.

TOMITA N, UEYAMA T, HASEGAWA S, YASUFUK T and UEDA Y (2004), 'Development of laser–arc hybrid welding robot system', *IIW Doc. XII-1791-2004*.

TONG H, UEYAMA T, NAKATA K and USHIO M (2003), 'High speed welding of aluminium alloy sheets using laser assisted alternating current pulsed metal inert gas process', *Science and Technology of Welding and Joining*, **8**(3), 229–234.

TRAUPE M, POSS R and ZENNER H (2002), 'Steigerung der Schwingfestigkeit geschweißter dünnwandiger Aluminiumbauteile durch Nachbehandlung', in *Schweißen und Schneiden 2002*, DVS–Berichte 220, Düsseldorf, DVS Verlag, 107–114.

TROMMER G and STAUFER H (2004), 'Vorteile addieren – Mit dem Laserhybrid-schweißen fertigt VW die Phaeton-Aluminiumtüren in besonders hoher Festigkeit', *MM Das IndustrieMagazin*, (27), 26–27.

UCHIUMI S, WANG J, KATAYAMA S, MIZUTANI M, HONGU T and FUJII F (2004), 'Penetration and welding phenomena in YAG laser–MIG hybrid welding of aluminium alloy', in Patel R, *Proc. 23rd International Congress on Applications of Lasers and Electro-Optics ICALEO 2004*.

UEYAMA T, TONG H, YAZAW I, HIRAMI M, KIHARA T, NAKATA K and USHIO M (2004), 'Aluminium alloy sheet welding by the laser AC pulsed MIG hybrid process', *Welding International*, **18**(5), 334–350.

VAIDYA W V, ANGAMUTHU K, KOCAK M, GRUBE R and HACKIUS J (2006), 'Strength and fatigue resistance of laser–MIG hybrid butt welds of an airframe aluminium alloy AA6013', *Welding in the World*, **50**(11/12), 88–97.

VERHAEGHE G (2007), 'Low-porosity laser welding of 12.7 mm thickness aerospace aluminium', in *Proc. 10th International Conference on Joints in Aluminium (INALCO 2007)*, 143–150.

VERHAEGHE G, ALLEN C and HILTON P (2007), 'Achieving low-porosity laser welds in 12.7 mm thickness aerospace aluminium using a Yb-fibre laser', in Vollertsen F, Emmelmann C, Schmidt M and Otto A, *Proc. 4th International WLT-Conference on Lasers in Manufacturing 2007*, Stuttgart, AT–Fachverlag, 17–24.

VERWIMP J and GEDOPT J (2007), 'Hybrid laser welding and friction stir welding applied to 6056 aluminium alloy', in Vollertsen F and Thomy C, *Proc. Applied Production Technology 2007 (APT'07) – Production of Aircraft Structures*, Bremen, BIAS Verlag, 109–122.

VERWIMP J, GEDOPT J, GEERINCKX E and VAN HAVER W (2006), 'Hybrid laser welding and friction stir welding applied to 6056 aluminium alloy', in Ostendorf A, *Proc. 25th International Congress on Applications of Lasers & Electro-Optics ICALEO 2006*, 970–978.

VERWIMP J, GEDOPT J, GEERINCKX E and VAN HAVER W (2007), 'Hybrid laser welding and friction stir welding applied to 6056 aluminium alloy', in *Proc. 10th International Conference on Joints in Aluminium (INALCO 2007)*, 157–162.

VOLLERTSEN F, SCHUMACHER J, SCHNEIDER K and SEEFELD T (2004), 'Innovative Welding Strategies for the Manufacture of Large Aircraft', *IIW Doc. XII-1832-04*.

VOLLERTSEN F and THOMY C (2005), 'Welding with fibre lasers from 200 to 17 000 W', in Ostendorf A, *Proc. 24th International Congress on Applications of Lasers & Electro-Optics ICALEO 2005*, 254–263.

WAGNER F, THOMY C, SCHILF M, SEEFELD T, KOHN H and VOLLERTSEN F (2006), 'Laser and laser hybrid welding of thick sheet aluminium and steel', in Brandt M and Harvey E, *Proc. 2nd Pacific International Conference on Applications of Lasers and Optics PICALO 2006*, 163–168.

WANG J, NISHIMURA H, FUJII K, KATAYAMA S, MIZUTANI M and UCHIUMI S (2007a), 'Penetration phenomena and gap tolerance in YAG laser-MIG hybrid welding of aluminum alloy', in *Proc. 10th International Conference on Joints in Aluminium (INALCO 2007)*, 151–156.

WANG J, TAKENAKA Y, HUNGU T, FUJII K and KATAYAMA S (2007b), 'Laser-MIG arc hybrid welding of aluminium alloy – comparison of melting characteristics between YAG laser and diode laser', *Welding International*, **21**(1), 32–38.

WIESNER S, RETHMEIER M and WOHLFAHRT H (2001), 'MIG and laser beam welding of aluminium die castings with wrought aluminium profiles', *Welding in the World*, **45** (Special Issue), 143–149.

WIESNER S, RETHMEIER M and WOHLFAHRT H (2005), 'MIG and laser welding of aluminium alloy pressure die cast parts with wrought profiles', *Welding International*, **19**(2), 130–133.

11

Hybrid laser–arc welding of dissimilar metals

C. THOMY, BIAS – Bremer Institut für angewandte Strahltechnik GmbH, Germany

Abstract: This chapter deals with hybrid welding of dissimilar metals, taking the example of aluminium–steel joints. After highlighting application potentials as well as challenges for such joints and reporting alternative processes, laser MIG hybrid welding is introduced as a potential alternative. Details are given on process and joint properties and their dependencies, focusing on microstructure, the effect of process parameters and mechanical and technological properties. Based on application studies, an assessment of future trends and developments in the use of hybrid welding for dissimilar metals such as aluminium–steel joints is attempted.

Key words: hybrid welding, aluminium–steel joints, laser–arc welding, microstructure, mechanical properties.

11.1 Introduction

In this chapter, the issue of hybrid welding of dissimilar metals is studied with use of the example of aluminium–steel joints. In section 11.2, the application potentials for such joints together with the associated challenges are highlighted, and the alternative processes investigated are discussed to provide the basis for assessing the use of laser–MIG hybrid welding for these material combinations. This process is then presented in detail in section 11.3, and process and joint properties and their dependencies are discussed in more detail in section 11.4. In particular, microstructure (11.4.1), the effect of process parameters in laser–MIG hybrid welding (11.4.2) and mechanical and technological properties (11.4.3) will be addressed for joining aluminium to steel. Section 11.5 illustrates the application potentials for laser–MIG hybrid welding of aluminium–steel joints, which is the basis for an assessment of future trends and developments in the use of hybrid welding for dissimilar metals (11.6). Information on all issues related to the welding of pure aluminium alloys should be taken from Chapter 10.

11.2 Specific aspects of and state-of-the-art in joining of dissimilar metals

11.2.1 Dissimilar metal combinations and their application potentials

The combination of materials with different properties is often required to provide products with optimised features. However, the differences in material properties, which often make them the optimum choice for the respective application, may yield considerable challenges for appropriate joining processes. A classical example for such challenges is the selection of appropriate filler materials for joining of austenitic to ferritic steels in apparatus engineering (see e.g. Strassburg and Wehner, 2000). However, in these applications, the basic alloying element (iron) is common for both joining partners, and the challenges again significantly increase if thermal joining of different metals such as aluminium to magnesium (Liu *et al.*, 2006) or aluminium to iron (i.e. steel) is attempted. In particular, the latter has been increasingly investigated since the past decade as, in the automotive industry, the demand for lightweight design and structures with optimised properties rose.

In order to select the appropriate process for joining aluminium to steel, two aspects have to be taken into account. First, the stage of the joining process in the process chain has to be considered. Basically, the joining of dissimilar metals can be performed during the production of semi-finished products such as tailored blanks or during the production of the structure itself. The first option has the advantage of a mostly two-dimensional joining task and excellent fit-up tolerances. However, the tailored blank in general and the joint in particular will have to show a good formability for the subsequent deep drawing process, which is usually required to obtain three-dimensional structural elements. On the contrary, joining of three-dimensional structural elements will not face the challenge of formability, but rather of poor fit-up tolerances.

Second, and associated with the previous aspect, the principal physical nature of the joining process, i.e. either thermal or non-thermal, has to be considered. Non-thermal joining processes such as bolting, riveting, clinching or adhesive bonding (Crane, 1967; Leuschen, 1996; Budde *et al.*, 1997; Hahn *et al.*, 2004) have demonstrated their fitness for joining structural elements e.g. in the car body. Although these joints are often characterised by very good mechanical properties e.g. in regard to stiffness (Budde and Pilgrim, 1995), their significant drawback is the adverse weight balance owing to the overlapping of the materials required by these joining processes (Klein, 1997). Therefore, in view of the basic aim of weight reduction as well as of obtaining an integral structure, thermal joining processes will be given a closer look in the following.

11.2.2 Challenges of joining dissimilar metals

One aspect of considerable importance for joining aluminium to steel in general and for thermal joining in particular is the difference in the basic properties of Fe and Al, such as melting temperature, heat conductivity and coefficient of thermal expansion (Table 11.1). The differences in thermal expansion in combination with the differences in the modulus of elasticity will result in thermally induced stresses, potentially leading to excessive distortion or residual stresses.

The fundamental challenge, however, arises from the formation of intermetallic phases between the two metals (Table 11.2, Fig. 11.1). Some of these phases, which are characterised by significant hardness values, are present in the joining zone and, owing to their brittleness, may have a detrimental effect on the static and dynamic strength of the joints (Sauthoff, 1995; Radscheidt, 1997; Schubert and Zerner, 1999; Zerner, 2002).

Table 11.1 Basic properties of iron and aluminium

	Unit	Iron	Aluminium
Symbol	–	Fe	Al
Density	g cm^{-3}	7.85	2.7
Melting temperature	°C	1563	660
Heat conductivity	W m K^{-1}	75	238
Coefficient of thermal expansion	1/K	12.3×10^{-6}	23.8×10^{-6}
Modulus of elasticity E	N mm^{-2}	210 000	72 000
Tensile strength R_m	N mm^{-2}	270–410	80
Yield strength $R_{p0.2}$	N mm^{-2}	180–250	35
Elongation at fracture A_5	%	30	42

Source: Klein (1997), Bargel and Schulze (2000), Ostermann (1998)

Table 11.2 Properties of intermetallic phases and structures in the system Fe–Al

Phase	Micro hardness HV
Fe_3Al	250–350
FeAl	400–520
$FeAl_2$	1000–1050
Fe_2Al_5	1000–1100
$FeAl_3$	820–980

Source: Radscheidt (1997).

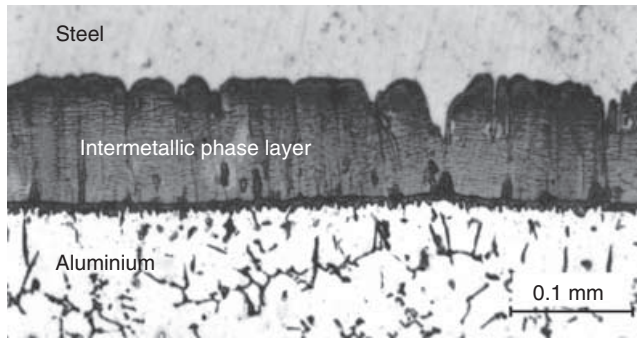

11.1 Example of an intermetallic phase layer in an inadequate aluminium–steel joint.

As the formation of these phases is mainly driven by diffusion (Achar *et al.*, 1980a), aside from the content of alloying elements (Radscheidt, 1997; Gebhardt and Obrowski, 1953; Rabkin and Rjabow, 1967), the time–temperature cycle to which the joining zone is subjected during joining is of significant importance. According to Achar *et al.* (1980b) it is generally assumed that, at lower temperature or higher cooling rate, the formation of intermetallic phases may be drastically reduced. Therefore, to tackle the challenges of both distortion and the detrimental effect of intermetallic phases, high-speed joining processes with low heat input are desirable. This should make hybrid welding a potentially attractive joining process.

11.2.3 Alternative processes for joining aluminium to steel

Studies on thermal joining of aluminium to steel range from conventional processes such as MIG (Andrews, 1962), WIG (Hartwig and Kouptsidis, 1978; Ghanam, 1968; Schultz, 1965), plasma (Winkelmann, 2003) and friction welding or explosion cladding (Achar *et al.*, 1980a; Lison, 1976) to the use of friction stir welding (Fukomoto *et al.*, 1996; Kawai *et al.*, 1998) and high-power beam processes such as electron beam welding (Dorn, 1969; Küber, 1970; Metzger and Lison, 1972; Bach *et al.*, 2005) and laser beam welding (Radscheidt, 1997; Zerner and Schubert, 1999; Zerner *et al.*, 1999; Kreimeyer *et al.*, 2002a; Kreimeyer *et al.*, 2002b). Some more recent work is summarised in Table 11.3.

With regard to joining aluminium to steel either for tailored blanks or for three-dimensional structural elements, aside from friction stir welding (Uzun *et al.*, 2005), mainly arc and laser beam processes, which are well-established for conventional, non-dissimilar joining, are discussed in the following. The basic challenge in all cases is to reduce heat input and

Table 11.3 Recent works on thermal joining of aluminium to steel

Joining process	References	Filler material	Joint geometry	Phase layer thickness
Brazing	e.g. Achar *et al.* (1980a)	Si-based	Overlap joint	n.a.
Soldering	e.g. Haferkamp *et al.* (2004)	$AlSi_{12}$, $ZnAl_4$	Overlap joint/butt joint	2 μm
Diffusion welding	Crane (1967)	n.a.	Butt joint	n.a.
WIG/MIG welding	Jüttner *et al.* (2003)	$AlSi_{12}$	Overlap joint/butt joint	2–3 μm
Cold metal transfer (CMT)	Bruckner *et al.* (2004)	n.a.	Overlap joint	2–3 μm
Plasma brazing	e.g. Winkelmann (2003), Kreimeyer *et al.*, 2004	$AlSi_{12}$	Overlap joint	<2 μm
Electron beam welding	Küber (1970)	$AlSi_{12}$	Overlap joint/butt joint	<2 μm
Laser-assisted pressure welding	Klein (1998)	n.a.	Overlap joint	No phase layer detected
Laser brazing	e.g. Haferkamp *et al.* (2004), Kreimeyer *et al.* (2001)	$AlSi_{12}$, $ZnAl_2$, $ZnAl_4$	Overlap joint/butt joint	1–2 μm
Resistance stud welding	Rudolf *et al.* (2004)	n.a.	Overlap joint	No phase layer detected
Friction welding	Streinz (1998)	n.a.	Butt joint	<0.8 μm
Friction- / arc stud welding	Achar *et al.* (1980a)	n.a.	Butt joint	No phase layer detected
Friction stir welding	e.g. Uzun *et al.* (2005)	n.a.	Overlap joint/butt joint	No phase layer detected
Explosive cladding	Achar *et al.* (1980a)	n.a.	Large area overlap joint	No phase layer detected

Note: n.a. = no information available.

increase cooling rate in order to minimise the thickness of the intermetallic phase layer.

Aside from some studies reporting efforts to optimise the time–temperature cycle in the joining zone by simple geometrical manipulations, e.g. a special MIG torch position to melt only the aluminium side (Jüttner *et al.*, 2003), mainly advanced arc processes with controlled heat input are considered for joining aluminium to steel. The CMT (cold metal transfer) process (Bruckner *et al.*, 2004) as well as the ColdArc process (Lorenz, 2005; Goecke, 2005); both essentially controlled MIG processes, have been applied successfully to the task. The intermetallic phase layer thickness was found to be in the range of 2–3 μm, resulting in a static strength of up to 175 MPa (Bruckner *et al.*, 2004). Winkelmann (2003) reported the use of a plasma arc for joining aluminium to steel in an overlap configuration and with zinc-based filler wires. However, as with all arc-based joining processes, the joining speed is relatively low, in this case in the range of 0.2 m min^{-1}.

Neglecting the process laser-assisted pressure welding specially designed for linear overlap joints only (Klein, 1998), flexible laser-based joining processes can generally be grouped into processes designed to melt only the aluminium side of the joint with or without filler wire and in laser brazing processes, trying to avoid the melting of both base materials.

In the latter processes, high-power diode lasers (Saida *et al.*, 2004) or Nd:YAG lasers (e.g. Waldmann *et al.*, 2001) are mostly used for standard seam geometries such as raised edge welds (Waldmann *et al.*, 2002) and fillet welds in overlap configuration (Mathieu, 2003). As filler materials, a wide range of alloy systems based on either zinc (e.g. Waldmann *et al.*, 2002), aluminium (e.g. Mathieu, 2003) and silver (Haferkamp *et al.*, 2004) is considered. Partly depending on the selection of filler materials as well as on the surface layer of the steel (zinc-coated or not), the use of flux is suggested. Phase layer thicknesses as low as 2 μm were obtained (Saida *et al.*, 2004). The joints achieved static strengths in the range of 180 to 200 MPa (Waldmann *et al.*, 2002; Mathieu, 2003), mostly failing in the heat-affected zone of the aluminium.

The other processing approach, i.e. melting the aluminium and wetting the steel with the aluminium melt has been pursued since the 1990s. Radscheidt and colleagues (Radscheidt, 1997; Zerner and Schubert, 1999; Zerner *et al.*, 1999) presented such a process for joining aluminium to steel in overlap configuration (sheet thickness ~1 mm), using a specially designed welding head. By optimising heat input, the formation of intermetallic phases could be restricted significantly (Sepold, 2001). In order to ensure a sufficient wetting, flux was applied.

For joining of aluminium to (preferably zinc-coated) steel in butt joint configuration, a laser-based joining process using either CO_2 or Nd:YAG laser (Kreimeyer *et al.*, 2002a) for sheet thicknesses in the range of 1 mm

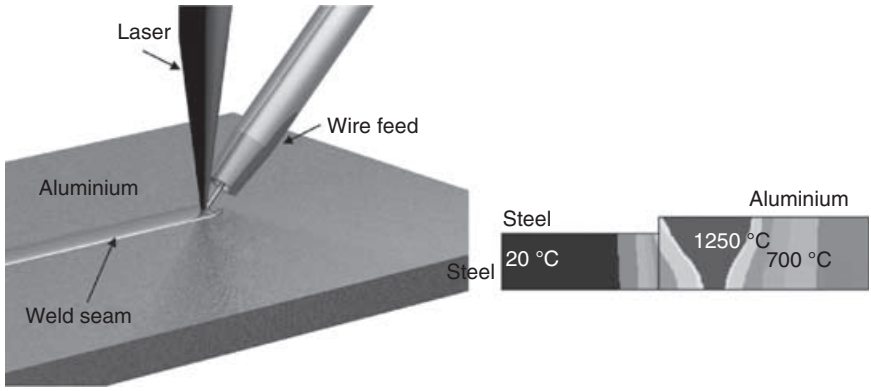

11.2 Process principle and temperature distribution for aluminium–steel butt joints obtained by laser beam welding (Kreimeyer *et al.*, 2002a).

was developed. The laser beam is positioned completely on the aluminium side of the joint to obtain a deep-penetration weld (Fig. 11.2). The molten aluminium then wets the steel sheet (to which flux is applied). For process stabilisation, filler wire is used. Crucial factors of influence are the exact positioning of the beam relative to the interfacial region between aluminium and steel and the use of specially designed clamping devices to avoid the opening of a gap during the process. Using an Nd:YAG-laser with 4 kW power, a joining speed of up to approx. 8 m min^{-1} was demonstrated, with the joints mostly failing in the aluminium.

11.2.4 Conclusions

In the past two decades, various processes have been proposed for joining steel to aluminium. With regard to the task of joining tailored blanks or three-dimensional structural elements, mainly arc or laser-based processes have to be considered. Whereas arc-based processes are mostly characterised by some gap bridging ability, but at a comparatively low joining speed, those laser-based joining processes including the melting of the aluminium base material demonstrated a significantly higher joining speed. However, they require a zero gap condition. Therefore, for both tasks, optimised yet flexible joining processes with good productivity are required. In particular, the joining of thicker sheets (>2 mm) and the reduction of fit-up and clamping requirements (in view of gap tolerance) should be aimed at. Moreover, the aspect of flux-reduced or flux-less joining is of persistent interest. As for the properties of the joints, a deepened insight into the composition and

influence of the intermetallic phase layer especially on the mechanical and technological properties of the joint is desirable.

11.3 Basic features of laser MIG hybrid welding for dissimilar metals

In laser MIG hybrid welding of dissimilar metals, which was first suggested by Kreimeyer and Vollertsen (2006) and developed further by Thomy *et al.* (Schilf *et al.*, 2007; Thomy *et al.*, 2007a; Thomy *et al.*, 2007b; Thomy *et al.*, 2007c; Thomy *et al.*, 2008; Wirth *et al.*, 2007a; Wirth *et al.*, 2007b), a laser beam (CO_2, Nd:YAG, Yb fibre or Yb:YAG) and a MIG–arc operated in the pulsed mode are used. In Fig. 11.3, the process principle is depicted. An aluminium and a steel sheet are arranged preferably in butt joint configuration, also allowing gap. The laser beam is positioned on the aluminium side. During joining, the edge of the aluminium sheet is molten, and together with the molten wire, the gap between the aluminium and the steel is bridged and the steel is wetted by the aluminium melt. The main task of the sub-process MIG welding is to create a large melt pool and to supply filler material to the melt pool to influence the metallurgy of the weld and increase the melt volume further, thus contributing to an improved wetting. The sub-process laser beam welding, which is operated in keyhole mode to supply the heat uniformly in the direction of depth, allows to increase the welding speed by stabilising the MIG arc, thus reducing heat input and, as

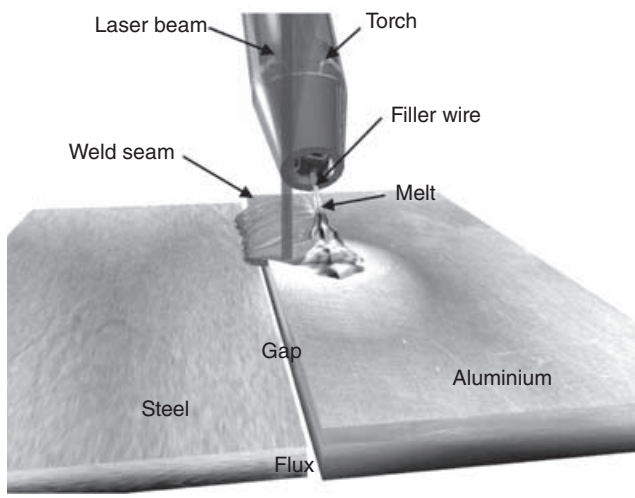

11.3 Principle of the laser MIG hybrid joining process.

a consequence, the negative effects of heat input such as excessive phase layer formation and distortion.

In general, the advantage of this process compared with most of the state-of-the-art laser-based processes is its ability of gap bridging of up to 1 mm (Kreimeyer and Vollertsen, 2006). Moreover, compared with arc-based joining processes, a higher processing speed, which is exceeding 6 m min^{-1} in thin-sheet applications, is achieved (Thomy *et al.*, 2008).

The most important parameters in this process for the given application are laser power, welding speed, MIG power, wire feed rate and the position of the MIG arc relative to the gap, which all have to be optimised to both obtain an adequate weld in the aluminium and a sufficient wetting of the steel with a minimum intermetallic phase layer. Thus, the challenges of hybrid welding of aluminium (see Chapter 10 for details) are combined with the specific challenges of joining dissimilar materials. The effect of the governing parameters on process and properties will be discussed in the next section.

11.4 Process and joint properties

The investigations reported in the following were carried out predominantly by Thomy *et al.* (Thomy *et al.*, 2007a; Thomy *et al.*, 2007b; Thomy *et al.*, 2008; Wirth *et al.*, 2007a; Wirth *et al.*, 2007b). Base materials were predominantly aluminium AA6016 (thickness: 1.15 and 2 mm) and zinc-coated steel DC05 + ZE (thickness: 1 mm); AlSi12 wire (diameter 1.2 mm) was used as filler material. In all cases, Flux F400NH (Fontargen) was applied on the uncoated face side of the steel sheets. Sheets were arranged in butt joint geometry with gap of 0–1 mm; the typical welding speed was in the range of 6.0 m min^{-1}.

11.4.1 Microstructure of dissimilar aluminium–steel joints

Figure 11.4 gives the top bead appearance and the cross-section of a typical aluminium–steel joint obtained by laser MIG hybrid welding. The laser

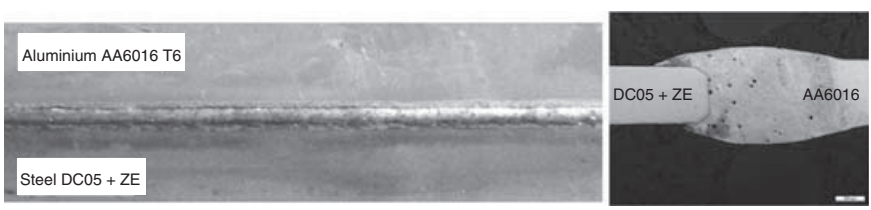

11.4 Top view and cross-section of a laser MIG hybrid welded aluminium–steel specimen.

power was 2.4 kW; the arc power was 2.49 kW. Welding speed and wire feed rate were 6 m min^{-1}. It is obvious from Fig. 11.4 that the seam is smooth and its width (i.e. the wetting length) is fairly constant over the seam length. There is no melting of the steel sheet, and the weld has only few small pores close to the face side of the steel sheet. This is attributed to the use of flux on the face side, which can contain humidity and, as a consequence, be a source of hydrogen to the melt pool.

A closer look on the cross-section of aluminium–steel joints by SEM reveals the existence of an intermetallic phase layer (Fig. 11.5). The images (SE- and BSE-composition measurement) are taken from the top, bottom and face side of the joining zone. The thickness of the phase layer is nearly

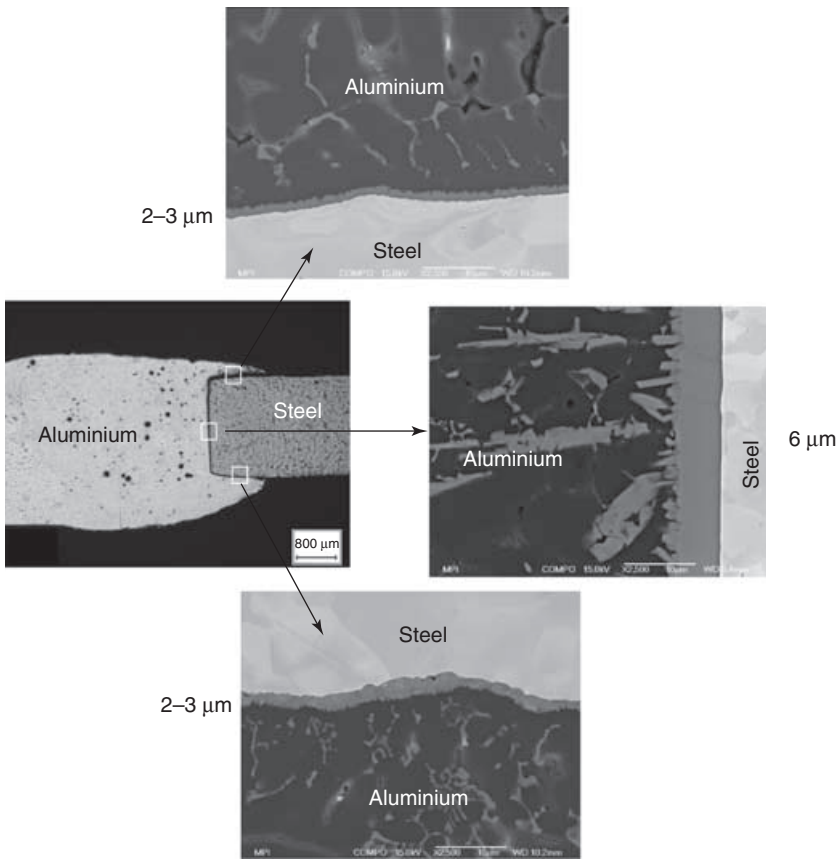

11.5 SEM images of the phase seam in the top, face and bottom region of a laser MIG hybrid welded aluminium–steel specimen aluminium EN AW-6056 (thickness 3.8 mm); steel THM 180BH + Z (thickness 1.95 mm)] (Courtesy: MPIE, Düsseldorf).

the same size on the top and the bottom side of the joining zone (2–3 μm). The phase layer on the face side has a thickness of approximately 6 μm. Obviously, the top and bottom phase seams have no needle-shaped structures growing into the aluminium on the intermetallic boundary. The phase seam on the face side, which is mostly associated with failure in tensile tests (see section 11.4.3), was analyzed by EDX and EBSD to gather further information on the composition of the phases (Fig. 11.6). The EDX results demonstrate that the phase seam contains aluminium as well as iron. The needle-shaped structures on the phase seam contain less iron than the phase seam. To clarify this situation, EBSD analysis was performed on this region (Fig. 11.6). It is obvious that the phase seam consists of two different Al–Fe structures. Using the data of the EDX and EBSD results, the two Al–Fe phases can be set to Al_3Fe and Al_5Fe_2. The phase Al_5Fe_2 forms a continuous layer between the aluminium and the steel. Crystal orientation analysis shows Al_5Fe_2 grains extending from the aluminium to the steel side with a length of 4–6 μm. The width of these grains is up to 7 μm in this area. The grains are oriented between the [100] and [010] zone. Only some small grains are oriented near the [001] zone axis (Fig. 11.7). Regarding crystal orientation, there seems to be a preferred growth direction for Al_5Fe_2 in

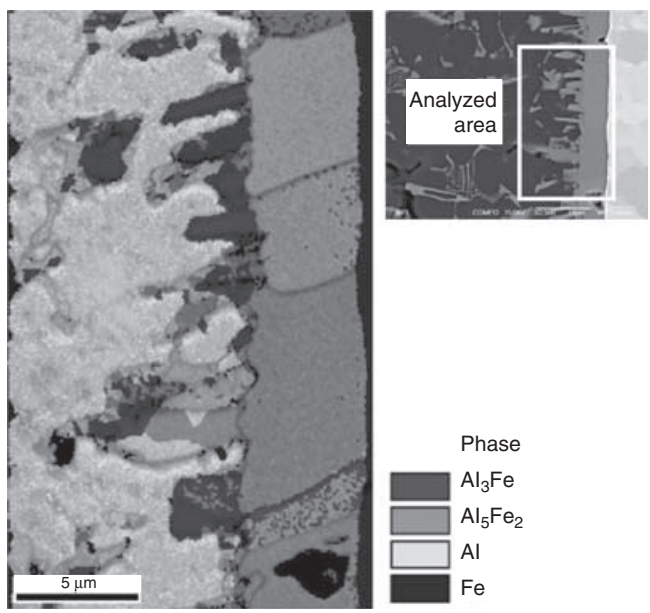

11.6 EBSD Image of part of the phase seam on the face side [aluminium EN AW-6056 (thickness 3.8 mm); steel THM 180BH + Z (thickness 1.95 mm)] (Courtesy: MPIE, Düsseldorf).

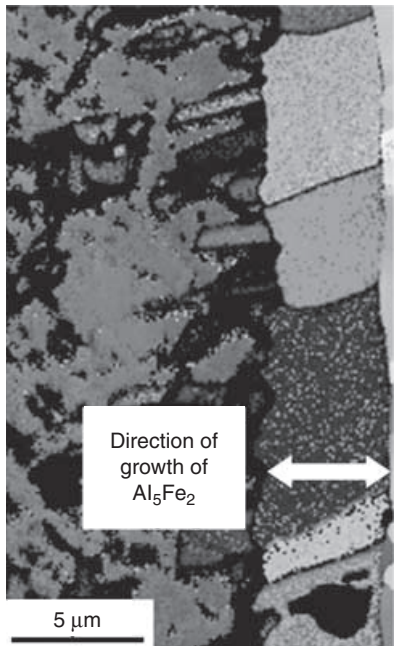

11.7 Orientation of the grains in the joining zone [aluminium EN AW-6056 (thickness 3.8 mm); steel THM 180BH + Z (thickness 1.95 mm)] (Courtesy: MPIE, Düsseldorf).

(001), which means that it is perpendicular to the steel sheet surface. The phase Al_3Fe forms columnar structures growing into the aluminium base material. The length of the columnar Al_3Fe structures can not be measured by this method, as the whole columns are likely not to be in the same plane.

As a result, it can be concluded that the intermetallic phase layer in the joining zone of aluminum-steel hybrid blanks produced by laser MIG hybrid joining consists of the two phases Al_3Fe and Al_5Fe_2. Initially, only the Al_3Fe-phase is created during heating by diffusion of Fe atoms into the aluminum as a layer between the two metal sheets. The continuous phase of Al_5Fe_2 is created by diffusion of Al atoms into the iron at temperatures above the melting temperature of aluminum (Radscheidt, 1997). This is in accordance with the results presented, because the intermetallic grains seem to grow from the aluminum to the steel as the grain size ranges over the whole phase seam. The formation of the needle-shaped Al_3Fe phase should be connected to the cooling at temperatures between 500 and 350 °C. As this phase is clearly visible on the face side of the aluminum–steel joint, the cooling rate in this region should have been much slower than on the top and bottom side of the joining zone. The phase layers on these sides do not contain any

obviously visible Al_3Fe needles. As the diffusion is dependent on time and temperature, the cooling interval between 500 and 350 °C must have been passed too fast for the visible formation of Al_3Fe needles. Concerning crack growth, the Al_3Fe phase is probably not responsible for the failure as the columnar shapes are protruding into the aluminum and are thus embedded into a ductile matrix. It is more likely that failure is associated with the brittle continuous Al_5Fe_2 phase seam. Therefore, the effect of process parameters on this phase and on further joint properties will be discussed in the next section.

11.4.2 Effect of process parameters in laser MIG hybrid welding of dissimilar aluminium–steel joints on their properties

In order to assess the effect of process parameters in laser MIG hybrid welding of aluminium to steel, aside from an evaluation of the seam surface quality and the results of tensile tests, the comparison of micro-geometrical parameters taken from cross-sections is helpful. In particular, the wetting length on top and bottom as well as the respective seam reinforcements can be used (Fig. 11.8). Moreover, phase layer thickness (Al_5Fe_2) on the top,

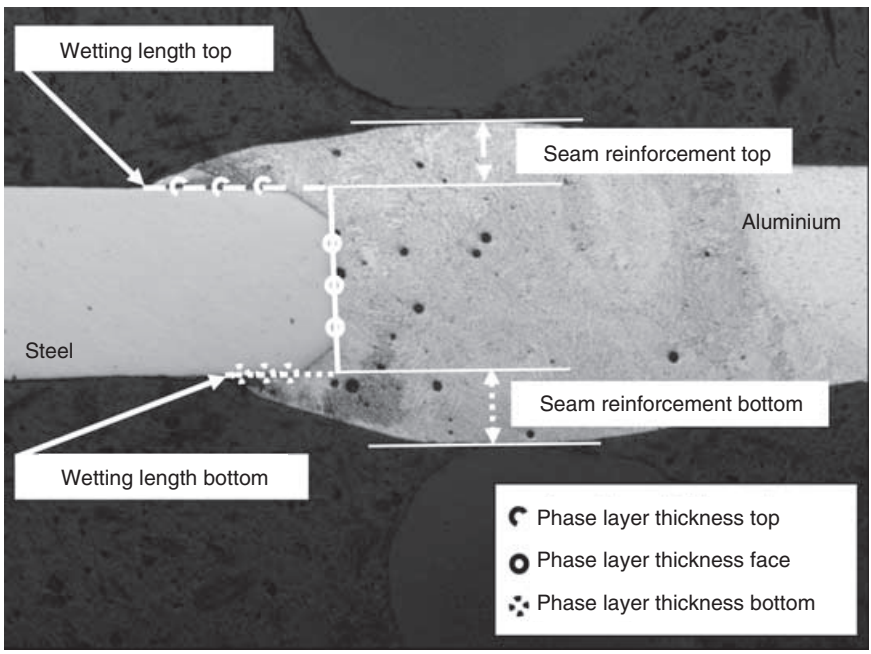

11.8 Micro-geometrical parameters for seam assessment.

bottom and face sides, taken in three equally distributed points and then averaged, is an important measure. In the following, the effect of laser power, MIG power, welding speed and position of the MIG arc relative to the aluminium sheet edge will be discussed for the case of Nd:YAG laser MIG hybrid welding with respect to wetting length, seam reinforcement, phase layer thickness and tensile strength (calculated relating to the aluminium cross-section).

On the top, bottom and face sides, there is a slight trend towards an increase in phase layer thickness with increasing laser power, which is attributed to a slower cooling time and therefore a longer time in the temperature interval promoting diffusion (Fig. 11.9). However, the phase layer thickness remains well below 4 μm. If the laser power exceeds 3300 W, there is a significant increase in phase layer thickness to 12 μm on the average at otherwise unchanged parameters, and cracking under the action of residual stresses occurs. However, if laser power is less than 3200 W, there is no significant effect on tensile strength, which is in the range of 180 MPa for all laser powers. Top and bottom wetting length as well as the respective seam reinforcements are not significantly affected as well.

A similar trend is found with MIG arc power, which was varied via arc current in from 2000 to 4000 W. Again, the phase layer thickness was less than 4 μm for all arc powers. However, owing to a destabilisation of the process with higher currents, the regularity of the seam especially in view of wetting length deteriorated slightly, and scatter in the tensile tests

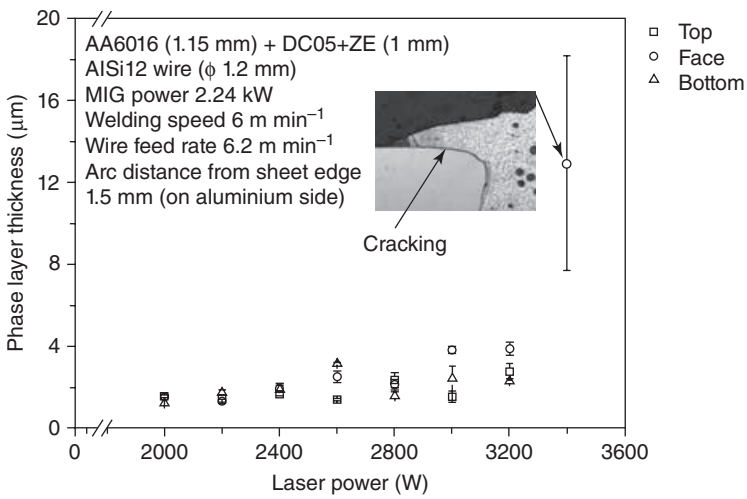

11.9 Effect of laser power on phase layer thickness in laser–MIG hybrid welding.

increased, which makes it recommendable to limit the arc power to approx. 3200 W to safely obtain a tensile strength of more than 170 MPa.

Welding speed at otherwise unchanged parameters (especially wire feed rate) has a significant influence on wetting behaviour. If welding speed is increased to more than approximately 6.5 m min^{-1} for a wire feed rate of 6.2 m min^{-1} (wire diameter 1.2 mm), wetting at the bottom side is insufficient. Further investigations demonstrated that wire feed rate and welding speed should be in the same range to provide sufficient amount of melt in the lower seam area. If this is not the case and wetting is insufficient, tensile strength is drastically reduced (Fig. 11.10). Moreover, wetting length decreases, and seam reinforcement increases with increasing welding speed, as the time of existence of the melt pool at a given location is decreased, thus decreasing the time available for wetting. The thickness of the intermetallic phase layer, however, is not affected by welding speed (for 5–7 m min^{-1}) and, provided sufficient wetting on both sides is obtained, the average tensile strength remains conveniently above 180 MPa.

The position of the MIG arc relative to the sheet edges is of crucial importance (Fig. 11.11). If the arc foot point (projection of the wire on the aluminium sheet) is further than 1.5 mm away from the sheet edge (for the given processing conditions, especially arc current), no wetting on the lower side occurs. However, moving the arc closer to the aluminium edge, phase layer thickness is increased. If the arc is positioned on the sheet edge or on the steel side, the process is greatly destabilised, and tensile strength is

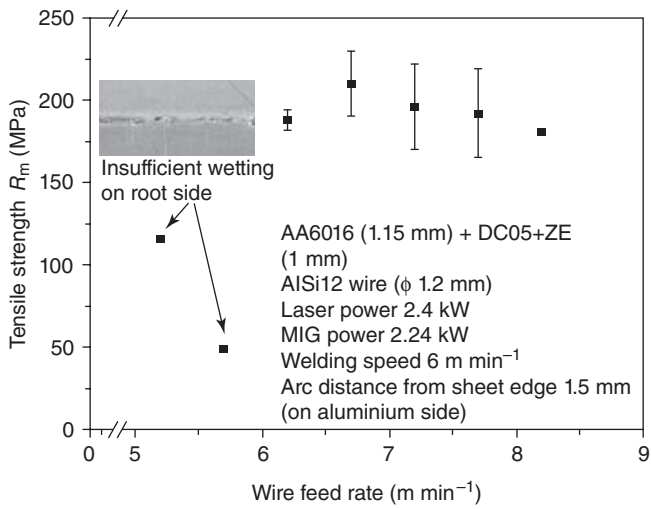

11.10 Effect of wire feed rate on tensile strength in laser–MIG hybrid welding.

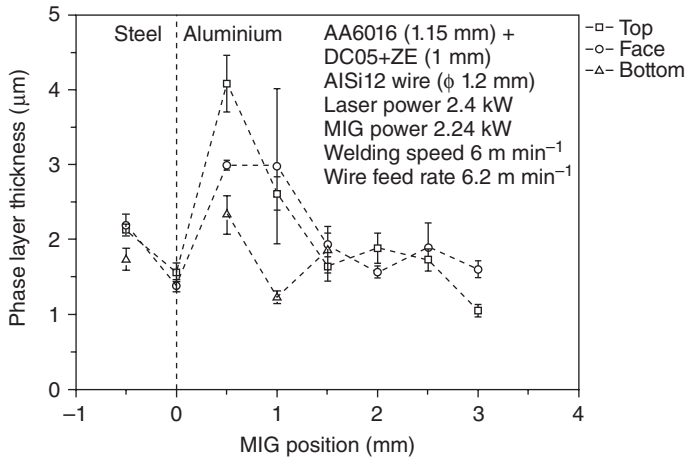

11.11 Effect of MIG position relative to sheet edge on phase layer thickness in laser–MIG hybrid welding.

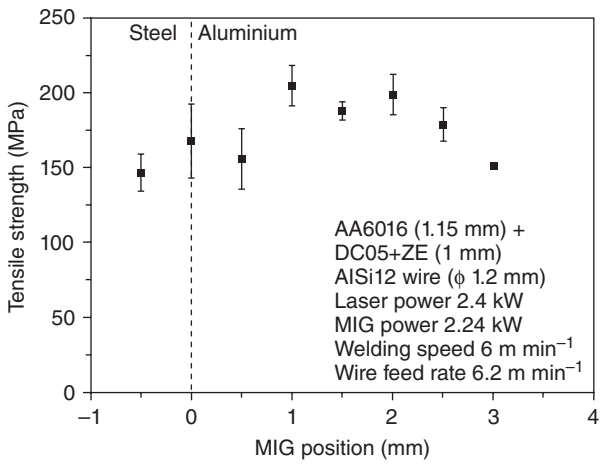

11.12 Effect of MIG position relative to sheet edge on tensile strength in laser–MIG hybrid welding.

reduced. For tensile strength, the best results are obtained for a MIG position between 1 and 2 mm from the sheet edge on the aluminium side (Fig. 11.12).

Based on the above considerations, a process parameter envelope to reproducibly produce aluminium–steel tailored hybrid blanks can be established, systematically varying parameters based on a restriction of heat

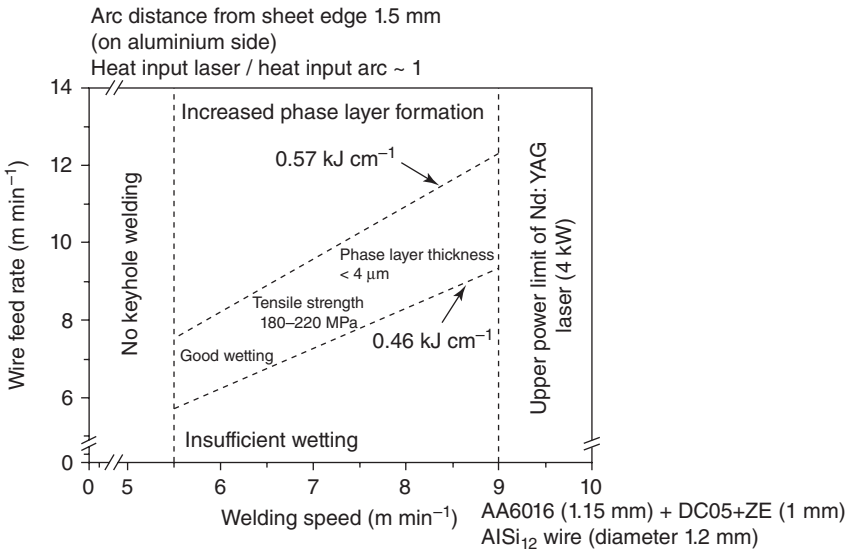
Arc distance from sheet edge 1.5 mm
(on aluminium side)
Heat input laser / heat input arc ~ 1
Increased phase layer formation
0.57 kJ cm−1
Phase layer thickness
< 4 µm
Tensile strength
180–220 MPa
0.46 kJ cm−1
Good wetting
Insufficient wetting
No keyhole welding
Upper power limit of Nd: YAG
laser (4 kW)
Wire feed rate (m min−1)
Welding speed (m min−1)
AA6016 (1.15 mm) + DC05+ZE (1 mm)
AlSi12 wire (diameter 1.2 mm)

11.13 Process parameter envelope for laser–MIG hybrid welding of aluminium to steel.

input between 0.46 and 0.57 kJ cm^{-1} and an approximately constant ratio of heat input by arc and laser beam of 1 (Fig. 11.13). In this parameter envelope, sufficient wetting is obtained, phase layer thickness is less than or equal to 4 µm and tensile strength is in the range of 180–220 MPa, which is in the range typical for all thermal joining processes for aluminium to steel (section 11.2.3).

11.4.3 Mechanical and technological joint properties

For specimens produced within the above parameter envelope, cracking under tensile load always occurs at the face side of the joint along the intermetallic phase layer and into the aluminium (Fig. 11.14). The crack typically seems to start at small imperfections such as pores and grow along the aluminium–steel interface in the intermetallic phase layer. The intermetallic phase layer remains on the steel side or on the aluminium side, a behaviour which is not consistent for different samples. When the crack reaches the edge of the steel sheet, it deviates into the aluminium seam. Fatigue data can be taken from Kreimeyer and Vollertsen (2006) and Thomy *et al.* (2007b).

In the bend test (Fig. 11.15) (bend angle 180°, bend radius 10 mm), the formability of aluminium–steel tailored hybrid blanks can be demonstrated.

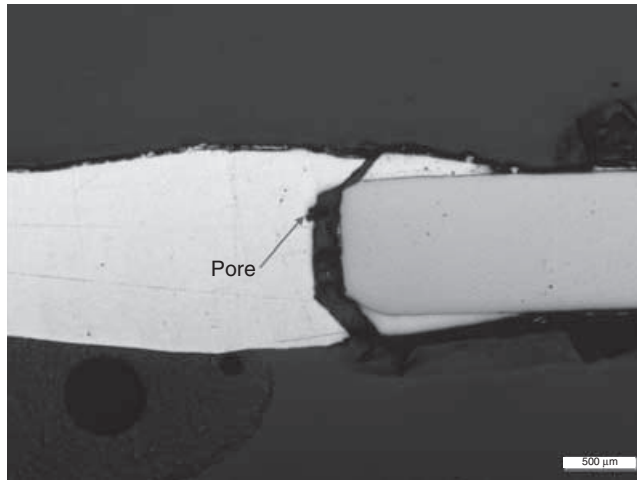

11.14 Cracking of an aluminium–steel specimen (AA6016 (thickness: 1.15 mm) and zinc coated steel DC05 + ZE (thickness: 1 mm)) under tensile load (tensile strength 193 MPa).

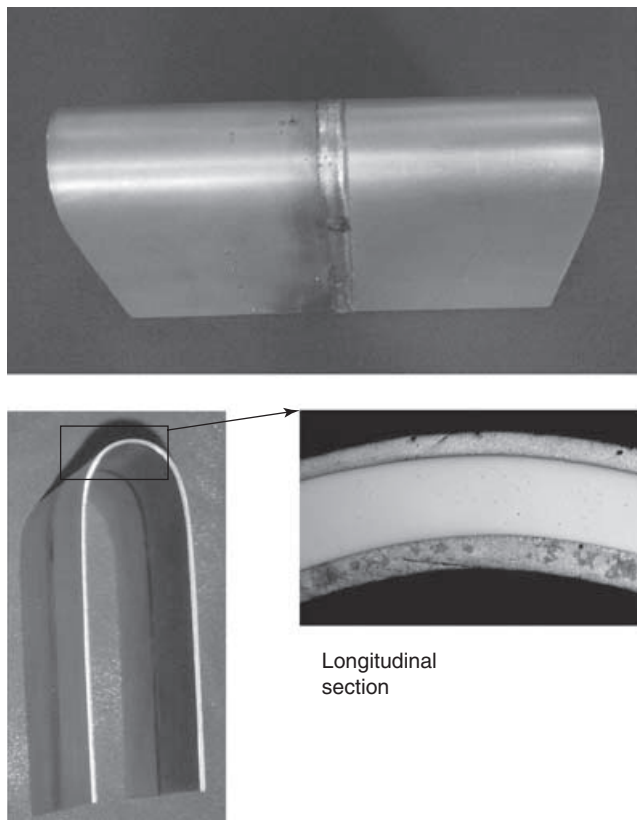

11.15 Bend test, radius 10 mm, angle 180° for AA6016 (thickness: 1.15 mm) and zinc-coated steel DC05 + ZE (thickness: 1 mm).

For these conditions, no cracks or delaminations in the seam occur. For multi-axial stress situations such as in deep drawing, formability may be an issue, as the limit drawing ratio in cup deep drawing is currently limited to 1.6. This requires special considerations for an optimum position of the seam in deep drawing.

11.4.4 Conclusions

From the above details, it can be concluded as follows:

- Feasible joints between aluminium and steel can be obtained by laser MIG hybrid welding, directing the process onto the aluminium and wetting the unmolten steel with the aluminium melt.
- An intermetallic phase layer is formed between the aluminium and the steel, consisting of Al_5Fe_2 with a preferred direction of growth rectangular to the face side of the plates, and adjacent needle-shaped Al_3Fe phases with no preferred direction of growth.
- Generally, the phase layer is thicker and contains more Al_3Fe in those areas of cross-section, where cooling rate is slower.
- Process parameters do have a significant influence on joint properties and should be selected as follows:
  - restrict laser power to minimise phase layer thickness;
  - restrict MIG power to stabilise the process and allow a tensile strength of more than 180 MPa;
  - choose a sufficient wire feed rate for a given welding speed to obtain sufficient wetting;
  - precisely position the MIG arc at an adequate distance from the sheet edge on the aluminium side.
- Based on these considerations, a parameter envelope can be established, which allows a reproducible production of joints with optimised properties, especially a tensile strength exceeding 180 MPa.
- For tensile load in butt joints, the crack grows along the intermetallic phase layer and deviates into the aluminium seam.
- For optimised processing conditions, tailored hybrid blanks can be produced, which withstand a bend test and yield a limit drawing ratio of 1.6.

11.5 Application potentials

One potential application for Nd:YAG laser MIG hybrid welding of dissimilar materials is the production of tailored hybrid blanks from aluminium- and zinc-coated steel. An example of such a tailored hybrid blank is displayed in Fig. 11.16. Both sheets with a length of 400 mm are

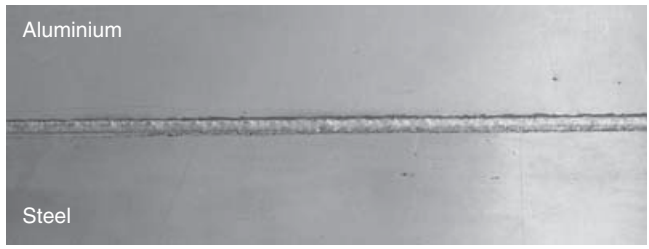

11.16 Example for an aluminium–steel tailored hybrid blank joined by laser MIG welding.

11.17 Aluminium–steel tailored hybrid tube joined by laser MIG hybrid welding.

joined at a competitive speed of 6 m min^{-1}. The tailored hybrid blank passes bend test and exhibits sufficient forming properties with a drawing limit ratio of 1.6 (section 11.4.3). Consequently, and taking into account the limits in formability, these hybrid blanks may be used in lightweight structures in a similar way to that of conventional tailored blanks.

Another application is the welding of tailored hybrid tubes or other three-dimensional structural elements (Thomy *et al.*, 2007a; Thomy *et al.*, 2007b). As an example, the tube displayed in Fig. 11.17 is produced by

Nd:YAG laser MIG hybrid welding (welding speed 4 m min^{-1}) from aluminium and zinc-coated steel tubes with a diameter of approximately 10 cm. Joint configuration is fillet welding in overlap configuration, with the aluminium tube on top. Similar elements and structures may be used for structural elements (e.g. axles) in the automotive industry.

In addition to the automotive industry, shipbuilding may also be a potential field of application. In modern shipbuilding (especially of yachts and military vessels), material combinations of aluminium and steel are already used in order to improve structural properties, particularly stiffness, weight and position of the centre of gravity. Owing to a beneficial influence on the position of the centre of gravity of the ship structure, the hull is normally manufactured from steel, whilst the upper decks or the deckhouse are made from aluminium alloys. A structural part of a yacht deckhouse (steel on the lower part of the demonstrator and aluminium on the upper part, thickness 3 mm each, length 1 m) joined in butt joint configuration by laser MIG hybrid welding using a CO_2 laser is shown in Fig. 11.18 (Schilf *et al.*, 2007; Thomy *et al.*, 2007c). With this demonstrator produced in an industrial environment, a static strength of up to 140 MPa was achieved. This is a significant improvement compared with the so-called 'Triclad®' profiles (explosion welded transition profiles between aluminum and steel) used in shipbuilding today.

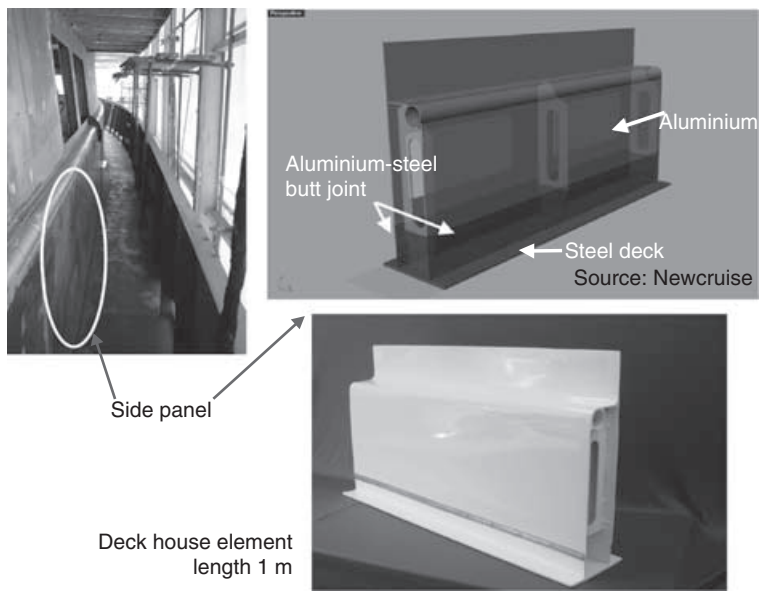

11.18 Concept for aluminium–steel in yacht construction and yacht deckhouse element produced accordingly (length: 1 m, material thickness: 3 mm).

The above examples illustrate the potentials for laser–MIG hybrid welding of aluminium to steel for tailored blanks as well as for structural applications. Although this process has not yet been applied in industrial production, it is to be expected that this will happen in the near future. Some future trends will be considered in section 11.6.

11.6 Future trends

The necessity for joining dissimilar materials such as aluminium and steel is certain to arise owing to the increasing demands for optimised, lightweight structures. Compared with other state-of-the-art thermal joining processes for such dissimilar material combinations, laser–MIG hybrid welding has the advantages of a high joining speed and good gap bridging ability. A further advantage is that hybrid welding can also be used for thicker aluminium–steel joints (3–5 mm). This should make laser MIG hybrid welding of aluminium to steel an attractive process for both tailored blanking and structural applications especially in the transportation industries.

However, there are still some challenges which have to be considered. Although the formation of intermetallic phases and the effects of process parameters are already well understood, fracture behaviour is still brittle, which may raise concerns in view of crash safety. Moreover, forming behaviour should be further enhanced to increase the flexibility in use of tailored hybrid blanks. Finally, some flux is still required, and only recently first trials using a coaxial laser–plasma hybrid welding process have demonstrated the feasibility of a completely flux-less joining using a coaxial laser–plasma hybrid welding process (Goecke *et al.*, 2008).

In conclusion, it should be expected that the first industrial applications for selected parts will be implemented in the next few years.

11.7 References

ACHAR D R G, RUGE J and SUNDARESAN S (1980a), 'Verbinden von Aluminium mit Stahl, besonders durch Schweißen', *Aluminium*, 56(2), 174–193.

ACHAR D R G, RUGE J and SUNDARESAN S (1980b), 'Metallurgical and mechanical investigations of aluminium–steel fusion welds', *Aluminium*, 56(6), 391–397.

ANDREWS D R (1962), 'Joining aluminium to mild steel by argon arc welding', *British Welding Journal*, (12), 650–658.

BACH F-W, BENIYASH A, LAU K and VERSEMANN R (2005), 'Joining of steel-aluminium hybrid structures with electron beam on atmosphere', *Advanced Materials Research*, (6–8), 143–150.

BARGEL H-J and SCHULZE G (2000), *Werkstoffkunde*, 7th ed., Springer, Berlin.

BERGMANN H W, WALDMANN H, GUYENOT M, HALDENWANGER H G and KORTE M (2000), 'Untersuchungsergebnisse zum Laserschweißen von Aluminium auf Stahl für

Außenhautanwendungen', in *Proc. European Automotive Laser Application EALA 2002*, Automotive Circle International, Berlin.

BRUCKNER J, HIMMELBAUER K and HACKL H (2004), 'Der CMT-Prozess und seine Möglichkeiten, im Speziellen das Fügen von Stahl mit Aluminium', in *DVS-Berichte 231*, Düsseldorf, DVS–Verlag, 201–204.

BRUCKNER J and HIMMELBAUER K (2005), '"Cold metal transfer" – Ein neuer Prozeß in der Fügetechnik', in *Schweißen und Schneiden 2005*, DVS-Berichte 237, Düsseldorf, DVS–Verlag, 32–43.

BUDDE L and PILGRIM R (1995), *Stanznieten und Durchsetzfügen*, Verlag Moderne Industrie, Landsberg.

BUDDE L, WIDDER T and BISCHOFF J (1997), 'Wärmearmes Fügen von Magnesiumwerkstoffen im Fahrzeugbau', *Adhäsion*, (10), 13–16.

CRANE C H (1967), 'Diffusion welding of dissimilar metals', *Welding Journal*, **46**, 23–31.

DORN L (1969), *Untersuchungen zum Elektronenstrahl-Schweißvorgang und zum Festigkeitsverhalten elektronenstrahlgeschweißter Metallverbindungen*, Dissertation, TU Hannover.

FUKOMOTO S *et al.* (1997), 'Evaluation of friction weld interface of aluminium to austenitic stainless steel joint', *Materials Science and Technology*, **13**(8), 679–686.

GEBHARDT E and OBROWSKI W (1953), 'Reaktionen von festem Eisen mit Schmelzen aus Aluminium und Aluminiumlegierungen', *Zeitschrift für Metallkunde*, **44**(1), 12–17.

GHANAM H M (1968), *Untersuchungen zum maschinellen WIG-Schweißen von Aluminium mit unlegiertem Baustahl für Punkt und Nahtverbindungen*, Dissertation, RWTH Aachen.

GOECKE S F (2005), 'Energiereduziertes Lichtbogen-Fügeverfahren für wärmeempfindliche Werkstoffe', in *Schweißen und Schneiden 2005*, DVS-Berichte **237**, Düsseldorf, DVS–Verlag, 44–48.

GOECKE S F, WILDEN J, JAHN S, REICH S, FEDTKE A, VOLLERTSEN F and THOMY C (2008), 'Technologiekette zum Produzieren, Reparieren und Recyceln von Produkten in Material-Mix-Bauweise – PROREMIX', *Die Verbindungs Spezialisten 2008*, DVS-Berichte **250**, Düsseldorf, DVS–Verlag, 375–378.

HAFERKAMP H, ENGELBRECHT L, OSTENDORF A, BUNTE J and CORDINI P (2004), 'Laserstrahllöten von tailored-hybrid-blanks aus nicht artgleichen Leichtbauwerkstoffen', in *DVS-Berichte* **231**, Düsseldorf, DVS–Verlag, 211–216.

HAHN O *et al.* (2004), 'Neuartige Stanzniet und Clinchverfahren zum Verbinden artverschiedener Werkstoffe', in *Schweißen und Schneiden 2003*, DVS-Berichte **232**, Düsseldorf, DVS–Verlag, 158–164.

HARTWIG H and KOUPTSIDIS J (1978), 'Schweißverbindungen zwischen AlMgSi0,5 und X5CrNi189 für das Vakuumsystem von Hochenergiebeschleunigern', *Schweißen und Schneiden*, **30**(2), 45–47.

JÜTTNER S, WINKELMANN R, FÜSSEL U, VRANAKOVA R and ZSCHETZSCHE J (2003), 'Fügen von Aluminium mit Stahl mittels Lichtbogenverfahren', in *Schweißen und Schneiden 2003*, DVS-Berichte **225**, Düsseldorf, DVS–Verlag, 377–382.

KAWAI G, OGAWA K and TOKISUE H (1998), Friction welding of 6061 aluminium alloy pipe to S25C carbon steel pipe', *International Journal of Off-Shore and Polar Engineering*, **8**(2), 144–147.

KLEIN B (1997), *Leichtbau-Konstruktion*, Friedr. Vieweg & Sohn, Braunschweig/Wiesbaden.

KLEIN R (1998), 'Laserstrahlfügen von verzinktem Feinblech und Al/St-Verbindungen', In *Proc. Dünnblechverarbeitung*, SLV München, 233–241.

KREIMEYER M, WAGNER F, ZERNER I and SEPOLD G (2001), 'Laserstrahlfügen von Aluminium mit Titan unter Verwendung eines optimierten Arbeitskopfs', in *DVS-Berichte 212*, Düsseldorf, DVS–Verlag, 317–321.

KREIMEYER M, WAGNER F, SEPOLD G, CRIQUI B and JOLY M (2002a), 'Kombiniertes Schweiß-Lötverfahren zum Fügen von Aluminium- und Stahlblechen im Stumpfstoß mit Hochleistungslasern', *Proc. Schweißen und Schneiden 2002*, DVS-Berichte 220, Düsseldorf, DVS–Verlag, 256–261.

KREIMEYER M, WAGNER F and SEPOLD G (2002b), 'Combined welding-brazing process for joining aluminium–steel tailored blanks with high power sources', in *Proc. IBEC 2002*, CD-ROM.

KREIMEYER M, WAGNER F and VOLLERTSEN F (2004), 'Einfluss von Zinkbeschichtungen beim Laserstrahlfügen von Aluminium-Stahl-Überlappverbindungen', in *DVS-Berichte 231*, Düsseldorf, DVS–Verlag, 223–227.

KREIMEYER F and VOLLERTSEN F (2006), 'Gap tolerant joining of aluminum with steel sheets using the hybrid technique', in Ostendorf A, *Proc. 25th International Congress on Applications of Lasers & Electro-Optics ICALEO 2006*, 947–952.

KÜBER B (1970), 'Schweiß- und Lötverbindungen zwischen Aluminium und Stahlwerkstoffen', *Aluminium*, **46**(4), 304–310.

LISON R (1976), 'Zur Problematik der Schweißverbindungen zwischen unterschiedlichen Werkstoffen unter besonderer Berücksichtigung des Schmelzschweißens', *Schweißen und Schneiden*, **28**(3), 89–92.

LEUSCHEN B (1996), 'Fügen von Stahl, Aluminium und deren Kombination – Karosseriefügeverfahren im Vergleich', in *VDI-Berichte Nr. 1264*, VDI-Verlag, Düsseldorf (1996), 113–131.

LIU L, LIU X and LIU S (2006), ' Microstructure of laser–TIG hybrid welds of dissimilar Mg alloy and Al alloy with Ce as interlayer', *Scripta Materialia*, **55**, 383–386.

LORENZ H (2005), 'ColdArc – der kalte Lichtbogen. Neuartige Technologie macht Unmögliches möglich', *Stahl*, (1), 34.

MATHIEU A (2004), 'Assembly of steel–aluminium by laser beam', in Patel R, *Proc. 23rd International Congress on Applications of Lasers and Electro-Optics ICALEO 2004*, October 4–7, San Francisco, 148–154.

METZGER G and LISON R (1973), 'Schweißverbindungen an unterschiedlichen Werkstoffen, an Beispielen von Werkstoffpaarungen, die für den Einsatz in der Kerntechnik von Bedeutung sind', *Bericht der Kernforschungsanlage Jülich, Jül-1011-RW*, Oktober 1972, 95pp.

OSTERMANN F (1998), *Anwendungstechnologie Aluminium*, Springer, Berlin.

RABKIN D M and RJABOW W R (1967), 'Das Schweißen von Aluminium mit Stahl', *Schweißtechnik*, **17**(10), 448–454.

RADSCHEIT C (1997), *Laserstrahlfügen von Aluminium mit Stahl*, BIAS Verlag, Bremen.

RUDOLF H, GRAUL M, DORN L and KOPPE K (2004), 'Widerstandsbolzenschweissen für Mischbauweise und hochfeste Verbindungen Hart- und Hochtemperaturlöten und Diffusionsschweißen', in *DVS-Berichte 231*, Düsseldorf, DVS–Verlag, 253–258.

SAIDA K, SONG W and NISHIMOTO K (2004), 'Laser brazing of aluminium alloy to steels with aluminium filler metals', in *DVS-Berichte 231*, Düsseldorf, DVS–Verlag, 232–237.

SAUTHOFF G (1995), *Intermetallics*, VCH Verlagsgesellschaft, Weinheim.

SCHILF M, WISCHHUSEN B-M, THOMY C, VOLLERTSEN F and METSCHKOW B (2007), 'Ansätze zum Laserstrahlfügen für Aluminium-Stahl-Verbindungen im Schiffbau', *Die Verbindungs Spezialisten 2007*, DVS–Berichte 244, Düsseldorf, DVS–Verlag, 286–290.

SCHUBERT E and ZERNER I (1999), 'Lasergestütztes Fügen von Werkstoffkombinationen', *Blech Rohre Profile*, (4), 76–81.

SCHULTZ H (1965), 'Verbinden unterschiedlicher Metalle durch Schutzgas- und Elektronenstrahlschweißen', *Schweißen und Schneiden*, **17**(7), 288–297.

SEPOLD G (2001) 'Potentiale lasergefügter Mischverbindungen. Hochleistungsfügeverfahren', in *Proc. 7. Internationales Aachener Schweißtechnik Kolloquium*, Aachen, Shaker–Verlag, Vol. 1, 159–170.

STRASSBURG F W and WEHNER H (2000), *Schweißen nichtrostender Stähle*, 3rd ed., Düsseldorf, DVS-Verlag.

STREINZ W (1998), 'Reibschweißen von Aluminium-Stahlgelenkwellen', in *Proc. Dünnblechverarbeitung*, SLV München.

THOMY C, WIRTH A, KREIMEYER M, WAGNER F and VOLLERTSEN F (2007a), 'Joining of dissimilar materials – new perspectives for lightweight design in the transportation industries', in *Proc. IIW International Conference Welding & Materials, July 01–08, 2007, Dubrovnik and Cavtat, Croatia*, 311–326.

THOMY C, WIRTH A, KREIMEYER M, WAGNER F and VOLLERTSEN F (2007b), 'Laser–MIG Hybridfügen von Aluminium–Stahl Leichtbaustrukturen', *Laser Technik Journal*, (4), 36–40.

THOMY C, WAGNER F, VOLLERTSEN F and METSCHKOW B (2007c), 'Lasers in the shipyard – laser joining of aluminum to steel for modern yacht construction', *Industrial Laser Solutions*, (11), 9–13.

THOMY C, WALTHER R and VOLLERTSEN F (2008), 'New developments when thermally joining hybrid materials in the automotive industry', in *Proc. 11th German and 8th European Automotive Conference 'Joining in Automotive Engineering', Apr. 24–25, 2008*, Automotive Circle International, Bad Nauheim, CD-ROM.

UZUN H, DALLE DONNE C, ARGAGNOTTO A, GHIDI T and GAMBRO C (2005), 'Friction stir welding of dissimilar Al6014-t4 to X5CrNi18-10 stainless steel', *Material and Design*, (26), 41–46.

WALDMANN H, BERGMANN J P, GUYENOT M, HALDENWANGER H-G and KORTE M (2001), 'A Study on Laser Welding of Aluminium to Steel for Automotive Skin Sheet Applications', in Duflou J R, Geiger M, Kals H J J, Shirvani B, Singh U P, *Proc. 9th International Conference on Sheet Metal*, Leuven, 2001.

WINKELMANN R (2003), 'Plasmaschweißen von Mischverbindungen', in *Proc. Dresdner Fügetechnisches Kolloquium 2003 – Klassische Technologien zur Herstellung neuer Fügeverbindunge*n, Dresden 13–14, März 2003, 1–7.

WIRTH A, KREIMEYER M, GNAUK J, THOMY C and VOLLERTSEN F (2007a), 'Analyses on the phase seam of a laser–MIG joined aluminum–steel sample', in Vollertsen F, Emmelmann C, Schmidt M and Otto A, *Proc. 4th International WLT Conference on Lasers in Manufacturing 2007*, Stuttgart, AT-Fachverlag, 111–115.

WIRTH A, THOMY C, WAGNER F and VOLLERTSEN F (2007b), 'Thermal joining of aluminium to other metals – processes, properties and applications', *Proc. 10th International Conference on Joints in Aluminium (INALCO 2007), Oct. 24–26, 2007, Osaka, Japan*, 125–130.

ZERNER I and SCHUBERT E (1999), 'Untersuchungen zur Phasensaumdicke beim Laserstrahlfügen von Aluminium-Stahl-Verbindungen', in *Proc. DFG-Schwerpunktprogramm Kurzzeitmetallurgie*, Bayreuth, 87–98.

ZERNER I, SCHUBERT E and SEPOLD G (1999), 'Diode lasers join aluminium to steel', Industrial Laser Solutions, (5), 23–28.

ZERNER I (2002), *Prozeßstabilisierung und Ergebnisse für das Laserstrahlfügen von Aluminium-Stahl-Verbindungen*, Bremen, BIAS–Verlag.

12

Hybrid laser–arc welding of steel

S. KATAYAMA, Osaka University, Japan

Abstract: Results of laser–arc welding, and the characteristics and proper welding conditions for hybrid welding of respective steels of different thickness are described. Hybrid laser–arc welding has been utilized to weld sheets or plates of steels such as mild steels, high tensile steels, Zn-coated steels and stainless steels in the industries of cars, shipbuilding pipelines, etc.

Key words: hybrid welding, stainless steel, Zn-coated steel, laser–arc welding, weld penetration.

12.1 Introduction

Laser welding is widely applied to joining of small or precise parts in various industrial fields. However, there are sometimes problems and defects in laser welding of sheets with a gap in transportation vehicles such as cars or thick plates in ships, pipelines and vessels. In order to overcome such problems and to improve both productivity and quality, hybrid laser–arc welding has been attempted all over the world.[1–30]

In this chapter, various results of hybrid laser–arc welding with CO_2, YAG, or fiber laser and TIG, MIG or MAG are summarized for respective steels to properly utilize the hybrid welding process in industrial applications. Since Steen and coworkers published their first paper about TIG augmented CO_2 laser welding,[31] the combinations of laser and arc have been developed as CO_2 laser and MIG or MAG, YAG laser and TIG, YAG laser and MIG or MAG, high power CO_2 laser and MIG or MAG, disk or fiber laser and MIG or MAG according to the development of fiber-delivered lasers and higher power lasers. Nozzles for hybrid welding have been developed.[1,2] The choice of gas is also important for steels. In the case of hybrid CO_2 laser and arc welding, Ar gas plasma affects the results and, thus, He gas mixtures (of 50 to 75%) are generally required.[1,3–5] With YAG, LD (laser diode), disk and fiber lasers, a process gas comprising mainly Ar and partly CO_2 or O_2 is normally selected for arc stability and bead surface shielding, and, for MIG/MAG, droplet detachment and spatter-free metal-transfer. The results obtained with a CO_2 laser may be similar with YAG or

fiber laser when the effect of gas plasma is suppressed by the use of a shielding gas of higher He content. The results with YAG, disk and fiber lasers should be essentially the same owing to an almost equal wavelength although the effects of power and power density should be considered further.

12.2 Hybrid laser–arc welding of steel and high tensile strength steel

Hybrid YAG laser–MAG arc bead-on-plate, butt joint or lap welding of low carbon steel, 590 MPa or 440 to 980 MPa steels were carried out to understand the effects of welding conditions on the weld penetration and mechanical properties.[7–9]

Pulsed MAG arc with Ar–20%CO_2 gas[7,8] or Ar–3%O_2 gas[9] at high arc voltage was utilized to perform stable welding by reducing spatters. The arc is generated toward the underneath plate and then a droplet flies away from the target after the disappearance of the arc, as shown in Fig. 2.4.[4] The droplets are liable to interfere with the incident laser beam when the target distance between a laser beam and a wire approaches 0 mm. No deviation of an arc is observed for a laser–arc distance of 9 mm, for example, and this is not, therefore, referred to as hybrid welding.[3] The optimum distance for deep penetration is normally about 2 to 4 mm.[7,9] Figure 12.1 shows the cross sections of weld beads produced by YAG laser, hybrid MAG arc–YAG laser and hybrid YAG laser–MAG arc welding at various traveling speeds under the same parameters.[7] (In this chapter, for example, when a laser optics head or arc torch is a leading heat source, YAG–MAG or MAG–YAG welding is used depending upon the heat sources arrangement.) The penetration depths of laser and hybrid weld beads decrease with an increase in the welding speed. Hybrid YAG laser–MAG arc welding does not make the penetration increase but increases the bead width drastically. On the other hand, hybrid MAG–YAG laser welding can deepen the penetrations of the laser welds. In the case of pulsed MIG with pure Ar gas instead of pulsed MAG, similarly hybrid MIG–YAG laser welding is more stable than hybrid YAG laser-MIG welding in terms of welding phenomena for the production of a sound weld of good surface appearance, as the surface and cross-section of the former weld is shown in Fig. 12.2.[7]

In the car industry, a lap joint and a fillet lap joint are normally used. In hybrid welding, the tolerance of a gap between butt joint sheets or lapped sheets increases owing to the use of arc and filler wire compared with laser welding, the weld bead width widens, and the maximum welding speed is increased several times faster than the arc welding.[9] Moreover, the joint strengths of hybrid welds are higher than those of spot welds and laser welds, as shown in Fig. 12.3.[9]

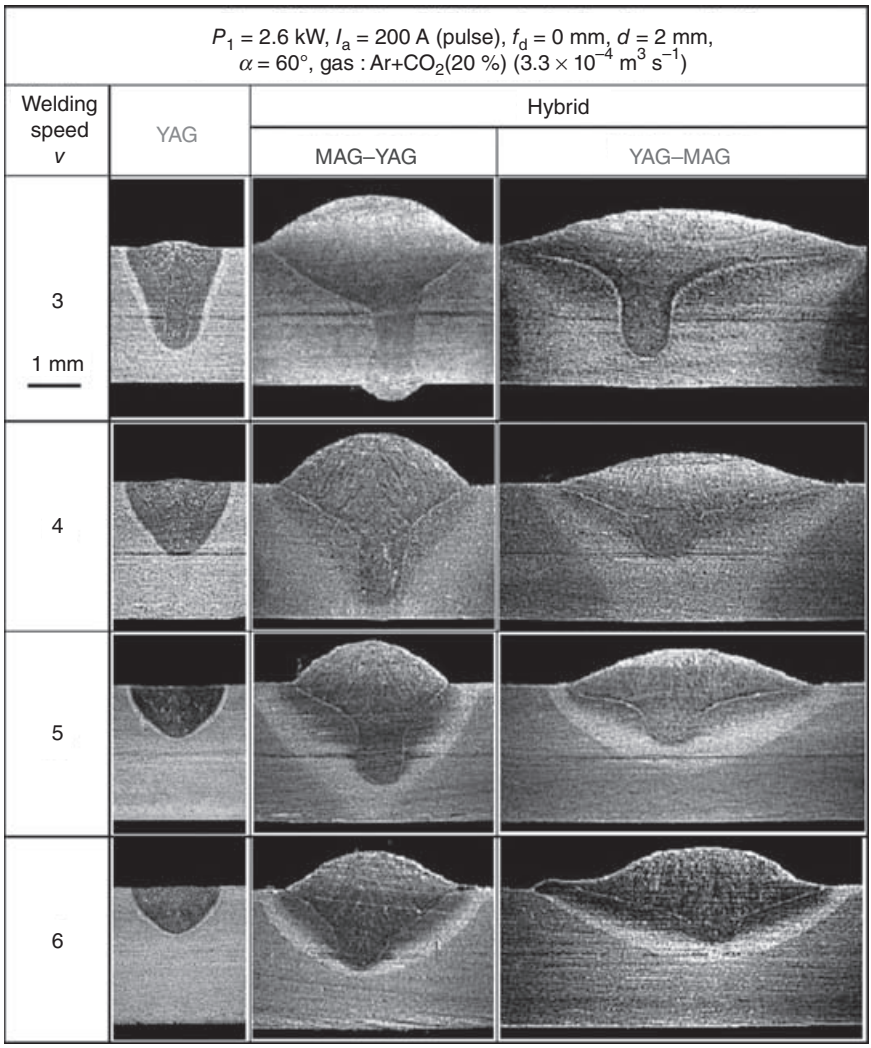

12.1 Cross-sections of weld beads produced by YAG laser, hybrid MAG–YAG laser and hybrid YAG laser–MAG welding at various traveling speeds.

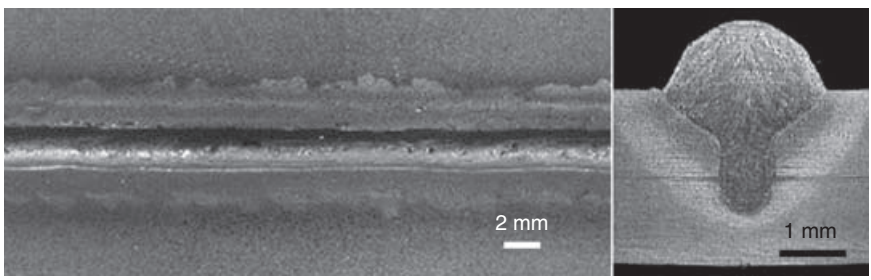

12.2 Surface and cross-section of hybrid MIG–YAG laser weld bead.

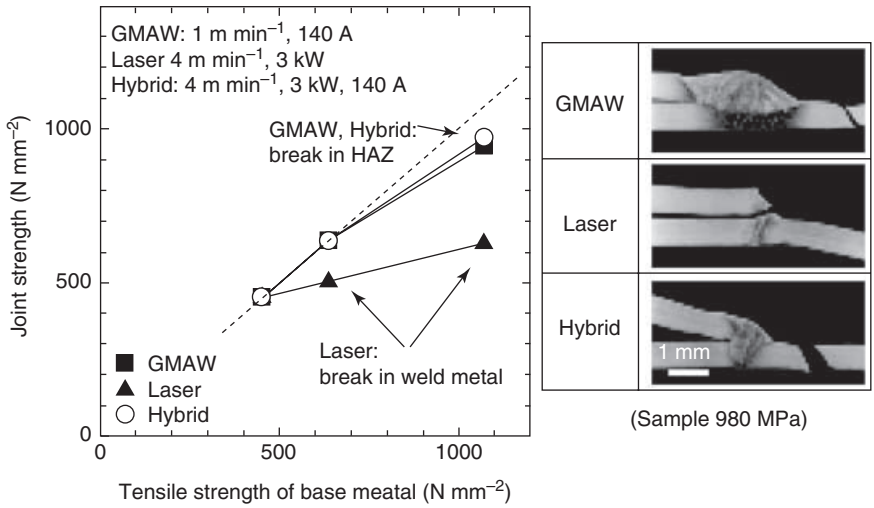

12.3 Comparison of joint strengths between spot, laser and hybrid welds, and cross-sections of specimens after test.

Figure 12.4 (a) and (b) exhibit surface appearances and cross-sections of hybrid YAG laser–MAG welds, showing the effects of laser power and arc current on the bead penetration geometry.[9] The increase in arc current leads to the slight increases in the deposited amount and the weld penetration, and the increase in laser power can further increase the penetration and weld fusion zone. Hybrid laser–arc welding can increase the gap tolerance in comparison with laser welding. The welding location also affects the weldable sheet gap, as shown in Fig. 12.5 (a) and (b).[9] In the case of the welding location shift to the lower sheet, the bridging gap decreases because the upper sheet does not melt. In the case of the shift to the upper sheet, welding is possible, but the penetration in the lower sheet becomes shallow.[9]

The hardness profiles across the welds are compared for different welding processes, as shown in Fig. 12.6 (a) and (b).[9] The maximum hardness of a hybrid weld is lower than that of a laser weld, but the width of the heat-affected zone of a hybrid weld is wider than that of a laser weld because of higher heat input. The joint strength increases with an increase in the throat thickness or welded area. It is confirmed in hybrid CO_2 laser–TIG arc welding of various high-strength steels that the hardness levels of hybrid weld metals decrease with an increase in the heat input.[10]

Hybrid welding of thick steel plates has been intensively studied by using CO_2 laser and MAG, then YAG laser and MAG and recently fiber laser and MAG for shipbuilding, pipelines, and so on.[1–16] Figure 12.7 shows the

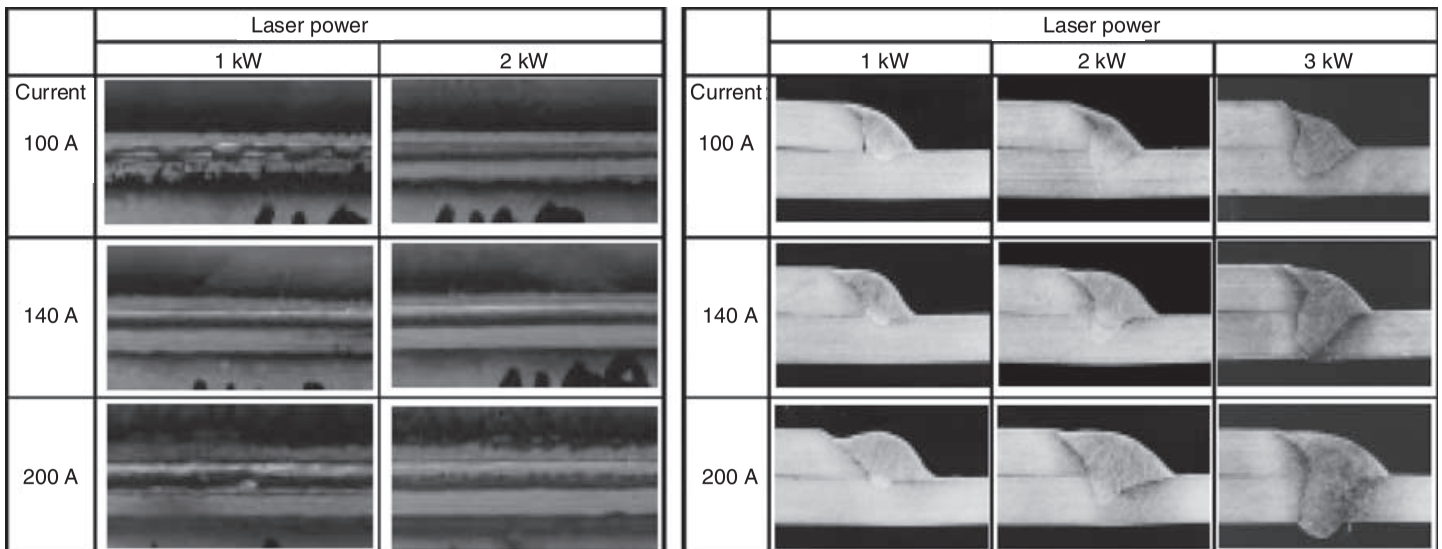

12.4 Surface appearances and cross-sections of hybrid YAG laser–MAG welds.

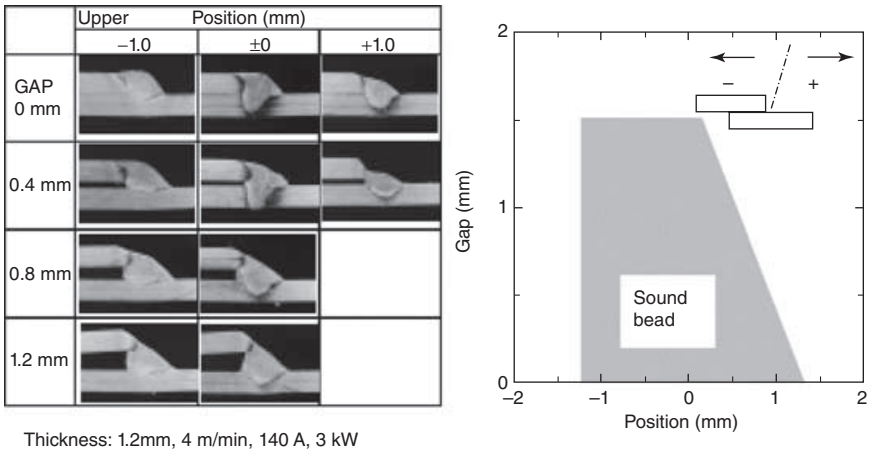

12.5 Effect of welding location on weldability of lap fillet sheets with gap, and process window for sound weld bead formation.

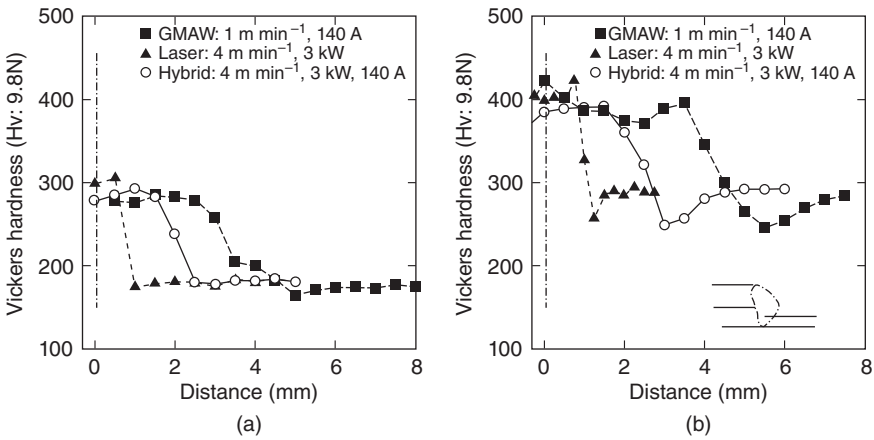

12.6 Comparison of hardness profiles across welds produced by different processes: (a) 590 MPa steel; (b) 980 MPa steel.

schematic representation of the LPLAC (leading path laser–arc combination) method for high-speed welding.[11] The lower butt joint is first welded with a CO_2 laser and the upper groove is deposited by MAG arc welding. A full penetration weld of an 8 mm thick mild steel plate was produced at the high speed of 3 m min^{-1} at 7 kW laser power and 9 kW arc power.[9] (It is demonstrated that a high quality fiber laser of 6 kW power and

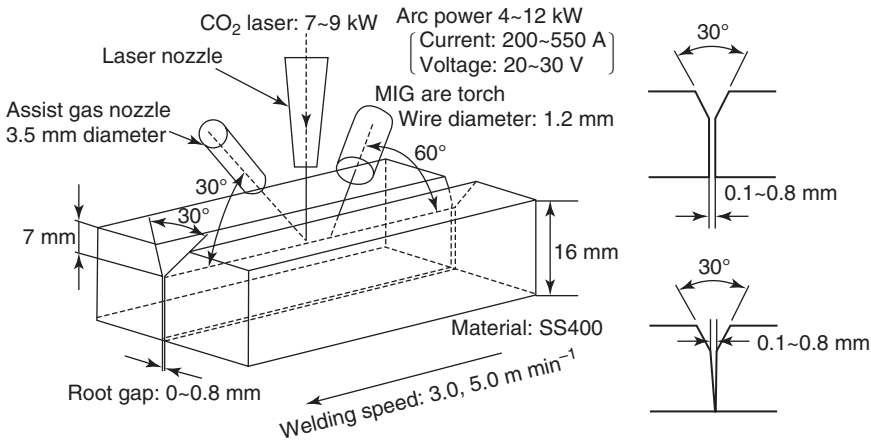

12.7 Schematic representation of LPLAC (leading path laser–arc combination) method.

0.5 MW mm^{-2} high power density can produce a full penetration weld in 8 mm thick stainless steel plate at 4.5 m min^{-1}, although the bead width is very narrow.[32])

In hybrid MAG-CO_2 laser welding of 15 mm thick structural steel plates by using the ILT integrated nozzle with an Ar–He–O_2 mixture, proper combinations of laser power and wire feeding rate, and laser power, welding speed and wire feeding rate are demonstrated for respective gaps up to 0.7 mm at 1.2 m min^{-1} in the flat position, and for respective gaps up to 3 mm in the horizontal position, respectively.[12] In the case of the flat position, the maximum allowable gap of 0.7 mm has been achieved in 15 mm thick steel plate without root preparation.[12] Drop through or sagging melt is liable to occur when the gap is wider or the root molten pool surface is oxidized and, therefore, the horizontal position and root surface protection of an inert gas may be chosen for thicker plates of over 15 mm. Cross-sections of optimized hybrid welds are presented in Fig. 12.8.[12] For thicknesses up to 25 mm, welds without any hot cracks and, if any, with only few small pores can be produced successfully.[12] The selection of V- or Y-shaped groove preparation in the range between 4° and 8° full angle and an appropriate welding speed is important in order to produce crack-free welds.[12]

Laser–GMA hybrid welding using 8, 20 and 30 kW fiber lasers was used to join low alloyed steel plates of 16 to 28 mm in thickness.[13] Multi-layer hybrid welding resulted in pore formation while single layer hybrid welding showed reasonable good results, although pores and cracks occurred under some conditions, as shown in Fig. 12.9 (a) and (b).[13]

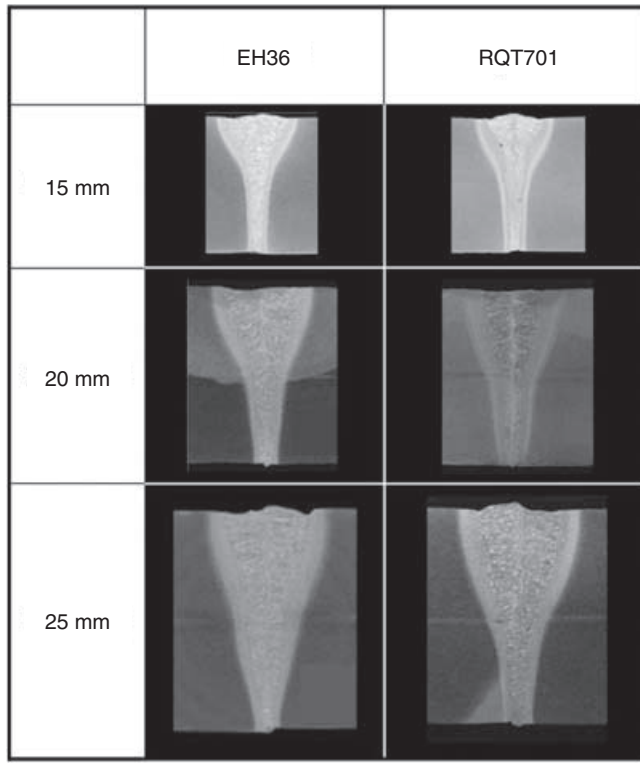

12.8 Cross-sections of optimized hybrid welds.

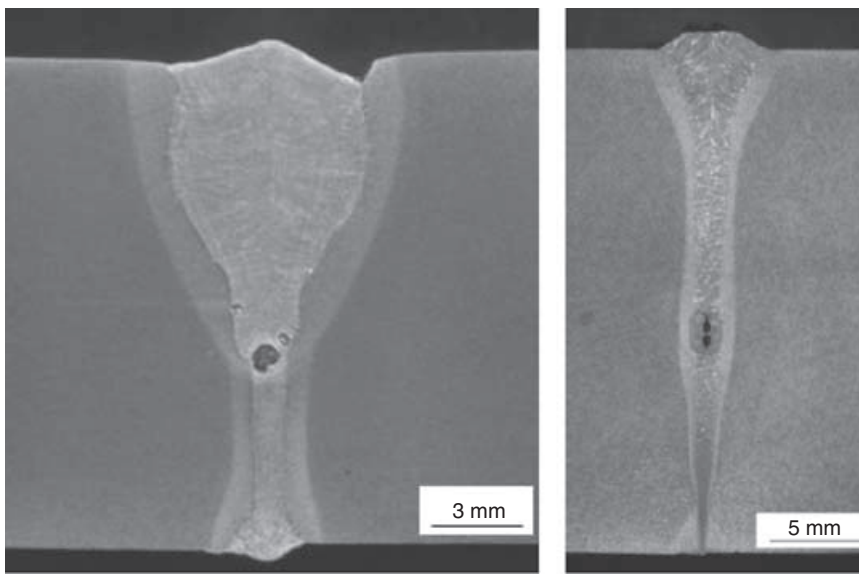

12.9 Examples of porosity (a) and pore or crack (b) in hybrid weld beads.

In Meyer Werft, properties of hybrid welds are evaluated by the destructive tests such as hardness measurements, tensile tests, notch impact tests, transverse and side bending tests, cross tensile tests and fatigue tests, and satisfactory results are obtained.[14,15] Thus, the manufacturing workshop is equipped with four high power CO_2 laser–MAG hybrid welding stations.[15] Recently hybrid laser–MAG welding with a fiber laser has been investigated for practical use. Moreover, highly efficient welds are produced by hybrid laser–GMA welding head with a tandem welding torch.[6,16]

12.3 Hybrid laser–arc welding of Zn-coated steel

Laser welding of low carbon steels and/or Zn-coated steels is practically applied for manufacturing car body and components, but the control of a gap between sheets (for example, 0.05 to 0.2 mm in lap welding of Zn-coated steel sheets) is required to produce sound welds. Especially in the case of the gap of 0 mm unsound weld beads with rough surfaces, pores or porosity are easily formed. Thus hybrid laser–arc welding of Zn-coated steels with YAG laser was investigated under various conditions[8,9,18–20].

It is emphasized to be more difficult to perform hybrid welding of Zn-coated steels than uncoated steels.[19] The process window for Zn-coated steels is much narrower than that for uncoated steels because of the Zn vapour atoms.[19] Nevertheless, it is demonstrated that sound lap welds can be formed in hybrid welding of Zn-coated steel sheets with 0 (zero) mm gap.[8] It may be attributed to the natural formation of a gap caused by deformation or distortion due to a higher heat input during hybrid welding.

The effect of shielding gas on pit or porosity on the bead surface and spattering is investigated in hybrid YAG laser–MAG welding of galvanealed steel fillet joint sheets without a gap in the flat position.[20] The CO_2 in the $Ar+CO_2$ shielding gas is effective in decreasing the pits, whilst O_2 decreases the size of pits but increases the number of pits.[20] Increasing the CO_2 and O_2 gas ratio in $Ar+CO_2$ and $Ar+O_2$ shielding gas deepens the penetration and widens the weld bead, respectively, and both increase spattering.[20] The effect of O_2 gas on penetration and the x-ray inspection results of hybrid welds made with respective gases are compared in Fig. 12.10, and the surface and cross-section of hybrid lap fillet joint weld with the $Ar+CO_2+O_2$ mixture shielding gas is exhibited in Fig. 12.11.[20] Consequently, the $Ar+CO_2+O_2$ mixture shielding gas is recommended for hybrid YAG laser-pulsed MAG welding of galvanealed steel in high-speed welding of automobiles because pits, porosity and spattering can be reduced.[20]

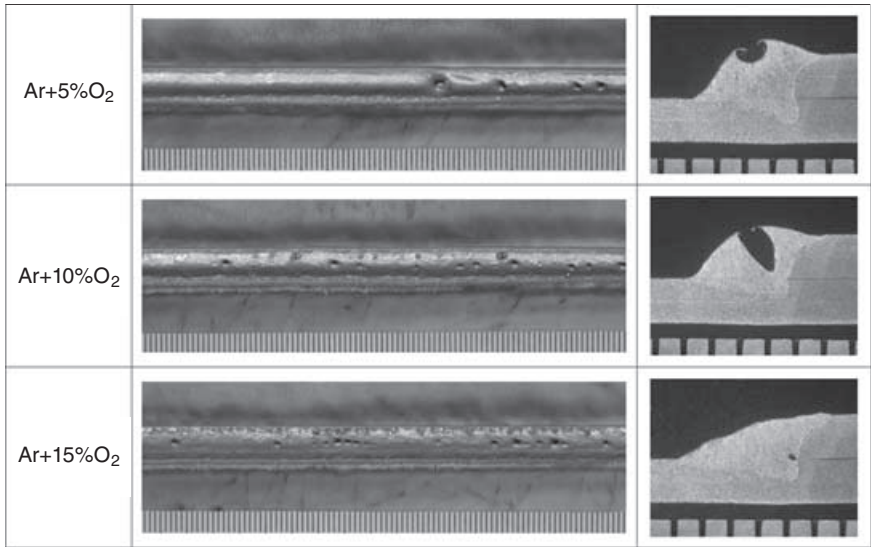

(a)

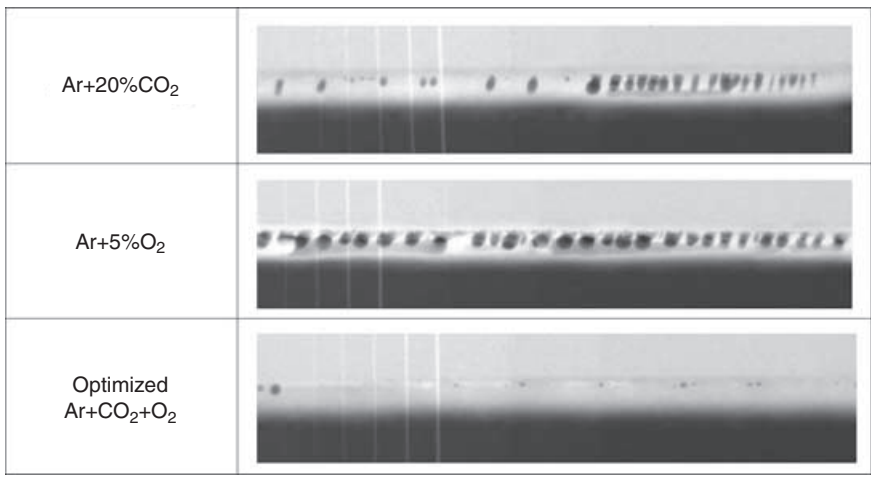

(b)

12.10 Effect of gas kind on weld penetration (a) and porosity formation (b) in hybrid welding of galvanealed steel sheets.

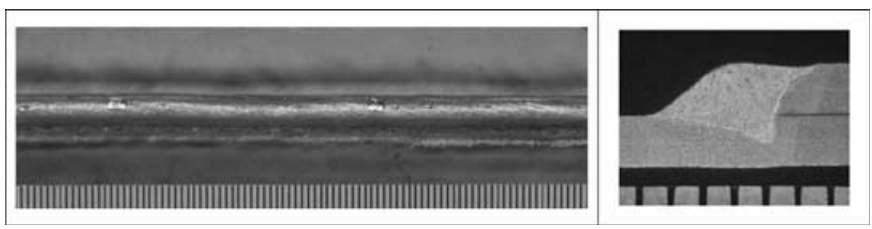

12.11 Example of hybrid weld bead with Ar+CO_2+O_2 mixture.

12.4 Hybrid laser–arc welding of stainless steel

The effects of parameters on penetration and porosity formation were investigated in hybrid welding using YAG laser and TIG arc under varying conditions, such as YAG–TIG or TIG–YAG, the distance between laser and arc, laser power, arc current, defocused distance, welding speed.[21–26] It is confirmed that a laser should be shot in the molten pool produced with the TIG arc to produce a deeply penetrated weld bead. The effects of surface tension and electromagnetic force on melt flows and penetration are also confirmed by high-speed video observation of plate surface and x-ray transmission observation of the molten pool inside. The detailed results were described in Chapter 2. To produce deeper penetration, hybrid YAG laser and double flux TIG welding with Ar+H_2 center gas and Ar environmental shielding gas has been developed.[25,26] Hybrid YAG–TIG welding using this double flux TIG arc was applied to the cover plate welding for a superconductive coil of stainless steel.[25,26]

Since duplex stainless steels offer highly economical combinations of strength and corrosion resistance owing to their chemical composition and their favorable microstructure of about 50% ferrite and about 50% austenite, they are used to build chemical and oil tanker vessels in shipbuilding industry and bridges.[27–30] In laser welding of duplex grades, the amount of ferrite is excessively high owing to the low heat input and rapid cooling rate.[28–30] Insufficient time for adequate austenite reformation can result in considerable chromium nitride precipitation within the ferrite grains in the HAZ and fusion zone, which, in turn, may have a detrimental effect on corrosion resistance and toughness.[27,29] Hybrid welding using filler wire and nitrogen shielding gas is preferred to form a higher content (near 50%) of austenite.[27–29]

12.5 References

1 PETRING D, FUHMANN C, WOLD N and POPRAWE R, 'Investigation and applications of laser–arc hybrid welding from thin sheets up to heavy section componests', *Proc. ICALEO 2003*, LIA, Session A 1–10, 2003.

2 TSUBOTA S, ISHIDE T, WATANABE M and AKABA T, 'Laser–arc hybrid welding system for various 3D welding – Development of coaxial laser welding head', *The 58th Annual Assembly of IIW*, Prague, IIW Doc. No. XII-1853-05 368-375 (CD), 2005.

3 THOMY C, SEEFELD T and VOLLERTSEN F, 'Laser GMA hybrid welding with various laser systems', *58th Annual Assembly of IIW*, IIW Doc. No. XII-1843-05 226-239 (CD), 2005.

4 SUGINO T, TSUKAMOTO S, NAKAMURA T and ARAKANE G, 'Fundamental study on welding phenomena in pulsed laser–GMA hybrid welding', *Proc. ICALEO 2005, Laser Materials Processing Conference*, LIA, Paper #302 108–116, 2005.

5 CHAE H, KIM C, KIM J and RHEE S, 'Development of hybrid laser–rotating arc welding process', *Proc. of the 4th International Congress, on Laser Advanced Materials Processing (LAMP)*, JLPS, Kyoto, 2006.
6 DILTHEY U and WIESCHEMANN A, 'Prospects by combining and coupling laser beam and arc welding processes, *Welding in the World*, **44**(3) 37–46, 2000.
7 NAITO Y, MIZUTANI M, KATAYAMA S and BRIAND F, *Presentation at 4th LAMP Conference*, JLPS, Kyoto, 2006.
8 ONO M, SHINBO Y, YOSHITAKE A and OHMURA M, 'Welding properties of thin steel sheets by laser–arc hybrid welding – Laser focused arc welding', *Proc. SPIE*, **4831** 369–374, 2002.
9 UCHIHARA M and FUKUI K, 'Laser–arc hybrid welding of automotive high strength steel sheets', *58th Annual Assembly of IIW*, Doc. No. XII-1854-05, 2005.
10 BRIAND F, DUBET O, LEFEBVRE P, BALLERINI G and NIKI K, 'Laser and hybrid welding of ultra high strength steels', *Proc. of 4th LAMP*, JLPS, Kyoto, 2006.
11 ABE N, KUNUGITA Y, MIYAKE S, HAYASHI M, TSUCHITANI Y and MIHARA T, 'The mechanism of high speed leading path laser–arc combination welding', *Proc. ICALEO '98*, LIA, Orlando, FL USA, Session F 37–45, 1998.
12 PETRING D, FUHRMANN C, WOLF N and POPRAWE R, 'Progress in laser–MAG hybrid welding of high-strength steels up to 30 mm thickness', *ICALEO 2007 Congress Proc.*, LIA, Orlando, FL USA, 300–307, 2007.
13 VOLLERTSEN F and GRUNENWALD S, 'Defects and process tolerances in welding of thick plates', *ICALEO 2008 Congress Proceedings, Laser Materials Processing Conference*, LIA, Temecula, CA USA, Paper 1004, 489–497, 2008.
14 ROLAND, F, and LEMBECK, H. 'Laser Beam Welding in Shipbuilding – Experience and Perspectives at Meyer Shipyard', *International Aachen Welding Conference; High Productivity Joining Processes, Fundamentals, Applications, Equipment*, Aachen, **1** 463–475, 2001.
15 LITMEYER M and LEMBECK H, 'Laser welding in shipbuilding – report of practical application', *Proc. of the 70th Laser Materials Processing Conference*, JLPS, Osaka Japan, 139–143, 2008.
16 HOWSE D S, SCUDAMORE R J and BOOTH G S, 'Yb fibre laser/MAG hybrid processing for welding of pipelines', *58th Annual Assembly of IIW*, IIW Doc. No. IV-880-05 383–393(CD), 2005.
17 YAPP D and KONG C-J, 'Hybrid laser–arc pipeline welding', *59th Annual Assembly of IIW*, IIW Doc. No. XII-1887-06, 2006.
18 HEDEGARD J, NERMAN P. ANDERSSON J, TOLF E and OHMAN E, 'High quality joining of galvanized steels, *Proc. JOM 11*, Helsingor, Denmark, 2003.
19 KAPLAN A F H, WIKLUND G and NILSSON T, 'The impact of zinc-coating on laser hybrid welding of steel', *ICALEO 2007 Congress Proceedings Laser Materials Processing Conf.*, LIA, Florida 345–352, 2007.
20 SATO T, KAMEI T and WADA K, 'Effect of shielding gas on weldability in YAG laser–GMA hybrid welding of galvanealed steel', *60th Annual Assembly of IIW*, IIW Doc. No. XII-1923-07, 2007.
21 NAITO Y, MIZUTANI M and KATAYAMA S, 'Observation of keyhole behavior and melt flows during laser–arc hybrid welding', *Proc. of the 22nd ICALEO '03*, Jacksonville, LIA, 2003, (CD: 1005).
22 NAITO Y, MIZUTANI M and KATAYAMA S, 'Penetration characteristics in YAG laser and TIG arc hybrid welding, and arc and plasma/plume behavior during welding

– welding phenomena in hybrid welding using YAG laser and TIG arc (First report)', *Quarterly Journal of the Japan Welding Society*, **24**(1) 32–38, 2006 (in Japanese).

23 NAITO Y, MIZUTANI M and KATAYAMA S, 'Electrical measurement of arc during hybrid welding – welding phenomena in hybrid welding using YAG laser and TIG arc (Third report)', *Quarterly Journal of the Japan Welding Society*, **24**(1) 45–51, 2006 (in Japanese).

24 KATAYAMA S, NAITO Y, UCHIUMI S and MIZUTANI M, 'Porosity preventive conditions and mechanisms in hybrid welding with YAG laser and TIG/MIG arc', *58th Annual Assembly of IIW*, Prague, IIW Doc. No. XII-1852-05, 348–358, 2005.

25 ASAI S, MINAMI K, SHIIHARA K, MAKINO Y, KANEHARA T and SHIBUI M, 'YAG–TIG hybrid welding process for coil cover plate of stainless steel', *58th Annual Assembly of IIW*, Prague, IIW Doc. No. XII-1855-05, 376–382, 2005.

26 SHIIHARA K, MAKINO Y, OGAWA T, ASAI S, KANAHARA T, SENDA I, OKUNO K, KOIZUMI N and MATUI K, 'Laser–arc hybrid welding for the cover plate of ITER TF coil', *ICALEO 2007 Congress Proc., Laser Materials Processing Conf.*, LIA, Florida 316–324, 2007.

27 VANDEWYNCKELE A, COUSO E V, OTERO J L A and LAMA M P, 'Laser–arc welding of duplex stainless steel', *ICALEO 2007 Congress Proc., Laser Materials Processing Conf.*, LIA, Florida 293–299, 2007.

28 WESTIN E M, KEEHAN E, STROM M and BROMSSEN B, 'Laser welding of a lean duplex stainless steel', *ICALEO 2007 Congress Proc., Laser Materials Processing Conf.*, LIA, Florida 335–344, 2007.

29 WESTIN E M and FELLMAN A, 'Laser hybrid welding of a lean duplex stainless steel', *ICALEO 2008 Congress Proc., Laser Materials Processing Conf.*, LIA, Florida 526–534, 2008.

30 FERSINI M, SORRENTINO S and ZILLI G, 'Duplex stainless steel for bridges construction: comparison between SAW and laser–GMA hybrid welding', *61st Annual Assembly of IIW*, Graz, IIW Doc. No. IV-960-08, 2008.

31 EBOO M, STEEN W M and CLARK J, 'Arc-augmented laser welding', *Proc. of 4th Int. Conf. on Advances in Welding Processes*, UK, 257–265, 1978.

32 KINOSHITA K, MIZUTANI M, KAWAHITO Y and KATAYAMA S, 'Phenomena elucidation in high power fiber laser welding of stainless steel', *Quarterly Journal of the Japan Welding Society*, **25**(1) 18–23, 2007 (in Japanese).

Index

AA6013, 123, 249, 252, 253, 255, 256
AA6014, 259
AA6016, 278
AA 6056, 117
AA6061, 234
AA6181, 259
A5052 alloy, 35, 43
A5356 alloy, 35
absorptivity, 51–3
AIMS standard, 117
Aker Yard, Finland, 187–8
ALFORM700M, 213
AlSil2 wire, 253, 278
aluminium
  CO_2 laser beam weld vs hybrid weld in AA6013 sheet
    dendritic structure, 252
    fatigue behaviour, 256
    grain size in the HAZ, 253
    microhardness gradient, 254
    surface appearance and cross section, 250
    tensile curves and fracture location, 255
  fusion welding of alloys, 219–28
    advantages and disadvantages of MIG welding, laser beam welding and laser MIG hybrid welding, 226
    hot-cracking susceptibility of EN AW-6XXX, 224
    temperature profiles and resulting microstructural zones, 222
    welded AA 6061 T6 hardness distribution, 223
  hybrid laser–arc welding, 216–62
    applications, 258–61
    future trends, 261–2
    overview on hybrid welding processes investigated, 228–31, 229–30
    roof segment of ICE train/ cross-section of the weld, 260
    specific features, 231–5
  and its alloys, 217–19
  mechanical properties of selected wrought alloys, 219
  parameters in hybrid welding, 235–45
    governing parameters, 235–6
    hybrid process parameters, 242–4
    sub-process arc welding parameters, 241
    sub-process laser beam welding parameters, 236–8, 240–1
  processes for hybrid laser–arc welding for alloys, 228–45
    energy input per volume of molten material for various welding processes, 232
    gap bridging capacities of various welding processes, 233
    properties of laser sources used, 237
  properties of Al99.99 at 20 °C, 218

properties of hybrid laser–arc welds, 245–58
fatigue behaviour, 256–7
hardness, 253–5
microstructure and cracking, 251–3
overview of base materials, joint types and properties investigated, 245, 246–7, 248–9
tensile strength, 255–6
visual inspection, macrosections and issue of porosity, 250–1
aluminium alloys, 42–3, 131–3 *see also* specific alloy
AA 6013 fatigue behaviour, 123
dendritic structure in upper section of fusion zone, 111
fatigue properties, 123
hardness, 114, 116
laser and hybrid welded cross-section, 111
microhardness gradient in CO_2 laser beam weld and hybrid weld, 115
microstructure of hybrid laser–arc welds, 110–11
strength, 117–18
tensile strength of square butt welds, 118
aluminium–steel joints
AA6016 and zinc-coated steel DC05 + ZE
bend test, 287
cracking, 287
application potentials, 288–91
aluminium–steel tailored hybrid blank, 289
aluminium–steel tailored hybrid tube, 289
concept for aluminium–steel in yacht construction and deckhouse, 290
basic properties of iron and aluminium, 272
considerations in selecting appropriate joining process, 271
cross-section showing intermetallic phase layer, 279
EBSD phase composition analysis, 280
future trends, 291
grains orientation in joining zone, 281
hybrid laser-arc welding, 270–91
intermetallic phase layer, 273
intermetallic phases, 272
laser–MIG hybrid welding
basic features, 277–8
effect of laser power on phase layer thickness, 283
effect of wire feed on tensile strength, 284
principle, 277
process parameter envelope, 286
micro-geometrical parameters for seam assessment, 282
principal physical nature of joining process, 271
process and joint properties, 278–88
effect of process parameters on laser MIG hybrid welding, 282–6
mechanical and technological joint properties, 286, 288
microstructure, 278–82
process principle and temperature distribution, 276
properties of intermetallic phases and structures in system Fe–Al, 272
recent works on thermal joining of aluminium to steel, 274
specific aspects of and state-of-the-art joining processes, 271–7
alternative processes, 273, 275–6
challenges of joining dissimilar metals, 272–3
dissimilar metal combinations and their application potentials, 271
top bead appearance and cross-section, 278
arc heat sources, 59–68
consumable electrodes, 62–4
basic metal transfer modes, 63

gas–metal arc welding, 62
ionisation grade vs temperature, 61
non-consumable electrodes, 64–8
common TIG welding process variants, 66
plasma torch, 67
tungsten inert gas welding, 65
arc welding, 3–15
brief history, 3–6
gas metal arc welding, 6–12
advantages, 11–12
disadvantages, 12
equipment, 6–7
filler wire, 8
power source advances, 10
shield gas, 7–8
gas tungsten arc welding, 12–15
advantages, 14
disadvantages, 15
equipment, 13–14
argon, 7–8, 29, 86, 89–90
Audi A8, 197, 259
austenitic–ferritic stainless steel, 109–10
austentite, 309
automated ultrasonic examinations, 137

bainite, 109
bead-on-plate welding, 238, 241, 244, 248
beam parameter product, 49–50
bend testing, 136
Blohm & Voss, Germany, 186
Böhler X 70-IG weld metal, 213
Böhler X 90-IG weld metal, 213
Boltzmann constant, 60, 171
Boltzmann distribution, 170
Boltzmann plot method, 170, 172
bremsstrahlung, 168, 173

carbon dioxide, 90
effect on hybrid weld bead cross section width, 96
and helium content effect on spatter of hybrid laser-MAG welding, 95
carbon dioxide laser, 57–8
carbon steel
hardness, 112–14
hardness distributions of laser weld, GMA weld and laser–GMA weld, 112
mechanical testing results for Yb fibre laser–MAG hybrid welds, 115
quenched and tempered HSLA S1100QL steel, 113
microstructure of hybrid laser-arc welds, 107–9
cross-section of an arc–laser hybrid weld in 12 mm structural steel, 107
effect of shielding gas CO_2 content, 108
microstructure of base metal, 108
microstructure of weld metal, 109
strength, 116–17
effect of gap on tensile strength, 117
strength and elongation of S1100QL, base metal, MAG and hybrid welds, 117
tensile strength of welded joints, 116
toughness, 118–20
Charpy energy in dependence to test temperature, 119
Charpy V-notch transition curve, 119
Cartesian directions, 209
Charpy V-notch test, 129, 136
Charpy V-notch transition curve, 181
CO_2 laser, 89, 193, 199, 200, 207, 302
cold Arc process, 275
cold metal transfer, 64, 275
cold working, 131
Com1 method, 98
Com2 method, 98
Com3 method, 98

construction steels
  excellent fatigue results of laser–MAG hybrid welds, 122
  fatigue properties, 120–2
  S–N curve of laser hybrid welds, 121
crack tip opening displacement tests, 136
critical pitting temperature, 123
cubic-face-centred structure, 217

deep-weld effect, 192, 204
DIN EN 515, 219
diode laser, 59, 86, 193
direct current electrode negative, 65–6
direct current electrode positive, 65–6
disc and fibre laser, 58–9
dissimilar metals *see* aluminium–steel joints
Doppler broadening, 171
duplex steel, 109–10

Eggert-Saha equation, 60
electron beam welding, 144
EN 439, 213
EN AW-5083, 252
EN AW-7020, 223
EN 440-G3Si1 solid wire, 181
EN ISO 13919–1:1996, level C, 130

FAT100 line, 182
ferrite, 108, 109, 309
fibre laser, 302
filler wire, 8
fillet lap joint, 300
Fincantieri, Italy, 188–9
flux cored arc welding, 5
FluxF400NF, 278
four-point bending, 182
Fraunhofer ILT, 100
Fresnel absorption, 173
friction stir welding, 144
Fronius TPS digital power source equipment, 199
Fronius-Wels, 200, 204
fusion welding, of aluminium alloys, 219–28
  effect of basic properties of aluminium, 220–1
    high coefficient of thermal expansion, 220
    high heat conductivity, 220
    hydrogen solubility of solid and liquid aluminium, 220–1
    surface layer of natural aluminium oxide, 220
  effect on joint properties, 221–5
    base metal and filler composition, 225
    heat input and heat flow, 224–5
  state-of-the-art processes and potential of hybrid welding, 225–8
fusion welding methods, 48
fusion zone, 253, 309

gas metal arc welding, 6–12, 121
  advantages, 11–12
  disadvantages, 12
  equipment, 6–7
    typical set up, 7
  filler wire, 8
  globular metal transfer, 9
  power source advances, 10
  pulsed spray transfer, 10–11
  real time adaptive control, 11
  shield gas, 7–8
  short circuit metal transfer, 8–9
  spray metal transfer, 9
  weld modes, 8
gas tungsten arcs, 71
gas tungsten arc welding, 12–15
  advantages, 14
  disadvantages, 15
  equipment, 13–14
    typical set up, 14
Gaussian beam, 50
Gaussian distribution, 163
Gaussian function, 163
German ICE train, 259, 260
globular metal transfer, 9

heat-affected zone, 112, 128, 144, 180, 205, 220, 221, 253, 309
heat conduction mode welding, 53
helium, 86, 89–90, 200
  and CO_2 content effect on spatter of hybrid laser-MAG welding, 95
  effect on hybrid weld bead cross section width in close-fitting I-butt joints, 95
  in He–Ar_2, effects on penetration depth of CO_2 laser–TIG hybrid weld, 94
helium shielding gas, 33
HL4000D laser, 212
HSLA S1100QL steel, 113, 114
HSLA-65 structural shapes, 121
hybrid CO_2 laser–TIG arc welding, 302
hybrid laser–arc welding, 28–44, xiii–xiv
  aluminium, 216–62
    applications, 258–61
    fusion welding of alloys, 219–28
    future trends, 261–2
    hybrid laser–arc welding processes for alloys, 228–45
    and its alloys, 217–19
    properties of hybrid laser–arc welds, 245–58
  arc heat sources, 59–68
    consumable electrodes, 62–4
    non-consumable electrodes, 64–8
  assessment of weld properties, 136–8
    defect detection using ultrasonic NDT, 132
    destructive testing, 136
    non-destructive testing, 136–8
  combinations of laser beams and arcs, 68–77
    available heat sources, 70
    basic setups, 69–75
    common operation point, 72
    geometrical arrangements, 70
    separate operation point, 74
    setups with more than 2 sources, 76–7
    two secondary heat sources, 76
dissimilar metals, 270–91
  application potentials, 288–91
  basic features of laser MIG hybrid welding, 277–8
  future trends, 291
  process and joint properties, 278–88
  specific aspects of and state-of-the-art processes, 271–7
dynamic behaviour, 34–5, 37
  arc and droplet behaviour, 36
  arc and plume behaviour during hybrid TIG–YAG welding, 34
  A5052 welds cross section, 35
  MIG welds vs hybrid YAG laser–MIG or MIG–YAG welds in steel with Ar gas, 36
effect of shielding gas, 85–103
  common types and physical properties of shielding gases, 86–92
  hybrid welding, 92–100
  mechanical properties of hybrid weld, 100–3
formation and prevention mechanism of porosity, 41–4
  melt flows, bubble, and porosity or no porosity, 44
  molten pool of hybrids, 41
  surface, cross section and x-ray inspection comparison, 43
  welding phenomena at 100 and 200 A, 43
future trends, 77–8
heat sources, 47–78
  common fusion welding methods, 48
  future trends, 77–8
laser beam heat sources, 48–55, 57–9
  beam characteristics, 49–51
  laser types, 55, 57–9
  welding modes, 51–5
laser-hybrid and laser-hybrid-tandem welding industrial robotic application, 192–215

applications and case studies in automotive industry, 195–9
applications in shipbuilding, 199–205
in automotive industry, 205–6
laser hybrid process for industrial applications, 193–5
laser hybrid welding system with three arcs, 211–14
laser tandem hybrid welding system, 209–11
in pipeline industry, 206–8
synergies by laser hybrid, 204–5
magnesium alloys, 143–75
laser beam and arc plasma interaction, 172–3
low-power laser–arc hybrid welding process, 145–62
numerical simulation, 162–8
practical application, 173–5
spectral diagnosis, 168–72
weldability, 144–5
melt dynamics and melt pool stability, 37–9, 41
melt flow patterns at 100A and 200A, 38
molten pool surface and ZrO_2 particle tracer at 100A in Ar gas, 37
molten pool surface and ZrO_2 particle tracer at 200A in Ar gas, 38
Pt diffusion in molten pool at 100A in Ar gas, 39
W particle motion at 100A, 40
W particle motion at 200A, 40
plasma characteristics in laser beam and arc interaction, 29–31, 33–4
arc voltage, current and high speed images variation, 32
hybrid laser–TIG and laser–MIG, 29
plume, plasma and keyhole behaviour during fibre, YAG and CO_2 welding, 32
plume and/or plasma formed TIG, YAG and hybrid TIG-YAG, 30
TIG arc and reflected laser beam during hybrid TIG-YAG welding, 33
type 304 steel behaviour during TIG and hybrid TIG-YAG, 31
voltage variation, 31
properties of joints produced, 106–24
corrosion properties, 123–4
fatigue properties, 120–3
hardness, 112–16
microstructure of welds, 106–11
strength, 116–18
toughness, 118–20
quality control and assessing weld quality, 127–39
shipbuilding applications, 178–91
approval of laser-based welding in shipbuilding, 179–84
industrial examples, 184–9
solidification flaws in welded structural steels, 129
steel, 299–309
and high tensile strength steel, 300–7
stainless, 309
zinc-coated, 307
weldability lobe, 130
weldability of typical structural materials, 127–34
aluminium alloys, 131–3
stainless steels, 133–4
structural steels, 127–31
weldability with respect to solidification flaw formation, 131
weld quality, 134–5
classification, 135
weld imperfections and defects, 134–5
hybrid laser–TIG welding
magnesium alloys, 143–75
cross section of dissimilar weld, 147
and TIG only stability, 148
hybrid MAG–CO_2 laser welding, 305

hybrid MAG–YAG laser welding, 300
hybrid MIG–YAG laser welding, 300
hybrid YAG laser–MAG arc bead-on-plate, 300
hybrid YAG laser–MAG arc welding, 300
hybrid YAG laser–MAG welding, 307
hybrid YAG laser–MIG welding, 300
hybrid YAG laser–pulsed MAG welding, 307
hybrid YAG–TIG welding, 309
hydrogen, 90–2

ILT integrated nozzle, 305
intermetallic phases, 272, 273, 275, 278, 279, 281, 284, 286, 288, 291

keyhole mode welding, 53–5
6-kW fibre laser, 187

lap joint, 300
laser, xiii *see also* specific lasers
laser beam heat sources, 48–55, 57–9
  beam characteristics, 49–51
    beam propagation of a Gaussian and a non-Gaussian beam, 49
  laser types, 55, 57–9
    beam parameter products vs laser power, 57
    carbon dioxide laser, 57–8
    comparison for typical materials processing laser sources, 56
    diode laser, 59
    disc and fibre laser, 58–9
    Nd:YAG laser, 58
  welding modes, 51–5
    conduction and keyhole mode laser beam welding, 53
    heat conduction mode, 53
    keyhole mode, 53–5
    penetration depth vs intensity, 54
    penetration mode, 55
    reflectivity values of selected metals at room temperature, 52
LaserBrazing, 193
laser–GMA hybrid welding, 305
laser–(GMAW) hybrid welding
  industrial robotic application, 192–215
LaserHybrid welding, 192
  applications and case studies in automotive industry, 195–9
    axle component from Daimler, 198
    economic advantages of welded component from automotive industry, 199
    laser beam hybrid welding at Audi, 197
    side panel in front of the driver's cabin, 199
    welded door, macro section and clamping device of Phaeton of VW, 196
  applications in shipbuilding, 199–203
    comparison of laser hybrid welding to alternative processes, 202
    macro section and lab set in combination with fibre laser from IPG, 204
    welding systems of a fillet weld, 203
  laser–(GMAW-tandem) hybrid welding process, 205–6
  metal transfer in the process, 195
  principle, 194
  principle of laser hybrid welding with three arcs, 212
  synergies, 204–5
    advantages of combining the processes, 205
  welding-head system for fabricating thick-walled tubes and pipes, 212
  weld seam geometry, 195
laser–MIG hybrid welding
  basic features, 277–8
  effect of laser power on phase layer thickness, 283
  effect of MIG position relative to sheet edge
    phase layer thickness, 285

tensile strength, 285
effect of process parameters, 282–6
arc power, 283–4
phase layer thickness, 283
position of the MIG arc relative to sheet edges, 284–5
process parameter envelope, 285–6
welding speed, 284
effect of wire feed on tensile strength, 284
principle, 277
process parameter envelope, 286
laser-single-wire welding, 206
laser–(tandem) hybrid welding, 209–11
component from automotive industry, 207
including laser, power sources, wire feeder, welding head, dividing wall and service station, 211
industrial robotic application, 192–215
pipe welding and macrosection of welded pipe, 209
principle, 206
on steel component, 207
laser welding, 15–25, 144
brief history, 15–18
development, 16–18
laser development, 15–16
and lasers, 18–25
advantages, 24
beam and optics, 21–2
conduction mode and keyhole mode weld definitions, 20
disadvantages, 24–5
equipment, 20–1
process gases and ancillary process equipment/considerations, 23–4
laser welding head, 23
leading path laser-arc combination, 304
Lindokote Shopprimer, 200
Local High Speed Bus, 210
local thermodynamic equilibrium, 170
analyses, 172
low-power laser-arc hybrid welding
hardness profile across weld
AZ31, 156
AZ61, 156
AZ91, 157
AZ61 to AZ31, 157
AZ91 to AZ31, 157
influence of welding parameters, 147–50
arc power, 147–8
arc power on weld penetration, 148
defocusing value, 149
distance between laser and arc, 150
distance between laser and arc on weld penetration, 151
focus value on welding penetration, 149
welding speed, 149
welding speed on welding quality, 150
magnesium alloys, 145–62
mechanical properties, 153–4, 156–8
results of fatigue test, 155
results of tensile tests, 155
microstructure, 150–3
AZ31 to AZ91 joint, 152
back scattering electron image of weld metal, 153
magnesium alloys AZ31, AZ61 and AZ91, 152
Mg, Al, Zn and O distribution within fusion zone, 154
welded joint by hybrid welding, 151
welded joint by TIG, 152
morphology of the welded seam, 145–7
plasma behaviour, 161–2
laser-induced plume/plasma of Mg alloy AZ31B during laser welding alone, 162
in welding process of magnesium alloy, 162
porosity, 158, 160–1
AZ31B weld joint, 158
element distribution in pore, 159

number of pores in weld metal using laser coaxial shielding, 160
number of pores in weld metal using laser lateral shielding, 161
pore formation sketch map, 159
LPLAC *see* leading path laser-arc combination

magnesium alloys
appearance of joints of AZ31 to AZ31 and AZ31 to AZ91, 147
conclusions and future trends, 175
cross section of laser–TIG hybrid welded magnesium alloys, 147
diagram of low-power laser-arc hybrid welding, 146
hybrid laser-arc welding, 143–75
infrared temperature measurement, 167–8
AZ31B Mg alloy plates, surface emissivity and corresponding temperature, 168
infrared image and zone analysis of S01 in hybrid welding, 168
sketch image, 167
laser beam and arc plasma interaction, 172–3
low-power laser-arc hybrid welding process, 145–62
numerical simulation, 162–6
heat source model of hybrid welding, 164
Rotary–Gauss body heat source model, 163
weld joints, 165
physical parameters of Mg, Al and Fe at their melting points, 144
practical application, 173–5
products of magnesium alloy autocycle, 174
products of magnesium alloy bicycle, 174
simulated vs experimental butt-welding result, 166
spectral diagnosis, 168–72
electron temperature and density, 170–2
local thermal equilibrium analyses, 172
spectra of TIG welding plasma and hybrid welding plasma, 169
welding plasma spectra acquisition, 168–70
temperature distribution at quasi-stable state
hybrid butt-welding, 165
TIG butt-welding, 166
weldability, 144–5
weld appearances and macrosections, 146
MAG tandem welding, 208
Marangoni effect, 53
martensite, 109
melt zone, 221
metal active gas, 302
metal active gas welding, 206
metal-arc inert gas welding, 144
metal inert/active gas welding, 89
metal inert gas, 5
Meyer Werft, Germany, 184–5
Meyer Werft Shipyard, 199, 202
micropores, 158
MIG welding, 200

Nd:YAG laser, 58, 86, 172, 194, 207, 208, xiii
Nd:YAG laser MIG hybrid welding
bead-on-plate-welding
effect of laser power on top bead appearance and arc zone geometry, 239
effect of arc current on penetration, 242
effect of distance between laser beam and arc on penetration, 243
governing parameters, 235
Nd:YAG laser plasma arc welding, coaxial

at workpiece on effective arc voltage ratio
effect of arc current and laser power, 239
effect of arc current and spot diameter, 240
Nd:YAG-MAG, 122
nitrogen, 90, 92
nitrogen laser cutting, 186
non-Gaussian beam, 50

Odense steel shipyard, Denmark, 189
optical output power, 49
oxygen, 90
content in Ar_2–O_2 mixture, effect on weld shape of TIG welds, 91
effects on hybrid YAG laser–TIG weld shape, 93

pearlite, 108, 109
penetration mode welding, 55
Planck constant, 60
plasma arc welding, 67–8, 144
plasma tungsten arcs, 71
porosity, 43
pulsed echo technique, 137
pulsed spray transfer, 10–11
pure CO_2-laser welding, 184

radiography, 136–7
Rayleigh length, 51
Rayleigh scattering, 33
real time adaptive control, 11
Rotary–Gauss body heat source model, 162–3, 164

Schuld Held Lasertechnik, 200
shielded metal arc welding, 121
shielding gas, 98 *see also* specific type of shielding gas
chemical and physical properties of gases commonly used in laser and arc welding, 87
combinations, 98
common types and physical properties, 86–92
active gases, 90
electrical conductivity of gases, 89
gas enthalpy, 88
inert gases, 86, 89–90
other gases, 90–2
thermal conductivity of gases, 88
effect of flow on weld penetration of hybrid laser–MAG welding, 97
effect on hybrid laser–arc welding, 85–103
effect on hybrid welding, 92–100
optimisation and effects of gas nozzle arrangement, 97–100
selection and effects of gas compositions, 92–4, 96–7
effect on mechanical properties of hybrid weld, 100–3
gas nozzle in hybrid CO_2 laser-TIG welding
arrangement, 98
effect on plasma shape and weld penetration depth, 99
effect on weld surface and cross-section shape, 99
requirements during hybrid laser–arc welding, 85–6
composition, 86
flow, 86
ionisation potential, 86
shielding gas flow effects on weld penetration of hybrid laser–MAG welding, 90
shipbuilding applications, of hybrid laser-arc welding, 178–91
approval of laser based welding, 179–84
effects of mismatching, 182–3
general, 179–80
main challenges, 180
mechanical properties, 180–2
unified guidelines, 183–4
arc welded deck panels for passenger ship, 179
Charpy V-notch transition curve, 182
first laser welded sandwich panels produced at Meyer Werft, 185

hardness profiles for welds in different steels, 181
of hybrid laser–arc welding, 178–91
industrial examples, 184–9
Aker Yard, Finland, 187–8
Blohm & Voss, Germany, 186
Fincantieri, Italy, 188–9
future applications, 189
Meyer Werft, Germany, 184–5
Odense steel shipyard, Denmark, 189
installation, laser head, and laser-source and MAG power supply, 188
installation and stiffener welding head and clamping tools, 186
installation and T-joint welding head and cross section, 187
laser installation at Odense Steel Shipyard and T-joint hybrid welding head, 190
layout of new pre-manufacturing workshop at Meyer Werft, 185
11 000 twenty foot equivalent container vessel at Odense steel shipyard, 189
world's biggest cruise ships built at Aker Yard, 184
short circuit metal transfer, 8–9
spot welding, 144
spray metal transfer, 9
S 960QL, 121
stainless steel, 133–4
austenitic stainless steels, 133
corrosion properties, 123–4
CPT for pickled weld surface and root surfaces, 124
duplex stainless steels, 134
ferritic stainless steels, 133
lean duplex LDX2101 weld microstructure, 110
martensitic stainless steels, 133
microstructure of hybrid laser–arc welds, 109–10
multi-pass hybrid weld, 110
Stark broadening, 171, 172
steel
comparison of hardness profiles across welds produced by different processes, 304
comparison of joint strengths between spot, laser and hybrid welds, 302
effect of gas kind on weld penetration and porosity formation, 308
effect of welding location on weldability of lap fillet sheets with gap, 304
hybrid laser–arc welding, 299–309
stainless steel, 309
steel and tensile strength steel, 300–7
zinc-coated steel, 307
hybrid weld bead with $Ar_2 + CO_2 + O_2$, 308
hybrid YAG laser–MAG welds, 303
optimised hybrid welds, 306
porosity and crack in hybrid weld beads, 306
representation of LPLAC method, 305
weld bead
hybrid MIG–YAG laser, 301
YAG laser, hybrid MAG–YAG laser and hybrid YAG laser–MAG welding, 301
Stefan–Boltzmann law, 167
structural steels, 127–31
fracture path deviation in impact and toughness testing, 129
self-quenching, 128
solidification flaws, 129–31
structural steel S235, 122
Submerged Arc welding process, 200
tailor-welded blanks, 200

ThyssenKruppMarine Systems, 186
TIG torch, 29
TIG torch method, 100
time ionised molten energy, 64
time-of-flight diffraction, 137

T-joints, 186
transverse tensile test, 136
Triclad, 290
Trumpf Laser technology, 199, 212
tungsten-arc inert gas welding, 144
tungsten inert gas welding, 5, 89
type 304 steel, 39, 42

ultrasonics, 137
uniaxial loading, 182

Vickers hardness, 136
voestalpine Stahl, 213, 214
Volkswagen Phaeton, 195
VW Phaeton, 258–9

wavelength λ, 49
welding *see also* specific welding process
  arc and laser, advantages and disadvantages, 3–25
weld metal, 112, 128, 180
weld modes, 8
weld quality, 134–5
  classification, 135
    cross sectional geometry, 135
    internal imperfections and defects, 135
    mechanical properties, 135
    penetration control – fillet welds only, 135
    surface defects, 135
  destructive testing, 136
  non-destructive testing, 136–8
    process monitoring, 137–8
    radiography, 136–7
    ultrasonics, 137
  weld imperfections and defects, 134–5

X80 steel, 207

YAG laser optics head, 29
Yttrium aluminium garnet laser, 302

zinc-coated steel DC05 + ZE, 278